



Eze, Anthonius Anayochukwu (2013) *Isometamidium transport and resistance in Trypanosoma brucei*. PhD thesis.

<http://theses.gla.ac.uk/4693/>

Copyright and moral rights for this thesis are retained by the author

A copy can be downloaded for personal non-commercial research or study, without prior permission or charge

This thesis cannot be reproduced or quoted extensively from without first obtaining permission in writing from the Author

The content must not be changed in any way or sold commercially in any format or medium without the formal permission of the Author

When referring to this work, full bibliographic details including the author, title, awarding institution and date of the thesis must be given

Glasgow Theses Service
<http://theses.gla.ac.uk/>
theses@gla.ac.uk

**Isometamidium transport and resistance
in *Trypanosoma brucei***

submitted by

Anthonius Anayochukwu Eze

BSc (Nig.), MSc.

in fulfilment of the requirements for
the degree of Doctor of Philosophy

**Institute of Infection, Immunity & Inflammation
College of Medical, Veterinary & Life Sciences
University of Glasgow**

September, 2013.

Abstract

Animal trypanosomiasis is a major hinderance to the growth of livestock farming in sub-Saharan Africa. Chemotherapy using isometamidium, diminazene and ethidium bromide has been the main control method in the absence of a vaccine against this disease. The effectiveness of these few trypanocides is severely threatened by the widespread development of resistance. Therefore, an understanding of the mechanism(s) involved in the development of resistance will assist in the development of screening protocols for easy identification of resistant cases prior to treatment, and also in finding ways to reverse the resistance. We studied the mechanism of resistance to isometamidium in bloodstream forms of *Trypanosoma brucei*. Resistance to isometamidium in *Trypanosoma brucei* was found to be composed of a reduced uptake of the drug and the modification of the F_1F_0 ATPase complex; active drug efflux by ABC transporters was not involved in the resistance mechanism, although efflux of ISM could be observed in both wild-type and resistant lines. Expression of the transporter gene *TbAT1*, as well as of *TbAT-E* and *TbAT-A*, in yeast, each resulted in increased ISM uptake. In addition, the V_{max} for the LAPT1 drug transport activity (Low Affinity Pentamidine Transporter) in ISM-resistant trypanosomes (clone ISMR1) was significantly reduced ($P < 0.05$; Student's t-test) compared to the wild type control. Also, two point mutations, namely G37A and C851A were found in the ATP synthase gamma subunit of the F_1F_0 ATPase complex of isometamidium-resistant trypanosomes. The resistant clones also lost their mitochondrial DNA and mitochondrial membrane potential and displayed various levels of cross-resistance to ethidium, diminazene, pentamidine and oligomycin. The C851A mutation introduced a stop codon in the open reading frame of the ATP synthase gamma gene. This mutation, when introduced into

the wild type *Tb427*, produced resistance to isometamidium, and cross resistance to diminazene, ethidium, pentamidine and oligomycin. C851A-ATP synthase gamma proves to be a dominant mutation that allows the rapid loss of mitochondrial DNA after just three days exposure of the parasites to 20 nM ISM or ethidium bromide. Finally, following a recent genome-wide loss-of-function RNAi screen that linked *TbAQP2* with pentamidine and melarsoprol cross resistance, we were able to demonstrate that *TbAQP2* encodes the HAPT1 in *T. brucei*, thus leaving us with the LAPT1 as the only known *T. b. brucei* drug transporter of unknown genetic origin. We however identified specific inhibitors for this transporter (LAPT1) that will be of use in its further characterization.

Table of Contents

1.	General Introduction	1
1.1.	African Trypanosomiasis	2
1.2.	History and Epidemiology of Trypanosomiasis	4
1.3.	Life cycle of trypanosomes	9
1.4.	Cell Biology of the trypanosomes	11
1.4.1.	The Glycosomes	12
1.4.2.	The mitochondria	15
1.4.3.	The variable surface glycoprotein.	17
1.5.	Molecular Biology of the Parasite	18
1.5.1.	Organisation and expression of the nuclear genome.	18
1.5.2.	The kinetoplast and its DNA.....	19
1.6.	Diagnosis of the disease	21
1.7.	Control methods	23
1.8.	Treatments for Human and Veterinary trypanosomiasis.....	24
1.9.	Uptake of trypanocides by the parasite	26
1.9.1.	Uptake of Eflornithine	27
1.9.2.	Uptake of the diamidines	27
1.9.3.	Uptake of arsenical-based trypanocides.....	29
1.9.4.	Uptake of suramin	30
1.9.5.	Uptake of the nitroheterocyclic trypanocides	31
1.9.6.	Uptake of Isometamidium (ISM).....	32
1.10.	Mechanism of action of trypanocides	32
1.11.	Biochemical targets for the development of new trypanocides.....	35
1.11.1.	Sterol biosynthesis	35
1.11.2.	Cysteine proteases	36
1.11.3.	Thiol metabolism.....	36
1.11.4.	Polyamine biosynthesis.....	37
1.11.5.	The glycosome.....	38
1.11.6.	RNA Processing.....	39
1.11.7.	The glycolipid anchor for variant surface glycoprotein (VSG)	40
1.11.8.	The proteasome	41
1.11.9.	Purine Salvage	42
1.11.10.	The Kinetoplast.....	45
1.11.11.	The Trypanosome Alternative oxidase.....	45
1.12.	Mechanisms of resistance to trypanocides	46
1.13.	Plans for the PhD project	49
2.	Materials and Methods	51
2.1	Materials.....	52
2.1.1	In vitro culture of bloodstream forms (BSF) of <i>T. b. brucei</i> , transformed yeasts and other cells.....	52
2.1.2	Induction of resistance to isometamidium and ethidium bromide in bloodstream forms of <i>T. b. brucei</i>	52
2.1.3	Alamar blue and propidium iodide drug sensitivity assays	52
2.1.4	In vitro uptake of isometamidium and [³ H]-pentamidine	53

2.1.5	Site-directed mutagenesis of genes of interest.....	53
2.1.6	Transfection of <i>T. b. brucei</i> (BSF), yeasts and <i>Leishmania mexicana</i>	53
2.1.7	Sequencing of genes of interest.....	54
2.1.8	Mitochondrial membrane potential Assays.....	54
2.1.9	Fluorescence microscopy.....	54
2.2	Methods.....	54
2.2.1	In vitro culture of bloodstream forms (BSF) of <i>T. b. brucei</i> , transformed yeasts and other cells.....	54
2.2.2	Induction of resistance to isometamidium and ethidium bromide in blood stream forms of <i>Trypanosoma brucei brucei</i>	56
2.2.3	Alamar blue and propidium iodide drug sensitivity assays.	57
2.2.4	Harvesting and purification of cells for uptake assays	59
2.2.5	In vitro uptake of isometamidium, [³ H] pentamidine and [³ H] diminazene.....	60
2.2.6	Molecular procedures utilized	61
2.2.6.1	Genomic DNA extraction	61
2.2.6.2	Primer design.....	61
2.2.6.3	Polymerase chain reactions (PCR).....	65
2.2.6.4	Site-directed mutagenesis.....	66
2.2.6.5	Generation of a TbAT-1 yeast expression vector.....	68
2.2.7	Transfection of <i>T. b. brucei</i> (BSF), yeasts and <i>Leishmania mexicana</i>	70
2.2.7.1	Transfection of <i>T. b. brucei</i>	71
2.2.7.2	Transfection of <i>Leishmania mexicana</i>	71
2.2.7.3	Transformation of yeast cells	72
2.2.7.4	Dilution of transformed trypanosomes (<i>L. mexicana</i>) and selection for clones.....	73
2.2.8	Sequencing of genes of interest.....	73
2.2.9	Mitochondrial membrane potential assays.....	74
2.2.10	Fluorescence microscopy.....	75
2.2.11	Infectivity studies in mice.....	75
3.	Isometamidium shares at least 1 transporter with pentamidine: Analysis of issues and possibilities.....	76
3.1.	Introduction.....	77
3.2.	Expression of <i>TbAT1</i> in yeast cells.....	78
3.3.	Isometamidium uptake through the P2 transporter.....	82
3.4.	Expression of TbAT-E1 and TbAT-E2 in Yeast and <i>Leishmania mexicana</i>	84
3.4.1.	Expression of <i>TbAT-E1</i> and <i>TbAT-E2</i> in yeast cells.....	84
3.4.2.	TbAT-E1 and TbAT-E2 Expression in <i>Leishmania mexicana</i>	87
3.5.	Expression of TbAT-A1, TbAT-A3 and TbAT-A6 in yeast and <i>Leishmania mexicana</i>	89
3.6.	RNAi of <i>TbAT-E</i> in 2T1.....	90
3.7.	Drug efflux by ABC transporters is not involved in ISM resistance in <i>T. brucei brucei</i>	92
3.8.	Discussions.....	97
3.9.	Conclusion.....	101

4. Development and characterization of clonal lines resistant to 1 μ M and 15 μ M isometamidium respectively.	102
4.1 Introduction	103
4.2 Induction of resistance	103
4.3 <i>In vitro</i> measurement of rate of multiplication.....	104
4.4 Assay for cross resistance to related trypanocides.....	105
4.5 Uptake studies and kinetic characterization	106
4.6 Sequencing and analysis of AT-like genes from resistant clones.....	108
4.7 Assay for sensitivity to oligomycin and FCCP	109
4.8 Measurement of the mitochondrial membrane potential.	111
4.9 Investigating the presence of kDNA in ISM-resistant clones	113
4.10 Sequencing and analysis of the ATP synthase gamma gene from the ISMR clones.....	115
4.11 Discussion	118
4.12 Conclusion.....	120
5. ISM resistant clones are dyskinetoplastic; evidence for a new resistance marker.....	121
5.1 Introduction	122
5.2 Site-directed mutagenesis of the wild type ATP synthase gamma gene to introduce the compensating mutation.....	122
5.3 Exposure of <i>Tb427 wt + S284*</i> clones to Isometamidium or Ethidium	128
5.3.1 <i>In vitro</i> measurement of resistance to trypanocides.....	130
5.3.2 The mitochondrial membrane potential.....	133
5.3.3 Fluorescent microscopy	134
5.3.4 Loss of Kinetoplast PCR.....	135
5.4 Sequencing of <i>Tb427 wt + S284*</i> clones 1I & 1E.....	136
5.5 Infectivity of ISMR and <i>S284*</i> clones in mice.....	138
5.6 Discussions.....	139
5.7 Conclusion.....	142
6. Aquaporin-2 expression enhances pentamidine but not ISM uptake: An investigation into the genetic identity of the High Affinity Pentamidine Transporter (HAPT1).	143
6.1. Introduction	144
6.2. Uptake of [³ H]-pentamidine by <i>Tb427 TbAT-E</i> dKO cells.	146
6.3. Effect of <i>TbAT-E1</i> and <i>TbAQP2</i> expression on drug sensitivity in <i>T. b. brucei</i> . 146	
6.4. [³ H]-Pentamidine uptake by <i>TbAQP2</i> expression in B48.....	148
6.5. The contribution of the <i>TbAQP2</i> to ISM uptake in <i>T. b. brucei</i>	152
6.6. Effect of <i>TbAQP2</i> expression on sensitivity to adenosine analogues	154
6.7. [³ H]-pentamidine uptake by 2T1 <i>TbAQP2</i> KO	156
6.8. Expression of synthetic aquaporin constructs in bloodstream forms of the <i>aqp2/aqp3</i> double null line.....	157
6.9. [³ H]-pentamidine uptake by <i>TbAQP2</i> expression in <i>Leishmania mexicana</i> . 159	
6.9.1. Effect of expression of <i>T. brucei</i> aquaporins on drug sensitivity of <i>Leishmania mexicana</i>	163

6.10.	Combination of Pentamidine and SHAM for synergistic studies.	166
6.11.	Sensitivity of High Affinity Pentamidine Uptake to inhibition by ionophores.	169
6.12.	Does the TbAQP3 gene also express a pentamidine transporter?.....	171
6.13.	Discussion.....	173
6.14.	Conclusion.....	174
7.	Test of a library of Bisphosphonium compounds for inhibitors of the Low Affinity Pentamidine Transporter (LAPT1).	176
7.1.	Introduction	177
7.2.	Bisphosphonium compounds as inhibitors of Pentamidine uptake through the LAPT1.	179
7.3.	Time-dependent toxicity of selected bisphosphonium compounds to trypanosomes.	184
7.4.	Discussion	188
8.	General Discussion	197
	Appendices.....	207
	Appendix A: General buffers, solutions and media.....	207
	Appendix B: Mitochondrial membrane potential graphics.	211
	Appendix C: DNA sequencing alignment of <i>TbAT-A</i> , <i>TbAT-E</i> , <i>TbAT1</i> and ATPase γ from ISMR clones.	230
	References	272

List of Figures

Figure 1.1 Classification of trypanosomes.....	3
Figure 1.2 The life cycle of <i>Trypanosoma brucei</i>	9
Figure 1.3 Sub cellular structure of the bloodstream form African trypanosome.....	11
Figure 1.4 Glycolysis and glycosomes in the bloodstream and procyclic forms of the African trypanosome.....	13
Figure 1.5 Mitochondrial inner-membrane potential in trypanosomes.....	21
Figure 1.6 Structures of drugs for (a) early stage and (b) late stage HAT.....	25
Figure 1.7 Structures of the most common trypanocides used in chemotherapy and chemoprophylaxis of livestock trypanosomiasis.....	25
Figure 1.8 Phylogenetic relationship between TbAT1, other AT-like genes (group I) and other nucleoside transporter genes (group II and IV).....	28
Figure 1.9 The distribution of trypanocidal resistance in sub-Saharan Africa.....	47
Figure 2.1 Dilution of trypanosomes and <i>L. mexicana</i> for clones.....	73
Figure 3.1 Agarose gel electrophoresis of <i>TbAT1</i> subcloned in pGEMT vector....	79
Figure 3.2 Agarose gel electrophoresis of BamHI and XhoI dropout of <i>TbAT1</i> from pDR195 vector.....	80
Figure 3.3 Vector map of <i>TbAT1</i> in pDR195 expression vector.....	81
Figure 3.4 Screen for <i>TbAT1</i> in yeast.....	81
Figure 3.5 Uptake of ISM by yeast cells expressing <i>TbAT1</i> and empty pDR195....	82
Figure 3.6 Uptake of ISM by <i>Tb427</i> wt and <i>TbAT-1</i> KO.....	83
Figure 3.7 Sensitivity to tubercidin in ISM resistant clone.....	84
Figure 3.8 Vector map of <i>TbAT-E1</i> in pDR195 expression vector.....	85
Figure 3.9 ISM uptake by MG887-1 yeast cells expressing <i>TbAT-E1</i>	85
Figure 3.10 ISM uptake by yeast cells expressing <i>TbAT-E2</i>	86
Figure 3.11 PCR screen of <i>TbAT-E2</i> and <i>TbAT-E1</i> in MG887-1 yeast cells.....	87
Figure 3.12 Graph of alamar blue on <i>TbAT-E</i> and <i>TbAT-A</i> expression in <i>L. mexicana</i> promastigotes.....	88
Figure 3.13 ISM uptake by yeast cells expressing <i>TbATA-1</i> and <i>TbATA-6</i>	89
Figure 3.14 PCR screen of <i>TbAT-A1</i> and <i>TbAT-A6</i> in MG887-1 yeast cells.....	90
Figure 3.15 Uptake of ISM by RNAi of AT-E in 2T1.....	91
Figure 3.16 Summary of repeats for ISM uptake by 2T1 RNAi of AT-E.....	92
Figure 3.17 Uptake of ISM by <i>Tb427</i> wt and ISMR15 clone 1.....	93
Figure 3.18 Uptake of ISM by <i>Tb427</i> wt, ISMR1 clone 3 and ISMR15 clone 1.....	94
Figure 3.19 Effect of tetracycline on rate of ISM efflux from cells and on the growth rate of ISMR1, ISMR15 and s427wt.....	95
Figure 3.20 Uptake of ISM by <i>Tb427</i> wt (from culture) in the presence of inhibitors of ABC transporters.....	96
Figure 3.21 Inhibition of ISM uptake by 100 μ M and 333 μ M concentrations of pentamidine (PENT), diminazene (DIM) and adenosine (ADO).....	97
Figure 3.22 Summary of drug uptake routes in <i>T. b. brucei</i> . equilibrative diffusion.....	98
Figure 4.1 Selection for resistance to ISM in concentration/passages.....	104
Figure 4.2 Rate of growth of the <i>Tb427</i> wt compared with the resistant clones.....	105
Figure 4.3 Sensitivity of the ISMR clones to trypanocides, assessed using the alamar blue assay.....	105
Figure 4.4 Isometamidium uptake in <i>Tb427</i> wt and resistant <i>T. brucei</i>	107

Figure 4.5 Alamar blue assay with oligomycin and FCCP on ISMR clones and <i>Tb427</i> wt.....	109
Figure 4.6 MMP measurement in <i>Tb427</i> wt, ISMR1 clone 3 and ISMR15 clone 1 after 1h incubation in 0.5 μ M ISM.....	112
Figure 4.7 MMP time points for <i>Tb427</i> wt exposed and unexposed to 0.5 μ M ISM.....	112
Figure 4.8 Fluorescence microscopy showing the absence of kinetoplast DNA in ISMR clones and <i>Tb427</i> wt.....	113
Figure 4.9 PCR showing the loss of maxi circle markers in ISMR clones.....	114
Figure 4.10 Mutation G37A replaces a negatively charged glutamic acid (E13) with a positively charged lysine (K13).....	116
Figure 4.11 Mutation C851A (S284*) replaces a serine residue with a stop codon.....	117
Figure 4.12 Model for explanation of the effects of oligomycin and FCCP on F_1F_0 ATPase.....	120
Figure 5.1 Sequencing data for <i>Tb427</i> wt + S284* ATPase γ clones.....	123
Figure 5.2 Sensitivity of <i>Tb427</i> wt + S284* ATPase γ clones to selected trypanocides in comparison to <i>Tb427</i> wt + wt ATPase γ	124
Figure 5.3 Sensitivity of <i>Tb427</i> wt + S284* ATPase γ clones to oligomycin.....	126
Figure 5.4 Mitochondrial membrane potential assay for <i>Tb427</i> wt + S284* ATPase clones.....	127
Figure 5.5 Fluorescence microscopy images showing DAPI stain of cellular DNA of <i>Tb427</i> wt + S284* ATPase γ clones 1 and 2.....	128
Figure 5.6 In vitro measurement of rate of multiplication of <i>Tb427</i> wt + S284* ATPase clones in ISM or EtBr.....	129
Figure 5.7 Cross-resistance to pentamidine by <i>Tb427</i> wt + S284* ATPase clones.....	130
Figure 5.8 Cross-resistance to ISM and diminazene by the <i>Tb427</i> wt + S284* ATPase clones.....	131
Figure 5.9 Cross-resistance to EtBr and oligomycin by the <i>Tb427</i> wt + S284* clones.....	132
Figure 5.10 MMP of <i>Tb427</i> wt + S284* ATPase clones, drug-free and after 1h incubation in 0.5 μ M ISM.....	133
Figure 5.11 Fluorescent microscopy of DAPI-stained images of <i>Tb427</i> wt + S284* ATPase γ clones 1I and 1E, showing apparent loss of kinetoplast.....	134
Figure 5.12 Fluorescent microscopy of DAPI-stained images of <i>Tb427</i> wt + S284* ATPase γ clones 3I and 3E, showing apparent loss of kinetoplast.....	134
Figure 5.13 Loss of kinetoplast PCR showing the loss of some markers for the mitochondrial DNA in <i>Tb427</i> wt + S284* ATPase γ clones 1E and I, and clones 3E and I.....	135
Figure 5.14 Sequence of the γ -subunit of the F_1F_0 -ATPase from <i>Tb427</i> wt + S284* clone 1 showing the trace data.....	136
Figure 5.15 Sequence of the γ -subunit of the F_1F_0 -ATPase from <i>Tb427</i> wt + S284* clone 1I showing the trace data.....	137
Figure 5.16 Sequence of the γ -subunit of the F_1F_0 -ATPase from <i>Tb427</i> wt + S284* clone 1E showing the trace data.....	137
Figure 5.17 Study of infectivity of ISMR and S284* ATPase γ clones in mice; plot of logarithm of average cell density for each group.....	138
Figure 5.18 Diagram showing the two domains of the F_1F_0 ATPase and the position of the γ subunit.....	140
Figure 6.1 Uptake of 30 nM [3 H]-pentamidine by <i>TbAT-E</i> -dKO + <i>Tb427</i> and <i>Tb427</i> wt control.....	146

Figure 6.2 Overview of drug sensitivity in a few selected cell lines compared to <i>T. b.</i> 427 wt.....	147
Figure 6.3 Effect of AQP2 expression on the sensitivity of B48 to cymelarsan.....	148
Figure 6.4 Low affinity [³ H]-pentamidine timecourse uptake by <i>TbAQP2</i> expression in B48.....	149
Figure 6.5 Summary of LAPT-mediated [³ H]-Pentamidine uptake.....	149
Figure 6.6 High affinity [³ H]-pentamidine timecourse uptake by <i>TbAQP2</i> expression in B48.....	150
Figure 6.7 Summary of HAPT-mediated [³ H]-Pentamidine uptake.....	151
Figure 6.8 Effect of <i>TbAQP2</i> expression on pentamidine sensitivity.....	152
Figure 6.9 Timecourse uptake of ISM by some selected cell lines.....	153
Figure 6.10 Summary of repeats for ISM uptake by some selected cell lines.....	153
Figure 6.11 Sensitivity of various <i>T. b. brucei</i> lines to adenosine analogues.....	155
Figure 6.12 Uptake of 30 nM [³ H]-pentamidine by <i>aqp2</i> null and wild-type control cells.....	156
Figure 6.13 Expression of synthetic aquaporin constructs in bloodstream forms of the <i>aqp2/aqp3</i> double null line.....	158
Figure 6.14 Timecourse uptake of 50 nM [³ H]-pentamidine, over 30 s.....	159
Figure 6.15 Timecourse uptake of 50 nM [³ H]-pentamidine, over 15 s, using <i>L. mexicana</i> promastigotes transformed with <i>TbAQP2</i>	160
Figure 6.16 Specific uptake of 100 nM [³ H]-pentamidine in <i>L. mexicana</i> promastigotes transformed with empty pNUS vector (control), <i>TbAQP2</i> ; and <i>TbAQP3</i>	161
Figure 6.17 Characterization of 20 nM [³ H]-pentamidine uptake in <i>L. mexicana</i> promastigotes expressing <i>TbAQP2</i>	161
Figure 6.18 Michaelis-Menten plot of 20 nM [³ H]-pentamidine uptake.....	162
Figure 6.19 Effect of expression of <i>T. brucei</i> aquaporins on drug sensitivity of <i>Leishmania mexicana</i>	164
Figure 6.20 Effect of expression of <i>T. brucei</i> aquaporins on sensitivity to ISM and Ethidium bromide in <i>Leishmania mexicana</i>	165
Figure 6.21 Demonstration of the effect of AQP genes on the sensitivity of <i>L. mexicana</i> to pentamidine.....	166
Figure 6.22 Sensitivity of selected cell lines to SHAM.....	167
Figure 6.23 Correlation between SHAM and pentamidine IC ₅₀ values.....	168
Figure 6.24 High affinity pentamidine uptake in <i>T. b. brucei</i> is sensitive to ionophores.....	170
Figure 6.25 Effect of different concentrations of ionophores on the MMP in <i>T. b. brucei</i>	171
Figure 6.26 Inhibition and Michaelis-Menten plots for the Low affinity [³ H]-Pentamidine uptake in <i>aqp2/3</i> double null and B48.....	172
Figure 6.27 Summary of uptake kinetics for <i>aqp2/3</i> double null and B48.....	173
Figure 7.1 Percentage inhibition of 1 μM [³ H]-pentamidine uptake by <i>Tb427</i> wt in the presence of indicated concentrations of bisphosphonium compounds.....	180
Figure 7.2 General structure of benzophenone-derived bisphosphonium salt derivatives with antileishmanial and antitrypanosomal activity.....	183
Figure 7.3 Propidium iodide real time assay showing the rate at which the selected bisphosphonium compounds kill trypanosomes.....	185
Figure 7.4 More propidium iodide real time assays, showing the rate at which selected bisphosphonium compounds kill trypanosomes.....	186

Figure 7.5 Structures of selected bisphosphonium compounds.....	187
---	-----

List of Tables

Table 2.1 List of primers used in this project.....	62
Table 4.1 Kinetic parameters of pentamidine uptake in different <i>Trypanosoma brucei</i> clones.....	106
Table 6.1 SHAM IC ₅₀ values in the presence of various concentrations of pentamidine.....	168
Table 7.1 Affinity of Selected Phosphonium compounds on the HAPT1 and LAPT1 diamidine transporters of <i>T. b. brucei</i>	181
Table 7.2 Antitrypanosomal activity of bisphosphonium salts having aliphatic and phenyl substituents.....	189
Table 7.3 Antitrypanosomal activity of bisphosphonium salts having substituted phenyl substituents.....	191
Table 7.4 Antitrypanosomal activity of monophosphonium salts.....	193

Dedication

To the Holy mother of God, and to the memory of my dear father.

Acknowledgement

I wish to acknowledge the invaluable instruction, guidance and encouragement given to me by my supervisor, Dr. H. P. De Koning during the course of my PhD programme. I am most grateful to him for allowing me to be myself. All the other members of the HDK group, both students and post docs, including Manal, Jane, Ibrahim, Abdulsalam, Juma, Daniel and Gordon were all a delight to work with. I also wish to acknowledge the members of the Barrett group with whom I worked in the lab, especially Eduard, Roy and Hyun. Mrs Caron Patterson, who shared office with me, and the Divisional secretary, Mulu Gedle deserve a special mention for their kindness and support whenever I ask. Also worthy of mention are the students and staff members of the 5th and 6th floor of the GBRC between 2009 and 2013 for being such great company. I feel indebted to Manal and Neils for helping me settle down in Glasgow when I arrived in 2009.

The support, understanding, goodwill and prayers offered for me by my siblings, Martha, Emmanuel, Solomon, Augustine, Chinazaoku and Afamefuna were indispensable to my progress. Together with my dearest Mum, Mrs Juliana Eze, my brothers and sisters stood by me through the years of this programme. Most importantly, I am grateful to the love of my life and my wife, Ogechi for her love and support and for believing in me.

Finally, I am very grateful to the commonwealth scholarship commission in the United Kingdom for the PhD scholarship award, and to Prof. P O J Ogbunude and my colleagues and friends in UNEC, Medical Biochemistry Department for their invaluable support.

Publications and presentations

Publications containing data presented in this thesis:

Munday, J. C., Eze, A. A., Baker, N., Glover, L., Clucas, C., Aguinaga Andrés, D., Natto, M. J., Teka, I. A., McDonald, J., Lee, R., Burchmore, R. J. S., Turner, M. C., Tait, A., McLeod, A., Mäser, P., Barrett, M. P., Horn, D. and De Koning, H. P. (2013). *Trypanosoma brucei* Aquaglyceroporin 2 is a high affinity transporter for pentamidine and melaminophenyl arsenic drugs and is the main genetic determinant of resistance to these drugs. *J Antimicrob Chemother*, **accepted**.

Taladriz, A., Healy, A., Perez, E. J. F., Garcia, V. H., Martinez, C. R., Alkhaldi, A. A. M., Eze, A. A., Kaiser, M., DeKoning, H. P., Chana, A. and Dardonville, C. (2012). Synthesis and Structure–Activity Analysis of New Phosphonium Salts with Potent Activity against African Trypanosomes. *J. Med. Chem.* **55**, 2606–2622

Publications containing data not present in this thesis:

Munday, J. C., Lopez, K. E. R., Eze, A. A., Delespaux, V., Abbeele, J. V. D., Rowan, T., Barrett, M. P., Morrison, L. J. and DeKoning, H. P. (2013). Functional expression of TcoAT1 reveals it to be a P1-type nucleoside transporter with no capacity for diminazene uptake. *Int J Parasitol Drugs Drug Res* **3**, 69-76.

Teka, I. A., Kazibwe, A., El-Sabbagh, N., Al Salabi, M. I., Ward, C. P., Eze, A. A., Munday, J. C., Mäser, P., Matovu, E., Barrett, M. P., De Koning, H. P., (2011). The diamidine diminazene aceturate is a substrate for the high affinity pentamidine transporter: implications for the development of high resistance levels. *Mol. Pharmacol.* **80**, 110-116.

Presentations

Eze, A. A., Gould, M. K., Donnelly, N., Stelmanis, V., Schnauffer, A. and de Koning, H. P. (2013). Mechanism of resistance to isometamidium in the protozoan parasite *Trypanosoma brucei brucei* (**poster presentation**), EMBO Young Scientists' Forum, Instituto de Medicina Molecular, Lisbon, Portugal, 15th and 16th July, 2013.

Eze, A. A., Wiatrek, D., Stelmanis, V., Munday, J. C. and de Koning, H. P. (2012). Uptake and mechanism of resistance to isometamidium in *Trypanosoma brucei brucei* (**poster presentation**), British Society for Parasitology spring meeting, Strathclyde University, Glasgow, United Kingdom, 2nd to 5th April, 2012.

Munday, J. C., Eze, A. A., Clucas, C., Aguinaga-Andres, D., Bleakley, A., Turner, M. C., MacLeod, A., Tait, A., Barrett, M. P. and De Koning, H. P. (2012). Aquaporin 2: A resistance marker for Pentamidine and Melarsoprol in *Trypanosoma brucei* (**oral presentation**), British Society for Parasitology spring meeting, Strathclyde University, Glasgow, United Kingdom, 2nd to 5th April, 2012.

Author's Declaration

I declare that the results presented in this thesis are mine, except when stated otherwise, and that this work has not been submitted for a degree at another institution.

Anthonius Anayochukwu Eze

July, 2013

Definitions/Abbreviations

AAT	African Animal trypanosomiasis
ADP	Adenosine diphosphate
AK	akinetoplastic
ANOVA	analysis of variance
ATP	Adenosine triphosphate
BSF	bloodstream form
bp	base pairs
BSA	bovine serum albumin
CCCP	Carbonyl cyanide m-chlorophenylhydrazone
CNT	concentrative nucleoside transporter
C851A	replacement of cytidine-851 with an adenosine
°C	degree celsius
Da	Dalton
dH ₂ O	distilled water
ddH ₂ O	distilled, de-ionized water
DFMO	α-difluoromethylornithine (eflornithine)
DK	dyskinetoplastic
DMSO	dimethylsulfoxide
DNA	deoxyribonucleic acid
dNTPs	deoxynucleotide triphosphates
<i>E. coli</i>	<i>Escherichia coli</i>
EC ₅₀	median effective concentration
EDTA	ethylenediaminetetraacetic acid
ENT	equilibrative nucleoside transporter
EtBr	ethidium bromide
FBS/FCS	foetal bovine serum/foetal calf serum
FCCP	Carbonyl cyanide 4-(trifluoromethoxy)phenylhydrazone
Fwd	forward
g	gram
gDNA	genomic DNA
GFP	green fluorescent protein
G37A	replacement of guanosine-37 with an adenosine
h	hour

^3H	tritium
HAPT1	high affinity pentamidine transporter
HAT	human African trypanosomiasis
HEPES	2-[4-(2-Hydroxyethyl)-1-piperazinylethanesulphonic acid
IC ₅₀	median inhibitory concentration
ISM	isometamidium
ISM _{R1}	ISM resistant trypanosome cloned out from 1 μM ISM
ISM _{R15}	ISM resistant trypanosome cloned out from 15 μM ISM
Kb	kilobase
kDNA	kinetoplast DNA
K _i	inhibition constant
K _m	Michaelis-Menten constant
KO	gene knock-out (deletion) line
LAPT1	low affinity pentamidine transporter
LB	luria broth
LS	long slender bloodstream form
M	molar concentration
min	minute
ml	millilitre
mM	millimolar
MMP	mitochondrial membrane potential
MOPS	3-(N-Morpholino)propanesulfonic acid
mRNA	messenger RNA
MW	molecular weight
ND	not determined
ng	nanogram
nM	nanomolar
PBS	phosphate-buffered saline
PCR	polymerase chain reaction
PMF	proton-motive force
P2	adenosine transporter encoded by <i>TbAT1</i> gene
rev	reverse
RFLP	restriction fragment length polymorphism
RNAi	RNA interference
rRNA	ribosomal RNA

rpm	revolutions per minute
R ²	correlation coefficient
SDS	sodium dodecyl sulfate
SEM	standard error of the mean
SHAM	Salicylhydroxamic acid
S284*	point mutation substituting serine with a stop codon
<i>T. b.</i>	<i>Trypanosoma brucei</i>
<i>TbAT1</i>	<i>Trypanosoma brucei</i> adenosine transporter 1 gene
<i>TbAQP2</i>	<i>Trypanosoma brucei</i> aquaporin-2 gene
<i>TbAQP3</i>	<i>Trypanosoma brucei</i> aquaporin-3 gene
<i>TbAT1</i> ^(-/-)	<i>TbAT1</i> gene deletion
<i>TbAT1</i> KO	<i>TbAT1</i> gene knock-out (deletion)
<i>T. b. b.</i>	<i>Trypanosoma brucei brucei</i>
<i>TbNT</i>	<i>Trypanosoma brucei</i> nucleoside transporters
tet	tetracycline
TFP di HCl	Trifluoperazine dihydrochloride
TMRE	Tetramethylrhodamine ethyl ester
UV	ultraviolet
µg	microgram
µl	microlitre
µM	micromolar
v	volume
V _{max}	maximum velocity
VSG	variant surface glycoprotein
w	weight
wt	wild type
W.H.O.	World Health Organization
xg	relative centrifugal force (RCF).

1. General Introduction

1.1. African Trypanosomiasis

African trypanosomiasis has been extensively studied and widely reported, and is actually a worldwide disease (Baral, 2010), which is caused by species of the *Trypanosoma* genus and is infectious to man as well as to domestic and wild animals (Osorio *et al*, 2008). *Trypanosoma brucei gambiense* (*T. b. gambiense*) and *Trypanosoma brucei rhodesiense* (*T. b. rhodesiense*) are responsible for the Human African trypanosomiasis (HAT) while *Trypanosoma brucei brucei* (*T. b. brucei*), *Trypanosoma congolense* (*T. congolense*) and *Trypanosoma vivax* (*T. vivax*) are responsible for the African animal trypanosomiasis (AAT) or nagana of cattle (Vanhamme & Pays, 2004). *Trypanosoma evansi* (*T. evansi*) causes surra in camels, *Trypanosoma equiperdum* (*T. equiperdum*) causes dura in horses (Vanhamme & Pays, 2004), while *Trypanosoma simae* (*T. simae*) is responsible for trypanosomiasis in pigs (Anene *et al*, 2001). In South America, *Trypanosoma cruzi* (*T. cruzi*) and *Trypanosoma theileri* (*T. theileri*) are both of medical and veterinary importance (Osorio *et al*, 2008), with *T. cruzi* causing Chagas' disease, or American trypanosomiasis in man. *T. theileri* is a species that is considered non-pathogenic in cattle, though it could become pathogenic in the presence of other diseases (Seifi, 1995). Apart from *T. evansi* which is mechanically transmitted by biting flies of the genera *Tabanus*, *Stomoxys*, *Atylotus* and *Lyperosia*, (Lun *et al*, 1993; Anene *et al*, 2001) and by the South and Central American vampire bats, *Desmodus rotundus* (Brun *et al*, 1998), through milk or during coitus (Brun *et al*, 1998); most other members of the genus *Trypanosoma* are cyclically transmitted through the bite of infected tsetse flies of the genus *Glossina* (Mäser *et al*, 2003) with the exception of *Trypanosoma cruzi* which is transmitted by infected blood-sucking bugs of the species *Triatoma infestans* (Bargues *et al*, 2006). The only trypanosome that is

mechanically transmitted (through copulation) and not through the agency of any known invertebrate vector is *T. equiperdum* (Claes *et al*, 2005; Brun *et al*, 1998). Similarly, *T. equiperdum* is the only species of African trypanosomes that lives as a tissue parasite (Claes *et al*, 2005); all other species of develop in the blood and tissue fluids of mammals as free-living organisms that never enter the cells of the host (Pays, 2006). These trypanosomes multiply extracellularly throughout their lifecycle in the blood and tissue fluids of vertebrates and in the alimentary canal of the tsetse fly (Clayton & Michels, 1996). Figure 1 illustrates the relationship between the different species of trypanosomes.

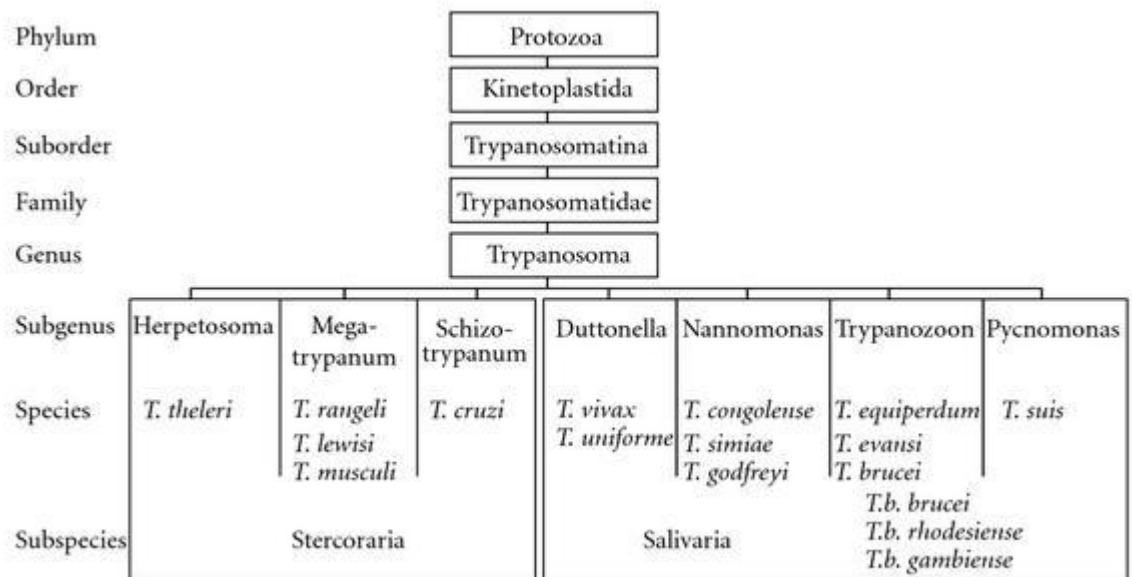


Figure 1.1 Classification of trypanosomes (Baral, 2010)

Trypanosomes cause relatively mild infections in wild animals, but cause a severe, usually fatal disease in domestic animals, the symptoms of which include fever, listlessness, emaciation, hair loss, discharge from the eyes, oedema, anaemia, and ultimately paralysis (Steverding, 2008). On the other hand, the clinical signs of dura ‘or dourine’ which include fever, local oedema of the genitals and mammary glands, cutaneous eruptions, incoordination, facial paralysis, ocular lesions, anaemia and emaciation, are marked by periods of

exacerbation and relapse, which usually end in death or possible recovery (Claes *et al*, 2005). Similarly, surra, caused by *T. evansi*, is an acute disease which leads to the death of the animals within two to eight weeks of infection, and is symptomized by progressive emaciation, oedema and nervous symptoms as well as anaemia, monocytosis and haemorrhages of visceral organs (Lun *et al*, 1993). A greater number of trypanosome species infect livestock animals, with a similar higher frequency of transmission by a larger number of *Glossina* species; veterinary trypanosomiasis therefore has the greater epidemic status, with a greater economic impact than the Human form of the disease in Africa (Baral, 2010).

Finally, a division of this disease into Human and Veterinary trypanosomiasis is only theoretical, since it had been confirmed that *T. b. rhodesiense*, also infect most domestic and wild mammals; the contribution of these animal reservoirs to the maintenance of *T. b. gambiense* infections is however still theoretical (Welburn *et al*, 2001;Massussi *et al*, 2009). These animals act as reservoirs of infection from which the human population can be reinfected, especially by *T. b. rhodesiense*, which is an established zoonotic parasite (Fèvre *et al*, 2006;Massussi *et al*, 2009). Hence, any programme aimed at controlling or eradicating the human form of this disease can only be successful if the simultaneous mass treatment of the domestic reservoir is also implemented (Onyango *et al*, 1966).

1.2. History and Epidemiology of Trypanosomiasis

The first accounts of human trypanosomiasis in modern times were provided by medical officers who worked for slave-trade companies, and these accounts described only the symptoms of the disease; Thomas Winterbottom and

John Aktins described the symptoms of the early and late stages of the disease respectively (Cox, 2004). In 1852, David Livingstone found the link between nagana in cattle and the bite of tsetse fly (Steverding, 2008). Forty three years later in 1895, the Scottish Pathologist, David Bruce discovered the causative agent of nagana to be *Trypanosoma brucei* (Steverding, 2008). This was followed in 1902 by the identification of *Trypanosoma brucei gambiense* (known then as *Trypanosoma gambiense*) as the causative agent of Human African Trypanosomiasis by the English Physician Joseph Everett Dutton after they were initially thought to be worms by Robert Michael Forde (Steverding, 2008). David Bruce was able to prove scientifically in the following year that sleeping sickness is transmitted by tsetse fly, but he erroneously proposed that transmission was mechanical (Cox, 2004). He accepted his error, and went ahead to describe the full life cycle of the trypanosomes within their tsetse fly host, after his earlier proposal was disproved by the German surgeon Friedrich Karl Kleine in 1909 (Cox, 2004). The two other causative agents of nagana, *T. congolense* and *T. vivax* were discovered in 1904 and 1905 by the Belgian physician Alphonse Broden and the German naval doctor Hans Ziemann (Steverding, 2008). *T. b. rhodesiense*, the other human trypanosome, was discovered in 1910 by parasitologists John William Watson Stephens and Harold Benjamin Fantham (Stephens & Fantham, 1910).

Three major epidemics of the Human trypanosomiasis occurred in Africa in the 20th century (Steverding, 2008). The first occurred between 1806 and 1906, mostly in Uganda and the Congo Basin (W.H.O., 2012), and resulted in the death of 300,000 and 500,000 people in the Congo Basin and the Busoga focus in Uganda and Kenya, respectively (Hide, 1999). The first set of trypanocides were arsenicals developed after the French physician Charles Louis Alphonse Laveran

and the French biologist Félix Mesnil found in 1902 that sodium arsenite was effective in infected laboratory animals (Cox, 2004). Hence the arsenical drug, atoxyl (aminophenyl arsonic acid), so named because it was initially thought to be non-toxic, was used to treat Human African Trypanosomiasis until the German physician Robert Koch found that it was in fact toxic to the optic nerve and led to blindness in 1.4% of the treated population (Steverding, 2008). Suramin (initially named Bayer 205 and then Germanin) was derived from the naphthalene urea compound, Afridol violet (fig. 2) by Wilhelm Roehl who tested more than 1000 colourless naphthalene urea derivatives while working for the German Bayer pharmaceutical company between 1905 and 1917 (Dressel, 1961). In 1919, tryparsamide was derived from atoxyl by American scientists, Walter Jacobs and Michael Heidelberger, and became the first drug for the second stage of Human trypanosomiasis since it was able to enter the central nervous system; however, it was still harmful to the optic nerve (Jacobs & Heidelberger, 1919). Both suramin and tryparsamide were employed to fight the second human epidemic of trypanosomiasis which occurred in many African countries between 1920 and 1940 (W.H.O., 2012). Mobile teams were also used in the control of this epidemic, together with other vector control measures and game destruction (De Raadt, 2005). Pentamidine was developed in 1937 for the treatment of the early stage of *T. b. gambiense* sleeping sickness by the English chemist Arthur James Ewins while working for May and Baker (Bray *et al*, 2003). This was followed in 1949 by the development of the arsenical drug melarsoprol, for treatment of the late stage *T. b. rhodesiense* sleeping sickness, by the Swiss chemist and microbiologist Ernst Friedheim. A number of drugs also became available for the treatment of animal trypanosomiasis in the 1950s, including the phenanthridine derivatives ethidium bromide and isometamidium chloride, the

aminoquinaldine derivative quinapyramine and the aromatic diamidine diminazene aceturate (Kinabo, 1993). The employment of these methods of control led to the almost complete disappearance of the disease by the mid 1960s. Surveillance was then relaxed, causing the reappearance of the disease and the most recent epidemic in 1970 (W.H.O., 2012). This epidemic of 1970 affected mainly Angola, Congo, Southern Sudan and the West Nile area of Uganda (De Raadt, 2005). Very little improvement was achieved before 1990 when eflornithine was introduced to replace melarsoprol for treatment of late stage *T. b. gambiense* sleeping sickness (Steverding, 2008). During this period, prevalence reached 50% in many villages in the Democratic Republic of Congo, Angola and Southern Sudan; sleeping sickness overtook HIV/AIDS as the greatest cause of mortality in those communities (W.H.O., 2012). In 2000 and 2001 respectively, WHO established public-private partnerships with Aventis Pharma (now sanofi-aventis) and Bayer HealthCare which enabled the creation of a WHO surveillance team, providing support to endemic countries in their control activities and the supply of drugs free of charge for the treatment of patients. Consequently, the total number of new cases of HAT reported per year in Africa has dropped from 37 991 in 1998 to 17 616 in 2004, with a further drop to 7139 in 2010. The current estimated number of actual cases is 30 000 (W.H.O., 2012). More than 500 new cases of the disease were found only in the Democratic republic of Congo in 2010. Angola, Central African Republic, Chad, Sudan and Uganda declared between 100 and 500 new cases while countries such as, Cameroon, Congo, Côte d'Ivoire, Equatorial Guinea, Gabon, Guinea, Malawi, Nigeria, United Republic of Tanzania, Zambia and Zimbabwe reported fewer than 100 new cases. Others including Benin, Botswana, Burkina Faso, Burundi, Ethiopia, Gambia, Ghana, Guinea Bissau, Kenya, Liberia, Mali, Mozambique,

Namibia, Niger, Rwanda, Senegal, Sierra Leone, Swaziland and Togo have not reported any new cases for over a decade (W.H.O., 2012).

Conversely, AAT remains a major constraint to the development of livestock in sub-Saharan Africa (Geerts, 2011). Animals kept in areas of moderate risk of trypanosomiasis have lower calving rates, lower milk yields, higher rates of calf mortality, and require more frequent treatment with preventive and curative doses of trypanocidal drugs than animals kept in trypanosomiasis free areas (Swallow, 1999). AAT occurs in 37 sub-Saharan countries where about 50 million cattle are exposed to the disease and about 35 million doses of trypanocides are used annually (Mattioli *et al*, 2004) in the prevention and treatment of the disease. The direct and indirect losses due to this disease are put at about US\$ 4.5 billion (Hursey, 2001).

The fight to eradicate trypanosomiasis in Africa is being coordinated by two key players: the Programme against African Trypanosomiasis (PAAT) and the Pan-African Tsetse and Trypanosomiasis Eradication Campaign (PATTEC). PAAT was set up in 1997 and is a joint programme of the FAO, WHO, OIE and the Inter-African Bureau for Agriculture (IBAR) of the African Union (Geerts, 2011). The PAAT approach is to link tsetse and trypanosome intervention to overall public health policies and to sustainable Agriculture and Rural Development (Mattioli *et al*, 2004). PATTEC however is a project of the AU-IBAR, launched in 2000, and its strategy is to apply area-wide principles to eliminate each pocket of tsetse infestation at a time; thus, creating a series of tsetse-free zones that can eventually be linked over a much larger area (Geerts, 2011).

1.3. Life cycle of trypanosomes

Trypanosomes arrive in the bloodstream of the mammalian host during a blood meal by an infected tsetse fly (Wang, 1995). The fly injects the metacyclic trypomastigote form of the parasite in its saliva before taking its blood meal (figure 1.2). Initially, the trypanosomes multiply locally at the site of the bite for a few days before entering the lymphatic system and the bloodstream, through which they reach other tissues and organs including the central nervous system (Chappuis *et al*, 2005). The metacyclic form of the parasite that was in the salivary gland of the fly is hence introduced into a mammal such as man, cattle, lions, antelopes, buffaloes, etc, where it differentiates into the long, slender, actively-dividing bloodstream form (Pays *et al*, 2006).

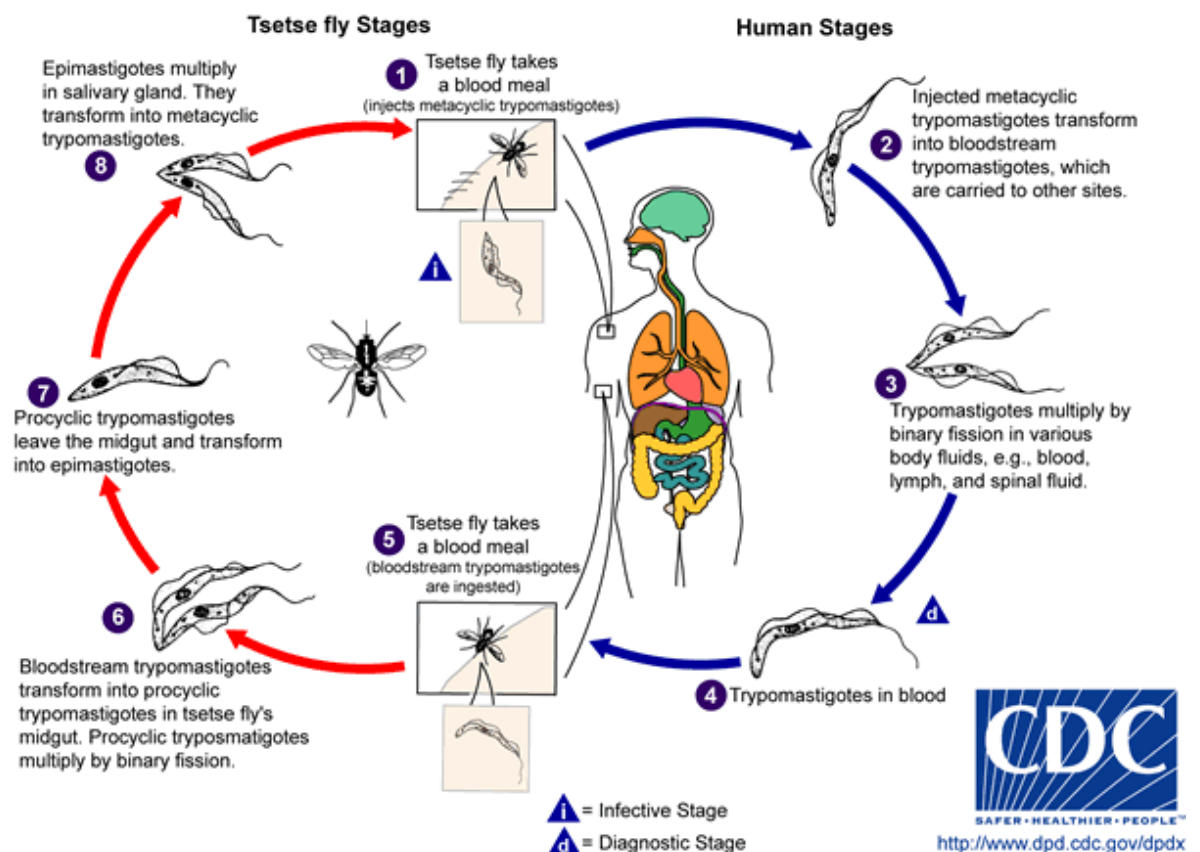


Figure 1.2 The life cycle of *Trypanosoma brucei*. Copyright Alexander J. da Silva and Melanie Moser, Centre for Disease Control Public Health Image Library. Reproduced from the CDC website: <http://www.dpd.cdc.gov/dpdx/HTML/TrypanosomiasisAfrican.htm>

This slender form is predominant in the blood and tissue fluids of the host during the period of increased parasitaemia that follows (Vassella *et al*, 1997). As the parasitaemia reaches its peak, the long, slender form differentiates into the short, stumpy non-dividing form of the parasite whose future is dependent on ingestion by tsetse fly. This differentiation from the long, slender form to the short, stumpy form is induced by a quorum-sensing signal, which is released by the parasite and characterized as the stumpy induction factor, SIF (Vassella *et al*, 1997). The finding that a lipophilic cAMP analog, 8-(4-chlorophenylthio)-cAMP (pCPTcAMP), was able to induce cell cycle arrest of bloodstream forms and slender to stumpy differentiation with high efficiency was considered an indication that endogenous production of cAMP by adenylate cyclases is sufficient to induce differentiation (Vassella *et al*, 1997). Stumpy formation *in vitro* was also induced by chemical treatments such as hydrolysable cAMP or the actual products of cAMP hydrolysis (Laxman *et al*, 2006) and troglitazone, a thiazolidinedione (Denninger *et al*, 2007). The short-stumpy form of the parasite is ingested by the tsetse fly and differentiates into the procyclic stage in the midgut lumen, while any long, slender form taken up alongside dies or differentiates into the stumpy form in the anterior midgut (Vickerman, 1985).

Trypanosomes exist only as trypomastigotes in the mammalian host, whereas the epimastigote form occurs during the development phase in the tsetse fly (Chappuis *et al*, 2005). A shift in growth temperature from 37 °C to 27 °C with simultaneous addition of *cis*-aconitase is believed to induce the differentiation to the procyclic form (Czichos *et al*, 1986). The procyclic form of the parasite divides rapidly in the midgut (Priest & Hajduk, 1994), then differentiates into the proventricular mesocyclic form which migrates to the tsetse salivary gland where it develops into the epimastigote, the form from

which the infective, non-dividing metacyclic form emerges via two intermediary stages (Vickerman, 1985). The metacyclic form can again be transferred to a mammalian host for the start of another round of the cycle.

1.4. Cell Biology of the trypanosomes

The African trypanosome has a long slender shape with a single flagellum (Vaughan & Gull, 2008) that exits the flagellar pocket at the posterior end of the cell (figure 1.3) and is attached to the cell body along its length (Vaughan & Gull, 2003). This flagellum originates from a basal body that is linked through the mitochondrial membrane to the mitochondrial genome, which is composed of a mass of catenated DNA called the kinetoplast (Matthews, 2005).

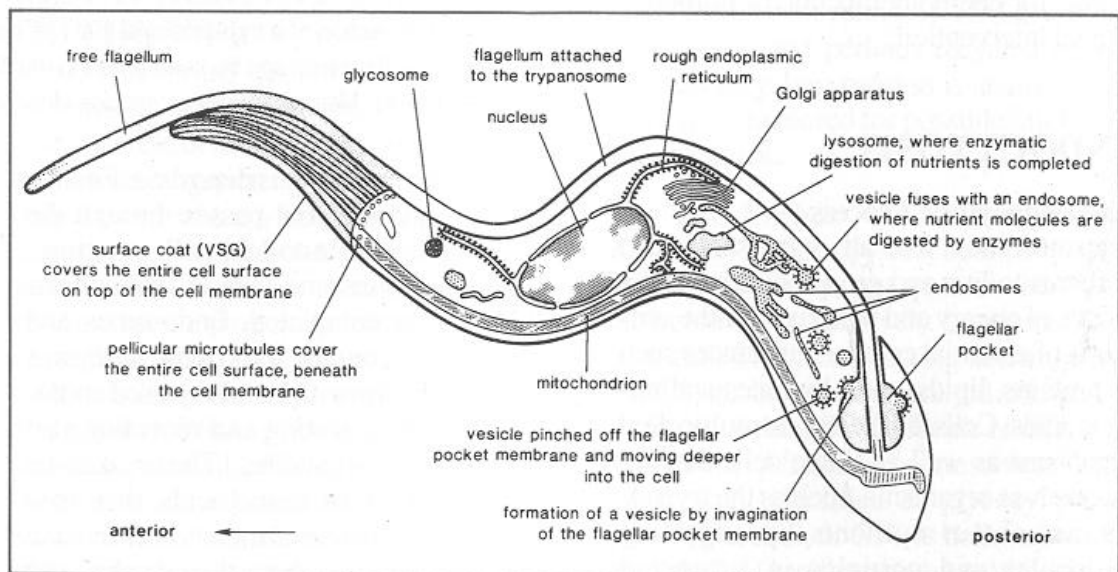


Figure 1.3 Sub cellular structure of the bloodstream form African trypanosome. The arrow shows the direction of travel of the parasite. Taken from ILRAD website:

<http://www.ilri.org/InfoServ/Webpub/fulldocs/ILRADre1989v7n1/endocytosis.htm>

The characteristic cell body shape is defined by a highly stable, highly cross-linked subpellicular microtubule cytoskeleton that lies under the cell membrane (Angelopoulos, 1970). The single-copy organelles (the flagellar pocket, flagellum, kinetoplast, mitochondrion and nucleus) are positioned

specifically within the cytoskeletal corset and are concentrated between the posterior and the centre of the cell (Matthews, 2005). The most posterior organelle is the mouth of the flagellar pocket, which serves as the only site of endo- and exocytosis (Overath & Engstler, 2004). The mitochondrion is a single elongated organelle that extends from the posterior to the anterior of the cell (Matthews, 2005). The procyclic form of *T. brucei* generates ATP from the amino acids that are abundant in their surroundings through mitochondrial-based pathways, and so can thrive in the absence of glucose or loss of glycolysis (ter Kuile, 1997). The bloodstream form on the other hand depends solely on the glycolysis of host glucose for ATP synthesis, hence the reduced mitochondrial function in this life cycle stage (Coley *et al*, 2011). The mitochondrial function of ATP generation is therefore performed in the bloodstream form by a different organelle: the glycosome.

1.4.1. The Glycosomes

Glycosomes are single-membrane organelles that compartmentalize the first seven enzymes of glycolysis and two enzymes of glycerol metabolism (Opperdoes & Borst, 1977) in addition to other pathways such as β -oxidation, ether lipid biosynthesis, sterol and isoprenoid biosynthesis, pyrimidine biosynthesis, purine salvage, the pentose phosphate pathway and gluconeogenesis (Parsons, 2004; Michels *et al*, 2000).

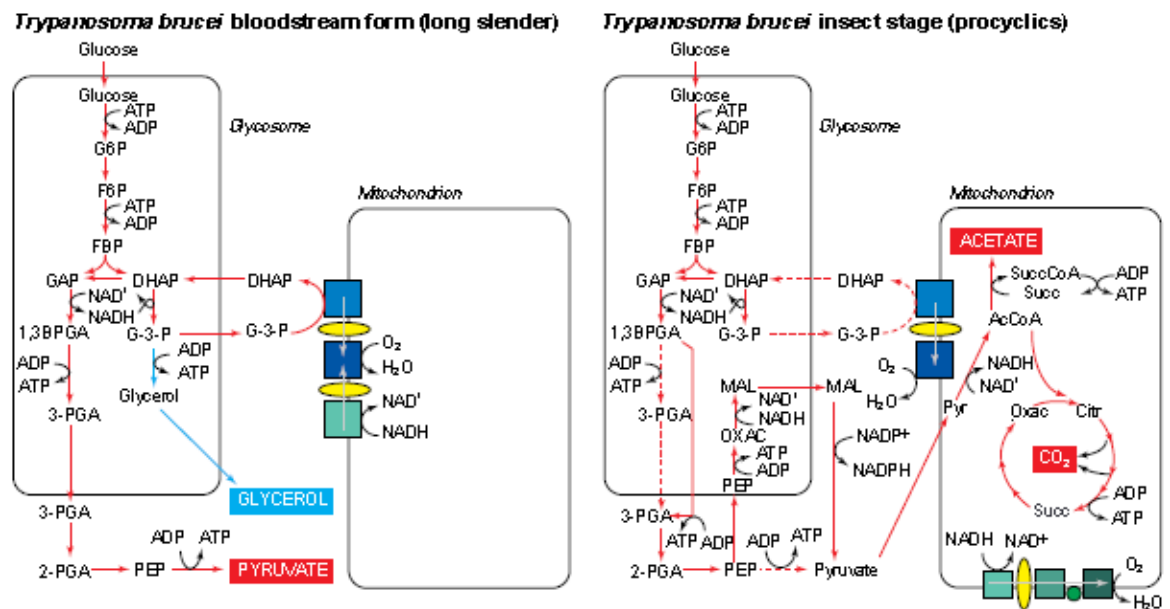


Figure 1.4 Glycolysis and glycosomes in the bloodstream and procyclic forms of the African trypanosome, taken from (Tielens & van Hellemond, 1998). Aerobic metabolism is shown in red and, when present, the anaerobic fermentation pathways are shown in blue. End-products are shown in boxes and dashed lines indicate relatively minor pathways. The enzyme complexes involved in electron transport are indicated by green and blue squares and the ubiquinone/ubiquinol pools are indicated by yellow ellipses. Abbreviations: AcCoA, acetyl-CoA; Citr, citrate; DHAP, dihydroxyacetone phosphate; FBP, fructose 2,6-bisphosphate; F6P, fructose 6-phosphate; GAP, glyceraldehyde 3-phosphate; G-3-P, glycerol 3-phosphate; G6P, glucose 6-phosphate; MAL, malate; Oxac, oxaloacetate; PEP, phosphoenolpyruvate; Pyr, pyruvate; Succ, succinate; SuccCoA, succinyl-CoA; 1,3BPGA, 1,3-bisphosphoglycerate; 2-PGA, 2-phosphoglycerate; 3-PGA, 3-phosphoglycerate.

Under aerobic conditions, the glycolytic enzymes convert glucose to 3-phosphoglycerate, which is then further metabolized to pyruvate with the resultant production of ATP by the cytosolic pyruvate kinase (Figure 1.4). The pyruvate is then secreted from the cell. Production and consumption of either ATP or NADH are balanced within the glycosomes (Coley *et al*, 2011). ATP is used up by the activity of the *T. brucei* hexokinase 1 and 2 (TbHKs) and phosphofructokinase (PFK), while it is regenerated by the activity of the glycosomal phosphoglycerate kinase (gPGK). Similarly, NADH production by

glyceraldehyde-3-phosphate dehydrogenase is balanced by NADH oxidation when glycerol 3-phosphate dehydrogenase (GPDH) metabolizes dihydroxyacetone phosphate (DHAP) to glycerol 3-phosphate (Gly-3-p). The resulting Gly-3-p is shuttled from the glycosome to the mitochondria where electrons are ultimately transferred to water through the activity of a glycerol 3-phosphate oxidase complex (consisting of a mitochondrial glycerol 3-phosphate dehydrogenase, ubiquinone, and trypanosomal alternative oxidase). The resultant DHAP is shuttled back to the glycosome to maintain its redox balance (Coley *et al*, 2011). Hence, the glycosome is not involved in net ATP synthesis. ATP synthesis occurs in the cytosol during the conversion of 2-phosphoglycerate to pyruvate (figure 1.4), giving a net production of two ATP molecules per molecule of glucose in the bloodstream form (Chaudhuri *et al*, 2006). The compartmentation of glycolysis in the glycosomes functions to regulate the pathway rather than to concentrate enzymes and metabolites of the pathway for an increased flux (Haanstra *et al*, 2008).

Under anaerobic conditions, or when the mitochondrial glycerol 3-phosphate oxidase is inhibited by salicyl hydroxamic acid (SHAM), glucose is metabolized at the same rate as under aerobic conditions, forming equal amounts of pyruvate and glycerol (Fairlamb *et al*, 1977). ATP production is reduced to half and the glycosomal NAD^+/NADH balance is maintained by the conversion of glycerol-3-phosphate to glycerol by glycerol kinase, which is a kinetically unfavourable reaction under normal conditions (Chaudhuri *et al*, 2006). Hence, bloodstream forms of *T. brucei* do not survive for long under anaerobic conditions. It has been demonstrated that SHAM alone kills *in vitro* culture of the bloodstream form within 24 hours, and that a reduction in the

trypanosome alternative oxidase level by RNAi is harmful to the parasites (Helfert *et al*, 2001).

In contrast, the glycosomes in the procyclic *T. b. brucei* contain additional enzymes and parts of pathways while the glycolytic pathway is down-regulated (Herman *et al*, 2008). Also, phosphoglycerate kinase is located mainly in the cytosol, hence 1,3-bisphosphoglycerate is not converted into 3-phosphoglycerate inside the glycosome (as in long slender forms) but in the cytosol (Tielens & van Hellemond, 1998). Most of the phosphoenolpyruvate produced in the cytosol from the glycosomal 1,3-bisphosphoglycerate re-enters the glycosome and is converted to malate which is shuttled out of the glycosome (figure 1.4) for oxidation to pyruvate which enters the mitochondrial Krebs cycle (Schnauffer *et al*, 2002). This shuttle ensures the maintenance of both redox and ATP/ADP balance within the procyclic glycosomes (Tielens & van Hellemond, 1998).

1.4.2. The mitochondrion

The mitochondrion of the early bloodstream form of *T. brucei* is tubular with hardly any cristae. The cytochromes, electron transport chain and most of the Krebs cycle enzymes are absent at this stage (Brown *et al*, 2006). It contains the glycerol 3-phosphate oxidase whose subunit, the trypanosome alternative oxidase is responsible for the oxidation of glycerol 3-phosphate from the glycosomes using oxygen as the electron acceptor (Clarkson *et al*, 1989). This electron flow to oxygen is not coupled to oxidative phosphorylation of ADP and does not generate a membrane potential (Bienen & Shaw, 1991). The mitochondrial membrane potential is however generated by the oligomycin-sensitive F_1F_0 -ATPase which acts in reverse as an ATP hydrolase, pumping protons from the matrix to the inter-membrane space at the expense of ATP

derived from substrate level phosphorylation (Nolan & Voorheis, 1992; Schnauffer *et al*, 2005). This potential is used for the import of nuclear-encoded mitochondrial proteins across the inner mitochondrial membrane (Bertrand & Hajduk, 2000).

The stumpy form of the parasite that follows is characterized by an increased specific activity of the F_1F_0 -ATPase (Bienen & Shaw, 1991), the development of tubular mitochondrial cristae and the synthesis of both proline and α -ketoglutarate oxidases in preparation for a switch to an amino acid-based energy metabolism (Vickerman, 1985). Therefore the procyclic form is able to oxidize proline and threonine for energy; more importantly, pyruvate instead of being excreted is rather metabolized to acetate in the mitochondrion, in which six out of the eight enzymes of the citric acid cycle have been shown to be active (van Hellemond *et al*, 2005). A fully functional electron transport chain is present and is coupled to oxidative phosphorylation of ADP to produce ATP by the mitochondrial ATP synthase (Williams, 1994; Brown *et al*, 2006). Studies in which ATP levels in procyclic trypanosomes were not lowered in the presence of 10 times excess of oligomycin were used to demonstrate that substrate level phosphorylation and the mitochondrial electron transport chain, but not the oxidative phosphorylation are essential to this life cycle stage (Coustou *et al*, 2003a). A more recent study uses the RNAi technique to demonstrate that the F_1F_0 -ATPase, and hence the oxidative phosphorylation, was still vital to the survival of the procyclics (Zikova *et al*, 2009). They have also been found to express all the enzymes for gluconeogenesis at this stage (van Hellemond *et al*, 2005). The epimastigotes of *T. cruzi* were found to resemble *T. brucei* procyclics in the use of proline as an important substrate, and in the incomplete catabolism of glucose to CO_2 and organic acids such as alanine and succinate

(Clayton & Michels, 1996). The transformation to the metacyclic form is believed to be accompanied by the repression of mitochondrial activity in preparation for infection of the mammalian host (Priest & Hajduk, 1994), since it was found that the metacyclic mitochondrion has the unbranched noncristate appearance of the bloodstream form mitochondrion (Vickerman, 1985).

1.4.3. The variable surface glycoprotein.

In order to survive the attack of the host antibody response during the bloodstream stage, the trypanosomal cell membrane is covered by a thick dense surface coat consisting of a monolayer of about 10^7 molecules of a single glycoprotein known as the variant surface glycoprotein (VSG) (Vanhamme & Pays, 2004; Pays, 2006; Pays *et al*, 2006). However, the VSG is highly immunogenic and can hence activate the host immune response; the parasite escapes this response by continuous antigenic variation achieved by repeated changing of the VSG loops which carry the trypanosomal antigenic determinants (Pays *et al*, 2006). According to Pays (2006), the reduction in the parasite population caused by the interaction of the parasite antigenic variation with the host immune response helps the parasite to prolong its infection by keeping the host alive, since the host must be alive for transmission by tsetse flies to occur (Pays, 2006).

Human serum, as well as sera from a few other related primates, is able to lyse the trypanosomes; only two subspecies of *Trypanosoma brucei*, namely *T. b. gambiense* and *T. b. rhodesiense* are able to resist this lysis by the human serum and hence are able to cause human infections (Pays, 2006). Human serum contains the trypanosome lytic factor, TLF which has been identified as the apolipoprotein L-1 of the HDL3 (Pays, 2006) and has been found to kill trypanosomes by creating a channel in the lysosomal membrane for the inflow of

chloride ions into the lysosome, a process that causes osmotic uptake of water and uncontrolled swelling of the lysosome until the parasite is ultimately lysed (Pays *et al*, 2006). The uptake of TLF by trypanosomes is mediated by the interaction of the HDL3-bound haptoglobin-related protein (Hpr) with a specific surface receptor on the parasite's cell surface, followed by endocytosis and fusion with the lysosome (Pays, 2006).

1.5. Molecular Biology of the Parasite

Trypanosomes have a two-unit genome, a nuclear genome and an unusual mitochondrial genome the kinetoplast, which holds about 20% of the total DNA of the organism (Hertz-Fowler *et al*, 2007). Possession of processes such as RNA editing, switching of the expression of alleles that code for the variable surface glycoprotein and the presence of an unusual mitochondrial DNA architecture are the unusual features that set the molecular biology of the trypanosomes apart (Preusser *et al*, 2012).

1.5.1. Organisation and expression of the nuclear genome.

Trypanosomes are diploid organisms. The genome contains 11 pairs of megabase-sized chromosomes (Palenchar & Bellofatto, 2006) in which the housekeeping genes (genes involved in the basic functions of the organism) are arranged in long polycistronic transcription units of up to 100 open reading frames (Preusser *et al*, 2012). There are also, in addition, about 5 intermediate-size chromosomes, sized between 200 and 900 kb, and about 100 minichromosomes (ranging in size from 50 to 150 kb) per trypanosome genome (Hertz-Fowler *et al*, 2007). The nuclear chromosomes are all linear and end in tandem repeats of the telomeric sequences [TTAGGG]_n (Hertz-Fowler *et al*,

2007), though some circular nuclear extrachromosomal DNA may be present (Alsford *et al*, 2003).

The trypanosomes possess three RNA polymerases: I, II and III. The RNA pol I transcribes mRNA for the variable surface glycoprotein as well as those for the procyclin in addition to its universal function of transcribing rRNA genes (Gunzl *et al*, 2003). All the remaining protein-coding genes are transcribed by the RNA pol II (Gunzl *et al*, 2007) while the tRNA and all the U-rich snRNA genes are transcribed by the RNA pol III (Palenchar & Bellofatto, 2006). The lack of specialized transcription factors associated with the RNA pol II suggests a lack of regulation of gene expression at the transcription initiation step; regulation of gene expression in trypanosomes occurs during transcript elongation, RNA processing and export, mRNA turn-over, translation and protein stability (Clayton, 2002). The protein-coding genes in trypanosomes are devoid of introns but trans-splicing and polyadenylation of the primary transcripts are required to generate mature mRNAs (Vanhamme & Pays, 1995). The Spliced Leader RNA acts as a splicing substrate during trans-splicing, cutting off mRNA from the primary transcript; it also attaches the m⁷G cap structure, derived from the Spliced Leader RNA, to each protein-coding mRNA during this process (Preusser *et al*, 2012).

1.5.2. The kinetoplast and its DNA

The kinetoplast DNA is made up of a few dozen maxicircles (23 kb each) and several thousand minicircles (1 kb each) (Roy Chowdhury *et al*, 2010). Maxicircles encode rRNAs, some mitochondrial proteins such as subunits of respiratory chain complexes, which include NADH dehydrogenase, cytochrome oxidase complexes I, II and III, cytochrome b (Melville *et al*, 2004) and the A6 subunit of the F₁F₀-ATPase (Schnauffer *et al*, 2005), and two guide RNAs

(Koslowsky, 2009). These subunits are however produced initially as precursor mRNAs which needs to be edited by insertion or deletion of uridine nucleotides at specific sites. The guide RNAs that act as templates in the editing process are encoded by the minicircles (Stuart *et al*, 2005).

The replication of the trypanosome kinetoplast involves the participation of two topoisomerases, a topoisomerase II (Wang & Englund, 2001) and a topoisomerase 1A (ScoCCA & Shapiro, 2008); the trypanosome genome was found to encode about five different topoisomerases (Klingbeil *et al*, 2007). The topoisomerases are responsible for releasing the individual minicircles before replication, so that they could be copied as free circular molecules. Other enzymes that take part in the replication of the kinetoplast DNA are DNA polymerases, DNA ligases and helicases; at least six DNA polymerases and two DNA ligases were found in the trypanosome mitochondrion, while the trypanosome genome encodes about eight helicases (Klingbeil *et al*, 2007) out of which six are mitochondrial (Liu *et al*, 2009).

Partial [dyskinetoplastidy (Dk)] or total [akinetoplastidy (Ak)] loss of kDNA keeps the trypanosome fixed in the bloodstream form; the tsetse fly is therefore eliminated from the life cycle and transmission between individual hosts becomes mechanical, allowing the parasite to spread outside the African tsetse belt (Lai *et al*, 2008). *T. equiperdum* and *T. evansi* differ only in that *T. equiperdum* contains fragments of kDNA maxicircles and is therefore dyskinetoplastid while *T. evansi* is akinetoplastid; hence both must have evolved from *T. brucei* after losing the ability to faithfully replicate their kinetoplast DNA (Lai *et al*, 2008). It was found that kDNA-deficient *T. brucei* and several strains of *T. equiperdum* and *T. evansi* need a mutation in the nuclear gene encoding the γ -subunit of the F_1 portion of the F_1F_0 -ATPase to survive the

loss of their kinetoplast (Lai *et al*, 2008). The loss of proton-pumping membrane component (F_0) of the ATP synthase in the Dk/Ak trypanosomes leads to a release of the soluble, catalytically active domain of the synthase (F_1) into the matrix. ATP hydrolysis by F_1 produces ADP, and the exchange of the ADP^{-3} for cytosolic ATP^{-4} via the inner-membrane ADP-ATP carrier, re-establishes the mitochondrial membrane potential, $\Delta\psi$ (Jensen *et al*, 2008)

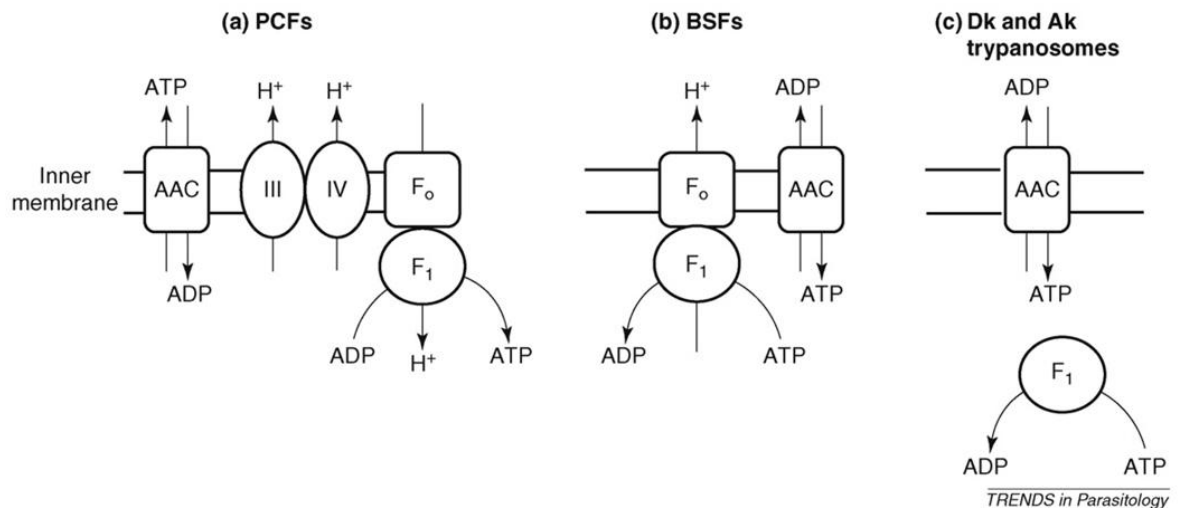


Figure 1.5 Mitochondrial inner-membrane potential in trypanosomes. Taken from Jensen *et al*, 2008. The ATP synthase is composed of F_0 , which is embedded in the inner membrane (IM) and translocates protons, and F_1 , which can either synthesize or hydrolyze ATP. The ATP-ADP carrier (AAC) mediates the exchange of ATP and ADP across the IM. (a) In the PCF, the electron transport machinery (only complex III and IV are shown) generates $\Delta\psi$, which is used to drive ATP synthesis, in addition to protein import and metabolite transport (not shown). (b) In the BSF, the ATP synthase runs backwards and uses ATP hydrolysis to pump protons across the IM to generate $\Delta\psi$. (c) In Dk or Ak trypanosomes, the F_0 portion of the ATP synthase is missing (e.g. owing to a lack of the kDNA-encoded subunit, A6), but the F_1 portion hydrolyzes ATP to ADP in the matrix. The exchange of ADP^{-3} with ATP^{-4} from the cytosol establishes $\Delta\psi$.

1.6. Diagnosis of the disease

Identification of trypanosomes was originally based on microscopic observation of morphology, morphometry and motility of the parasites in host

tissues. The recent development of molecular techniques such as restriction enzymes, sequencing, DNA probing and polymerase chain reaction (PCR) has made significant input into trypanosome identification, characterisation and diagnostic accuracy at various taxonomic levels (Desquesnes & Davila, 2002). The level of accuracy that a system of diagnosis demands may depend on the purpose in view. For instance, the simple presence of pathogenic trypanosome can be sufficient for a decision on the treatment for AAT but not for HAT; hence identification of the trypanosome species, sub-species, type or even isolate can be necessary for medical, sanitary, taxonomic, epidemiological or research purposes (Desquesnes & Davila, 2002). The first methods of DNA identification were DNA sequencing techniques and synthesis of DNA probes, followed by PCR, and a combination of both methods (Majiwa *et al*, 1994).

Genetic characterisation of trypanosomes was based initially on isoenzyme electrophoresis (Godfrey *et al*, 1987) and Restriction Fragment Length Polymorphism analysis, RFLP (Kanmogne *et al*, 1996a). These methods though successful, are limited by the requirement of a substantial amount of parasite material. The PCR-based DNA finger-printing techniques have overcome this limitation (Simo *et al*, 2008), and include the Random Amplification of Polymorphic DNA, RAPD (Kanmogne *et al*, 1996b), minisatellites and microsatellites DNA amplification techniques (MacLeod *et al*, 2000; Biteau *et al*, 2000) and Mobile Genetic Element PCR, MGE-PCR (Tilley *et al*, 2003). These methods are used to study the genetic diversity of trypanosomes, and have generated important epidemiological information on the relationship between trypanosome strains and their potential role in the heterogeneity of disease foci, and also in the generation and maintenance of HAT foci (Tilley *et al*, 2003).

1.7. Control methods

Trypanosomiasis can be controlled by either checking the spread of the vector or by controlling the parasites, or a combination of both methods (Delespaux *et al*, 2008). Vector control methods include the use of insecticides (sprayed as aerosol into the atmosphere or sprayed on the animals on which tsetse feed), the use of baits and (or) traps, and the use of the sterile insect technique (SIT) (Simarro *et al*, 2008). Traps are not usually employed as a means of eradication of flies from an infested area, but to reduce populations of tsetse to levels that reduce the challenge or risks to humans and animals, and to forestall the re-invasion of flies from a previously cleared area (Grant, 2001). Their efficiency can however be improved by the addition of strips of insecticide-treated material or chemical attractants, and by arranging in a straight line in riverine areas; these traps are a cheap means to very impressive reduction of tsetse populations, without any unwanted side effects (Grant, 2001).

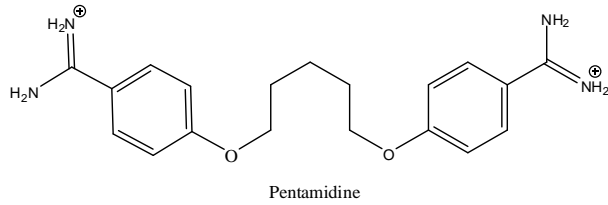
Aerial and ground spraying of organochlorine insecticides, such as dichlorodiphenyltrichloroethane and dieldrin, as practiced in Africa between the 1940s and the 1980s has been stopped because organochlorines persist for many years in the environment and so induce Cytochrome P450 activities which cause trypanocidal resistance in the exposed animals (Boibessot *et al*, 2006). Indiscriminate spraying of all vegetations (whether they are resting sites for tsetse or not) caused heavy mortality of reptiles, small mammals, fish, birds and insects in the Southern African savannah (Grant, 2001). Besides, the aerosol technique is rather expensive, with a high infrastructural-support requirement; SIT is similarly a costly technique whose feasibility can be drastically reduced in areas infested by multiple species of tsetse flies (Simarro *et al*, 2008). The

possibility of vaccine development for the control of the parasite is ruled out by the expression of antigenic variation by the blood stream forms of trypanosome (Wilkes *et al*, 1997); hence, the control of trypanosomiasis relies principally on treatment and prophylaxis (Anene *et al*, 2001).

1.8. Treatments for Human and Veterinary trypanosomiasis.

Four drugs are currently approved for the treatment of HAT, depending on the causative trypanosome subspecies and on the stage of the disease (Fairlamb, 2003). Drugs for the treatment of late stage trypanosomiasis are those that are able to cross the blood-brain barrier to kill the parasites in the cerebrospinal fluid and brain parenchyma (Fèvre *et al*, 2006), and they include melarsoprol (effective against both *T. b. rhodesiense* and *T. b. gambiense*) and eflornithine (effective only against *T. b. gambiense*) while pentamidine and suramin are for the treatment of the early stage disease (Barrett & Gilbert, 2006). Nifurtimox has been used in the past for patients suffering from eflornithine- or melarsoprol-resistant trypanosomiasis (Fairlamb, 2003) but was never licensed as mono-therapy for HAT due to the severity of its side-effects. The action of the above-mentioned clinically-approved drugs is marred by a range of severe side-effects that are sometimes life-threatening. Recently, nifurtimox-eflornithine combination treatment (NECT) was compared to eflornithine monotherapy in the treatment of second-stage *T. gambiense* infection, and was found to be as efficacious as the eflornithine monotherapy (Priotto *et al*, 2009). In addition, NECT was found to be safer since it proved to be half as toxic as the standard eflornithine monotherapy, cured HAT in a shorter period of administration than the monotherapy, and has a lower propensity for resistance by trypanosomes (Priotto *et al*, 2009).

a. Early-stage trypanosomiasis.



b. Late-stage trypanosomiasis

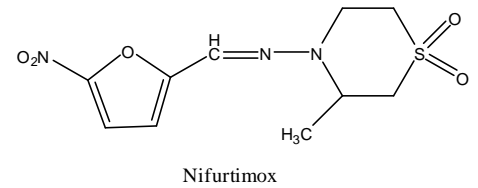
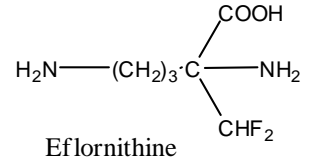
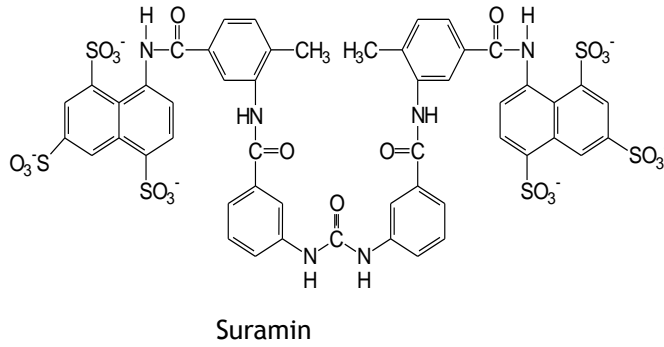
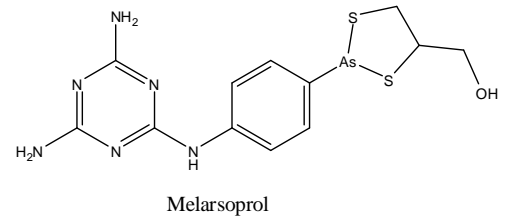


Figure 1.6 Structures of drugs for (a) early stage and (b) late stage HAT.

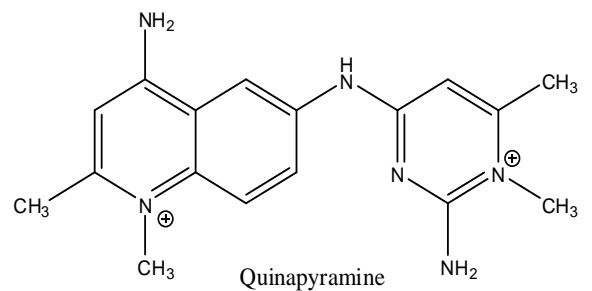
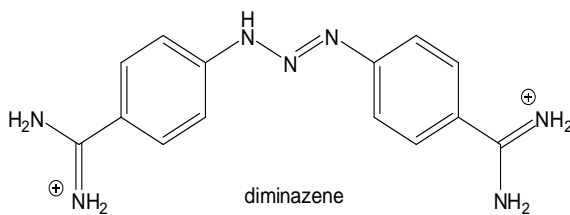
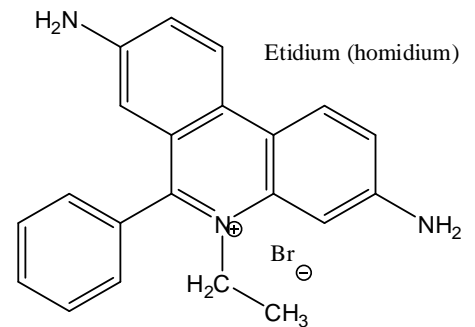
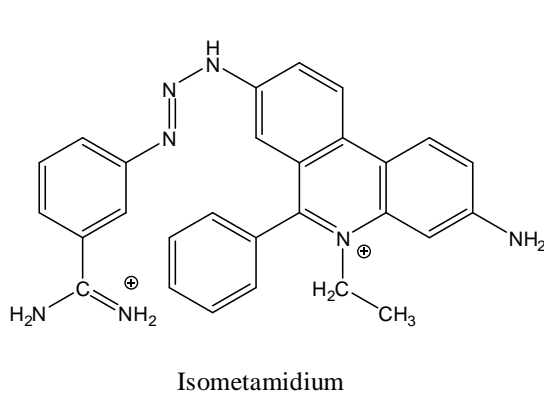


Figure 1.7 Structures of the most common trypanocides used in chemotherapy and chemoprophylaxis of livestock trypanosomiasis.

Chemotherapy and chemoprophylaxis of African animal trypanosomiasis (AAT) make use of three compounds, namely: diminazene, an aromatic

diamidine; homidium, a phenanthridine; and isometamidium, a phenanthridine-aromatic amidine (Leach & Roberts, 1981; Wilkes *et al*, 1995). Isometamidium is essentially a fusion compound of homidium and part of the diminazene molecule (Delespaux & de Koning, 2007). Delespaux and his colleagues (2008) were of the opinion that homidium should be removed from the drug market because of its toxic mutagenic properties. They argued that removal of this drug from the market would not affect the treatment of AAT adversely, since diminazene aceturate can replace it for chemotherapy while isometamidium becomes the sole chemoprophylactic agent. Similarly, treatment and prophylaxis of trypanosomiasis caused by *T. evansi* rely on quinapyramine, suramin and melarsen oxide cystemine (cymelarsan) (Leach & Roberts, 1981).

1.9. Uptake of trypanocides by the parasite

Uptake of drugs, an important factor in the determination of the efficacy of every anti-parasitic drug, may be by passive diffusion, endocytosis, receptor-facilitated uptake or transporter-facilitated uptake (de Koning, 2001a). Each mode of uptake has its specific implication when considering drug action, selectivity and the development of resistance; hence, lipophilic drugs can cross membranes by simple diffusion and will enter all cells while hydrophilic drugs need help to cross bio-membranes (de Koning, 2001a). Generally, uptake that is facilitated by either receptors or membrane transporters can be a basis for selective chemotherapeutic action against the parasite, if the cells of the host do not express a homologous protein or if the transporter (or receptor) expressed by the host has a much lower affinity (or rate of uptake) for the drug (de Koning, 2001a). However, the disadvantage of selective uptake is that the parasite may develop resistance to the drug when the receptor or membrane transporter is lost or mutated (de Koning, 2001a).

1.9.1. Uptake of Eflornithine

Uptake of eflornithine in bloodstream forms of *T. b. brucei* was found to be non-saturable, up to 10 mM concentration, and was therefore attributed to passive diffusion (Bitonti *et al*, 1986). A similar conclusion was drawn from eflornithine uptake studies in bloodstream forms of *T. b. gambiense* and *T. b. rhodesiense* (Iten *et al*, 1997). But since this proposed mode of uptake for eflornithine could not explain reduced rate of uptake observed in resistant cells (and in the absence of any identified extrusion mechanism or metabolism of eflornithine by the parasite), it was suggested that a combination of passive and facilitated diffusion be considered (de Koning, 2001a). The transporter responsible for this facilitated diffusion component has been identified as the amino acid transporter expressed by the TbAAT6 gene (Vincent *et al*, 2010). Deletion of this gene in the resistant line and the RNAi knockdown of its expression both resulted in about 40 fold resistance to eflornithine compared to the wild type trypanosomes; in addition, ectopic expression of this gene in the resistant line restored wild type sensitivity to eflornithine (Vincent *et al*, 2010).

1.9.2. Uptake of the diamidines

Pentamidine and diminazene aceturate are diamidines used for the treatment of early-stage human African trypanosomiasis caused by *T. b. gambiense* and for African animal trypanosomiasis, respectively (de Koning, 2008). Pentamidine uptake in the procyclic form is mediated by a single high-affinity proton-driven symporter, PPT1 (procyclic pentamidine transporter) (de Koning, 2001b), while both pentamidine (de Koning, 2001b) and diminazene (Barrett *et al*, 1995) seem to be transported by the P2 aminopurine transporter in the bloodstream form of *T. brucei brucei*. However, only 50 to 70% of the pentamidine transport in the bloodstream form was mediated by P2 while the

remaining 30 to 50% of the transport was carried out by a low-capacity high affinity pentamidine transporter (HAPT1) and a high-capacity low affinity pentamidine transporter (LAPT1) (de Koning, 2001b). The genes that encode the HAPT1 and the LAPT1 are not currently known, but have been speculated to be closely related to TbAT1 that codes for P2 (de Koning *et al*, 2005). This phylogenetic relationship is shown in figure 1.8.

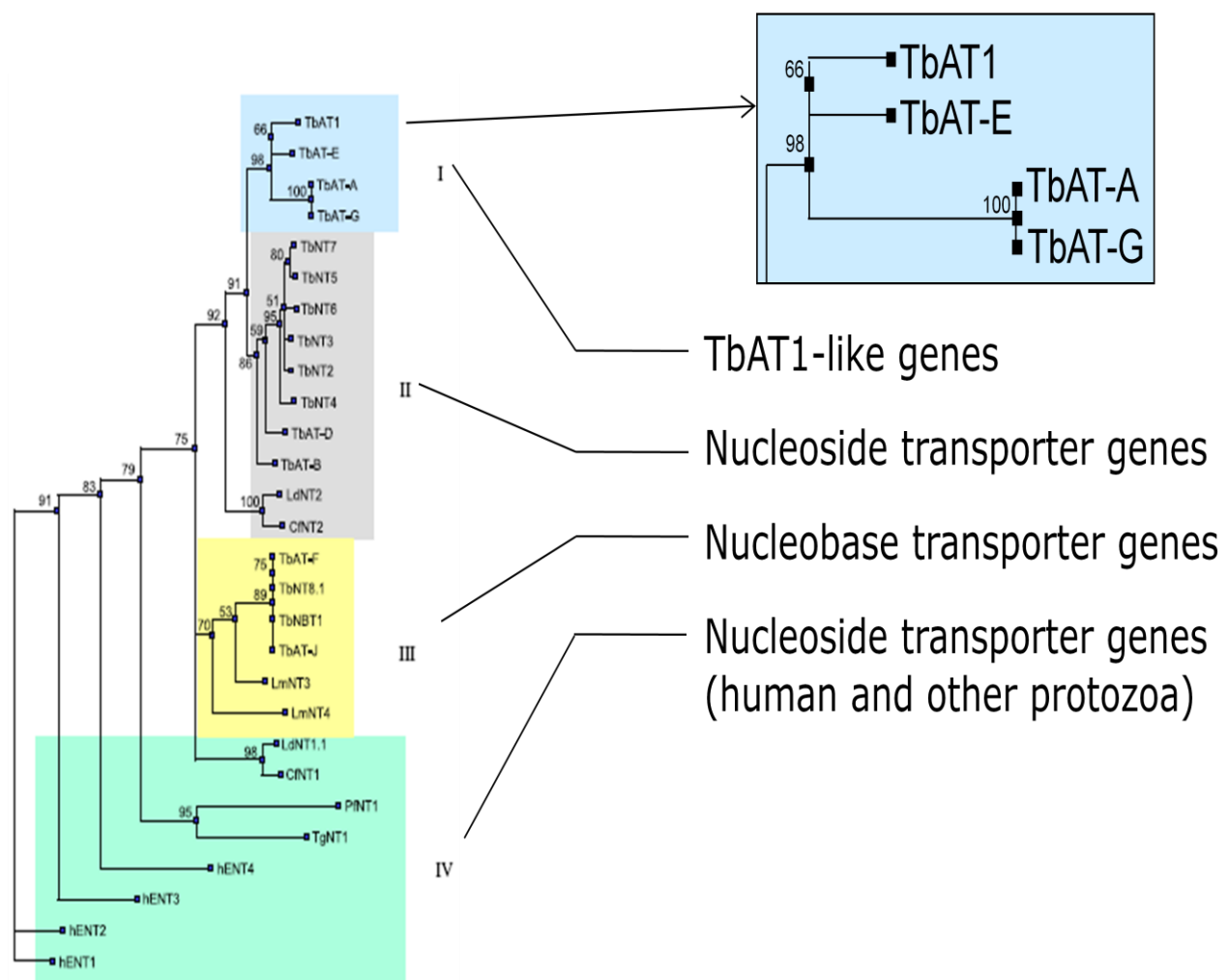


Figure 1.8 Phylogenetic relationship between TbAT1, other AT-like genes (group I) and other nucleoside transporter genes (group II and IV). Reproduced from (de Koning *et al*, 2005)

In contrast, uptake of diminazene aceturate was shown to be principally mediated by P2 (de Koning *et al*, 2004). These observations seem to be in agreement with the occurrence of resistance to diminazene but not to pentamidine in the field because a change or mutation in the gene TbAT1 that codes for P2 (Mäser *et al*, 1999), would almost entirely prevent the uptake of diminazene by trypanosomes (de Koning, 2008). Since pentamidine can be taken up by three different transporters, as stated above, it was suggested that it would take at least the simultaneous loss of the P2 and HAPT activities to cause a high level pentamidine resistance (de Koning, 2008).

Recently, a set of genome-wide, loss-of-function RNA interference (RNAi) library screens in *T. brucei* was used to demonstrate that two closely related aquaglyceroporins, AQP2 and AQP3, play a major role in pentamidine and melarsoprol cross-resistance (Alsford *et al*, 2012). This role was finally assigned specifically to AQP2, and it was demonstrated that from its function, AQP2 may correspond to HAPT1 but for the fact that it is restricted to the flagellar pocket (Baker *et al*, 2012).

1.9.3. Uptake of arsenical-based trypanocides

Of the available melaminophenyl arsenicals, which include melarsoprol, cymelarsan, trimelarsan and melarsen oxide, melarsoprol is the only arsenical licensed for the treatment of human African trypanosomiasis (late stage), while cymelarsan is licensed for the treatment of trypanosomiasis in camels (de Koning, 2001a). Melarsoprol is amphipatic, and will diffuse through cell membranes (Barrett & Gilbert, 2006). However, melarsoprol is very quickly metabolized to the more hydrophilic melarsen oxide in plasma (96% clearance within an hour) (Burri *et al*, 1993). Uptake of melarsoprol (melarsen oxide) by *T. brucei* was found to be mediated by P2 (Mäser *et al*, 1999; Delespaux & de

Koning, 2007). This finding is supported by these observations: P2 is inhibited with high affinity by melaminophenyl arsenicals (de Koning & Jarvis, 1999); expression of TbAT1 gene in yeast makes the yeast sensitive to arsenicals (Mäser *et al*, 1999); TbAT1 (P2) is mutated or altered in some melarsoprol resistant clones (Carter & Fairlamb, 1993; Stewart *et al*, 2010). Nevertheless, the finding that the *in vitro* effect of melarsen oxide on $\Delta tbat1$ *T. b. brucei* could be counteracted by pentamidine was the basis for the prediction that P2-independent uptake of melarsen oxide was mediated by HAPT (Matovu *et al*, 2003; Bridges *et al*, 2007). Hence, it is highly possible that the concomitant loss of P2 and HAPT results in high levels of resistance to both diamidines and melaminophenyl arsenicals, while the loss of P2 alone leads to only moderate loss of sensitivity for melarsoprol and some diamidines but high levels of resistance for other diamidines, including diminazene (de Koning, 2008). Finally, studies in which *L. major*, *L. infantum* and *L. tarentolae* all became hypersensitive to both arsenic and antimony after transfection with LmAQP1 suggest that these metalloids are taken up via the aquaporins (Gourbal *et al*, 2004).

1.9.4. Uptake of suramin

When the charge and size of suramin is considered (the molecule contains six negative charges at physiological pH), it becomes unlikely that the drug could be taken up by a specific transporter (de Koning, 2001a). Also the quantity of charge carried by the molecule rules out the possibility of passive diffusion of suramin into the trypanosomes (Vansterkenburg *et al*, 1993). Suramin binds strongly to low density lipoproteins and other serum proteins, including transferrin, for which trypanosomes express receptors; these complexes could therefore be taken up through receptor-mediated endocytosis; hence, it was

proposed that suramin is probably taken up by trypanosomes while bound to LDL (Vansterkenburg *et al*, 1993). This view has been changed by the outcome of the genome-wide tetracycline-inducible RNA interference (RNAi) library screens which identified a bloodstream stage-specific invariant surface glycoprotein (ISG75) family as being responsible for suramin uptake (Alsford *et al*, 2012). ISG75 was found to be responsible specifically for suramin binding, and the drug was found to be accumulated in the trypanosomal lysosome (Alsford *et al*, 2012). Suramin-ISG75 complex is then degraded by proteases to release suramin which is subsequently transported into the cytoplasm by MFST, a putative major facilitator superfamily transporter (Fairlamb, 2012).

1.9.5. Uptake of the nitroheterocyclic trypanocides

Nifurtimox and benznidazole are the main nitroheterocycles used to treat Chagas disease (Wilkinson and Kelly, 2009). Megazol is efficacious against both *T. cruzi* (Filardi & Brener, 1982) and *T. brucei* (Enanga *et al*, 1998), while nifurtimox is used to treat infections by *T. cruzi* (Docampo *et al*, 1981). Megazol was found to inhibit the uptake of adenosine by P2, with a display of high affinity for this transporter; this was to be expected since the drug has the structural motif recognised by P2 (Barrett *et al*, 2000). Nevertheless, arsenical-resistant parasites deficient in P2 were found to remain sensitive to megazol, suggesting that in spite of its ability to interact with P2, the drug seems to also be taken up across the membrane by passive diffusion (Barrett *et al*, 2000). Similarly, the uptake of nifurtimox into *T. cruzi* was found to be by passive diffusion across the cell membrane (Tshako *et al*, 1991), while studies on the route of uptake into *T. brucei* is yet to be done (Barrett & Gilbert, 2006).

1.9.6. Uptake of Isometamidium (ISM)

Uptake of ISM involves the permeation of both the plasma and the mitochondrial membranes, since it has been demonstrated that ISM is accumulated in the kinetoplast of both *T. congolense* (Wilkes *et al*, 1995) and *T. brucei* (Boibessot *et al*, 2002). The transport was found to be energy-dependent, as it was very sensitive to the metabolic inhibitor SHAM/glycerol (Sutherland *et al*, 1992); it was inhibited by ethidium, but not by either diminazene, melarsoprol or quinapyramine (de Koning, 2001a). And since resistance to ISM was found to always be associated with cross-resistance to ethidium (Peregrine *et al*, 1997), it was suggested that ISM and the structurally related ethidium might share the same route of uptake (de Koning, 2001a).

The P2 transporter may be responsible for part of the ISM uptake in *T. brucei brucei*, as evidenced by the inhibition of P2-mediated uptake of adenosine by ISM (de Koning, 2001a), but the low level of cross resistance between diminazene and ISM suggests that this mode of uptake may not be significant (Delespaux & de Koning, 2007). In summary therefore, ISM may be carried across the trypanosomal cell membrane by facilitated diffusion, and then later actively sequestered in the mitochondria, using the energy of the mitochondrial potential (de Koning, 2001a). This correlates with the observation that ISM diffuses out of resistant trypanosomes, with low mitochondrial potential, when placed in ISM-free medium (de Koning, 2001a).

1.10. Mechanism of action of trypanocides

Pentamidine, diminazene aceturate, isometamidium chloride and ethidium bromide were found to promote the cleavage of *T. equiperdum* minicircle DNA at therapeutically relevant concentrations; the cleavage sites

map to distinct positions in the minicircle sequence, and each drug has a different cleavage pattern (Shapiro & Englund, 1990). This effect was attributed to possible inhibition of a mitochondrial type II topoisomerase by these trypanocides. A more recent study however states that point mutations in the topoisomerase II gene are not involved in isometamidium resistance (Delespaux *et al*, 2007). Another study that compared the distribution and metabolism of isometamidium and ethidium bromide in the trypanosomes found that trypanosomes take up isometamidium faster than ethidium bromide; and whereas isometamidium accumulated in the kinetoplast and remained unmetabolized, ethidium bromide was more widely distributed throughout the trypanosome, and was found to have undergone hydroxylation and methylation reactions (Boibessot *et al*, 2002). A recent study has shown that ethidium bromide kills trypanosomes by blocking the initiation of minicircle replication (Roy Chowdhury *et al*, 2010). According to the study, ethidium bromide is transported into the mitochondrial matrix by the mitochondrial membrane potential. The killing of dyskinetoplastic trypanosomes by ethidium bromide was explained by a possible inhibition of nuclear DNA replication, and this mechanism was also proposed for isometamidium based on the similarity in the structure of these two trypanocides.

Melarsoprol, a melaminophenyl-based arsenical known for its toxic side effects, is taken up into the trypanosomes through the P2 aminopurine transporter (Carter & Fairlamb, 1993). It inhibits trypanosome pyruvate kinase, phosphofructokinase, and fructose-2,6-bisphosphatase, hence blocking glycolysis (Wang, 1995). An alternative mechanism is the formation of melarsen-trypanothionine adduct (Mel T) which inhibits trypanothione reductase (Fairlamb *et al*, 1989). The formation of Mel T was however the mechanism that

was recently confirmed using the high-throughput technology that gave results suggesting that this adduct was toxic to trypanosomes (Alsford *et al*, 2012).

Most proteins involved in the mechanism of action of suramin reside in the lysosomes of the trypanosomes and include the AP1 adaptin complex, lysosomal proteases and major lysosomal transmembrane protein, N-acetylglucosamine biosynthetic enzymes as well as ornithine decarboxylase (ODC) and about three other enzymes involved in spermidine biosynthesis (Alsford *et al*, 2012). Most of the lysosomal proteins were found to act through the agency of the bloodstream-stage-specific invariant surface glycoprotein ISG75 (Alsford *et al*, 2012).

Eflornithine acts as an irreversible suicide inhibitor of ornithine decarboxylase; hence, inhibiting the synthesis of polyamines in trypanosomes as well as in mammalian cells (Van, I & Haemers, 1989; Bellofatto *et al*, 1987). But trypanosomes are more sensitive to eflornithine than mammalian cells (Bellofatto *et al*, 1987). Inhibition of ornithine decarboxylase leads to a decrease in the levels of putrescine, spermidine and trypanothione, which causes a general decrease in the biosynthesis of DNA, RNA and proteins (including the variant surface glycoprotein) (Fairlamb, 2003). This decrease in the synthesis of the variant surface glycoprotein reduces parasitic antigenic variation, thus increasing the efficiency of the host immune response (Van, I & Haemers, 1989). Eflornithine is therefore more of a cytostatic than a cytotoxic drug (Fairlamb *et al*, 1987)

Nitroheterocyclic compounds such as nifurtimox and benznidazole are both pro-drugs that must be activated within the trypanosome by the action of a NADH-dependent, mitochondrially localized, bacterial-like, type I nitroreductase (NTR) (Wilkinson *et al*, 2008). This enzyme is expressed by the parasite but not

by the host, and is the basis for the selectivity of this class of drugs as well as for the development of two new classes of anti-trypanosomal agents, nitrobenzylphosphoramidate mustards and aziridinyl nitrobenzamides (Wilkinson *et al*, 2011).

1.11. Biochemical targets for the development of new trypanocides.

The ideal drug against trypanosomiasis would need to meet the following criteria: it should cross the blood-brain barrier in order to be able to deal with the cerebral stages of the disease where the need for new drugs is highest; it should be active against both *T. b. gambiense* and *T. b. rhodesiense*, and also against other species of *Trypanosoma*; there should be a very low tendency for the development of resistance against such a drug; lastly, such drug should be very cheap (Luscher *et al*, 2007). Selective toxicity against any microbial pathogen can be achieved through selective binding of drug to a specific microbial target; through a common target being vital to a pathogen but not to a host cell; or through the selective uptake of drugs into the pathogens (Barrett & Gilbert, 2006). For a compound to act as a drug, it must be able to inhibit a specific target within the parasite (Barrett, 2000). There are a large number of trypanosomal enzymes and/or biochemical pathways that have been established as possible targets for the development of new trypanocides (Wilkinson & Kelly, 2009). Some of these possible targets are discussed next.

1.11.1. Sterol biosynthesis

Both *T. brucei* and *T. cruzi* were found to possess active sterol biosynthetic pathways (Hinshaw *et al*, 2003). Most of the genes that encode enzymes in the ergosterol biosynthetic pathway in *T. cruzi* have been identified and

characterized (Wilkinson & Kelly, 2009); hence, inhibitors of oxidosqualene cyclase were found to be effective against *T. cruzi in vitro*, though the *in vivo* effects were yet to be determined (Hinshaw *et al*, 2003). *T. brucei* can however take in cholesterol from the host bloodstream, though it has this pathway (Coppens & Courtoy, 2000).

1.11.2. Cysteine proteases

A number of trypanosomal cysteine proteases have been identified and biochemically characterised, including the cathepsin L-like enzymes cruzipain (of *T. cruzi*) and brucipain (of *T. brucei*) (Wilkinson & Kelly, 2009), both members of the C1 cysteine proteases. These C1 peptidases are either essential to the survival of the parasite or important as virulent factors which contribute to disease pathogenesis, and are therefore potential serodiagnostic markers, vaccine candidates and drug targets (Caffrey & Steverding, 2009). This was earlier demonstrated by the killing of *T. brucei* with the benzyloxycarbonyl-phenylalanine-alanine diazomethane cysteine protease inhibitor; the target of this inhibitor was originally presumed to be brucipain, until it was proved by genomic analysis that the actual target was tbcatsB, a cathepsin B-like protease of *T. brucei* (Mackey *et al*, 2004). Hence, tbcatsB was the most likely target of the protease inhibitor, and as such is a potential target for drug development, since it was shown to be very useful in host serum protein degradation by the parasite (Mackey *et al*, 2004).

1.11.3. Thiol metabolism

Leishmania and trypanosomes are unique in their employment of trypanothione instead of glutathione in the control of their intracellular reducing environment (Werbovetz, 2000). Obviously, the presence of trypanothione reductase instead of glutathione reductase in trypanosome makes trypanothione

an essential cofactor mediating the redox balance in the parasite, and trypanothione reductase a potential target for the development of chemotherapy (Wang, 1995). A number of compounds found to inhibit trypanothione reductase activity have been identified, with some of them exhibiting trypanocidal activity (Wilkinson & Kelly, 2009). Similarly, Galarreta and co-workers identified three new heteroaromatic frameworks (harmaline, pyrimidobenzo thiazine, and aspidospermine) as the basis for inhibition of *T. cruzi* trypanothione reductase. Interestingly, none of the new-found compounds inhibited glutathione reductase, a property that qualified them as potential trypanocides (Galarreta *et al*, 2008).

1.11.4. Polyamine biosynthesis

The polyamine biosynthetic pathway is unique in being the target of the only clinically proven trypanocide with a known mechanism of action (Willert & Phillips, 2008). The trypanocidal activity of the ornithine decarboxylase inhibitor, eflornithine, has validated polyamine biosynthesis as a target for the development of new trypanocides (Taylor *et al*, 2008). Therefore, in addition to ornithine decarboxylase, S-adenosylmethionine decarboxylase and spermidine synthase must also have vital functions in trypanosomes (Fairlamb & Bowman, 1980), which qualifies them as potential targets for the development of chemotherapy, provided they also have unique features for selective inhibition (Wang, 1995). In fact, it has been found that ornithine decarboxylase and S-adenosylmethionine decarboxylase are the most likely rate-limiting steps in polyamine biosynthesis (Willert & Phillips, 2008); hence, both are potential drug targets, since the polyamine, spermidine must be synthesized by this pathway for conjugation to glutathione to form trypanothione (Taylor *et al*, 2008).

1.11.5. The glycosome

The trypanosomes need to switch the variable surface glycoproteins fast enough to escape the host antibody response (Donelson & Rice-Ficht, 1985). Inhibition of any of the glycosomal glycolytic enzymes should therefore block the glycolytic pathway and kill the bloodstream trypanosomes efficiently (Clarkson, Jr. & Brohn, 1976). Furthermore, structural comparison of *T. brucei brucei* glycosomal glyceraldehyde-3-phosphate dehydrogenase (GAPDH) against the homologous human muscle enzyme showed that in the NAD⁺ binding region, amino acid differences that occur between the two enzymes could provide opportunities for the design of selective inhibitors by replacing the 2' and 3' adenosine ribose hydroxyl group with substituents extending in the direction of the changed amino acids (Verlinde *et al*, 1994). It was found that 2'-deoxy-2' (3-methoxybenzamido) adenosine (a derivative of adenosine) inhibited the human GAPDH only marginally, but inhibited the parasite enzyme 45-fold when compared with adenosine (Verlinde *et al*, 1994). Although the efficiency of this inhibitor still needs considerable improvement, and *in vivo* testing against trypanosomes needs to be done, this finding was a positive step towards the design of a new trypanocide (Wang, 1995). The compound, 3 - (diethylphosphono) - propenal, with a K_i of 66 μM for *T. brucei* GAPDH (about 600 times lower than the K_i for the rabbit-muscle enzyme) was reported to be the best inhibitor for the parasite enzyme (Verlinde *et al*, 2001). It was found to kill cultured trypanosomes with a LD_{100} 0.3 μM (Verlinde *et al*, 2001).

Finally, facilitated diffusion system was found to be employed by the bloodstream form of *T. brucei brucei* in the uptake of D-glucose from the blood of the host (Gruenberg *et al*, 1978). This membrane transport process was found to be the rate-limiting step of glucose metabolism in the trypanosomes

(Gruenberg *et al*, 1978;Eisenthal *et al*, 1989). Nevertheless, the uptake process was found to be very fast, apparently to keep pace with the high rate of glucose metabolism in the trypanosomes (Eisenthal *et al*, 1989). Two different glucose transporters were found to be expressed differentially between the bloodstream and the procyclic forms; THT1 (for trypanosome hexose transporter) genes are expressed in the bloodstream forms, while THT2 genes are expressed in the procyclic forms (Bringaud & Baltz, 1993). The glucose transporter system of *T. brucei* also differed from the human transporter in hexose specificity and drug sensitivity; hence the parasite glucose transporter could be a target for chemotherapeutic intervention (Bringaud & Baltz, 1993).

1.11.6. RNA Processing

The rate of transcription during the development of *T. brucei brucei* is not controlled by the employment of specific promoters (Wang, 1995). The promoters for the VSG genes and the gene that codes for procyclin (a major surface antigen of the procyclic forms of *T. brucei brucei*) are mostly constitutive (Pays *et al*, 1990). Therefore, control of the stage-specific expression of VSG and procyclin genes is not carried out at the transcription initiation level, but most probably by interfering with the elongation and stability of the specific transcripts (Pays *et al*, 1990), or the posttranscriptional level (Wang, 1995). Many of the transcription units for protein-encoding genes in trypanosomes are polycistronic, containing tandemly arranged genes with interstitial noncoding spacer regions; thus one of the major roles of *trans* splicing is the production of mature mRNAs from these polycistronic precursors (Agabian, 1990). Furthermore, *trans* splicing serves as the first important step in the regulation of gene expression in trypanosomes (Agabian, 1990). Hence, it has

been proposed that uniqueness and importance of *trans* splicing should make the process an ideal target for the development of new trypanocides (Wang, 1995).

1.11.7. The glycolipid anchor for variant surface glycoprotein (VSG)

The VSG of bloodstream African trypanosomes is attached to the cell surface by a glycosyl phosphatidylinositol (GPI) anchor that contains myristate as its only fatty acid component; hence the trypanosomal VSG differs from mammalian GPI-anchored proteins in containing exclusively myristate (14:0, a fully saturated 14-carbon fatty acid) in its GPI moiety (Ferguson & Cross, 1984). The GPI is synthesized as a precursor, glycolipid A, that is subsequently linked to the VSG polypeptide (Masterson *et al*, 1989). On using a cell-free system for GPI biosynthesis, it was found that a product of the system, glycolipid A' was identical to glycolipid A save for the fact that its fatty acids are more hydrophobic than myristate; glycolipid A' was converted to glycolipid A in the final phase of trypanosome GPI biosynthesis, through highly specific fatty acid remodelling reactions involving deacylation and subsequent reacylation with myristate (Masterson *et al*, 1990). Obstruction of the process of fatty acid remodelling or acyl exchange, or the introduction of an analogue to replace myristate in GPI may result in suppression of the development of the bloodstream form of trypanosomes (Wang, 1995). A study of the utilization of heteroatom-containing analogs of myristate in the biosynthesis of GPI in a cell-free system and in intact trypanosomes showed that the specificity of fatty acid incorporation depends on chain length rather than on hydrophobicity (Doering *et al*, 1991). One of the analogues of myristate, 10-(propoxy)decanoic acid was highly toxic to bloodstream forms of trypanosomes in culture; it had little effect

on cultured procyclic trypanosomes and no effect on mammalian cells (Doering *et al*, 1991).

1.11.8. The proteasome

The proteasome is a multi-subunit proteinase complex that plays a critical role in intracellular protein degradation (Steverding, 2007). The eukaryotic proteasome is a 26S multifunctional proteinase complex composed of the 20S core proteolytic particle and the 19S regulatory complex (Coux *et al*, 1996). The 20S core particle in which the proteolytic activities reside is a barrel-shaped structure made up of four rings; two outer rings consisting of seven distinct α -subunits and two inner rings made up of seven different β -subunits (Steverding, 2007). Three of the β -subunits of each inner ring contain the three major proteolytic activities of the proteasome, commonly referred to as the peptidyl-glutamyl peptide hydrolysing activity, the trypsin-like activity, and the chymotrypsin-like activity located on the β 1, β 2, and β 5 subunits, respectively (Steverding, 2007). The proteasome of *T. brucei* resembles those of mammalian cells structurally (Steverding, 2007), however, the *T. brucei* 20S proteasome appears less complex than that of the mammalian cells as it shows fewer protein spots in two-dimensional gel electrophoresis than its mammalian homologue (Claverol *et al*, 2002).

The substrate specificity of the trypanosomal proteasome differs from that of mammalian cells (Steverding, 2007). Similarly, inhibitor studies show that mammalian proteasome differs from its trypanosomal homologue in its response to inhibitors (Steverding, 2007). For instance, two epoxyketones, epoxomicin [Ac(methyl)-Ile-Ile-Thr-Leu-EX] and YU101 [Ac-homoPhe-Leu-Phe-Leu-EX] were tested and found to inhibit the chymotrypsin-like activity of the rat proteasome much more strongly than that of the trypanosomal proteasome

(Glenn *et al*, 2004). Epoxomicin also inhibited the trypsin-like activity of the trypanosome proteasome very strongly, while YU101 inhibited the same activity rather moderately (Glenn *et al*, 2004). It was therefore suggested that the structure of epoxomicin could be altered to produce a more potent trypanocide with an improved inhibition of the trypsin-like activity of the trypanosomal proteasome (Glenn *et al*, 2004). Using fluorogenic peptides as substrates, the trypanosomal proteasome was found to possess a high trypsin-like but a low chymotrypsin-like activity, while the reverse was found to be the case with the mammalian homologue (Hua *et al*, 1996). This finding suggests that proteasome inhibitors could be designed to specifically target the trypsin-like activity of the trypanosomal proteasome; such new drugs would rarely be toxic to the host cells whose proteasomes have a low trypsin-like activity (Steverding, 2007).

1.11.9. Purine Salvage

A unique biochemical feature of parasitic protozoa is their complete dependence on the salvage of preformed purines from their vertebrate and invertebrate hosts, either in the form of nucleosides or as nucleobases (Landfear *et al*, 2004). The uptake of these purine nucleosides or nucleobases from the host system has been identified as the first step in the salvage pathway, and is carried out by various nucleoside or nucleobase transporters located in the plasma membrane of the parasite (Landfear *et al*, 2004). All the protozoan nucleoside and nucleobase transporters that have been identified were grouped as members of the equilibrative nucleoside transporter (ENT) family (Landfear *et al*, 2004). The interest in purine transport arose from the fact that purine salvage has been found to be essential to the survival of the parasites, and because purine transporters mediate the uptake into the parasites, of a range of cytotoxic drugs, many of which are purine analogues (Carter *et al*, 1995).

Twelve transporters of the ENT family (designated TbAT1 and TbNT2 - TbNT12) are expressed by the parasite (Ortiz *et al*, 2009). The TbAT1 gene was found to encode the transport activity previously designated as P2 (Mäser *et al*, 1999), which was originally found to transport adenosine and adenine into the intact bloodstream form (TbAT1 is actually bloodstream form-specific) of the parasite (Carter & Fairlamb, 1993). This implies that pentamidine transport may be mediated by 5 different transporters (TbAT1, HAPT1, LAPT1, TbNT11.1 and TbNT12.1) in the bloodstream form, unless future studies prove that HAPT1 and LAPT1 are identical to TbNT11.1 and TbNT12.1, respectively (Ortiz *et al*, 2009). TbNT2 - TbNT7 are P1 type nucleoside transporters; TbNT2, TbNT5, TbNT6 and TbNT7 were found to be high affinity adenosine/inosine transporters (with K_m values $<5\mu\text{M}$), while TbNT5, and to a lesser extent TbNT6 and TbNT7 also mediate the transport of hypoxanthine (Sanchez *et al*, 2002). Ribonuclease protection assays showed that TbNT2 - TbNT7 are all expressed in the bloodstream form *T. brucei*, while the TbNT2 and TbNT5 genes are also expressed in the procyclic form (Sanchez *et al*, 2002).

The procyclic form of *T. b. brucei* was found to express one high affinity purine specific nucleobase transporter (H1), which was described as a nucleobase/proton symporter (de Koning & Jarvis, 1997a). The second procyclic purine nucleobase transporter (TbNBT1 or H4) however lacks this specificity but exhibits a high affinity for all natural purine nucleobases as well as uracil, guanosine and allopurinol (Burchmore *et al*, 2003). Similarly, in the bloodstream form, two transporters for hypoxanthine, described as guanosine-sensitive (H2) and guanosine-insensitive (H3), were found (de Koning & Jarvis, 1997b). H2 was shown to be a proton/hypoxanthine symporter capable of transporting guanosine

and some pyrimidine bases, while H3 showed high affinity and selectivity for purine nucleobases only (de Koning & Jarvis, 1997b).

It is quite clear from the above that the bloodstream form of *T. brucei*, like other protozoa, expresses multiple purine transporters with overlapping substrate specificities (de Koning *et al*, 2005). The implication is that it would be very difficult to starve the trypanosomes of purines by inhibiting all these transporters (Luscher *et al*, 2007), since trypanosomes have been found to react to purine starvation by up-regulation of their purine transporters, and by expression of higher-affinity permeases (de Koning, 2001b). It may however be useful to consider designing nucleobase or nucleoside analogues that will only be recognized by the parasitic enzymes, and whose nucleotide products will turn out poisonous to the parasite (Wang, 1995).

Quite a number of enzymes in the purine salvage pathway can also be selectively inhibited by use of specific analogues (El Kouni, 2003). For instance, phosphoribosyltransferases play an important role in purine salvage in most parasites, and are therefore considered as targets for drug design (El Kouni, 2003). More importantly, xanthine is a substrate for parasitic purine phosphoribosyltransferases, but not for the mammalian host enzyme (Reyes *et al*, 1982). Hence, xanthine analogues may be employed to inhibit the parasitic phosphoribosyltransferases selectively in order to interfere with purine salvage in the parasite but not the host (El Kouni, 2003). The effect of this interference will be potentiated by the common lack of *de novo* purine biosynthesis in the parasites (El Kouni, 2003). In cases where the parasite can salvage the purines using other enzymes (for instance, the kinase reaction), then the introduction of xanthine analogues as “subversive substrates”, which would be activated to

toxic nucleotides only in the parasite, may be preferable to inhibitors of specific salvage enzymes (El Kouni, 2003).

1.11.10. The Kinetoplast

The existence of dyskinetoplastic or akinetoplastic trypanosomes tends to suggest that kDNA is not essential for viability of BSFs and therefore would not be a drug target (Roy Chowdhury *et al*, 2010). Results of some other studies however indicate that RNA editing proteins and the A6 subunit of ATP synthase, are essential in BSF trypanosomes (Schnauffer *et al*, 2005), and since the compensating mutation (described in 1.5.2) occurs at a low frequency, kinetoplast DNA and proteins involved in its replication and expression should be valid drug targets in bloodstream forms (Roy Chowdhury *et al*, 2010).

1.11.11. The Trypanosome Alternative oxidase

Since trypanosomes lack lactate dehydrogenase (Wang, 1995), the NADH produced in the glycosomal glycolytic pathway must be reoxidized via a dihydroxyacetone phosphate (DHAP) α -glycerophosphate (α -GP) shuttle which consists of a glycosomal NAD⁺-dependent α -GP dehydrogenase and a mitochondrial α -GP oxidase (Visser & Opperdoes, 1980). The oxidase cannot function under anaerobic conditions, causing α -GP, NADH, and ADP to accumulate to high concentrations in the glycosome; these accumulated metabolites can inhibit the glycerol kinase (GK)-catalyzed conversion of the accumulated α -GP and ADP to glycerol and ATP (Visser & Opperdoes, 1980). Also, α -GP oxidase can be inhibited by salicylhydroxamic acid (SHAM) to bring *T. brucei brucei* to a condition similar to anaerobiosis; glycolysis can then be completely blocked under this condition by inhibiting the GK-catalyzed reversible reaction with glycerol, with the resultant lysis of the trypanosomes within minutes (Clarkson, Jr. & Bohn, 1976). Mice infected with *T. b.*

rhodesiense were completely cured 24 hours after injection with a combination of SHAM and glycerol. The parasites however reappeared in the blood of the mice, and killed them a few days later; an occurrence attributed to either the existence of a few resistance cells in the initial parasite population, or the failure to reach the effective trypanocidal levels of SHAM and glycerol in some tissues, resulting in survival of parasites in those tissues (Clarkson, Jr. & Bohn, 1976).

1.12. Mechanisms of resistance to trypanocides

Resistance is the inheritable, temporary or permanent loss of the original sensitivity of a microbial population to a drug; resistance is not usually absolute since resistant parasites can still be eliminated at much higher drug dosages, but this concentration may be harmful to the host (Matovu *et al*, 2001). Management practice and the nature of the drug are both important factors in the induction of resistance. For instance, it is believed that the nature of ethidium bromide as a potent mutagen may enhance selection for resistance (Matovu *et al*, 2001). Block treatment is a traditional management practice used in the control of nagana; this practice has increased the magnitude of the resistance problem in nagana when compared to human trypanosomiasis where hospitalization aids adequate drug administration (Matovu *et al*, 2001). Hence drug resistant trypanosomes from animals are far more prevalent in Africa (Matovu *et al*, 2001).

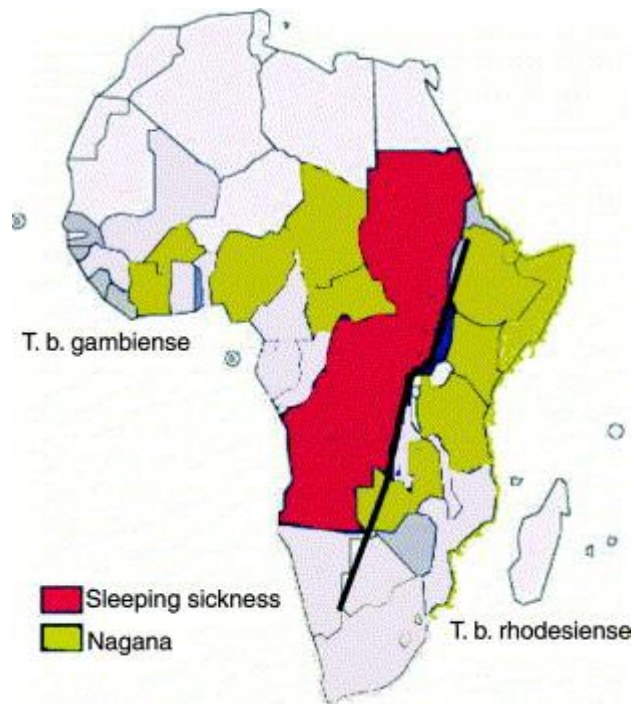


Figure 1.9 The distribution of trypanocidal resistance in sub-Saharan Africa. Taken from Matovu *et al.*, 2001.

Studies have shown that drugs must enter the interior of the cell in sufficient quantities in order to kill the parasite (Matovu *et al*, 2001). Sutherland and his co-workers (1992) proposed an inverse relationship between ISM uptake by trypanosomes and resistance, in which an increase in resistance by parasites could be attributed to a reduction in drug accumulation caused by a change in a specific cell-surface receptor or transporter and/or the involvement of a drug efflux mechanism (Sutherland *et al*, 1992). It is generally accepted that drug accumulation differs between ISM-sensitive and ISM-resistant trypanosomes, with reduced net drug uptake enhancing the survival of the latter in the presence of drug concentrations which are lethal to the sensitive parasites (Matovu *et al*, 2001). This was shown to be true by studies in which sensitive and resistant *T. b. rhodesiense* were cultured in medium with tryparsamide, followed by bioassay of supernatants against sensitive trypanosomes. It was found that supernatants in which resistant parasites had been incubated was still able to kill susceptible trypanosomes, indicating that the former had not absorbed any appreciable

quantity of the drug from the medium (Matovu *et al*, 2001). The implication of this model is that the loss of a particular membrane transporter involved in the uptake of trypanocides would cause the cross-resistance to the drugs it transports; for instance, the loss of the P2 transporter causes a cross-resistance between melarsoprol and diminazene aceturate (Delespaux & de Koning, 2007). It is therefore not safe to introduce diminazene aceturate for human use since it could cause an increase in resistance to melarsoprol, the only approved drug for late stage sleeping sickness (Delespaux & de Koning, 2007).

Reduction of net drug uptake could be as a result of either decreased drug import or increased drug export (Mäser *et al*, 2003). The transporters usually involved in the export of drugs are those of the ABC superfamily; large membrane proteins with two ATP-binding cassettes per transporter (Mäser *et al*, 2003). The best known members of this superfamily are the P-glycoproteins that function in the elimination of foreign molecules from the cell (Upcroft, 1994), and are therefore useful in the active detoxication of the cytosol (Matovu *et al*, 2001). Three ABC transporter genes were identified in *T. brucei*: TbMRPA, TbABC2, and TbABC3; and all three were found to be expressed in both the bloodstream and the procyclic forms (Mäser & Kaminsky, 1998). TbMRPA has been localized to the plasma membrane in the bloodstream form of *T. b. brucei* (Shahi *et al*, 2002), and an over-expression of TbMRPA in trypanosomes was found to increase resistance to melarsoprol (Shahi *et al*, 2002). It was nevertheless proposed that of the three possible mechanisms of resistance to arsenicals and antimonial drugs (loss of uptake, failure to activate the drug and active extrusion), the only mechanism relevant to anti trypanosomal drugs concerns the loss of uptake (Shahi *et al*, 2002). Alternative mechanisms of resistance, such as failure to undergo apoptosis (as triggered by the

trypanocide), have been suggested (Mäser *et al*, 2003). These different possible mechanisms are however not mutually exclusive, and may complement each other to produce high levels of resistance (Mäser *et al*, 2003).

1.13. Plans for the PhD project

ISM is the only recommended prophylactic drug, and is widely used in the treatment of, and protection against, trypanosome infections in cattle and small ruminants across sub-Saharan Africa (Afework *et al*, 2006). Resistance to ISM usually goes with cross-resistance to ethidium bromide (Peregrine *et al*, 1997), and since diminazene aceturate is employed for curative purposes only, as it is cleared too rapidly to give longer-term protection (Delespaux *et al*, 2008), resistance to ISM is a serious problem in many parts of sub-Saharan Africa (Afework *et al*, 2006).

Probably, the main cause of drug resistance in African trypanosomes is changes to specific transporters in the plasma membrane that are responsible for the internalisation of the drug (Bray *et al*, 2003). Therefore, the presence of a mutation in the nucleotide transporter gene, TbAT1 in *T. b. brucei* was linked to ISM resistance (Afework *et al*, 2006). However, LAPT1 has been identified as the resistance marker for EtBr and ISM, with the TbNT2/P1, TbAT1/P2 and HAPT1 transporters making minor contributions to the transport of both drugs (Dietrich and De Koning, unpublished). Certainty about this has been hampered by lack of specific inhibitors for the diamidine transporters, and LAPT in particular. This project therefore aims:

- i. to identify specific inhibitors of the LAPT1 transporter;
- ii. to identify the transporter of ISM in *T. b. brucei* at the biochemical and molecular level;

- iii. to determine the mechanism of resistance to ISM in *T. b. brucei*.

2. Materials and Methods

2.1 Materials.

2.1.1 In vitro culture of bloodstream forms (BSF) of *T. b. brucei*, transformed yeasts and other cells.

HMI-9 powder was purchased from Invitrogen, heat-inactivated fetal calf serum was from PAA laboratories, Austria while NaHCO₃ was purchased from BDH. β-mercaptoethanol was a product of Sigma. For the synthetic complete medium minus uracil, D-glucose was purchased from Fisher Scientific while yeast nitrogen base without amino acids was bought from Sigma. The amino acids for the synthetic complete drop out mix were all purchased from Sigma; while the Bacto-agar was bought from BD. Peptone for the yeast extract-peptone-dextrose and adenine medium (YPAD) was supplied by Formedium Ltd., England, while the yeast extract was a product of Sigma. HOMEM for culturing *Leishmania promastigotes* was purchased from Life technologies corporation, U.K.

2.1.2 Induction of resistance to isometamidium and ethidium bromide in bloodstream forms of *T. b. brucei*.

Isometamidium used throughout this project was in the form of Samorin donated by Merial, while Ethidium bromide was supplied by Sigma. Stock solutions of these and most other drugs used in this project were made in dimethyl sulfoxide (DMSO) purchased from Sigma.

2.1.3 Alamar blue and propidium iodide drug sensitivity assays

Resazurin sodium salt and propidium iodide were both purchased from Sigma, so also was digitonin. The library of bisphosphonium compounds were synthesized by our collaborator, Dr. Christophe Dardonville of Instituto de

Quimica Medica, Spain, while the RT compounds were synthesized by Dr Richard Tidwell of the University of North Carolina, Chapel Hill, USA.

2.1.4 In vitro uptake of isometamidium and [³H]-pentamidine

[³H]-Pentamidine isethionate was supplied by Amersham, and contains 3.26 TBq/mmol. Unlabelled pentamidine isethionate was however purchased from Sigma. The constituents of the assay buffer were purchased as follows: Hepes, NaCl, KCl, NaHCO₃, MgCl₂·6H₂O, MgSO₄·7H₂O were supplied by BDH, NaH₂PO₄·2H₂O by MERCK, while CaCl₂·2H₂O and MOPS were purchased from Sigma. Mineral oil, di-*n*-butylphthalate and SDS were produced by Sigma, while the Optiphase 'Hisafe' 2 scintillation fluid was supplied by Perkin Elmer.

2.1.5 Site-directed mutagenesis of genes of interest.

Pfu Turbo DNA polymerase was purchased from Stratagene while Dpn I restriction enzyme was produced by Promega.

2.1.6 Transfection of *T. b. brucei* (BSF), yeasts and *Leishmania mexicana*

Go Taq polymerase and the dNTPs were bought from Promega, while the Luria broth (LB) media and Luria broth agar were supplied by Sigma. The primers used in this project were all synthesized either by Sigma or by Eurofins MWG Operon. Phusion high fidelity polymerase was produced by New England Biolabs while the ultra pure agarose used was supplied by Invitrogen. The Lithium acetate, polyethyleneglycol and ethylenediaminetetraacetic acid (EDTA) used for yeast transformation were supplied by Sigma while the Tris-HCl was produced by MP Bio medicals, Germany.

2.1.7 Sequencing of genes of interest.

pGEM-T Easy vector was purchased from Promega, while the plasmid extraction and gel extraction kits were bought from Macherey-Nagel. The competent XL1 strains of *Escherichia coli* were purchased from Stratagene initially, but were subsequently prepared in-house using the calcium chloride method (Sambrook & Russell, 2001).

2.1.8 Mitochondrial membrane potential Assays.

Phosphate buffered saline (PBS) was supplied in tablet form by Sigma. Other reagents used namely, tetramethylrhodamine ethyl ester (TMRE), valinomycin and Troglitazone were also produced by Sigma.

2.1.9 Fluorescence microscopy

Methanol was purchased from Fisher Scientific while vectashield mounting medium (containing 4',6-Diamidino-2-phenylindole dihydrochloride, DAPI) was supplied by Vector Laboratories, U. S. A.

2.2 Methods

2.2.1 In vitro culture of bloodstream forms (BSF) of *T. b. brucei*, transformed yeasts and other cells.

Five different published strains of *T. b. brucei* (BSF) were used in this project namely, 1) *Trypanosoma brucei brucei* 427 wild type from which the following other strains were derived; 2) TbAT1/P2 knock out (KO) was derived from *T. b. b.* 427 wt by sequential replacement of both alleles of TbAT1 gene with resistance markers for the antibiotics neomycin and puromycin (Matovu *et al*, 2003); 3) TbAT1-KO B48 was derived from TbAT1-KO by selection in increasing pentamidine concentrations until these cells also lost the high affinity

pentamidium transporter, HAPT1 (Bridges *et al*, 2007); 4) 2T1 cells were derived from *T.b.b.427* wt by the incorporation of a T7 RNA polymerase driven by an inducible ribosomal RNA; 2T1 also displays an improved transfection efficiency compared to *T.b.427* wt (Alsford *et al*, 2005); 5) RNAi of ATE1 in 2T1 cells was performed by transfecting with the plasmid, pHDK02 to knock down the expression of ATE1 gene (Teka, 2011). These trypanosome strains were all maintained *in vitro* in HMI-9 medium (Hirumi & Hirumi, 1989) containing 10% fetal calf serum (FCS) and 14.3 µl of β-mercaptoethanol per litre at pH 7.4. The parasites were incubated at 37 °C under 5% CO₂ and sub-cultured every 48 hours.

The *Saccharomyces cerevisiae* strain MG887-1 (*fcy2-*) used in this project was made to be auxotrophic for uracil by Gillissen and colleagues by the excision of truncated URA3 gene with *EcoRI* and *SmaI* from pΔura3 (Gillissen *et al*, 2000). *S. cerevisiae* MG887-1 was grown on solid YPAD medium plates (see Appendix A) at 30 °C and sub-cultured to a fresh plate once a week. Transformed *S. cerevisiae* MG887-1 was plated on synthetic complete medium minus uracil (see Appendix A).

Leishmania mexicana (*L. mexicana*) promastigotes (M379) were grown in HOMEM medium (pH 7.4) supplemented with 10% heat-inactivated fetal calf serum (FCS) at 27 °C. Cultures were passaged into fresh medium twice weekly.

Competent XL1 strains of *Escherichia coli*, used for cloning of *T. b. brucei* genes of interest after they have been subcloned into the appropriate plasmid vectors, were stored as glycerol stabilates at -80 °C. After transformation, XL1 cells were cultured overnight in LB broth containing 100 µg/ml ampicillin at 37 °C.

Stabilates were regularly prepared from all parasitic strains used in this project for long term storage. Cell cultures of density between 10⁶ and 2 x 10⁶

were diluted in a 1:1 proportion by a 30% glycerol mixture in the corresponding culture medium, thus ending up with cells in a 15% glycerol/media mix. 1 ml aliquots of this mix was transferred into properly labelled cryo vials and kept at -80 °C for at least 24 hours before transferring to liquid N₂ storage.

Cells from stabilates were returned to culture by thawing at room temperature. The entire 1 ml of thawed stabilate was added to 10 ml of warm medium, incubated on the appropriate incubator and passaged the next day or as necessary.

2.2.2 Induction of resistance to isometamidium and ethidium bromide in blood stream forms of *Trypanosoma brucei brucei*.

Induction of resistance to ISM or EtBr in *Tb427* wt was started from a concentration of 0.05 nM for either drug in complete HMI-9 media after this concentration was arrived at using halving dilutions in 96-well plates to determine the concentration at which trypanosomes can survive in the drug. This halving dilution for the determination of start concentration was done with ISM alone, starting from its IC₅₀ of 23.4 nM, since the IC₅₀ of ISM is much lower than that of EtBr. Trypanosomes were incubated in the drug-containing media, while the concentration of each drug was slowly increased; the ISM concentration was increased to 1 µM before the first set of clones was selected by plating out (designated ISMR1). Similarly, the EtBr concentration was raised to 4 µM before individual clones were generated. These were named EBR4. ISMR clones were generated as ISM concentration was raised until the last set of clones were generated from 15 µM ISM and was named ISMR15.

2.2.3 Alamar blue and propidium iodide drug sensitivity assays.

Alamar blue end point assays were used to estimate the cytotoxicity of drugs and potential drugs candidates to parasitic cells *in vitro* (Räz *et al*, 1997). Viable parasites are able to reduce the dye (converting resazurin to the fluorescent resorufin) to the fluorescent metabolite which is measured. Since a linear correlation exists between the strength of the fluorescence and the density of viable cells (Räz *et al*, 1997), the amount of living cells can be estimated from the fluorescence values. Sigmoidal dose-response curves with variable slopes were generated using the GraphPad Prism software to plot the fluorescence values against the logarithm of drug concentration, and the EC₅₀ values (effective concentration that inhibits growth by 50%) were estimated automatically.

Alamar blue dye was prepared by dissolving 12.5 mg of Resazurin sodium salt in 100 ml of phosphate buffered saline (PBS) at pH 7.4. The mixture was filter-sterilized and stored at -20 °C in foil-wrapped tubes to shield from exposure to light. Test compounds were diluted to 200 µM in the corresponding medium, starting from a 20 mM stock solution in DMSO (water or ethanol if the compound is insoluble in DMSO). 200 µl of this solution was added to the first well of the 96-well plate, while 100 µl of fresh medium was added to the remaining wells. Halving dilution was done by taking 100 µl from the first well into the second, mixing well by pipetting up and down several times before moving 100 µl from the second to the third well, and so on. The last well was left drug-free. 100 µl of 2×10^5 cells (trypanosomes) or 2×10^6 cells (leishmania) was introduced to all wells, giving a final concentration of 100 µM in the first wells and 10^5 cells (trypanosomes) in all wells. 20 µl of alamar blue dye was

added to all wells after incubating at 37 °C and 5% CO₂ for 48 hours, and the plate was read 24 hours later in the Fluostar Optima at 530 nm and 590 nm, excitation and emission respectively. For *Leishmania* promastigotes, the dye was added after 72 hours from the start of the assay, and the plate was read 48 hours after. A modified alamar blue assay was employed to magnify the difference in ISM sensitivity between *Tb427* wt and *Tb427* wt cells expressing mutated ATPase γ gene. In the modified assay, 5×10^3 cells/ml final cell density was used, and the assay was incubated at 37°C and 5% CO₂ for 72 hours before addition of alamar blue dye, and the plates were read 18 hours after.

Propidium iodide real time assay measures fluorescence over 250 cycles (8 hours) and was used to estimate how quickly a drug kills trypanosomes. Propidium iodide binds to nucleic acids to produce fluorescence, and this happens when the test agent causes the cell to lyse. 500 μ M of each drug was prepared in HMI-9 medium and 200 μ l of it introduced into the first wells. Halving dilutions were performed, as in alamar blue, up till the 9th wells while 100 μ l of 40 μ M digitonin in HMI-9 (positive control) was added to the 10th. 100 μ l of fresh media was added to the 11th wells while the addition of 200 μ l of 5×10^6 cells was alternated with 200 μ l of fresh media on the last column. Two rows were prepared for each drug as described above; 100 μ l of 10^7 cells in 18 μ M propidium iodide was introduced into the first 11 wells of the first row (the 12th already contains 200 μ l 5×10^6 cells/ml in HMI-9). 18 μ M propidium iodide in HMI-9 was also added to the first 11 wells of the 2nd row for the same drug (the 12th already holds 200 μ l of HMI-9 medium). Hence, the final concentrations of each drug were from 250 μ M to 0.98 μ M, 9 μ M of propidium iodide and 5×10^6 cells/ml. Plates were then read in the plate mode using the Fluostar Optima

(BMG Labtech) at 544 nm and 620 nm, excitation and emission respectively. EC50 values were subsequently determined using the prism software.

2.2.4 Harvesting and purification of cells for uptake assays

Trypanosome cultures of between 300 ml and 600 ml were set up in order to achieve the cell density of the order of 10^8 cells/ml needed for uptake assays. After 48 hours of incubation (in HMI-9, at 37 °C and 5% CO₂), parasites were harvested while in the mid-log phase of growth by centrifugation at 1100 x g for 10 min, followed by a double wash in assay buffer (pH 7.3) before a final resuspension and adjustment of density to $\sim 10^8$ cells/ml in assay buffer. Cells were usually left for 20 - 30 minutes on the bench (with intermittent gentle shaking) before use to allow them to adapt to the conditions of the experiment. *Leishmania* cells for uptake were grown up in cultures of between 150 ml and 300 ml, and were harvested in much the same way as for trypanosomes, after 72 hours of incubation.

Yeast culture for uptake was initiated as a starter culture in 5 ml synthetic complete medium minus uracil (SC-URA) which was incubated for 6 hours at 30 °C in a shaker-incubator before the addition of an extra 45 ml of the same medium followed by incubation overnight. Cells were harvested by centrifugation at 1100 x g for 10 minutes at 4 °C, followed by a double wash of the pellet in assay buffer (without glucose). The cells were then re-suspended in assay buffer at a density of about 10^8 cells/ml, and the cell suspension divided in three tubes which were kept on ice. Each tube was used for one set of triplicates after being left on the bench for 15 minutes to return to room temperature.

2.2.5 In vitro uptake of isometamidium, [³H] pentamidine and [³H] diminazene.

Uptake of ISM was monitored using the innate fluorescence as described for DB829, other diamidines and ethidium bromide (Ward *et al*, 2010). A 20 μM solution of ISM was prepared in the appropriate medium, and 100 μl of this solution was layered on 100 μl of oil mix (1:7 mixture of light mineral oil and di-*n*-butylphthalate) in a microfuge tube and mixed with 100 μl of trypanosome suspension in the same media. This mixture was incubated on the bench for the appropriate time before uptake was stopped by centrifugation at 12500 \times g for 1 min. The oil and media were carefully removed with a 200 μl pipette tip attached to a vacuum pump before incubation of pellet in 50 μl (1:8) 0.1N HCl/methanol buffer for 1hr at room temp. Fluorescence was thereafter measured in the Fluostar Optima at 355 nm and 620 nm, excitation and emission respectively (Wilkes *et al*, 1995).

Assay for the uptake of [³H]-pentamidine and [³H]-diminazene was carried out using the general uptake assay technique as described by De Koning (2001b). The concentration of the permeants was adjusted to suit the affinity of the transporter of interest for the particular permeant. For instance, HAPT1 with a K_m value of 36 ± 6 nM (De Koning, 2001b) is fully saturated by 1 μM of permeant; hence HAPT1-mediated uptake was usually measured using 30 nM [³H] permeant concentrations or less. On the other hand, LAPT1 with a K_m value of 56 ± 8 μM (De Koning, 2001b) requires millimolar concentrations to saturate, and so LAPT1-mediated uptake was usually measured at 1 μM [³H] permeant concentrations. When HAPT1 activity was studied in s427 wt, 1 mM unlabelled adenosine was usually added to saturate the P2 transporter (Bridges *et al*, 2007). All uptake assays were performed in triplicate and all parameters were determined

independently at least three times unless stated otherwise. 100 μl of [^3H] permeant solution (containing 2 x the desired permeant concentration in assay buffer) was layered on 300 μl of oil mix in a microfuge tube. Uptake assays were then initiated by adding 100 μl of cell suspension at $\sim 10^8$ cells/ml, followed by incubation on the bench for a pre-determined time. Uptake was stopped by the addition of 1 ml of 1 mM unlabelled permeant in assay buffer and subsequent centrifugation at 12500 x g for 45 seconds. The tubes were then flash frozen in liquid nitrogen and the bottom (containing the cell pellet) cut off and collected in numbered scintillation vials containing 300 μl of 2% sodium dodecyl sulphate (SDS). Vials were incubated at room temperature for 30 minutes to solubilise the pellets before the addition of 3 ml Optiphase 'Hisafe' 2 scintillation fluid. Scintillation count was determined on the 1450 Microbeta Liquid Scintillation and Luminescence Counter (PerkinElmer Lifesciences) after an overnight incubation at room temperature.

2.2.6 Molecular procedures utilized

2.2.6.1 Genomic DNA extraction

Genomic DNA extraction for polymerase chain reaction (PCR) was done using the Nucleospin tissue kit (Macherey-Nagel) and the standard protocol for human or animal tissue and cultured cells. DNA concentrations were measured on the NanoDrop ND 1000 spectrophotometer, and DNA samples were stored at -20°C .

2.2.6.2 Primer design

The primers were designed to flank the gene of interest, one complementary to the sequence upstream of the 5' end and the other complementary to the sequence downstream of the 3' end. Primers may be

designed to incorporate restriction sites when it will subsequently be ligated into a specific vector. Whenever possible, primer sequences were designed to have between 50 to 60% GC content and to have a G or C at both ends.

Primers for site-directed mutagenesis PCR were designed to be complementary to each other so they could anneal to the opposite strands of the sequence of interest. They were designed to be between 25 and 45 nucleotides in length with the desired mutation in the middle and about 10 to 15 nucleotides of correct sequence on both sides. They were also designed to begin and end in C or G nucleotides and to have at least 40% GC content.

Primer use	Primer sequence	Fragment size
TbAT-1 forward. TbAT-1 reverse	5'-CTCGAGATGCTCGGGTTTGA ^{CT} CA-3' 5'-GGATCCCTACTTGGGAAGCCCCTC3-'	1404 bp
Forward,ATE Reverse,ATE	5'-GCCGTTGTGTGGGGTGTC 5'-TATTAGCGCCATCCCGCC	~750 bp
TbATA forward. TbATA reverse	5'-ACTCAAAGGTGTGCTGGCTG-3' 5'-CGGCGGTGTCAAATCCAAG-3'	1500 bp

ATPase Forward	γ 5'CGGCGGCCGCATGTCAGGTAACTTCGTCTTTACAAAG	937 bp
ATPase Reverse	γ 5'-ATAGGATCCCTACTTGGTTACTGCCCTTCCCAG	
Fwd: ATPase γ mutagenesis	5'-CTTTCTGCTATGAGTTAGTTGGAGGCAATGCG-3'	5567 bp
Rev: ATPase γ mutagenesis	5'CGCATTGCCTTCCAACCTAACTCATAGCAGAAAG-3'	
A6 Forward	5'-AAAAATAAGTATTTTGATATTATTAAAG-3'	381 bp
A6 Reverse	5'-TATTATTA ACTTATTTGATC-3'	
ND4 Forward	5'-TGTGTGACTACCAGAGAT-3'	256 bp
ND4 Reverse	5'-ATCCTATACCCGTGTGTA-3'	
ND5 Forward	5'-TGGGTTTATATCAGGTTTATTTATG-3'	395 bp
ND5 Reverse	5- CCCTAATAATCTCATCCGCAGTACG-3'	
ND7 Forward	5'-ATGACTACATGATAAGTA-3'	161 bp
ND7 Reverse	5'- CGGAAGACATTGTTCTACAC-3'	

<p>Forward: Actin</p> <p>Reverse: Actin</p>	<p>5'-CCGAGTCACACAACGT-3'</p> <p>5'-CCACCTGCATAACATTG-3'</p>	<p>456 bp</p>
<p>Fwd: TbAT1 Screen in yeast</p> <p>Rev: TbAT1 Screen in yeast</p>	<p>5'-CTCGAGATGCTCGGGTTTGA CTCA-3'</p> <p>5'-CATCGCCTCCGTGGGGGTC-3'</p>	<p>789 bp</p>
<p>Fwd: pDR195 screen in yeast, REF: TbAT1</p> <p>Rev: pDR195 screen in yeast, REF: TbAT1</p>	<p>5'-GCGGCATTTTGCCTTCCTGT-3'</p> <p>5'-CCAATGCTTAATCAGTGAGGCACC-3'</p>	<p>815 bp</p>
<p>Fwd: ATA-1, ATA-6 screen in yeast</p> <p>Rev: ATA-1, ATA-6 screen in yeast</p>	<p>5'-GGATGCTTGGCTTCGGTTCT-3'</p> <p>5'CTGTGACTCATCTTTCGGGA-3'</p>	<p>1404 bp</p>

<p>Fwd: pDR195 screen in yeast, REF: ATA1, ATA6.</p> <p>Rev: pDR195 screen in yeast, REF: ATA1, ATA6.</p>	<p>5'-CGTAGAACCAGCCGCACA-3'</p> <p>5'-AAAGGGGGATGTGCTGCAAG-3'</p>	<p>1780 bp</p>
<p>Fwd: pDR195 screen in yeast, REF: ATE1, ATE2.</p> <p>Rev: pDR195 screen in yeast, REF: ATE1, ATE2.</p>	<p>5'-GCGGCATTTTGCCTTCCTGT</p> <p>5'-CCAATGCTTAATCAGTGAGGCACC</p>	<p>~810 bp</p>

Table 2.1 List of primers used in this project. Restriction endonuclease recognition sequences and mutated nucleotides are shown in colour.

2.2.6.3 Polymerase chain reactions (PCR)

PCR was employed in the amplification of DNA sequences for various purposes in the course of this project work. Go Taq polymerase was used for routine PCR screening, Phusion polymerase was employed when high fidelity amplification was necessary and *Pfu Turbo* DNA polymerase (QuickChange Site-Directed mutagenesis kit) was used for the site-directed mutagenesis. The

thermal cycler used was a product of G-STORM. PCR with Go Taq polymerase was done using 1 unit of the enzyme in 20 μ l, and following the manufacturer's instruction. Similarly, PCR with Phusion polymerase was done using 1 unit of Phusion DNA polymerase in 50 μ l of PCR reaction, also following the manufacturer's instruction.

2.2.6.4 Site-directed mutagenesis

The endogenous replacement construct for the site-directed mutagenesis of ATPase γ was based on the pEnT6-GFP tagging plasmids generated by Kelly et al, (2007), and the wildtype ATP synthase gamma version of the construct was generated and supplied by Matt Gould and Achim Schnauer (University of Edinburgh). PCR primers were designed to amplify the WT ATP synthase gamma gene from genomic DNA, with a NotI-recognition sequence immediately 5' and a BamHI-recognition sequence immediately 3' of the open reading frame. A 260 bp region of the ATP synthase gamma 3' Untranslated Region (UTR) was also amplified with HindIII and NotI recognition sequences at the 5' and 3' ends, respectively. The pEnT6B-GFP vector (B means blast) was restriction enzyme digested with HindIII and BamHI to remove the GFP and TY tag sequence. The PCR products were also digested with their respective restriction enzymes and ligated in a single reaction into the pEnT6-Blast vector backbone to give one circular plasmid.

Templates for site-directed mutagenesis were supercoiled double stranded DNA plasmids bearing the gene of interest. The desired mutation was incorporated in the primers, so that the PCR replicates the plasmid to carry the mutation. The non-mutated parental DNA templates were sourced from *Escherichia coli* and were therefore methylated. PCR for site-directed

mutagenesis was done with 2.5 units of Pfu Turbo DNA polymerase in 50 µl of PCR reaction, following the manufacturer's instruction.

Dpn I was thereafter employed to selectively digest the methylated template plasmids as follows: 10 units of *Dpn*I restriction enzyme and 10 µl Promega buffer B were added to the above PCR product which was then pipetted up and down to mix and centrifuged for a few seconds before it was incubated at 37 °C for 1 hour. The mutated, circular, nicked double-stranded DNA plasmid was subsequently transformed into XL1 blue *E. coli* as described below in 2.2.6.5. Transformed *E. coli* cells were plated out on ampicillin-containing agar plates (100 µg/ml ampicillin) and incubated overnight at 37 °C. Next day, colonies were selected, streaked on fresh ampicillin-containing agar plates (numbered and incubated at 37 °C overnight) while the residual bacteria on the tips were used to grow up overnight cultures on a 37 °C shaker. Cultures were minipreped using the Nucleospin plasmid kit from Macherey-Nagel, and plasmid concentration measured on the Nano-drop spectrophotometer. The plasmids were then sent for sequencing to check for the presence of the desired mutation. Sequencing was done by Eurofins MWG, and a colony bearing plasmids with the desired mutation was grown up in ampicillin-containing LB broth, overnight on a 37 °C shaker. Mutated plasmids were extracted the next day and used for the transfection of trypanosomes as described below in section 2.2.7.1. The pEnT6B-GFP vector was linearized with NotI to enhance integration into the trypanosome genome. The linearized plasmid was purified using the Nucleospin PCR clean up kit from Macherey-Nagel, and concentrated using the ethanol precipitation method as follows: Twice the volume of 100% ethanol and 0.1 times volume of 3 M NaCl were added to the DNA solution and mixed. DNA appeared as a white fluff and was removed to a new tube with a pipette tip,

washed twice in 1ml 70% ethanol, air-dried and re-suspended in a suitable volume of sterile distilled water.

2.2.6.5 Generation of a TbAT-1 yeast expression vector.

2.2.6.5.1 Copying of gene of interest and sub-cloning into pGEMT.

The primers for 3' and 5' ends of TbAT-1 were designed to incorporate a *Bam*HI restriction enzyme site and an *Xho*I site respectively, to facilitate the insertion of the gene into the final vector. The PCR reaction was done using the Phusion DNA polymerase, and the PCR product was A-tailed to facilitate insertion into the pGEMT Easy vector, as follows: 1 µl 10 mM dATP, 10 µl Go Taq reaction buffer and 1 unit of Go Taq polymerase were added to the PCR product and incubated at 72°C for 15 minutes. Loading dye was then added to the reaction and it was separated on an agarose gel electrophoresis, using 1% agarose gel and visualized with SYBR safe. The correct band (1404 base pairs) was identified under ultraviolet light, cut out and purified using the Macherey-Nagel gel and PCR purification kit. Purified DNA was sub-cloned into pGEMT easy vector as follows: 5 µl 2 x buffer, 3 units of T4 ligase and 0.5 µl pGEM-T vector were added to 3.5 µl gel-extracted DNA and incubated for 1 hour at room temperature.

2.2.6.5.2 Transformation into competent *E. coli* cells.

TbAT-1 in the pGEMT vector was transformed into XL1-blue *E. coli* as follows: An aliquot of XL1-blue *E. coli* was defrosted on ice; 5 µl of TbAT1 ligation in pGEMT was put in an eppendorf tube followed by 50 µl of XL1-blue cells; the transformation was incubated on ice for 30 minutes, heat-shocked for 45 seconds at 42 °C and incubated again for 2 minutes on ice. This was followed by the addition of 100 µl of LB broth and 45 minutes incubation at 37 °C with

shaking. The transformation was finally spread on an ampicillin-containing agar plate (100 µg/ml ampicillin) and incubated at 37 °C overnight.

2.2.6.5.3 PCR screen of colonies

The following day, colonies were screened by PCR; bacterial colonies were picked from the agar plate with sterile 200 µl pipette tips, streaked on a new LB agar plate, numbering each streak and dipping each tip thereafter in the PCR tube bearing the corresponding number. The new agar plate was incubated at 37 °C overnight and PCR using the universal primers, M13F and M13R, was done followed by electrophoresis on 1 % agarose gel. Positive colonies were identified and overnight cultures were set up from the numbered streaks on the new agar plate. An overnight culture of pDR195-transformed *E. coli* was also set up, and both cultures were mini-prepped the next day using the Nucleospin plasmid kit from Macherey-Nagel.

2.2.6.5.4 Digestion of DNA with restriction enzymes

Test restriction digest of *TbAT-1* in pGEMT was done with the restriction enzymes, *Bam*HI and *Xho*I and subsequently electrophoresed on agarose gel to confirm that the restriction enzymes will cut out the right size of product. Cultures that gave the correct size of drop out were restriction-digested along with the yeast expression vector (pDR195) as follows: 45 µl of mini-prepped DNA was placed in an eppendorf tube together with 7 µl of 10 x bovine serum albumin, 7 µl Promega buffer C, 30 units of *Xho*I, 30 units of *Bam*HI and incubated overnight at 37°C on a heat block. Digest reactions were electrophoresed the next day, and the bands for *TbAT-1* obtained from pGEMT and linearised pDR195 expression vector were both gel-extracted.

2.2.6.5.5 Ligation of digested DNA into the final vector.

This was followed by the ligation of TbAT-1 and pDR195 expression vector in a 10 µl ligation reaction made up of 1 µl 10 x buffer, 3 units of T4 ligase, 2 µl pDR195 vector backbone and 6 µl TbAT-1 insert in a sterile eppendorf tube. The ligation was incubated at 4°C overnight, and then transformed into XLI blue *E. coli* as described above. Colonies were screened by PCR as stated earlier (section 2.2.6.5.4) and positive colonies were test-digested with the corresponding restriction enzymes, and colonies which dropped out correct size of band were sequenced to confirm that start and stop sites were present correctly. The correct colony was then grown up in an overnight culture, mini-prepped as before, and plasmid DNA used to transform *Saccharomyces cerevisiae* MG887-1.

2.2.7 Transfection of *T. b. brucei* (BSF), yeasts and *Leishmania mexicana*

TbAT1 KO B48 cells were transfected with TbATE1, TbATE2, A728G-TbATE2, TbAQP2 (all sub-cloned into pHD1336) and empty pHD1336 vector; Tb427 wt cells were transfected with wt ATPase γ and C851A (S284*) ATPase γ , both sub-cloned into pEnT6B-GFP vector (B = blasticidin); *Saccharomyces cerevisiae* MG887-1 was transformed with TbATA1, TbATA3, TbATA6, TbATE1, TbATE2 and TbAT1/P2 (all sub-cloned into pDR195) and empty pDR195; *L. mexicana* promastigotes (M379) were transfected with TbATA1, TbATA3, TbATA6, TbATE1 and TbATE2 (all sub-cloned into pNUS-HCN vector) and pNUS-HCN empty vector (Tetaud *et al*, 2002).

2.2.7.1 Transfection of *T. b. brucei*

10 µg of pHD1336-based plasmid DNA and 2×10^7 trypanosome cells were used for each transfection. Cells were counted and the volume of culture required for transfection was removed and centrifuged at 1500 x g for 10 minutes. The supernatant was completely removed and the cell pellet was re-suspended in the pre-determined volume of T-cell buffer. 10 µg of plasmid was placed in each labelled cuvette, while distilled water was placed in the control cuvette. 100 µl of cell suspension in T-cell buffer was transferred to each plasmid-containing cuvette and also to the control, and the cuvettes were all pulsed in Amaxa Nucleofection machine with program X-001. Cells were transferred into pre-warmed HMI-9 medium and allowed to recover for 8 - 16 hours at 37 °C and 5% CO₂. Relevant antibiotics were then added before the cells were diluted out for clones.

2.2.7.2 Transfection of *Leishmania mexicana*

Each transfection was performed on 10^7 cells *Leishmania mexicana* M379 WT cells using 10 µg of pNUS-HcN-based plasmid DNA (Tetaud *et al*, 2002). Cells were counted and the volume of culture needed for the plasmids removed and centrifuged at 1000 x g for 10 minutes. The supernatant was removed, and cells were washed in 5 ml HOMEM medium, centrifuged again at 1000 x g for 10 minutes before the supernatant was removed completely and the cell pellet re-suspended in the pre-determined volume of T-cell buffer. 10 µg of plasmid was placed in each labelled cuvette, while distilled water was placed in the control cuvette. 100 µl of cell suspension in T-cell buffer was transferred to each plasmid-containing cuvette and also to the control, and the cuvettes were all pulsed in Amaxa Nucleofection machine with program U-033. The cuvettes were subsequently placed on ice for 10 minutes before the parasites were transferred

into 10 ml pre-warmed HOMEM medium and allowed to recover for 16 - 18 hours. G418 (50 µg/ml) was then added before the cells were diluted out for clones.

2.2.7.3 Transformation of yeast cells

5 ml YPAD medium was inoculated with an MG887-1 yeast colony, and grown overnight at 30 °C. Next day, cells were sub-cultured into 30 ml fresh medium at 2×10^6 cells/ml and incubated to 2×10^7 cells/ml (takes about 5 hours at 30°C). 25 ml of culture at 2×10^7 cells/ml were centrifuged at 1100 x g for 10 minutes, washed in 10 ml sterile distilled water, re-centrifuged, re-suspended in 1ml sterile distilled water and transferred to a 1.5 ml sterile microfuge tube. The cells were centrifuged again at 2700 x g, re-suspended in 1 ml sterile 1 x TE/LiAc, and centrifuged one final time at 2700 x g before being re-suspended in 0.25 ml 1 x TE/LiAc at a final density of 4×10^9 cells/ml. 100 µl of this cell suspension was mixed with 5 µl of plasmid DNA and 2 µl single stranded carrier DNA (10 mg/ml salmon sperm DNA, boiled and quick-chilled on ice) in a 1.5 ml sterile microfuge tube. The mixture was incubated for 10 minutes at room temperature followed by the addition of 300 µl sterile PEG/LiAc/TE and subsequent incubation at 30 °C for 60 minutes with shaking. 43 µl of DMSO was added and mixed before the tube was heat-shocked at 42 °C for 5 minutes. This was followed by centrifugation at 2700 x g and a wash in 1 ml 1 x TE, another centrifugation and a final re-suspension in 500 µl of 1 x TE. The cells were then plated on a synthetic complete medium minus uracil agar. Incubation was at 30 °C for between 24 and 48 hours, until colonies were visible.

2.2.7.4 Dilution of transformed trypanosomes (*L. mexicana*) and selection for clones

After transformation, trypanosomes or *L. mexicana* were cloned by dilution in HMI-9 or HOMEEM medium as shown below in 50 ml centrifuge tubes.

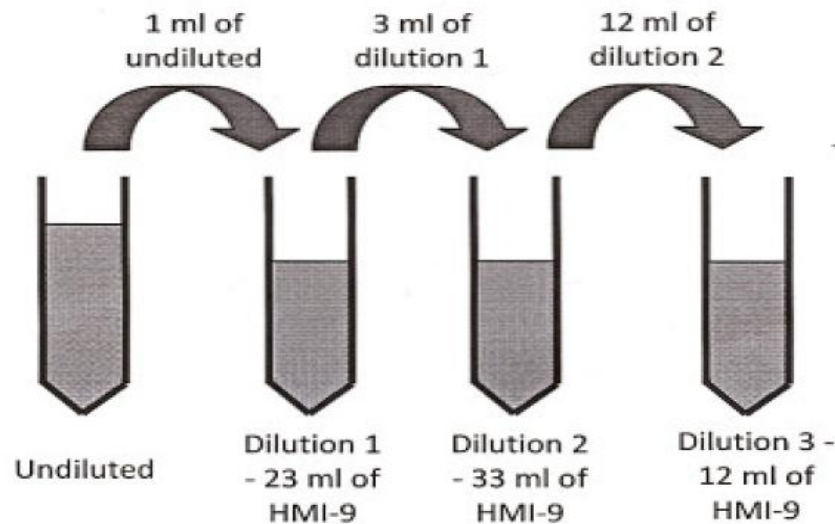


Figure 2.1 Dilution of trypanosomes and *L. mexicana* for clones. Dilution was done at about 16 hours after transfection (immediately after introducing the selective antibiotic). Antibiotic selection combines with dilution to produce clonal lines.

Each dilution was then plated out in 96 well plates at 200 μ l per well. Hence plate 1 (containing dilution 1) would be at 1/24 times dilution, while plates 2 and 3 would be at 1/288 and 1/576 times dilution respectively. Clones were usually obtained from plates 2 and 3.

2.2.8 Sequencing of genes of interest.

Each gene for sequencing was duplicated by PCR with Phusion DNA polymerase. The PCR product was a-tailed and subsequently sub-cloned into the pGEMT easy vector as described above in section 2.2.6.5.1. The resulting ligation was transformed into XLI blue *E. coli* and colonies of transformed bacteria were screened for the presence of the DNA insert. PCR to screen for all DNA inserted

in pGEMT was with standard primers M13F and M13R. Overnight cultures of positive colonies were grown, miniprep and test-digested with the relevant restriction enzyme. DNA samples that dropped out the correct size of band were sent to be sequenced either by Source BioScience or Eurofins MWG Operon. Sequences were ultimately aligned with CLC genomic workbench 5.5.1.

Sequencing of PCR products was also carried out following a PCR clean-up step with the Nucleospin PCR clean up kit from Macherey-Nagel. Samples for sequencing were sent to Eurofins MWG Operon.

2.2.9 Mitochondrial membrane potential assays.

Fluorescence Activated Cell Sorting Technology (FACS) was employed in the determination of the change in mitochondrial membrane potential (MMP) due to exposure of trypanosomes to isometamidium, valinomycin and troglitazone in culture. Valinomycin (100 nM) and troglitazone (10 μ M) were employed as negative and positive controls respectively. MMP was evaluated using tetramethylrhodamine ethyl ester (TMRE) at 25 nM conc (Ibrahim *et al*, 2011).

Cell cultures were centrifuged and the density adjusted to 10^6 cells/ml in fresh HMI-9 media. Four different cultures were set up for each cell line as follows: drug-free, isometamidium (500 nM), valinomycin (100 nM) and troglitazone (10 μ M). After incubation of these cultures for a predetermined time (at 37 °C and 5% CO₂), 1 ml of cells (10^6 cells/ml) was centrifuged for 10 min at 1500 x g (room temp.). The pellet was re-suspended in 1 ml of PBS containing 25 nM TMRE and incubated at 37 °C for 30 min in the absence of the test compounds. Samples were subsequently placed on ice for at least 30

minutes before analysis by flow cytometry using the FL2-Height detector and CellQuest software.

2.2.10 Fluorescence microscopy.

Fluorescence microscopy was employed to visualize the presence or absence of kinetoplasts in the isometamidium resistant clones. Trypanosome cultures were counted and the density adjusted to 5×10^5 cells/ml in fresh HMI-9 media. 50 μ l of this cell suspension was spread out on a microscope slide and allowed to dry. The slides were placed in ice-cold methanol overnight at -20°C to fix the parasites to the slides. Slides were subsequently removed from the methanol, dried in a fume hood and stored at 4°C . Rehydration of the slide was done by gently putting 1 ml of PBS on the slide and allowing to stand for 5 min. The PBS was gently removed by inclining the slide on a soft tissue, and a drop of vectashield mounting medium containing DAPI (4',6-Diamidino-2-phenylindole dihydrochloride) was placed on the slide before covering with a cover slip. The slide was then viewed under the Delta vision microscope.

2.2.11 Infectivity studies in mice.

Infectivity study was done with the clones generated for ISM resistance to test their ability to mount and sustain an infection. Twenty female ICR mice were procured from Harlan, UK. They were allowed 7 days to acclimatize before being used for the experiment. The study was done in 4 groups of 5 mice, and each group was inoculated with one of *Tb427* wt, ISMR1 clone 3, ISMR15 clone 1 and *Tb427* wt + S284* ATPase γ clone 3. 200,000 trypanosome cells in phosphate-buffered saline, PBS were inoculated per mice via the intra peritoneal route. Blood was drawn from tail puncture and diluted 1:10 in lysis buffer for counting.

3. Isometamidium shares at least 1 transporter with pentamidine: Analysis of issues and possibilities.

3.1. Introduction.

It is now banal to state that new drugs are needed for the treatment of African trypanosomiasis. Few drugs are available for the treatment of this disease both in man and in livestock even though chemotherapy is the main method of control. Development of new drugs can however be achieved through the elucidation of the mode of action and the underlying mechanisms of resistance to existing drugs (Carter *et al*, 1995). The identification of the membrane transporters responsible for the uptake of the available trypanocides will enhance the development of new methods of diagnosis and improve the treatment of drug-resistant sleeping sickness (Mäser *et al*, 1999), since the development of resistance to most trypanocides has been linked to a reduction in drug accumulation. Hence, alterations to the P2 aminopurine transporter have been implicated in resistance of trypanosomes to melaminophenyl arsenicals (Carter & Fairlamb, 1993) and to diamidines (Carter *et al*, 1995). Some reports also found a role for the P2 transporter in isometamidium transport in *T. b. brucei* (Afework *et al*, 2006;Mäser *et al*, 1999), although the level of contribution to this process was not quantified. We have investigated these claims, and also assessed the contribution of other closely related pentamidine transporters to the uptake of isometamidium in *T. b. brucei*.

This chapter presents the results of studies on the membrane transport of isometamidium. These studies aimed to identify the transporters of isometamidium in *Trypanosoma brucei brucei* in order to determine their contribution to the uptake, and resistance to the trypanocide. Three candidate transporters were studied, namely: the P2 aminopurine transporter encoded by the *TbAT1* gene (Mäser *et al*, 1999;Stewart *et al*, 2010), the *TbAT-E1* allele and

the *TbAT-A* genes. Each was expressed either in yeast or *Leishmania mexicana*, and the contribution to isometamidium uptake measured.

Finally, the contribution of drug efflux by ABC transporters to ISM resistance was investigated. These transporters are known to use the energy of ATP to export drugs from cells against a concentration gradient (Mäser *et al*, 2003) Hence, clinical drug resistance cases experienced during the treatment of many diseases have been attributed to the activities of these multidrug resistance proteins, MRPs (Deeley *et al*, 2006). Expression of some efflux pump genes in *E. coli* produced a multidrug resistance phenotype (Swick *et al*, 2011), while some inhibitors of microbial efflux pumps significantly enhanced the antimicrobial effects of cationic phenothiazinium dyes on *Staphylococcus aureus* (Tegos *et al*, 2008). Similarly, antimony resistance in *Leishmania donovani* promastigotes was attributed to the activity of multidrug resistance-associated protein (MRP)-like pumps that were in resistant isolates (Mandal *et al*, 2009), and efflux pumps were also found to expel pentamidine from the cytosol of resistant *Leishmania mexicana* while the cytosolic pentamidine in the wild type cells was accumulated in the mitochondria, driven by the high mitochondrial membrane potential (Basselin *et al*, 2002). Since it had been found that the trypanosome genome contains three ABC transporter genes, all of which are expressed in both the bloodstream and procyclic forms (Mäser & Kaminsky, 1998), we studied the possible contribution of drug efflux to ISM resistance in the ISMR clones.

3.2. Expression of *TbAT1* in yeast cells.

The *TbAT1* gene was sub-cloned into the pGEMT vector to create sticky ends needed for ligation into the final expression vector. The size of the *TbAT1*

gene is 1404 bp; hence, sub-cloning into pGEMT generated a product of about 1600 bp (figure 3.1).

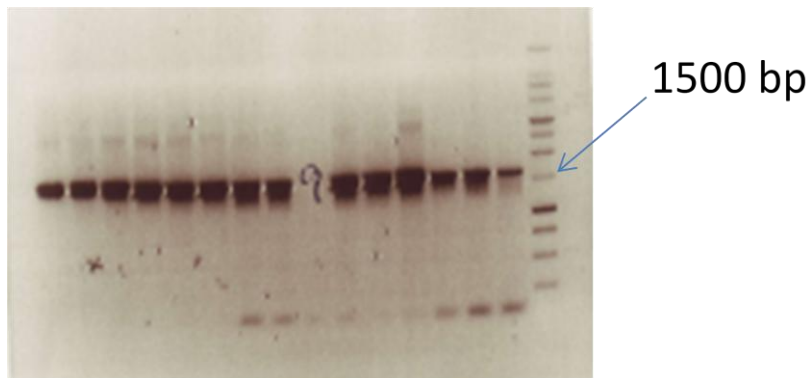


Figure 3.1 Agarose gel electrophoresis of *TbAT1* subcloned in pGEMT vector. Bands represent the PCR screen of XLI blue *E. coli* colonies using M13F and M13R primers, after transformation with *TbAT1* subcloned in pDR195 plasmid.

TbAT1 was cut out of pGEMT using *XhoI* and *BamHI* restriction enzymes. The same restriction enzyme pair was used to linearize the pDR195 expression vector (figure 3.3), cutting out the sequence between the restriction sites, before *TbAT1* was ultimately ligated into the yeast expression vector pDR195. After ligation into pDR195, a test restriction digest was performed to check for correct ligation. The bands at ~6 kb (figure 3.2) represent the empty pDR195 vector, while the bands at ~1.5 kb represent *TbAT1* genes dropped out of the expression vector by the restriction enzymes.

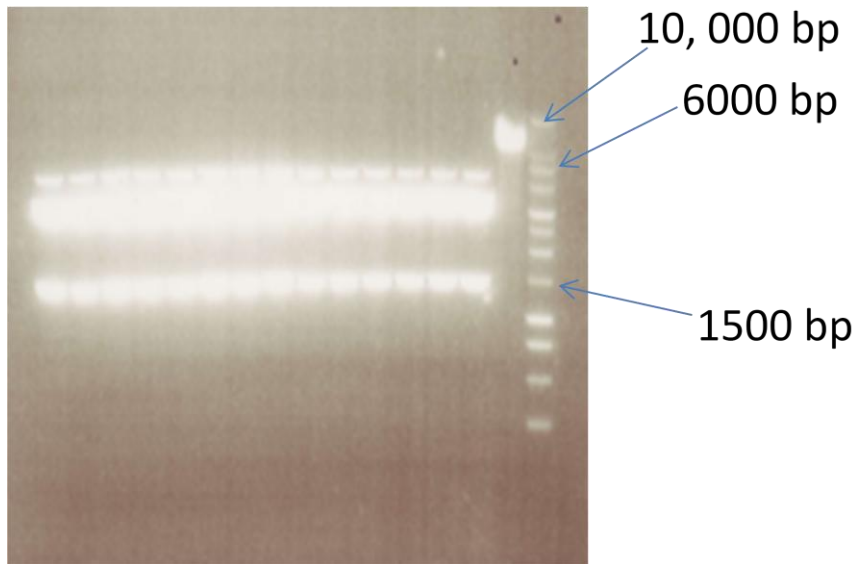


Figure 3.2 Agarose gel electrophoresis of *Bam*HI/*Xho*I dropout of *TbAT1* from pDR195 vector. *TbAT1* was excised from *TbAT1*/pDR195 plasmid, after ligation, to check for correct insertion into the plasmid. Bands at ~6kb represent linearised pDR195 plasmid, while bands at ~ 1.5kb represent *TbAT1* restriction drop out. The single band at ~ 8kb represents intact *TbAT1*/pDR195 plasmid.

TbAT1 in pDR195 was subsequently sequenced to ensure that start and stop sites are present correctly before the construct was used to transform yeast cells. The transformed yeast was then screened by PCR using primers that copied a segment of the *TbAT1* (789 bp, figure 3.4). The presence of the plasmid was also demonstrated by PCR with primers that copied a section of the Ampicillin resistance gene (815 bp; figure 3.4). Primer sequences were presented in table 2.1.

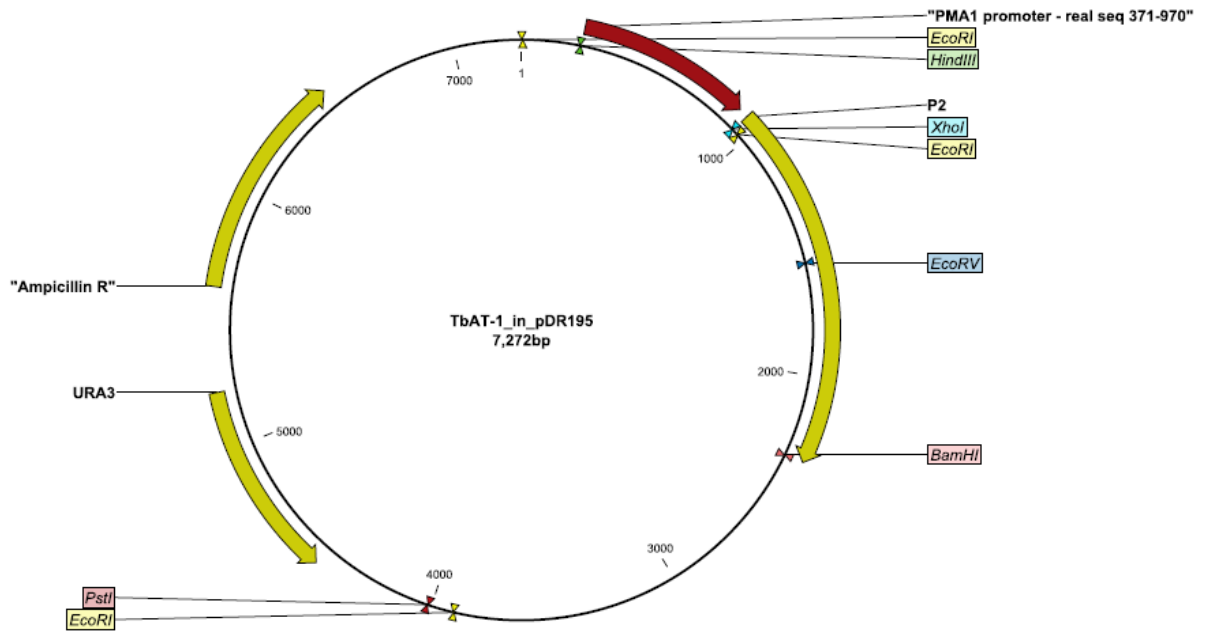


Figure 3.3 Vector map of *TbAT1* in pDR195 expression vector. This was generated by subcloning *TbAT1* into the *XhoI/BamHI* site in pDR195 plasmid.

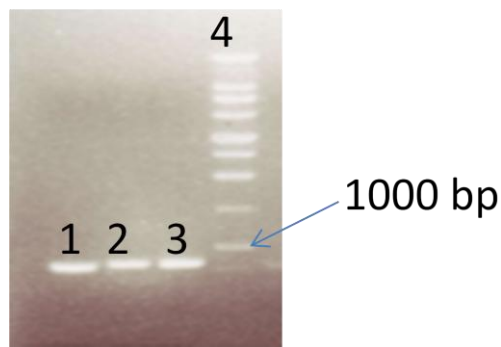


Figure 3.4 Agarose gel electrophoresis of PCR screen for *TbAT1* in yeast. **Band 1:** *TbAT1* gene in *TbAT1*-expressing yeast; **2:** pDR195 vector in *TbAT1*-expressing yeast; **3:** pDR195 in empty vector control yeast; **4:** 1 kb ladder. The nucleotide sequences of the primers used were presented in table 2.1.

3.3. Isometamidium uptake through the P2 transporter.

Yeast cells expressing TbAT1 showed a clear increase in the amount of isometamidium (ISM) taken up, which was significant from the 6th minute of uptake, compared to cells expressing the empty pDR195 vector (figure 3.5).

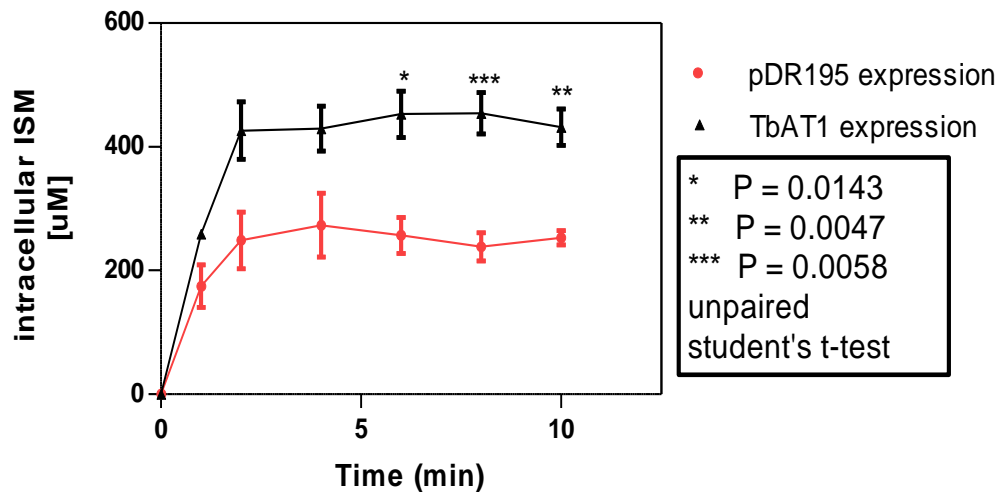


Figure 3.5 Uptake of ISM by MG887-1 yeast cells expressing TbAT1 and empty pDR195. Assay was performed in triplicate with 9×10^7 cells/ml of *TbAT1* expressing yeast and 1.026×10^8 cells of pDR195-transformed yeast (control) in assay buffer at room temperature; [ISM] = 10 µM. Yeast cells were harvested from culture as described in section 2.2.4, and ISM uptake monitored using the same method described for trypanosomes in section 2.2 5.

Next, the rate of ISM uptake was determined in *TbAT1* KO cells (*TbAT1*^(-/-) or wild type *Tb427* cells from which the *TbAT1* gene has been deleted) When the rate of uptake in the wild type *Tb427* was however compared to that in *TbAT1* KO cells (*TbAT1*^(-/-)), no significant difference was found (figure 3.6). This suggests that the contribution to the uptake of ISM by *TbAT1* or P2 in *T. b. brucei* is very minimal. The rate of ISM uptake was only 20% lower when the *TbAT1* gene was deleted (figure 3.6). Hence the contribution to the *in vitro* uptake of ISM by the P2 transporter may be put at just 20 %. However, it must be

remembered that the P2 expression level is very low in cultured cells, compared to in vivo levels (Ward *et al*, 2011), thus the real contribution of P2-mediated ISM uptake may be much higher.

Tubercidin sensitivity in *T. brucei* can be used as an indicator for TbAT1 expression levels (Geiser *et al*, 2005;Munday *et al*, 2013). The significant cross resistance to tubercidin in ISM resistant clone 3 (ISMR1 clone 3 is an ISM resistant trypanosome line selected by growing in the presence of ISM; sections 2.2.2 & 4.2) is a further strong indication that ISM is transported by the P2 transporter, as P2 expression appears to be much-reduced in the ISM-resistant strain (figure 3.7). The significant difference between the IC₅₀ found for ISMR1 clone 3 and that found for the *TbAT1* knock out may be an indication that the P2 transporter is still partly functional in the resistant clone whereas it has been deleted in the *TbAT1* KO. Consistent with this interpretation, the *TbAT1* open reading frame from ISMR1 was cloned and sequenced, but no mutations in the coding sequence were found (appendix C).

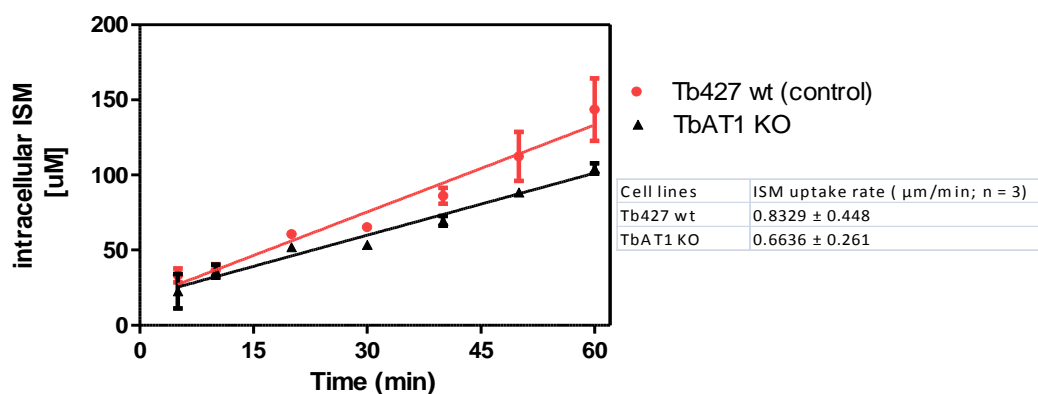


Figure 3.6 Uptake of ISM by Tb427 wt and *TbAT-1 KO*. Assay was performed in triplicate with 1.48×10^8 cells/ml of *Tb427* wt and 1.08×10^8 cells/ml of *TbAT1*^(-/-) in complete HMI-9 medium

(+ 10% fetal bovine serum) at room temperature; [ISM] = 10 μ M. ISM uptake was measured as described in section 2.2.5. Experiment shown is representative of three independent assays performed in triplicate and showing similar outcomes.

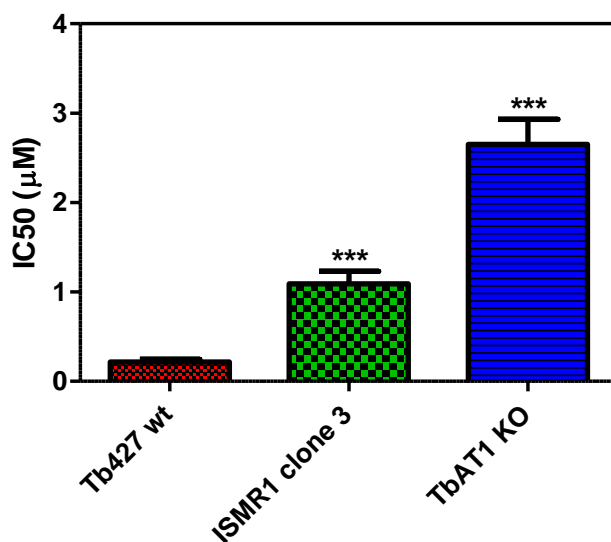


Figure 3.7 Sensitivity to tubercidin in ISM resistant clone, ISMR1 clone 3. IC₅₀ values were determined from alamar blue assays with tubercidin, using 10⁵ cells/ml of each cell line (section 2.2.3). Each bar represents the average of three independent assays; errors bars are SEM. ***P < 0.01, one way ANOVA with Turkey's correction, using Graphpad prism 5.0.

3.4. Expression of TbAT-E1 and TbAT-E2 in Yeast and *Leishmania mexicana*.

3.4.1. Expression of *TbAT-E1* and *TbAT-E2* in yeast cells.

Cloning of *TbAT-E1* into pDR195 (figure 3.8) was performed by Dr Jane Munday. The expression of this gene in yeast was done by Dagmara Wiatrek, an exchange student from Poland; *TbAT-E2* was cloned and expressed in yeast by Mounir El Mai, a student from France (both with my involvement and supervision). Yeast cells expressing *TbAT-E1* were found to display a significantly higher uptake of ISM compared to the empty vector-expressing control (P<0.05 even before the 2nd minute of uptake; figure 3.9). Figure 3.9 is a graph of the

mean of four independent uptake assays. *TbAT-E2* expression in yeast also increased the uptake of ISM significantly but only in the 6th minute of uptake (figure 3.10), and to a lesser extent compared to *TbAT-E1*. Figure 3.10 is a graph of a single assay performed in triplicate.

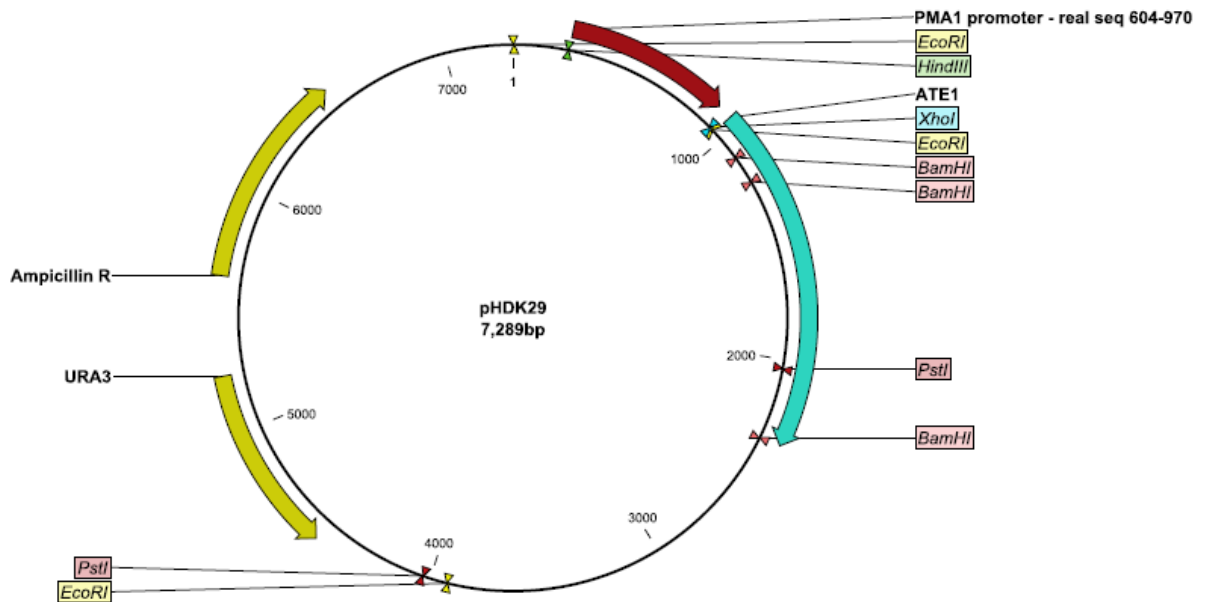


Figure 3.8 Vector map of *TbAT-E1* in pDR195 expression vector. This was generated by subcloning *TbAT-E1* into the *XhoI/BamHI* site in pDR195 plasmid.

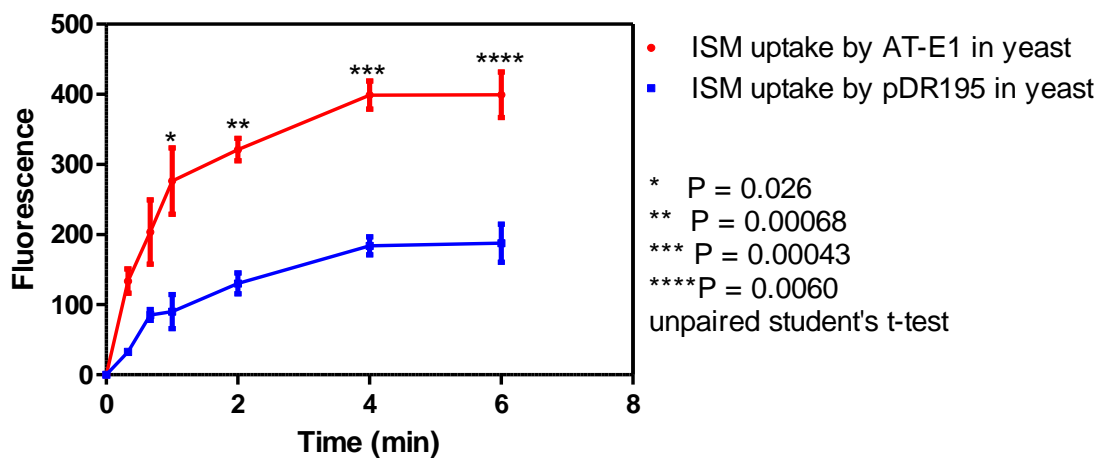


Figure 3.9 ISM uptake by MG887-1 yeast cells expressing *TbAT-E1*; [ISM] = 10 μ M. Graph is a plot of the mean of 4 independent assays. Each of the assays was performed in triplicate with $\sim 10^8$

cells/ml of *TbAT-E1* expressing yeast and pDR195-transformed yeast (control), respectively, in assay buffer at room temperature; [ISM] = 10 μ M. Yeast cells were harvested from culture as described in section 2.2.4, and ISM uptake monitored using the same method described for trypanosomes in section 2.2 5.

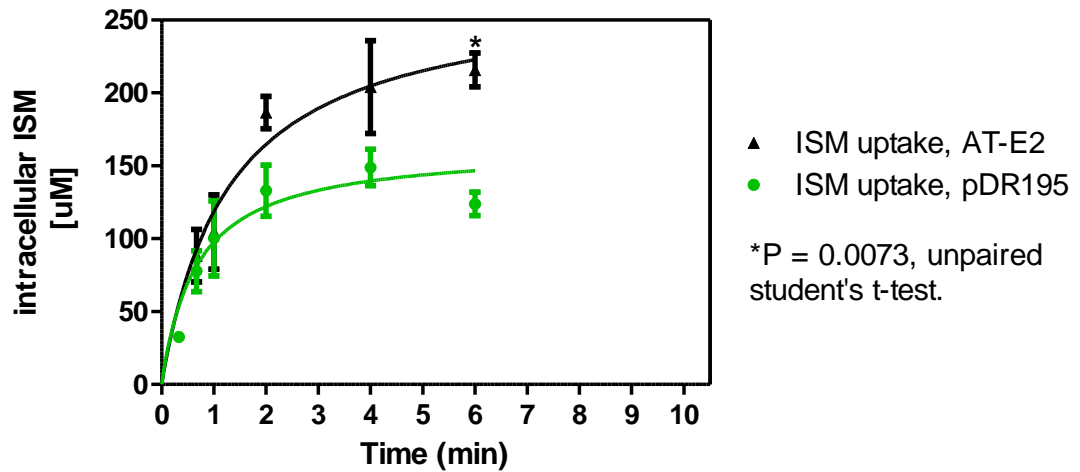


Figure 3.10 ISM uptake by MG887-1 yeast cells expressing *TbAT-E2*. Assay was performed in triplicate with 6.32×10^7 cells/ml of *TbAT-E2* expressing yeast and 7.96×10^7 cells of pDR195-transformed yeast (control) in assay buffer at room temperature; [ISM] = 10 μ M. Yeast cells were harvested from culture as described in section 2.2.4, and ISM uptake monitored using the same method described for trypanosomes in section 2.2 5.

Primers used for PCR to check for the presence of the inserted genes in the transformed yeast were presented in table 2.1. *TbAT-E1* and *TbAT-E2* were each amplified to give a PCR product of ~750 bp (figure 3.11). A segment of the ampicillin gene sequence was amplified (~810) to demonstrate the presence of pDR195 plasmid (figure 3.11).

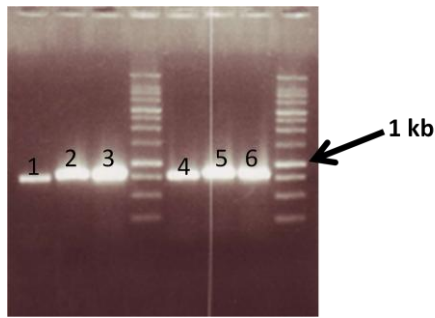


Figure 3.11 Agarose gel electrophoresis of PCR screen of MG887-1 yeast cells transformed with *TbAT-E2* and *TbAT-E1*. Band 1 and 4: *TbAT-E2* and *TbAT-E1* respectively, amplified from *TbAT-E2* and *TbAT-E1* transformed yeast cells; 2 and 5: pDR195 vector in E2 and E1 expressing yeasts respectively; 3 and 6: pDR195 vector in empty vector yeasts. The primers used were presented in table 2.1

3.4.2. *TbAT-E1* and *TbAT-E2* Expression in *Leishmania mexicana*

TbAT-E1 and *TbAT-E2* were both cloned into pNUS-HcN vector (Tetaud *et al.*, 2002) by Dr Jane Munday who also did the expression of *TbAT-E1* in *L. mexicana*. The expression of *TbAT-E2* in *L. mexicana* was however done by me. The expression of *TbAT-E1* did not increase the susceptibility of *L. mexicana* to pentamidine. Susceptibility to ISM was however increased significantly by *TbAT-E1* expression in *L. mexicana*, ($P < 0.05$; figure 3.12). This correlates with the increased ISM uptake found for *AT-E1* expression in yeast (figure 3.9). In addition to *TbAT-E1*, *TbAT-E2*, *TbAT-A1* and *TbAT-A3* all increased diminazene sensitivity when expressed in *Leishmania mexicana* (figure 3.12). Amphotericin-B was included as control.

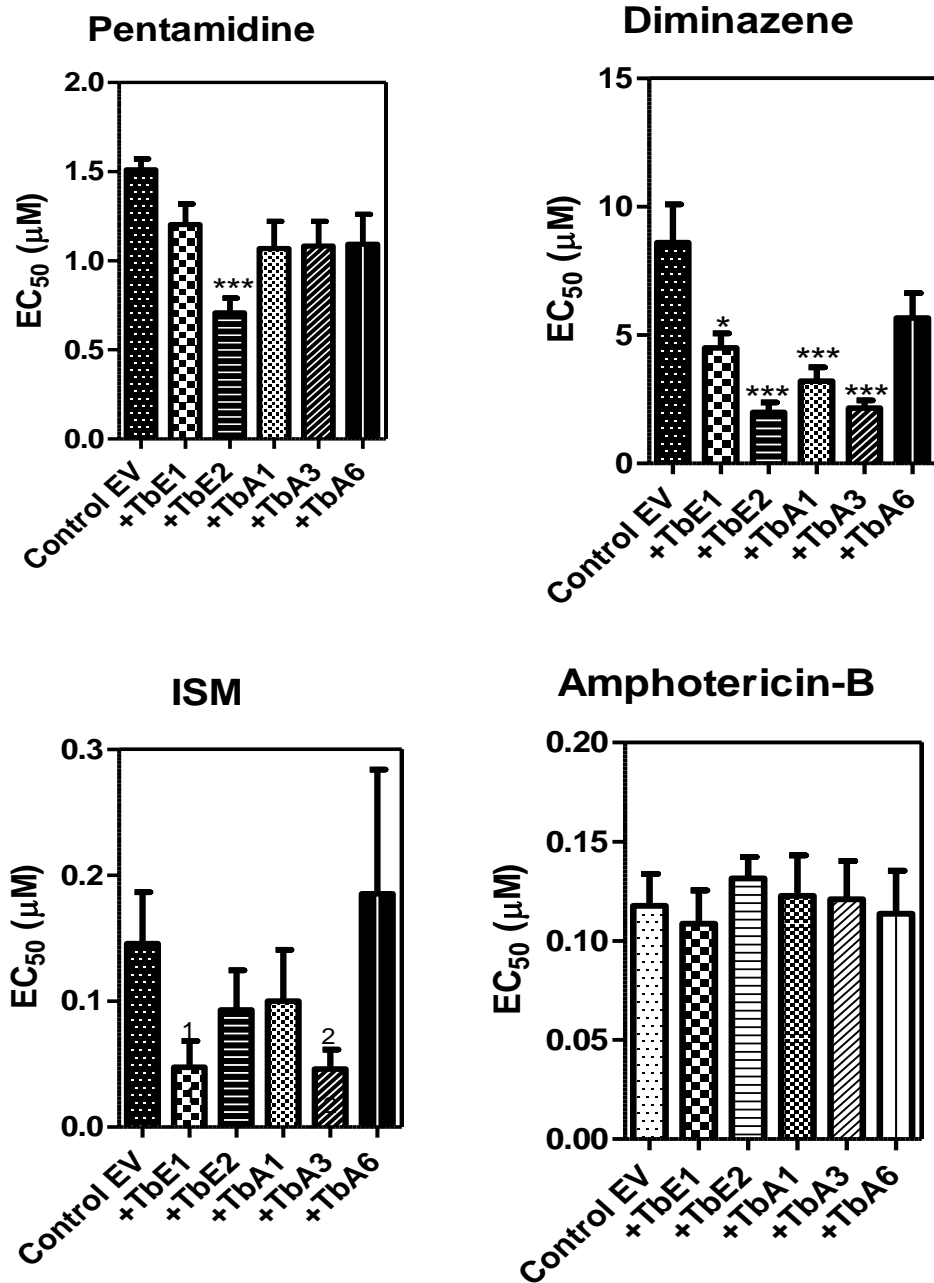


Figure 3.12 Sensitivity of *TbAT-E* and *TbAT-A* transformed *L. Mexicana* promastigotes to Pentamidine, Diminazene and ISM. EC₅₀ (IC₅₀) values were determined from alamar blue assays using 10⁶ cells/ml of each cell line (section 2.2.3). Each bar represents the average of at least three independent assays; errors bars are SEM *P<0.05, ***P<0.01(one way ANOVA with Turkey's correction, using Graphpad prism 5.0); 1P = 0.049, 2P = 0.04 (unpaired students't-test).

3.5. Expression of TbAT-A1, TbAT-A3 and TbAT-A6 in yeast and *Leishmania mexicana*.

TbAT-A was found to have multiple copies in *Trypanosoma brucei*. These were cloned in pDR195 and pNUS vectors and expressed in yeast and *L. mexicana* respectively by Dr. Jane Munday and a Masters student, Luke Woodford. The rate of ISM uptake was increased on the expression of *TbAT-A1* and *TbAT-A6* in MG887-1 yeast; however significant increase in ISM uptake was found only for *AT-A1* expression, from the first full minute of uptake onwards (figure 3.13).

Expression of each of *TbAT-A1*, *TbAT-A3* and *TbAT-A6* in *L. mexicana* led to an increase in susceptibility to ISM, though not statistically significant except for *TbAT-A3* (figure 3.12), while *TbAT-A6* was the least sensitive to ISM. This is not a surprising observation since *TbAT-A6* has about 44 nucleotides missing from its sequence when compared to *TbAT-A1* and *TbAT-A3*.

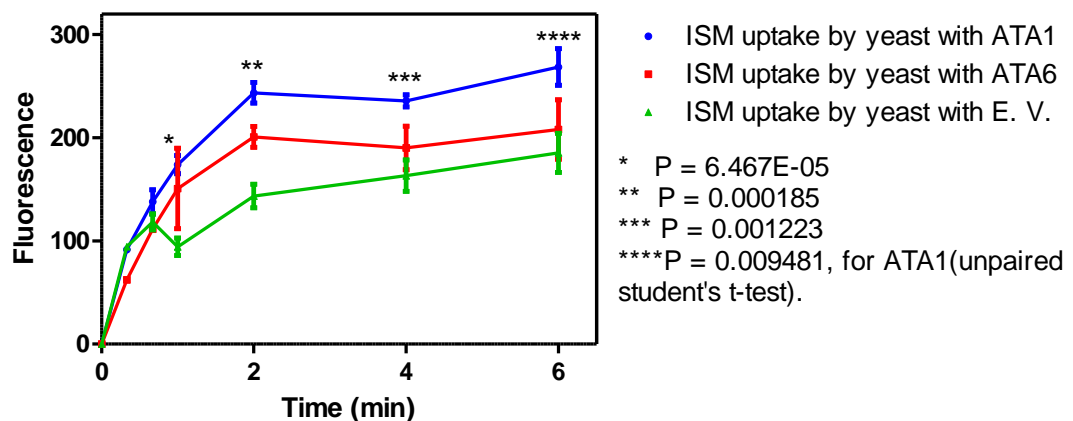


Figure 3.13 ISM uptake by yeast cells expressing *TbATA-1* and *TbATA-6*. Graph is the average of 2 independent repeats. Each of the assays was performed in triplicate with $\sim 10^8$ cells/ml of *TbAT-A1* expressing yeast, *TbAT-A6* expressing yeast and pDR195-transformed yeast (control), respectively, in assay buffer at room temperature; [ISM] = 10 μ M. Yeast cells were harvested from culture as described in section 2.2.4, and ISM uptake monitored using the same method described for trypanosomes in section 2.2 5.

Screen of transformed yeast cells was done by PCR using primers that amplify *TbAT-A1* and *TbAT-A6* (~1400 bp each; figure 3.14). Amplification of the *URA3* gene was employed to demonstrate the presence of the pDR195 expression vector (~1800 bp; figure 3.14). An additional PCR reaction to amplify the PMA1 promoter + the downstream sequence (~1000 bp; figure 3.14) was done on the empty vector yeast.

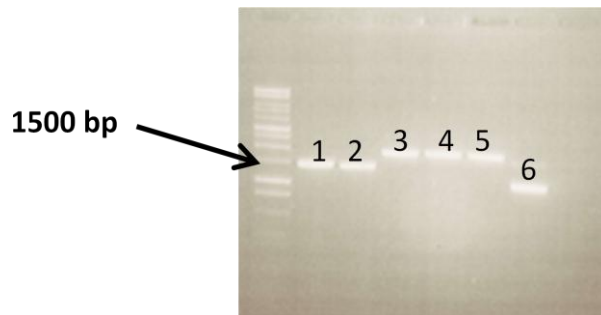


Figure 3.14 Agarose gel electrophoresis of PCR screen of *TbAT-A1* and *TbAT-A6* in transformed MG887-1 yeast cells. Bands 1 and 2, *TbAT-A1* and *TbAT-A6* respectively amplified from *TbAT-A1* and *TbAT-A6* transformed yeast cells; 3, 4 and 5, *URA3* gene in *TbAT-A1*, *TbAT-A6* and empty vector expressing yeast cells respectively; 6, pDR195 vector in empty vector expressing yeast cells. The primers used were presented in table 2.1.

3.6. RNAi of *TbAT-E* in 2T1

RNA interference, RNAi was used to decrease the cellular levels of *TbAT-E* expression in 2T1 cells. The 2T1 strain was generated to eliminate the problems created by variable expression levels at different rRNA spacer loci. Hence, 2T1 enhances integration at a tested and marked locus, thereby eliminating the need to screen multiple recombinant clones to identify those that display desirable features (Alsford & Horn, 2008). RNAi of *AT-E* was performed by my colleague, Ibrahim Teka, a former PhD student in our group (Teka, 2011). RNAi of *AT-E* caused an average reduction in the rate of uptake of ISM to 45 % of the original rate on the induction of RNAi (Fig. 3.15). This reduction was however found to be statistically insignificant ($p=0.070$; figure 3.16) in an unpaired t-test due to

variations between individual experiments which may be due to variations in the phase of life of the parasites at the time of mobilization for uptake or differences in the room temperature value on the individual experiment days (each assay was performed at room temperature). However, in a paired t-test, the reduction was found to be significant ($p = 0.04$; figure 3.16), suggesting that the difference between samples within the individual experiments was consistently significant.

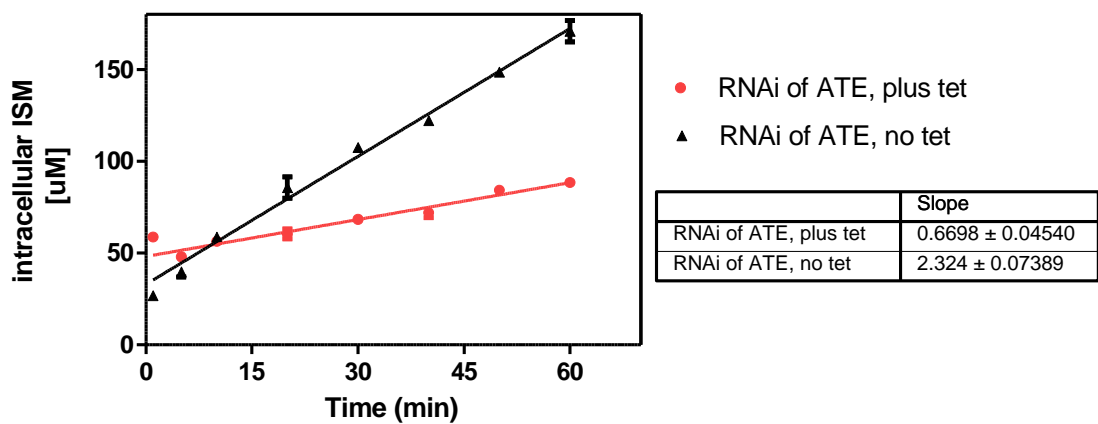


Figure 3.15 Uptake of ISM by RNAi of *AT-E* in 2T1 Tetracycline at 1 $\mu\text{g/ml}$ final concentration was added to the culture 48 hours before ISM uptake to induce RNAi of *AT-E*. Assay was performed in triplicate with $\sim 10^8$ cells/ml of induced and non-induced cell lines in complete HMI-9 medium (+ 10% fetal bovine serum) at room temperature; $[\text{ISM}] = 10 \mu\text{M}$. ISM uptake was measured as described in section 2.2.5. Experiment shown is representative of three independent assays performed in triplicate and showing similar outcomes. The slope of each line represents the rate of uptake ($\mu\text{M}/\text{min}$).

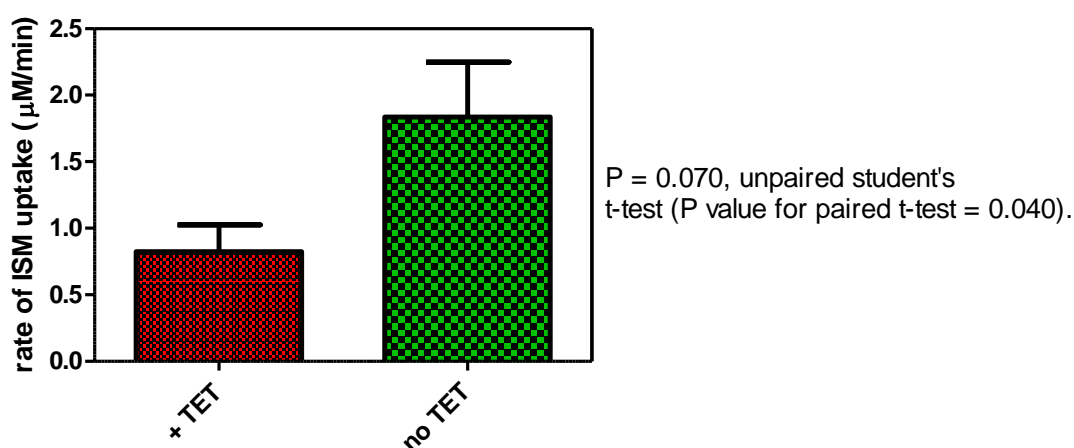


Figure 3.16 Summary of repeats for ISM uptake by 2T1 RNAi of *AT-E*. Bar graphs represent average of rate of ISM uptake and SEM obtained from 3 independent assays done in triplicate, and represented by the graph in figure 3.15.

3.7. Drug efflux by ABC transporters is not involved in ISM resistance in *T. brucei brucei*.

It was recently found that a combination of ISM with tetracycline or enrofloxacin killed resistant trypanosomes much more effectively than ISM alone (Delespaux *et al*, 2010). This finding supports the hypothesis that tetracycline can inhibit ABC transporters (Chopra & Roberts, 2001; Warburton *et al*, 2013) thus compromising the activity of these transporters, thereby reducing the rate of efflux and hence reversing the drug resistance (Delespaux *et al*, 2010). We investigated the relevance of this hypothesis in our resistant clones by carrying out a series of ISM uptake in the presence or absence of tetracycline.

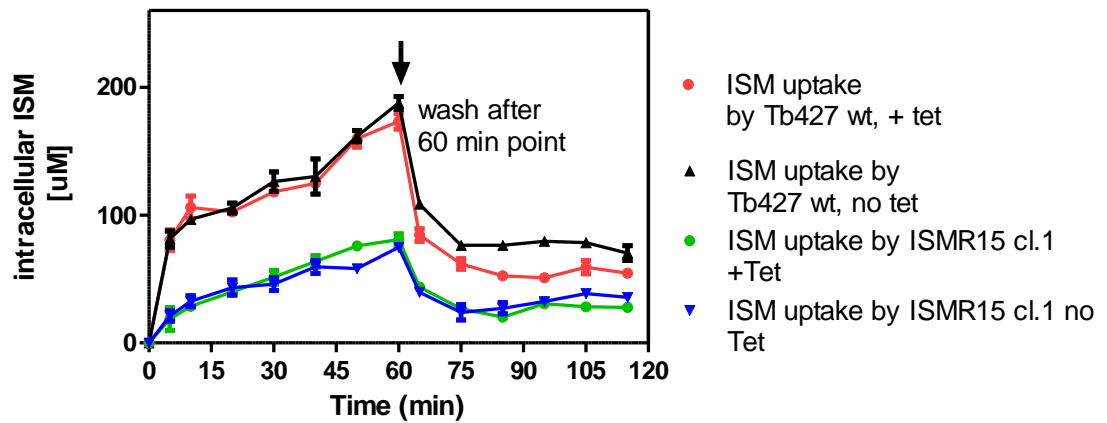


Figure 3.17 Uptake of ISM by Tb427 wt and ISMR15 clone 1 Assay was performed in triplicate with 1.50×10^8 cells/ml of *Tb427* wt and 2.13×10^8 cells/ml of ISMR15 clone 1 in complete HMI-9 medium (+ 10% fetal bovine serum) $\pm 40 \mu\text{M}$ ($17.78 \mu\text{g/ml}$) tetracycline at room temperature (fluorescence was normalised for different cell densities); $[\text{ISM}] = 10 \mu\text{M}$. ISM uptake was measured essentially as described in section 2.2.5, except that cells were washed, after the 60th minute time point, by centrifuging for 5 minutes at 2600 rpm and 4°C (to remove ISM) and subsequently resuspended in ISM-free media to continue the assay.

Though we were able to clearly demonstrate ISM efflux after washing out the drug and placing the cells in fresh medium, there was no difference in the rate of efflux of ISM in ISMR15 clone 1 in the presence or absence of tetracycline, as evidenced by the overlapping graphs of uptake (figure 3.17). This indicates that tetracycline-inhibitable ABC transporters are not involved in drug extrusion in ISM resistant *T. brucei brucei*. Also, the drop in the level of intracellular ISM after the 60th minute wash and re-suspension in tetracycline-containing media is uniform in both the wild type and resistant lines (figure 3.18). This clearly demonstrates that ABC transporter activity may not be involved in ISM resistance.

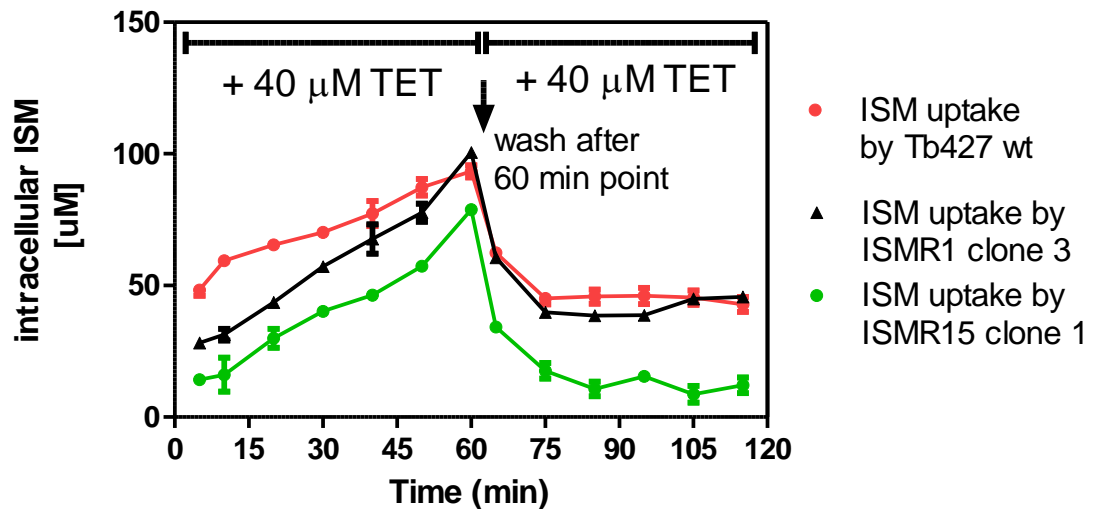


Figure 3.18 Uptake of ISM by Tb427 wt, ISMR1 clone 3 and ISMR15 clone 1 Assay was performed in triplicate with 2.04×10^8 cells/ml of *Tb427* wt, 2.68×10^8 cells/ml of ISMR1 clone 3 and 2.62×10^8 cells/ml ISMR15 clone 1 in complete HMI-9 medium (+ 10% fetal bovine serum) + 40 μ M (17.78 μ g/ml) tetracycline at room temperature (fluorescence was normalised for different cell densities); [ISM] = 10 μ M. ISM uptake was measured essentially as described in section 2.2.5, except that cells were washed, after the 60th minute time point, by centrifuging for 5 minutes at 2600 rpm and 4°C (to remove ISM) and subsequently re-suspended in tetracycline-containing ISM-free media to continue the assay.

Next, Tb427 wt, ISMR1 clone 3 and ISMR15 clone 1 were all exposed to either 5 μ M ISM alone, or 5 μ M ISM in the presence of 40 μ M (17.78 μ g/ml) tetracycline, for six hours, after which they were all washed and re-suspended in fresh, drug-free HMI-9 media and the rate of recovery and multiplication monitored by 12 hourly cell count (figure 3.19). The resistant clones exposed to ISM + tetracycline did not become more sensitive to ISM compared to those exposed to ISM alone (figure 3.19). This demonstrates that tetracycline-sensitive ABC transporters are not involved in resistance to ISM in *T. brucei brucei*.

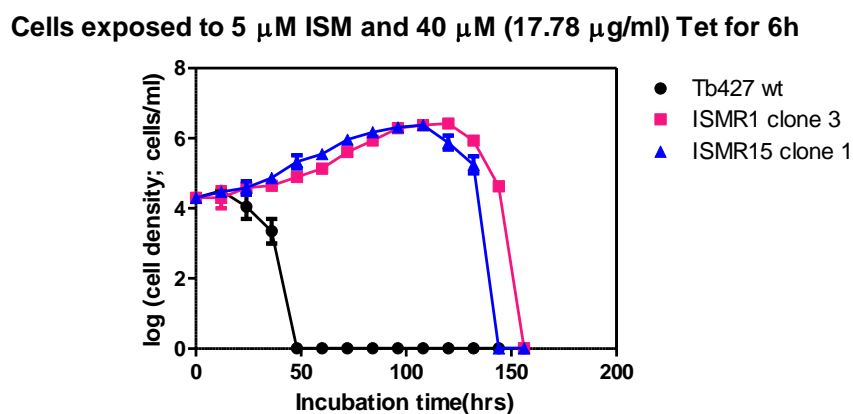
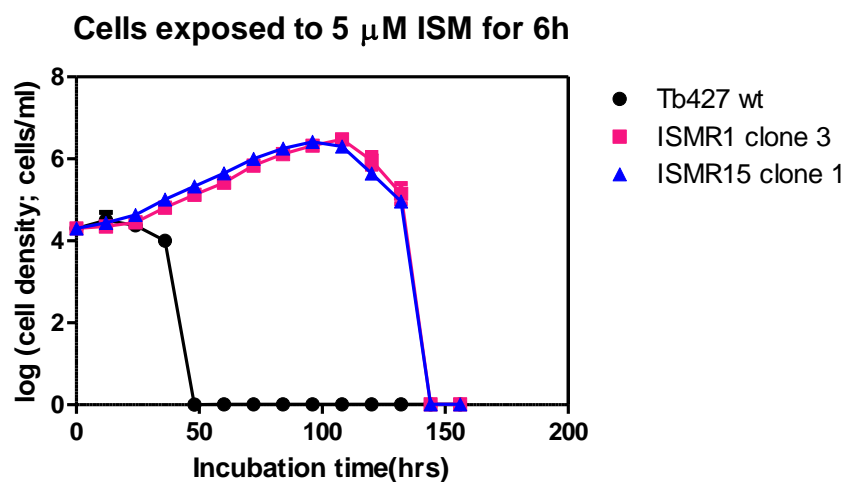


Figure 3.19 Effect of tetracycline on rate of ISM efflux from cells and on the growth rate of ISMR1, ISMR15 and s427wt. Each cell line at 2×10^4 cells/ml was exposed to either 5 μ M ISM alone or 5 μ M ISM + 40 μ M (17.78 μ g) tetracycline for six hours before centrifugation and resuspension in fresh, drug-free HMI-9 medium. Cells were subsequently counted every 12 hours. Each graph is the average of two independent growth measurements

Since tetracycline had no effect on the efflux of intracellular ISM in *T. brucei brucei*, we screened a number of compounds known to either inhibit ABC transporters directly or compromise energy transduction within the cells, as the ABC transporters are ATP-dependent. Uptake of 10 μ M ISM was measured in the presence or absence of 50 μ M concentration of each inhibitor (1 μ M for

valinomycin). Carbonyl cyanide m-chlorophenylhydrazone (CCCP), valinomycin and oligomycin reduced ISM uptake to 60%, 59.5% and 49.6% respectively. Though these reductions were not statistically significant ($P=0.06$; figure 3.20), we decided to investigate the effect of oligomycin on ISM uptake since it had earlier been demonstrated that oligomycin specifically inhibits the F_1F_0 -ATPase of the trypanosomes (Schnauffer *et al*, 2005). Our findings on the contributions of the F_1F_0 -ATPase to ISM uptake and sensitivity are presented in chapters 4 and 5. Pentamidine did not inhibit ISM uptake at 50 μM (figure 3.20). This observation goes contrary to our hypothesis that at least part of the ISM uptake in *T. brucei brucei* is mediated by a pentamidine transporter.

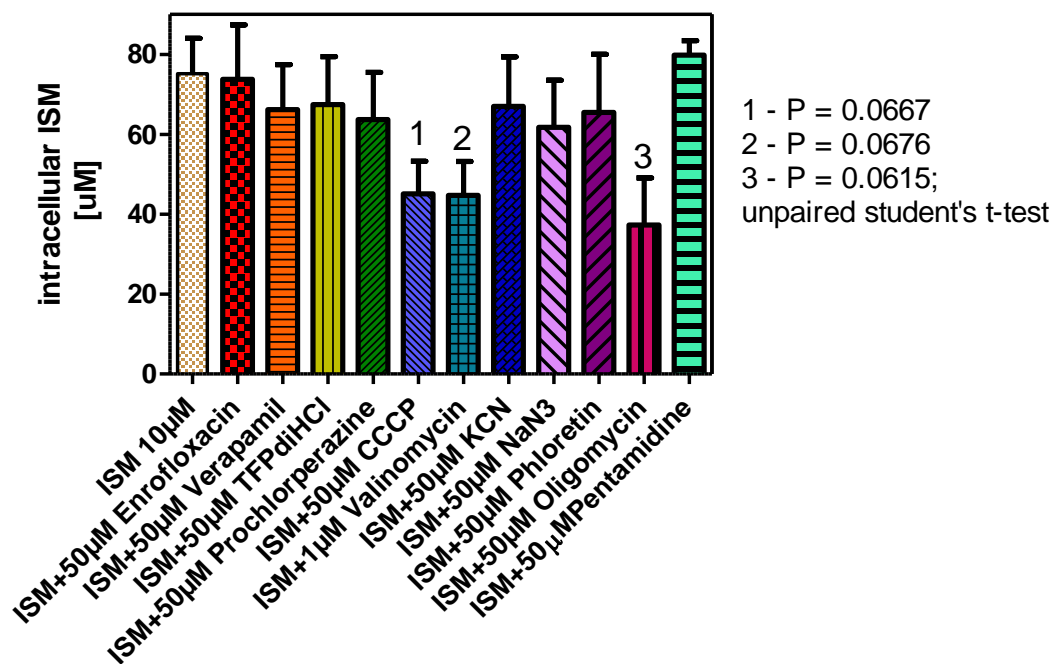


Figure 3.20 Uptake of ISM by Tb427 wt (from culture) in the presence of inhibitors of ABC transporters. Assay was performed in triplicate with $\sim 10^8$ cells/ml of *Tb427* wt in complete HMI-9 medium (+ 10% fetal bovine serum) at room temperature; [ISM] = 10 μM and inhibitor concentrations are as indicated. ISM uptake was measured as described in section 2.2.5; incubation was for 20 minutes. Each bar represents the average of 3 independent repeats; error bars represent the SEM.

Therefore, in order to investigate this finding further, we increased both the concentration of pentamidine and the incubation time (figure 3.21). On increasing the pentamidine concentration from 50 μM to 100 μM , a 13% inhibition of uptake was achieved while a 26% inhibition of uptake was found with 333 μM pentamidine (figure 3.21). There was a 100% ISM uptake in the presence of 333 μM of adenosine (which saturates TbAT1/P2) while 100 μM and 333 μM diminazene significantly reduced uptake of ISM to 62% and 50.2% respectively (figure 3.21).

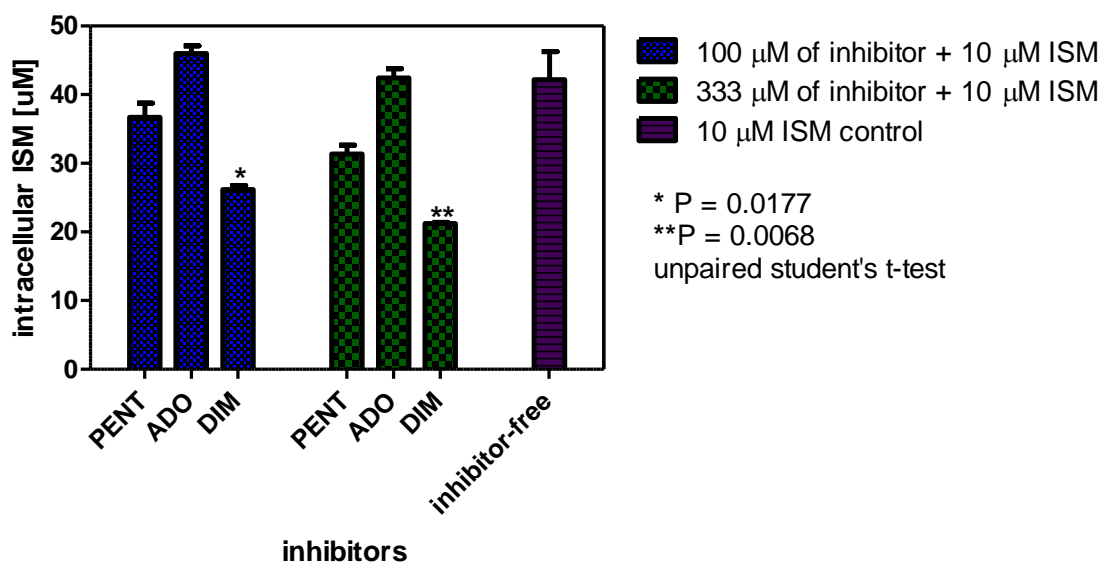


Figure 3.21 Inhibition of ISM uptake by 100 μM and 333 μM concentrations of pentamidine (PENT), diminazene (DIM) and adenosine (ADO). Assay was performed in triplicate with $\sim 10^8$ cells/ml of *Tb427* wt in complete HMI-9 medium (+ 10% fetal bovine serum) at room temperature; [ISM] = 10 μM . ISM uptake was measured as described in section 2.2.5; Incubation was for 30 minutes Each bar represents the average of 3 independent experiments. (ISM-free control experiment was done once, also in triplicate); error bars represent the SEM.

3.8. Discussions

TbAT1 encodes the P2 transporter that transports adenosine, adenine, melaminophenyl arsenicals, and diamidines (Carter & Fairlamb, 1993;Matovu *et*

al, 2003;de Koning *et al*, 2004). However, when this gene was expressed in yeast it mediated the uptake of adenosine which was strongly inhibited by isometamidium and the melaminophenyl arsenicals (melarsoprol and melarsen oxide) but insensitive to pentamidine and diminazene aceturate (Mäser *et al*, 1999). But P2 mediates pentamidine uptake in *T. b. brucei*, and adenosine uptake in *T. b. brucei* was found to be strongly inhibited by pentamidine (Carter *et al*, 1995;de Koning & Jarvis, 1999). Hence the insensitivity of TbAT1 expression in yeast to pentamidine was attributed to the possible absence of a trypanosomal cofactor or modification required for diamidine recognition (Mäser *et al*, 1999).

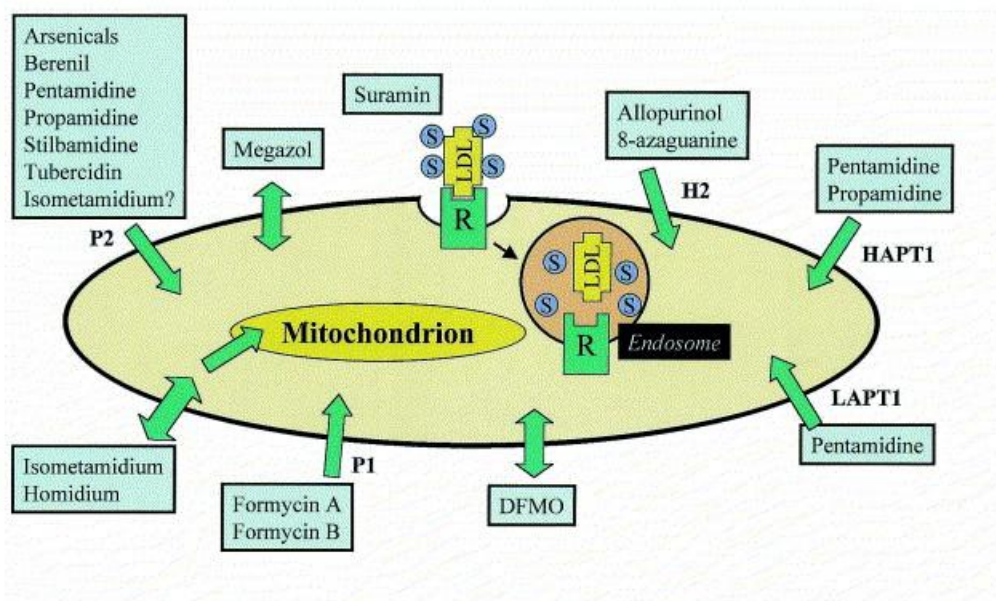


Figure 3.22 Summary of drug uptake routes in *T. b. brucei*. Equilibrative diffusion (facilitated or simple) is shown by double-headed arrows; suspected active transport is shown by single-headed arrows. R = low-density lipoprotein receptor; S = suramin molecule. Figure taken from De Koning, 2001.

Currently, P2 is the only pentamidine transporter in the trypanosomes that has been fully characterized at both the biochemical and molecular levels (figure 3.22). The current situation is that research findings suggest that 3 pentamidine transporters exist in *T. brucei brucei*, namely the P2 transporter,

the High affinity pentamidine transporter (HAPT1) and the Low affinity pentamidine transporter (LAPT1); however, the genes encoding either the HAPT1 or the LAPT1 are yet to be found and the most likely candidates for these roles are the closely related genes, *TbAT-E*, *TbAT-A* and *TbATG* (de Koning *et al*, 2005).

Our findings indicate that P2 transporter activity accounts for about 20% of ISM uptake in *T. b. brucei*, but this just failed to reach a significant level (figure 3.6). Inhibition studies were not done on the uptake in yeast, but there was a significant increase in uptake of ISM due to the expression of *TbAT1* in yeast. The significant insensitivity to tubercidin found in the ISMR1 resistant clone (figure 3.7) also suggests that a reduced expression or activity of *TbAT1* contributes to ISM resistance. ISM uptake through the P2 transporter should however be sensitive to inhibition by both adenosine and diminazene. But only diminazene was able to inhibit this uptake significantly in our wild type *T. b. brucei* ($P < 0.01$, student's t-test; figure 3.21).

ISM uptake assays in yeast cells expressing *TbAT-E1* indicate that the transporter encoded by the *TbAT-E1* makes a major contribution to the uptake of ISM in *T. b. brucei* (figures 3.9). This is evidenced by the significantly increased ISM accumulation ($P < 0.05$) due to expression of the gene in yeast. Similarly, significantly increased susceptibility ($P < 0.05$) to ISM was observed with the expression in *Leishmania mexicana* (figure 3.12). The second allele of *TbAT-E*, the *TbAT-E2* also produced a significantly increased ISM uptake in yeast, but this assay was done only once. Conversely, the expression of *TbAT-E2* in *L. mexicana* did not produce a significantly increased sensitivity to ISM (figure 3.12).

Furthermore, *TbAT-A* was also expressed in yeast and tested for ISM uptake. *TbAT-A1* and *TbAT-A6* are two alleles (copies) of this gene and both were tested for ISM uptake. *TbAT-A1* expression produced a significantly increased uptake of ISM in yeast (figure 3.13). *TbAT-A* was expressed in null mutants of *Leishmania* deficient in purine nucleoside or nucleobase uptake and was found to be a high affinity purine transporter, designated *TbNT11.1* and *TbNT11.2* (Ortiz *et al*, 2009). *TbNT11.1* was also able to transport pentamidine when expressed in *Xenopus oocytes* (Ortiz *et al*, 2009). However, when we expressed each of the three sequences for *TbAT-A*, namely *TbAT-A1*, *TbAT-A3* and *TbAT-A6* in *L. mexicana*, there was no significant difference in pentamidine sensitivity between each of them and the empty vector expression (figure 3.12). Furthermore, the alignment of the nucleotide sequences for *TbAT-A1*, *TbAT-A3*, *TbNT11.1* and *TbNT11.2* could not give a clear picture of which of the two alleles, *TbNT11.1* or *TbNT11.2* corresponds to either *TbAT-A1* or *TbAT-A3* because each one varied with about the same number of nucleotides from the other (see appendix). *TbAT-A1* differed from *TbNT11.1* and *TbNT11.2* by 9 and 10 nucleotides, respectively, while *TbAT-A3* differed from both *TbNT11.1* and *TbNT11.2* by 10 nucleotides each. Since *TbAT-A1* also varies from *TbAT-A3* by 8 nucleotides, it is therefore possible that either could be the *TbNT11.1*. Similarly, *TbAT-E*, designated *TbNT12.1* in the same paper, was expressed in *Xenopus oocytes* and was found to mediate the uptake of both adenine and pentamidine (Ortiz *et al*, 2009). The nucleotide sequence for *TbNT12.1* also differed from *TbAT-E1* and *TbAT-E2* by 15 and 16 nucleotides, respectively, and since the variation between *TbAT-E1* and *TbAT-E2* is about 16 nucleotides, it is not clear which of them will be the *TbNT12.1*. Our findings on pentamidine uptake by *TbAT-E1* will be presented in chapter 6.

Finally, our findings suggest that drug efflux by ABC transporters is not involved in the resistance of *T. b. brucei* to ISM. This contradicts the findings by Delespaux *et al* (2010), that the antibiotics tetracycline and enrofloxacin potentiated the effects of isometamidium against ISM-resistant *T. congolense* strains; the explanation given was that both antibiotics are substrates for ABC-transporters (Delespaux *et al*, 2010) and thus competitively inhibit ISM-efflux. However, we did not find any effects of tetracycline on the growth of *T. b. brucei*, either in the presence or absence of isometamidium (figure 3.19). In addition, the inability of verapamil or enrofloxacin to produce a significant reduction in ISM uptake supports our conclusion that, at least in *T. brucei*, ABC transporters do not seem to be involved in ISM efflux (figure 3.20). Earlier reports of inability of verapamil to reverse resistance to ISM in *T. b. brucei* and in *T. congolense* are consistent with our findings (Wilkes *et al*, 1997; Kaminsky & Zweygarth, 1991). Furthermore, assuming that the theory of up-regulation of ABC transporters in resistance was true for *T. b. brucei*, then intracellular ISM levels in the resistant clones should be near constant after wash and re-suspension in 40 μ M tetracycline, instead of rapidly decreasing (figure 3.18).

3.9. Conclusion

ISM uptake is transporter-mediated in *T. b. brucei* and is not the result of diffusion as figure 3.22 suggests. The balance of evidence suggests that P2 mediates the uptake of ISM in *T. b. brucei*, but may not facilitate a large proportion of the flux. Similarly, the *TbAT1*-like gene *TbAT-E1* also expresses a transporter that is able to transport ISM. It is also clear that the efflux mechanism does not contribute to ISM resistance in *T. b. brucei*.

**4. Development and characterization of clonal lines
resistant to 1 μ M and 15 μ M isometamidium
respectively.**

4.1 Introduction

The control of African trypanosomiasis relies solely on chemotherapy in the absence of large-scale vector control programmes or any hope for a vaccine against the disease in the near future (Delespaux & de Koning, 2007). Most of the drugs currently in use against African trypanosomiasis (sleeping sickness in humans; Nagana in cattle) have been in use for a very long time and are threatened by resistance. In many ways, the situation is worse for the treatment of the veterinary condition as there is widespread resistance to the only two drugs available to treat the condition in sub-Saharan Africa, namely diminazene aceturate and isometamidium (Sow *et al*, 2012; Jamal *et al*, 2005; Matovu *et al*, 1997; Geerts *et al*, 2001). Hence, nagana is still a major constraint to the development of livestock in thirty-seven countries of sub-Saharan Africa (Geerts, 2011). In addition, domestic animals and livestock are able to act as reservoirs for the human infective species of *T. brucei* (Hide *et al*, 1994), particularly in the case of *T. b. rhodesiense*. There is thus an urgent need to improve on the control measures against African Animal Trypanosomiasis. This can be achieved partly by increasing the effectiveness of the few available drugs through reducing the rate of development of drug resistance in the field. It is therefore important that the mechanism of resistance to isometamidium and other veterinary trypanocides be fully elucidated to help develop a method for its resolution and also for the easy identification of resistant trypanosomes. We induced resistance to isometamidium in our 427 laboratory strains, and characterized the resistant phenotype at the biochemical and molecular levels.

4.2 Induction of resistance

It took a period of nine months to adapt the wild type *T. brucei brucei* 427 wt to survive and multiply in 1 μM concentration of ISM and an additional

three months to raise this level of resistance to 15 μM ISM. Cells were incubated in the designated ISM concentration for at least 14 passages (not shown on graph) before being cloned out to ensure complete viability in ISM at that conc. The clones produced from 1 μM were designated ISMR1 while those produced at 15 μM were called ISMR15.

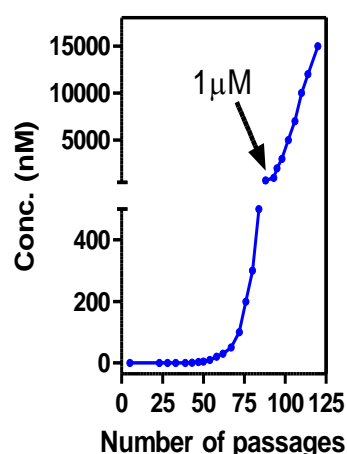


Figure 4.1 Selection for resistance to ISM in concentration/passages. Cells were cultured in increasing concentrations of ISM, starting from 0.05 nM ISM, in HMI-9 medium. Cells were cultured in a particular ISM concentration for > 10 passages before cloning out (or moving to the next ISM concentration; section 2.2.2). Cloning out was done in drug-free medium, and clones were maintained in drug-free HMI-9 medium.

4.3 *In vitro* measurement of rate of multiplication

Analysis of the rate of growth of ISMR1 clone 3 and ISMR15 clone 1 using the one way ANOVA found no significant difference between their growth rate and that of the wild type *T. b.427*. However it should be noted that *Tb427* wt was able to attain the stationary phase of growth after 48 hours of growth while both resistant clones reached the same phase after 72 hours of growth (figure 4.2).

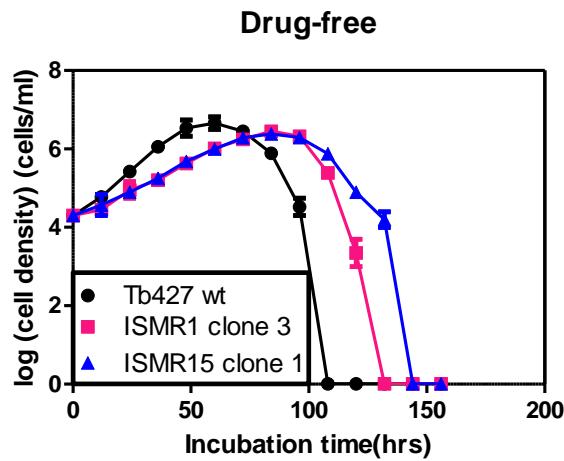


Figure 4.2 Rate of growth of the *Tb427* wt compared with the resistant clones. Cultures were initiated in drug-free HMI-9, starting from a seeding density of 2×10^4 cells/ml for each cell line. Cells were subsequently counted every 12 hours to monitor the cell density.

4.4 Assay for cross resistance to related trypanocides

ISMR1 clone 3 was found to be 44-fold resistant to ISM compared to the wild type control while ISMR15 clone 1 was 121-fold resistant (figure 4.3).

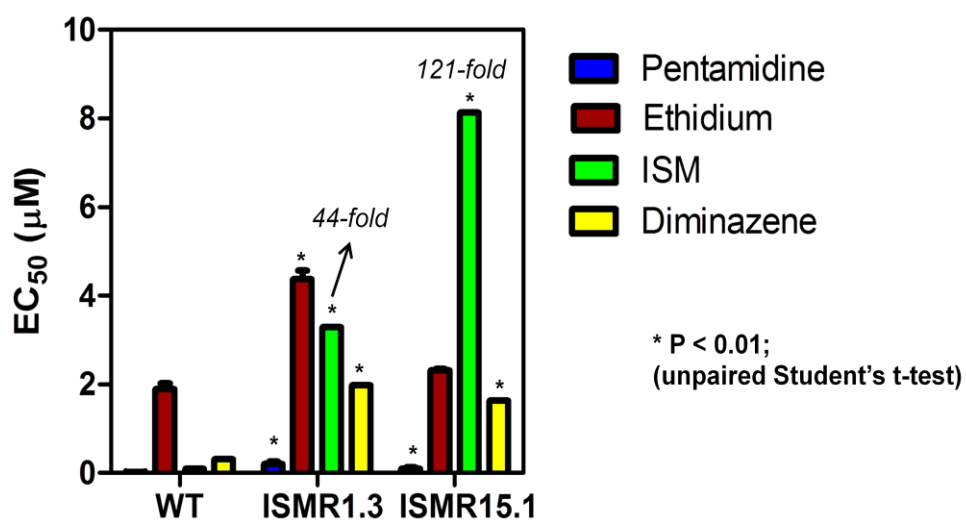


Figure 4.3 Sensitivity of the ISMR clones to trypanocides. EC_{50} values were determined from alamar blue assays using 10^5 cells/ml of each cell line and incubating the assay at $37^\circ C$ and 5%

CO₂ for 48 hour before addition of alamar blue dye. Fluorescence was measured 24 hours after addition of dye. (section 2.2.3). Each bar represents the average of at least three independent assays; errors bars are SEM; *P < 0.01, unpaired Student’s t-test.

Both clones were in addition significantly cross resistant to pentamidine, diminazene and to ethidium bromide (figure 4.3; p < 0.01, unpaired Student’s t-test). Only a minor increase in ethidium EC₅₀ values was observed for the two strains, whereas slightly higher cross-resistance for pentamidine (33-fold; n = 5) and diminazene (9-fold; n = 5) were observed in ISMR1, clone 3. Interestingly, the further adaptation to 15 μM ISM only did not increase resistance to any of the other drugs tested.

4.5 Uptake studies and kinetic characterization

Uptake of [³H] pentamidine was characterized in the ISMR clones in order to check whether any of the known pentamidine transporters have been altered in the clones.

	HAPT1						LAPT1			
	Km AVG	SE	Vmax AVG	SE	Propamidine Ki AVG	SE	Km AVG	SE	Vmax AVG	SE
WT 427	0.036	0.0060	0.0044	0.0004	4.6	0.7	56	8	0.85	0.15
TbAT1-KO	0.029	0.0080			13.0	3.0	50	17		
B48	not detectable						56	7	0.82	0.2
ISMR1	0.059	0.014	0.0043	0.0016	16.9	4.8	38	7	0.32	0.06

Table 4.1 Kinetic parameters of pentamidine uptake in different *Trypanosoma brucei* clones. [³H]-Pentamidine uptake was monitored as described in section 2.2.5. K_m (μM) and V_{max} (pmol/10e7 cells/s) values were subsequently derived from the Michaelis-Menten saturation curve. ISMR1 clone 3 showed a significantly reduced LAPT1 activity (P < 0.05, unpaired Student’s t-test) compared to the same transporter activity in *Tb427* wt. Values of K_m and V_{max} shown are averages of at least 3 independent determinations.

The V_{max} of LAPT1 was significantly reduced in ISMR1 clone 3 (P = 0.043, unpaired Student’s t-test). This suggests a decrease in the number of LAPT1

molecules on the plasma membrane of the trypanosomes. The significantly reduced K_m ($P = 0.018$, unpaired student's t-test) means that the organism balances reduced expression of the LAPT1 with an increased affinity (lower K_m) for pentamidine. Since pentamidine is not the physiological ligand for this transporter, it suggests that pentamidine shares at least some functional group(s) with the physiological substrate and it is for this functional group that the affinity was increased.

Similarly, ISM uptake measured by the innate fluorescence was significantly reduced in ISMR1 ($P < 0.01$; figure 4.4), compared to the wild type.

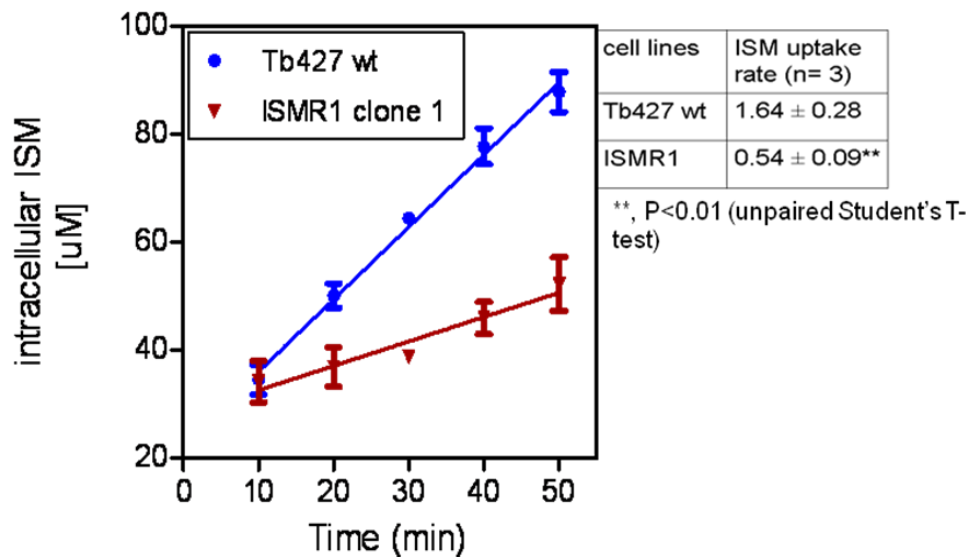


Figure 4.4 Isometamidium uptake in *Tb427* wt and resistant *T. brucei*. Assay was performed in triplicate with $\sim 10^8$ cells/ml of *Tb427* wt and ISMR1 clone 1 in complete HMI-9 medium (+ 10% fetal bovine serum) at room temperature; [ISM] = 10 μM . ISM uptake was measured as described in section 2.2.5. Experiment shown is representative of three independent assays performed in triplicate and showing similar outcomes. The slope of each line represents the rate of uptake ($\mu\text{M}/\text{min}$).

4.6 Sequencing and analysis of AT-like genes from resistant clones.

AT-like genes sequenced include *TbAT1*, *TbAT-E* and *TbAT-A*. Each gene was amplified from the ISMR1 and ISMR15 clones and *Tb427* wt by PCR with Phusion polymerase using the specific primers listed in table 2.1, A-tailed, sub-cloned into pGEMT easy vector and sent for sequencing.

10 colonies each transformed with *TbAT1* gene from *Tb427* wt and ISMR15 clone 1, respectively, and 9 from ISMR1 clone 3 were sequenced. The sequences from the two clones were identical to those from *Tb427* wt, except for a single G to A nucleotide substitution at position 1127 (found in only 2 of the 10 colonies from ISMR15 clone 1). This substitution changes the codon TGC (for cysteine, uncharged but polar) to TAG (for tyrosine, also uncharged but polar) resulting in a conservative mutation. The sequence alignment result is presented in appendix C.

Five colonies transformed with *TbAT-E* gene from ISMR15 clone 1 were sequenced, and none had any unique nucleotide change (all nucleotide changes found in these colonies were also present in either *TbAT-E1* or *TbAT-E2*). Three of the colonies were identical to *TbAT-E1* while the remaining two differed from *TbAT-E1* by 5 nucleotide changes (they were however identical to *TbAT-E2* at those 5 positions). *TbAT-E2* however differed from all the sequenced colonies and from *TbAT-E1* by possessing some 8 unique nucleotide changes (appendix C).

Twelve colonies transformed with *TbAT-A* from ISMR15 clone 1 and 15 colonies from ISMR1 clone 3 were sequenced, but none showed any unique nucleotide change when aligned with wild type sequences for *TbAT-A1* to 6. The 44 nucleotide deletion characteristic of *TbAT-A5* and *TbAT-A6* were present in five of the sequences from ISMR15 clone 1 and in six from ISMR1 clone 3,

suggesting that these two main types of sequences for *TbAT-A* (complete and incomplete) can co-exist in a single clone. None of the sequenced colonies had the *TbAT-A3* allele, since none had the distinguishing adenine nucleotide at position 327. All the other alleles of *TbAT-A* and all the sequenced colonies had a G nucleotide at that position (appendix C).

4.7 Assay for sensitivity to oligomycin and FCCP

Carbonylcyanide-p-trifluoromethoxyphenylhydrazone (FCCP) is a proton ionophore known to uncouple oxidative phosphorylation by transporting protons across the phospholipid bilayer membrane of the mitochondria (Benz & McLaughlin, 1983). Oligomycin on the other hand, inhibits F_1F_0 ATPase activity by causing a conformational change in the F_0 portion of the complex that is transmitted to F_1 , resulting in an impaired binding of the substrate in the catalytic sites (Penefsky, 1985). It causes this change in conformation by binding to the OSCP (oligomycin sensitivity conferral protein) subunit of F_0 (Schnauffer *et al*, 2005).

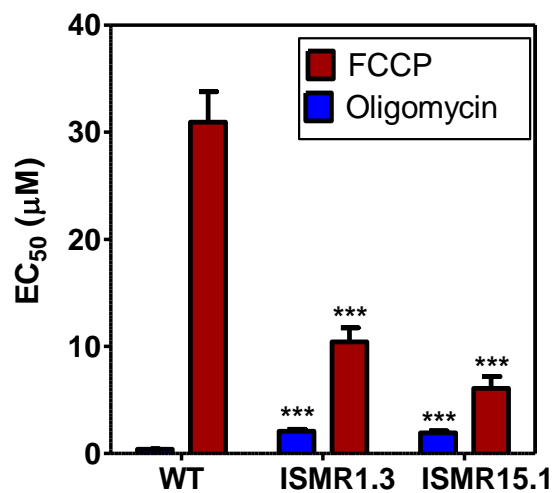


Figure 4.5 Alamar blue assay with oligomycin and FCCP on ISMR clones and *Tb427* wt. EC₅₀ values were determined from alamar blue assays using 10⁵ cells/ml of each cell line (section 2.2.3).

Each bar represents the average of at least 3 independent repeats and SEM; ***P < 0.001, unpaired Student's t-test.

Alamar blue was initially done with a number of compounds that either inhibit ATP production or directly inhibit ABC transporters. Compounds such as enrofloxacin, verapamil, TFP diHCl, prochlorperazine, CCCP, FCCP, valinomycin, oligomycin, potassium cyanide and sodium azide were tested on the ISMR clones and *Tb427* wt. FCCP and oligomycin are the only ones of the inhibitors tested (full results not presented) that gave EC₅₀ values differing significantly (P < 0.001, unpaired Student's t-test) between the ISMR clones and *Tb427* wt (figure 4.5). ISMR1 clone 3 and ISMR15 clone 1 were both 5-fold more resistant to oligomycin than the control *Tb427* wt. This relative insensitivity to oligomycin led us to the prediction that the F₁F₀ ATPase complex has been compromised, since it was found that the insensitivity of *T. evansi* to oligomycin was due to its possession of an altered F₁F₀ ATPase complex (Schnauffer *et al*, 2005). Similarly, our theory of a compromised F₁F₀ ATPase in ISMR clones explains the increase in susceptibility to FCCP. The wild type F₁F₀ ATPase is fully functional and utilizes the energy of ATP to maintain the mitochondrial membrane potential (MMP) in *Tb427* wt by pumping out protons; this explains why *Tb427* wt has a significantly higher EC₅₀ for the proton ionophore than the resistant lines with a dysfunctional proton pump (P < 0.001, unpaired Student's t-test). The ISMR clones, whose F₁F₀ ATPase is impaired and cannot pump protons out as quickly as FCCP activity allows them into the mitochondria, cannot maintain the MMP and these strains are thus more sensitive to FCCP. Therefore, we next assessed whether the MMP was different in the resistant clones.

4.8 Measurement of the mitochondrial membrane potential.

Time point measurement of the MMP was done for *Tb427* wt, ISMR1 clone 3 and ISMR15 clone 1 after 1 h, 3 h and 5 h incubation in 0.5 μ M ISM. The first hour results are presented in figure 4.6. The untreated control MMP value for both ISMR1 clone 3 and ISMR15 clone 1, representing their steady-state MMP, was found to be highly significantly reduced ($P < 0.001$, unpaired Student's t-test) when compared to the value for the untreated control *Tb427* wt. Similarly, the 1h MMP value for the ISM-treated ISMR1 and ISMR15 clones was significantly lower ($P < 0.01$, unpaired Student's t-test) than the value for ISM-treated *Tb427* wt. Comparing the MMP values for the ISM-treated versus the non-treated *Tb427* wt at the third and fifth hours (figure 4.7), the values for the ISM-treated cells were found to be significantly reduced ($P < 0.001$, unpaired student's t-test). This indicates strongly that ISM is responsible for the significant reduction in the MMP values of the ISMR clones; i.e. incubation with ISM over several hours reduced the MMP, as the positively charged drug accumulates inside the mitochondrion, and one adaptation seems to be the lowering of the MMP, reducing the driving force for ISM uptake across the mitochondrial membrane.

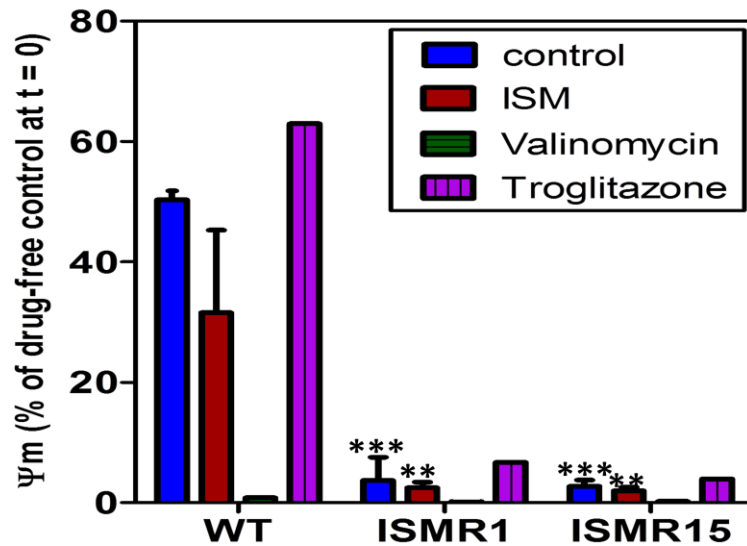


Figure 4.6 MMP measurement in *Tb427* wt, ISMR1 clone 3 and ISMR15 clone 1 after 1h incubation in 0.5 μM ISM in HMI-9 at 37°C and 5% CO₂ (control cells were incubated for 1h in drug-free HMI-9 medium). Cells were also incubated in 100 nM valinomycin and 10 μM troglitazone for 30 minutes as control (details in section 2.2.9) Each bar represents the average of at least 3 independent repeats and SEM; ***P < 0.001, **P < 0.01, unpaired Student’s t-test

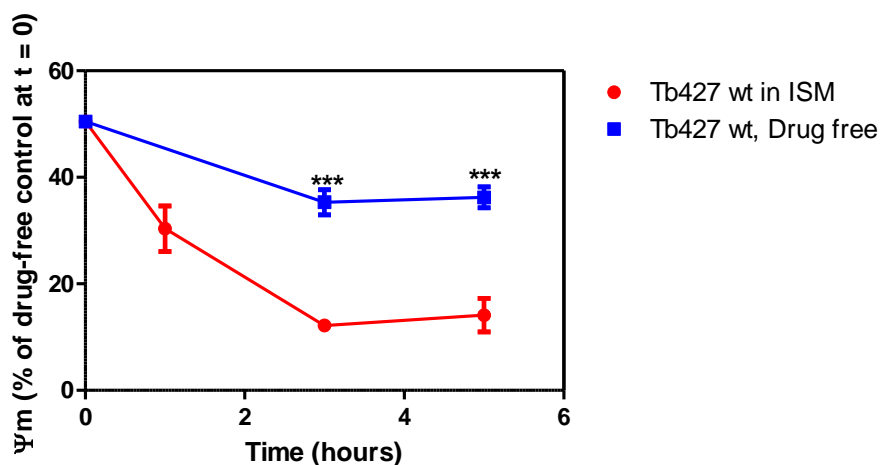


Figure 4.7 MMP at 1h, 3h and 5h time points for *Tb427* wt exposed and unexposed to 0.5 μM ISM. 10⁶ *Tb427* wt cells were incubated in HMI-9(drug free control) and in 0.5 μM ISM dissolved in HMI-9 medium, respectively, at 37 °C and 5% CO₂ for 1h, 3h and 5h before the MMP values were determined (details in section 2.2.9). ***P < 0.001, unpaired Student’s t-test

4.9 Investigating the presence of kDNA in ISM-resistant clones

The function of generating the MMP by the F_1F_0 ATPase is still essential in the bloodstream form *Tb427* wt, despite the stripped-down mitochondrial function in this life cycle stage (Schnauffer *et al*, 2005). The F_1F_0 ATPase complex is partially encoded in the mitochondrial DNA (Schnauffer *et al*, 2005), and oligomycin sensitivity is a conclusive marker for the presence of a functional kinetoplast DNA and a mitochondrial system for protein synthesis (Opperdoes *et al*, 1976). After finding that the ISMR clones had lost both their MMP and oligomycin sensitivity we therefore investigated the presence of kinetoplast DNA in these clones.

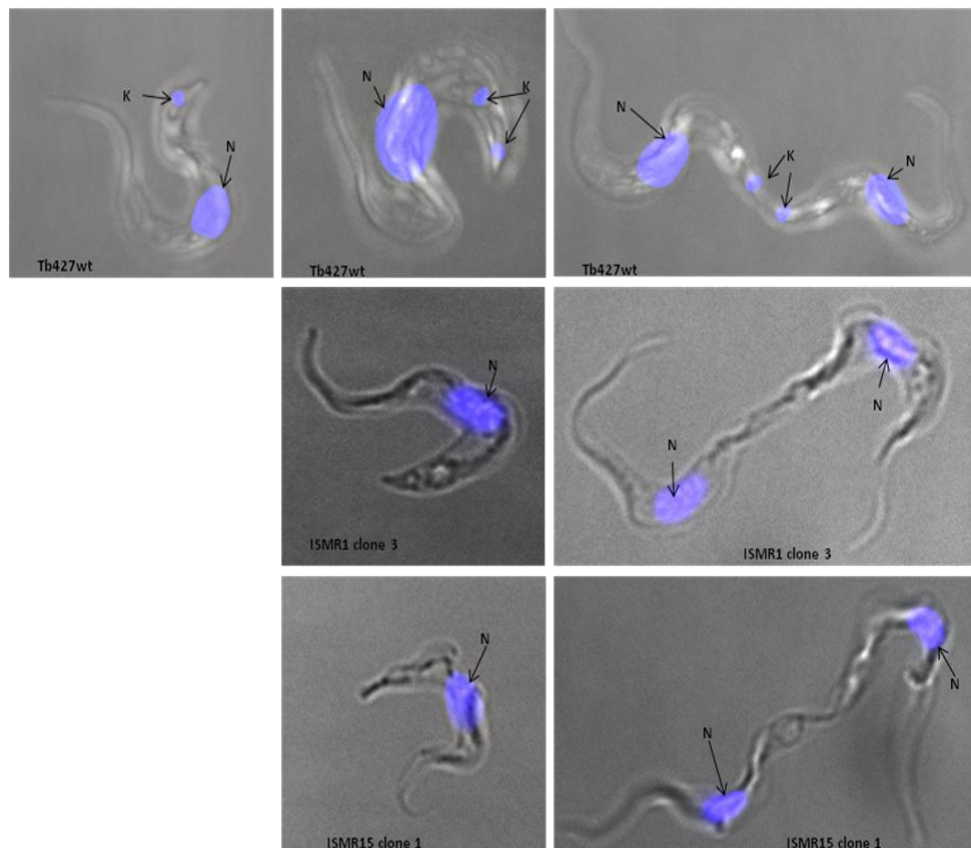


Figure 4.8 Fluorescence microscopy showing the absence of kinetoplast DNA in ISMR clones; *Tb427* wt is included as control. N = nucleus, K = kinetoplast. ISMR1 and ISMR15 were both selected for resistance to ISM by incubating in 1 μ M and 15 μ M ISM, respectively (figure 4.1). Both

clones lost their kDNA (kinetoplast DNA) during the selection process, as demonstrated above. The cells were not exposed to ISM as part of the fluorescence microscopy.

Fluorescence microscopy using DAPI stain to view the DNA content of the cells showed that the ISMR clones have lost their kinetoplast DNA (figure 4.8). This finding was confirmed by PCR for some maxi circle markers (figure 4.9). Maxi circle genes in the mitochondria encode ATPase subunit 6 (A6) and NADH dehydrogenase subunits, ND4, ND5 and ND7 (Bhat *et al*, 1990; Vondruskova *et al*, 2005). These mitochondrial genes are located in the kinetoplast and are usually intact in *Tb427* wt which serves as the positive control. Also, actin which is a nuclear gene was also used as an internal control (to demonstrate presence of the nuclear DNA). Hence, the presence or absence of these maxi circle genes demonstrated by PCR reactions can serve as conclusive evidence of the presence or loss of these genes (and their loss indicates that the kDNA may have been compromised) as shown in figure 4.9.

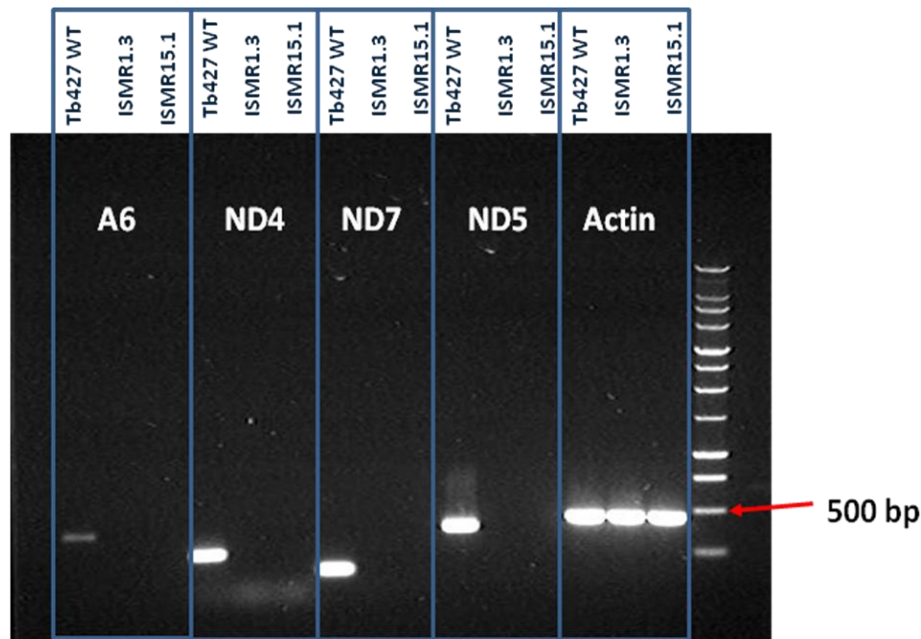


Figure 4.9 PCR showing the loss of maxi circle markers in ISMR clones. The nuclear-encoded gene Actin was included as a control. A6 = ATPase subunit 6; ND4, ND5, ND7 = NADH dehydrogenase subunits 4, 5 & 7 respectively.

The result of the DAPI staining and the PCR together led us to the conclusion that the ISMR clones must have lost their kinetoplast which contains the kDNA, and since ATPase subunit 6 (A6) gene is in the kDNA and is essential for their survival, we looked at the possibility that they have developed a compensation mutation (Schnauffer *et al*, 2005).

4.10 Sequencing and analysis of the ATP synthase gamma gene from the ISMR clones.

Schnauffer and colleagues (2005) suggested that the loss of the mitochondrial gene products (especially A6 which is a subunit of the F_1F_0 ATPase) must be compensated for by mutation of the ATP synthase γ subunit to enable dyskinetoplastic trypanosomes to survive the loss of their kinetoplast (Schnauffer *et al*, 2005). These mutations alter the F_1F_0 ATPase complex and compensate for the loss of the mitochondrial gene products (Schnauffer *et al*, 2005), hence they are called compensating mutations. The γ subunit is the central part of the F1 domain that protrudes from the membrane into the matrix and contains the nucleotide binding and catalytic sites (Atwal *et al*, 2004). ATP synthase γ gene from the ISMR clones and *Tb427* wt was amplified with Phusion polymerase, A-tailed and sub-cloned into pGEMT easy vector and sequenced to check for the presence of mutations. The mutations identified are presented in figures 4.10 and 4.11.

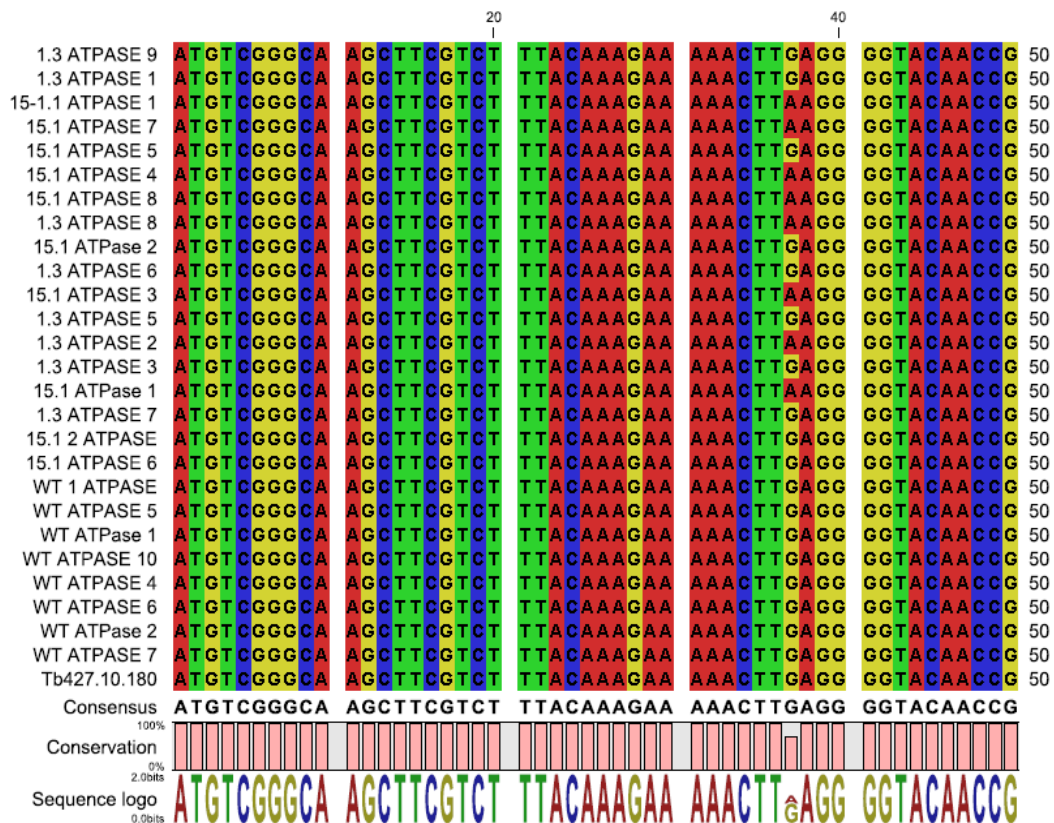


Figure 4.10 Sequence of the ATPase gamma gene from *Tb427* wt, ISMRI clone 3 and ISMR15 clone 1. ATPase γ gene from each cell line was amplified by PCR, sub-cloned in pGEMT and cloned in XLI blue *E. coli*; plasmids extracted from colonies of transformed *E. coli* were subsequently sequenced (details in section 2.2.8). Mutation G37A replaces a negatively charged glutamic acid (E_{13}) with a positively charged lysine (K_{13}), and is therefore a non-conservative mutation of the central subunit of the F_1 (catalytic) domain of the F_1F_0 ATPase.

The first mutation, G37A (E13K) replaced a glutamic acid (acidic amino acid, GAG) with a lysine (basic amino acid, AAG). This mutation is clearly heterozygous (only one of the two alleles was mutated) since it appeared in about half of the colonies sequenced for each of the ISMR clones while the other half bore the wild type GAG codon (figure 4.10).

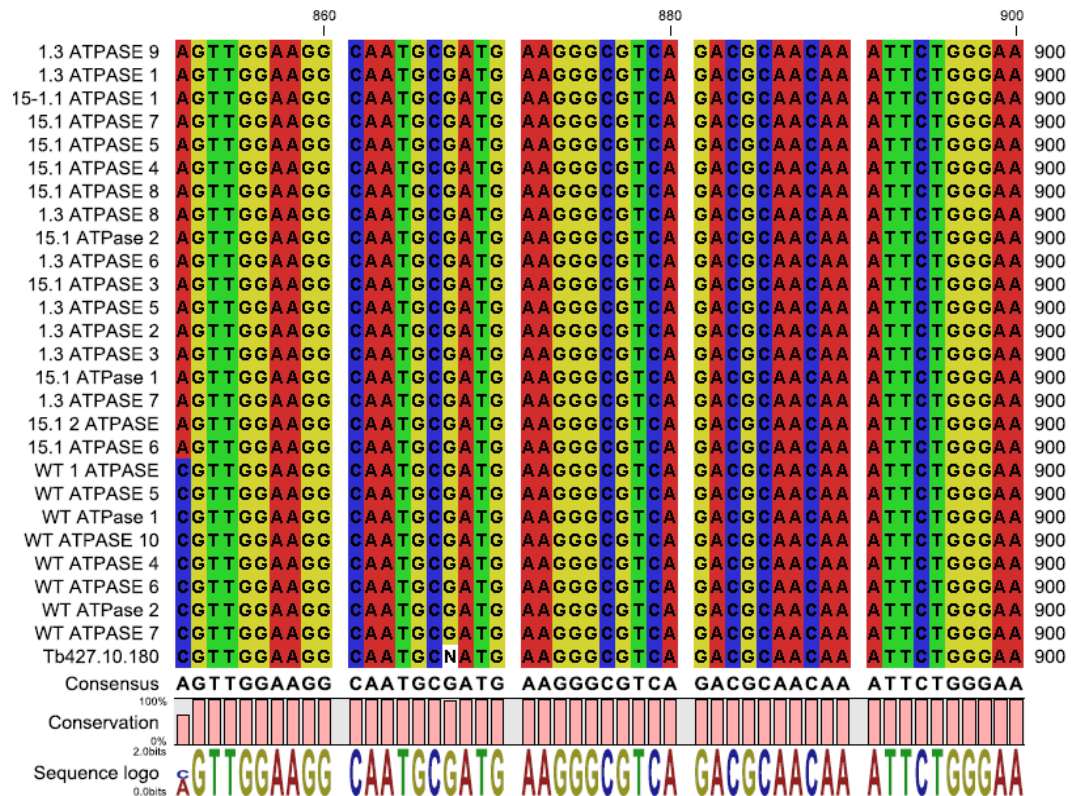


Figure 4.11 Sequence of the ATPase gamma gene from *Tb427* wt, ISMRI clone 3 and ISMR15 clone 1 (Sequencing was done exactly as described in legend to figure 4.10). Mutation C851A (S284*) replaces a serine residue with a stop codon, thereby truncating the γ -subunit of the F1 domain at a point 22 amino acids upstream the actual stop codon.

The second mutation, C851A replaced a serine residue (TCG) with a stop codon (TAG), and is clearly homozygous (both alleles were mutated) since the point mutation appeared in all the colonies sequenced for each ISMR clone (figure 4.11). This point mutation terminates the amino acid sequence of the γ -subunit prematurely, cutting off the last 22 amino acids (at the carboxyl terminal) before the actual stop codon for the gene. We assessed the significance of this sequence truncation by introducing this exact mutation into *Tb427* wt and found that this mutation C851A-ATPase has a significant effect on the function of *T. brucei brucei* F₁F₀ ATPase since it was able to make the organism significantly resistant to ISM and EtBr (findings are presented in chapter 5).

4.11 Discussion

Our results suggest that the rate of cell division in *Tb427* was reduced on the induction of resistance to ISM (figure 4.2). This is consistent with the finding that ISMR clones have lost much of their MMP since it is MMP that drives the import into the mitochondria of proteins encoded by nuclear genes (Schnauffer *et al*, 2005). Therefore, since the mitochondrion needs to grow and divide as part of the cell division programme, and this growth depends on the insertion of newly synthesized constituents, resulting in expansion of the various compartments of each mitochondrion (Neupert, 1997), a reduction in MMP should reduce the rate of this transport of proteins, mitochondrial growth and ultimately cell division. Similarly, infectivity is a direct function of cell multiplication since every trypanosome cell can synthesize only a single variant surface glycoprotein (VSG) antigen (due to transcriptional control of gene expression); hence, antigenic variation is maintained by the differential and successive expression of a large number of different antigen genes (Pays, 1985). This suggests that infectivity is therefore indirectly dependent on MMP in *T. b. brucei* (findings from infectivity studies in mice are presented in chapter 5).

Apart from the very high resistance to ISM in the ISMR clones, cross resistance was also developed to the related phenanthridine, ethidium bromide and to the diamidines, pentamidine and diminazene (figure 4.3). Cross resistance to diminazene is consistent with the cross resistance to tubercidin (figure 3.7) which is a marker for a defective P2 transporter; it is also consistent with the reduction of rate of ISM uptake to half by 333 μ M diminazene (figure 3.21). When all these are put together with the cross resistance to pentamidine (figure 4.3) and the inhibition of ISM uptake by pentamidine (figure 3.21; statistically insignificant), we can say that ISM is transported by a pentamidine

transporter that also transports diminazene, and that can only be the P2 transporter (de Koning *et al*, 2004; Stewart *et al*, 2010). This builds on the observations reported in Chapter 3 and is further evidence that P2 is partly responsible for ISM uptake. The reduction in V_{\max} found for the low affinity pentamidine transporter, LAPT1 in ISMR1 clone 3 indicates that the expression of this transporter was down-regulated in the resistant line. This piece of evidence suggests a role for LAPT1 in ISM uptake as well. Part of the difficulty in studying ISM uptake seems to be that multiple transporters contribute to the process, none of them contributing a very major part of the total flux.

FCCP works against the F_1F_0 ATPase complex by creating a channel to return protons into the mitochondria as the enzyme pumps them out to create the essential MMP. Oligomycin on the other hand is a specific inhibitor of the F_0 subunit of the F_1F_0 ATPase complex (Coustou *et al*, 2003b); it binds to the OSCP (oligomycin sensitivity conferral protein) subunit of F_0 (Schnauffer *et al*, 2005). Hence, the loss of sensitivity to oligomycin is an indication that the F_1F_0 ATPase complex has been altered as is the case in dyskinetoplastid and akinetoplastid trypanosomes that have lost the F_0 subunit (section 1.5.2). Figure 4.12 summarizes our understanding of the effect of oligomycin and FCCP on ISM uptake and MMP. It is clear from the investigation that the high level of ISM resistance was multi-factorial, with adaptations reducing total drug uptake through TbAT1/P2 and probably through LAPT1, and the loss of kinetoplast and MMP, enabled by the mutation in the γ -subunit of the mitochondrial ATPase.

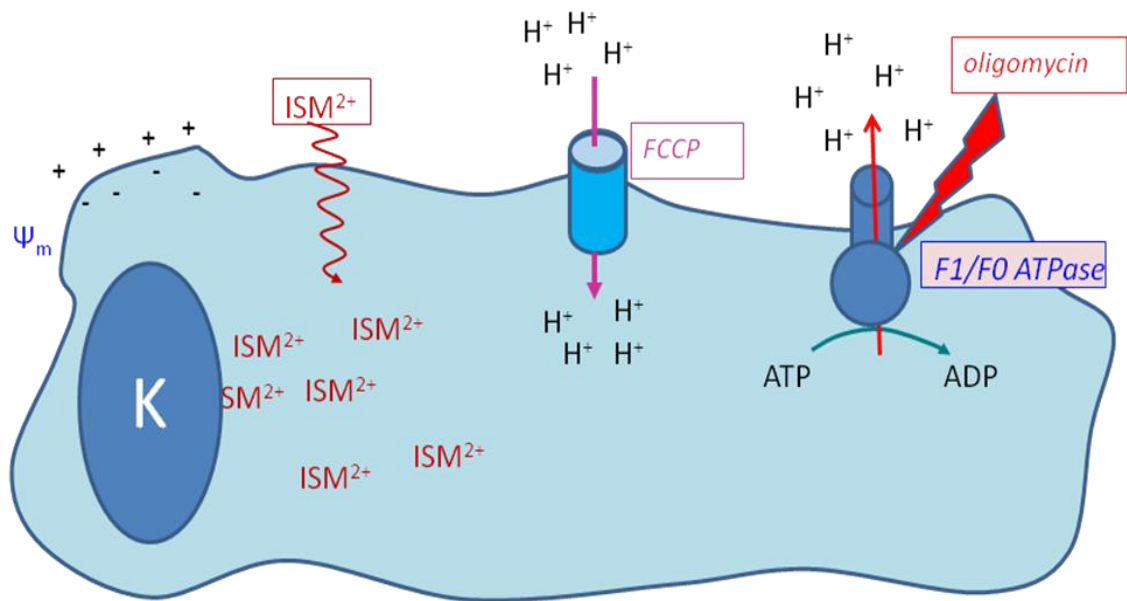


Figure 4.12 Model for explanation of the effects of oligomycin and FCCP on F₁F₀ ATPase. The F₁F₀ATPase uses the chemical energy of ATP to pump out protons from the mitochondrial matrix, creating a membrane potential, Ψ_m which facilitates ISM uptake. This potential can be wastefully dissipated in the presence of FCCP which creates a channel for the movement of protons back into the matrix.

4.12 Conclusion

ISM is transported into the trypanosomal mitochondria, down the MMP which is created and maintained by the F₁F₀ ATPase complex. This MMP is critical to the biogenesis of the mitochondria since it aids the import of proteins and other factors synthesized in the cytosol into the mitochondria.

**5. ISM resistant clones are dyskinetoplastic;
evidence for a new resistance marker**

5.1 Introduction

The knowledge of drug targets within the parasites is absolutely necessary for the judicious use of drugs especially when one is faced with resistance to a particular trypanocide and is trying to determine the best choice of drug to administer (Matovu *et al*, 2001). This knowledge is also very vital in making the choice of a drug pair to administer together as a combination therapy. In this case, a sound knowledge of the mechanism of action of the different drug candidates will certainly help in the selection of the pair that acts on different metabolic targets so that their combination produces a synergy (Matovu *et al*, 2001). The intracellular target of ISM is yet to be elucidated. The results presented in chapter 4 have so far been correlative. Hence, we have demonstrated the loss of the mitochondrial DNA and mitochondrial membrane potential, and a set of mutations in the ATPase gamma gene of our resistant clones which are missing in the wild type strain. In this chapter, we demonstrate the importance of these changes to ISM resistance by reconstructing the resistance phenotype in the wild type *Tb427*.

5.2 Site-directed mutagenesis of the wild type ATP synthase gamma gene to introduce the compensating mutation

Of the two mutations identified in the ISM resistant clones, the nonsense mutation (S284*, C851A) was chosen for analysis because we believe that this mutation should have a greater impact on the ATP synthase gamma gene since it introduced a stop codon within the open reading frame of the gene, thus truncating the expected gene product. Site-directed mutagenesis was carried out on the construct, pEnT6-Blast + wt ATPase γ , as outlined in section 2.2.6.4 and colonies of *E. coli* transformed with the mutated plasmid, pEnT6-Blast +

S284* ATPase γ were sequenced to check that the mutation was correctly introduced. One of the colonies found to have been transformed with the correctly mutated plasmid was grown in an overnight culture and mini-prepped to extract the mutated plasmid which was subsequently linearised with the *NotI*, purified with the Macherey-Nagel PCR clean up kit and concentrated by precipitation with ethanol. The resulting DNA sample was quantified on a nano-drop Spectrophotometer and the volume containing 10 μ g of DNA was used to transfect *Tb427* wt cells. Three clones were subsequently selected under drug pressure, namely *T.b.427* wt + pEnT6-Blast-S284*-ATPase γ clones 1, 2 and 3 (will be referred to as *Tb427* wt + S284* ATPase γ clones in this chapter). ATP synthase gamma from the selected clones were generated by PCR, sub-cloned into pGEMT easy vector and sent to be sequenced to check for the presence of the compensating mutation, correct integration of the plasmid and to determine the genotype after the mutation (whether only one or both of the alleles of the ATP synthase was replaced by the mutated plasmid).

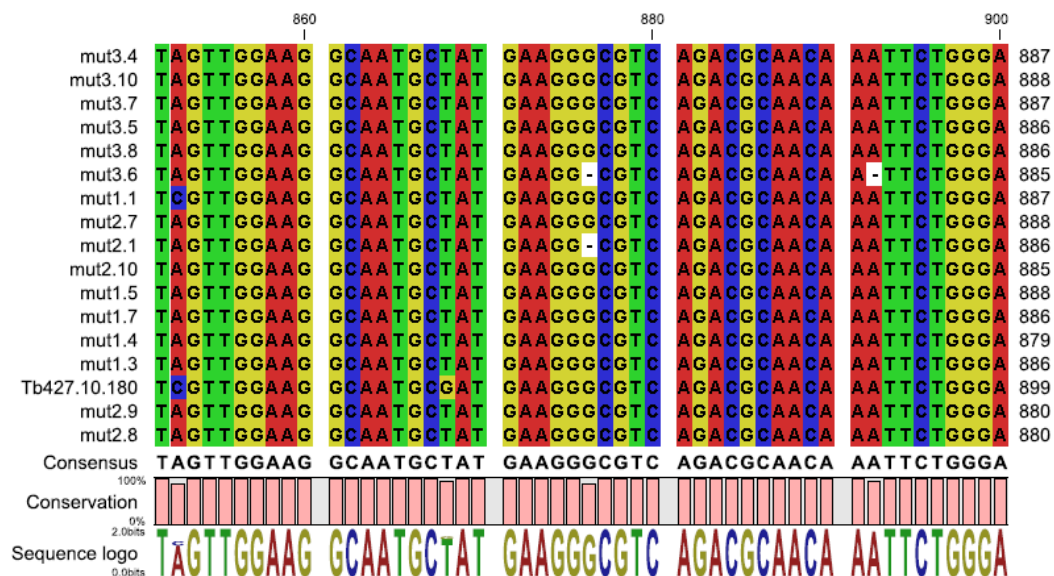


Figure 5.1 Sequence of the ATPase gamma gene from *Tb427* wt + S284* ATPase γ clones, immediately after transformation with pEnT6-Blast + C851A. ATPase γ . ATPase γ gene from each cell line was amplified by PCR, sub-cloned in pGEMT and cloned in XLI blue *E. coli*; plasmids extracted from colonies of transformed *E. coli* were subsequently sequenced (details in section

2.2.8). Mut1.3 used in the figure means *E. coli* colony number 3 of those transformed with ATP synthase gamma gene from *Tb427* wt + S284* ATPase γ clone 1, etc. (figure 5.18 shows the position of the gamma subunit in the F_1F_0 ATPase complex).

The mutation (C851A) can be seen to be visibly present in all the colonies sent for sequencing except in colony 1 of those picked for *Tb427* wt + S284* ATPase γ clone 1 (mut1.1) which bears the wild type C nucleotide (figure 5.1). This result clearly indicates that *Tb427* wt + S284* ATPase γ clone 1 is heterozygous for the C851A mutation (only one allele of the ATP synthase gamma was replaced by the mutated plasmid) while *Tb427* wt + S284* ATPase γ clones 2 and 3 were both homozygous for the same mutation (both alleles of the ATP synthase gamma were replaced by the mutated plasmid). Thus, *Tb427* wt + S284* ATPase γ clone 1 still has one copy of the wild type gene while *Tb427* wt + S284* ATPase γ clones 2 and 3 carry the compensating mutation on both alleles of their ATP synthase gamma gene. To assess the effect of the introduced mutation on the wild type cell function, we measured the sensitivity to selected trypanocides, as well as the mitochondrial membrane potential. We also did fluorescence microscopy (DAPI staining) to check for the presence of the mitochondrial DNA.

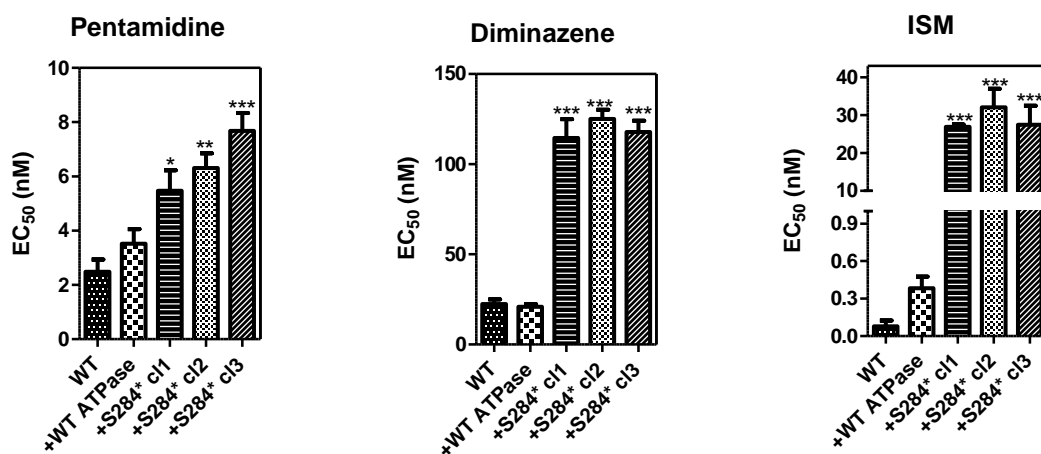


Figure 5.2 Sensitivity of *Tb427* wt + S284* ATPase γ clones to selected trypanocides in comparison to *Tb427* wt + wt ATPase γ . EC₅₀ values were determined by a modified alamar blue

assay; plates were seeded with 5×10^3 cells/ml density of all cell lines, incubated at 37°C and 5% CO₂ for 72 hours before addition of alamar blue dye. Fluorescence values were measured 18 hours after the addition of dye (details in section 2.2.3). WT = *Tb427* wt; +WT ATPase = *Tb427* wt + wt ATPase γ ; +S284* cl1 = *Tb427* wt + S284* ATPase γ clone 1; etc. *P < 0.05, **P < 0.01, ***P < 0.001, one way ANOVA using Graphpad prism 5.0 (n = 4).

The alamar blue assay protocol was modified to amplify differences in drug sensitivity between the clones. This amplification was achieved by incubating the cells in ISM or EtBr long enough for them to lose their kDNA (72 hours was found to be sufficient for the cells to lose their kinetoplasts). Hence, the seeding density was reduced from 10^5 cells/ml to 5×10^3 cells/ml; alamar blue dye was added after 72 hours of incubation and the fluorescence was measured exactly 18 hours after. All three clones, *Tb427* wt + S284* ATPase γ clones 1, 2 and 3 were significantly more resistant to ISM, diminazene and pentamidine than both controls *Tb427* wt and *Tb427* wt + wt ATPase γ , when analysed by one way ANOVA, using the PRISM software (figure 5.2). All three clones were much more resistant to ISM (at least 100 folds) and EtBr (at least 240 folds) than to diminazene (5 folds) and oligomycin (5 folds), when compared to *Tb427* wt + wt ATPase γ ; resistance to pentamidine amounted to only about 2 folds in all the clones (figure 5.2). The cross-resistance to oligomycin directly indicates that the γ -subunit of the organisms' F₁F₀-ATPase has been compromised.

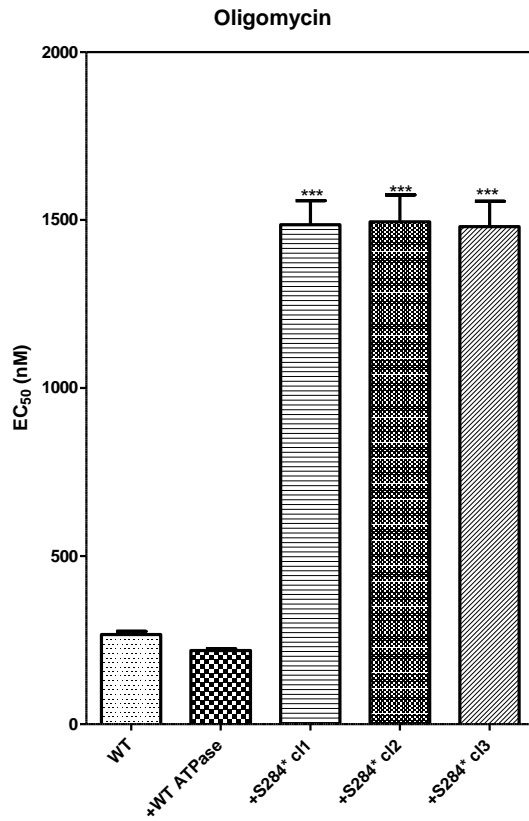


Figure 5.3 Sensitivity of *Tb427* wt + S284* ATPase γ clones to oligomycin. EC₅₀ values were determined by a modified alamar blue assay; plates were seeded with 5×10^3 cells/ml density of all cell lines, incubated at 37°C and 5% CO₂ for 72 hours before addition of alamar blue dye. Fluorescence values were measured 18 hours after the addition of dye (details in section 2.2.3). WT = *Tb427* wt; +WT ATPase = *Tb427* wt + wt ATPase γ ; +S284* cl1 = *Tb427* wt + S284* ATPase clone 1; etc. ***P < 0.001, one way ANOVA using Graphpad prism 5.0 (n = 4).

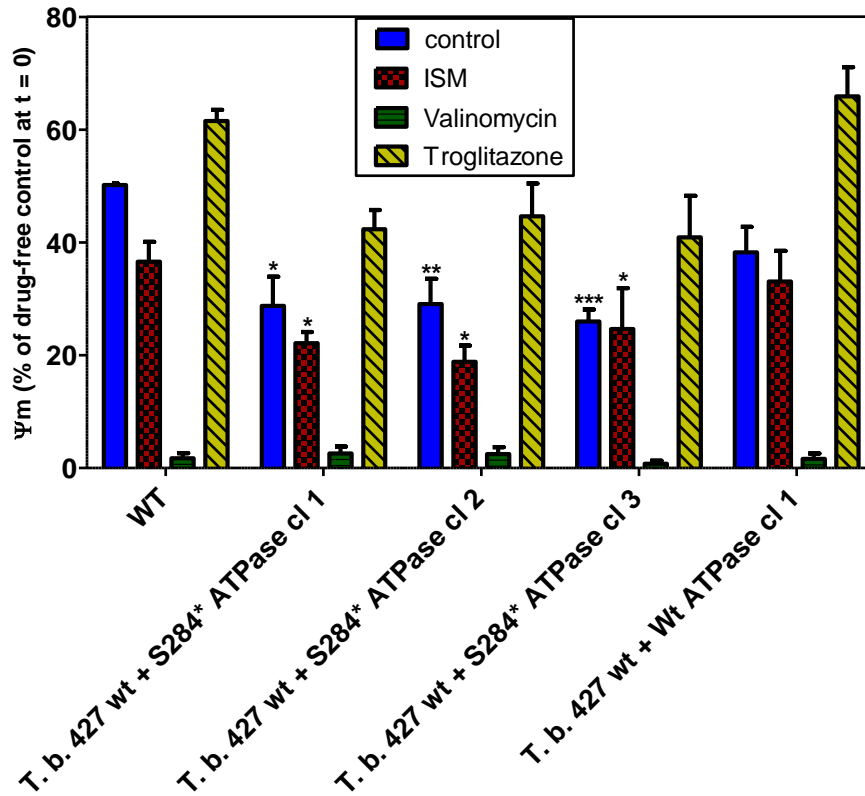


Figure 5.4 Mitochondrial membrane potential assay for *Tb427 wt + S284** ATPase clones. Cells were incubated in 0.5 μ M ISM for 1h, in 100 nM valinomycin or 10 μ M troglitazone for 30 minutes; all samples were then centrifuged at 1500 x g and resuspended in 25nM TMRE (tetramethylrhodamine ethyl ester; section 2.2.9). All control cells were incubated for 1h in fresh HMI-9 media. *Tb427 wt* control cells were used to calibrate the flow cytometer to 50% before measurements are made for other cell types (more details in section 2.2.9). * $P < 0.05$, ** $P < 0.01$, *** $P < 0.001$, unpaired Student's t-test (n = 3).

A measurement of the mitochondrial membrane potential of the *Tb427 wt + S284** clones indicates that significant reductions in the mitochondrial membrane potential have already occurred. Though the individual mitochondrial membrane potential values are not as low as those found for the ISMR clones; the significantly reduced mitochondrial membrane potential values at this stage indicate that a reduced mitochondrial potential may be necessary for ISM resistance.

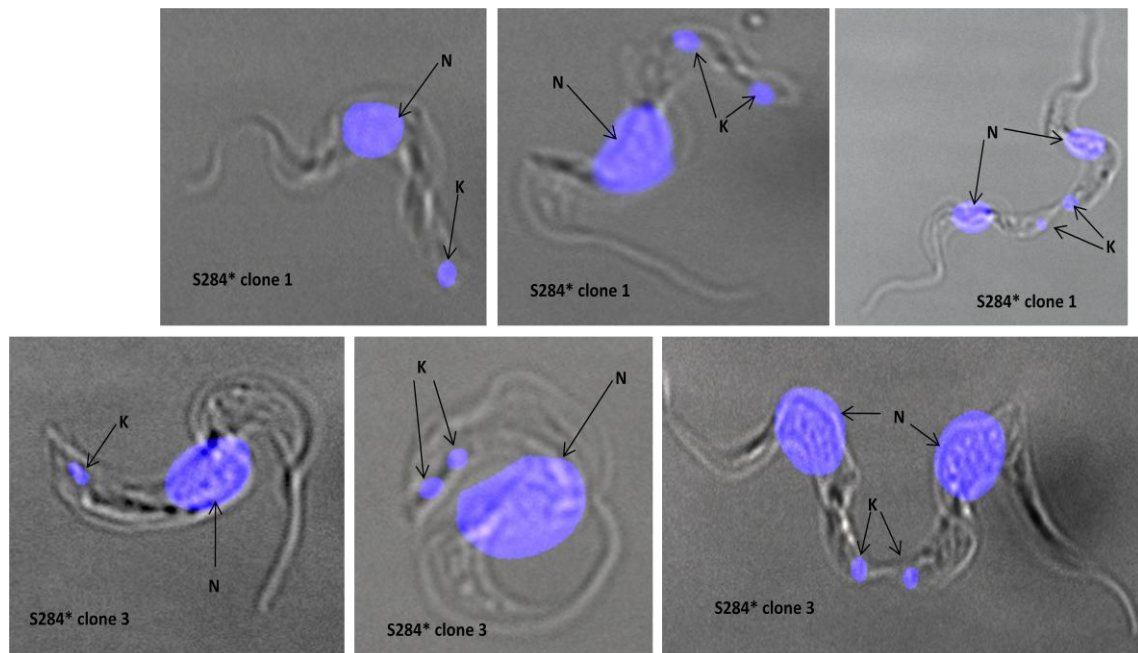


Figure 5.5 Fluorescence microscopy images showing DAPI stain of cellular DNA of *Tb427* wt + S284* ATPase γ clones 1 and 2. S284* clone 1 = *Tb427* wt + S284* ATPase γ clone 1, etc.

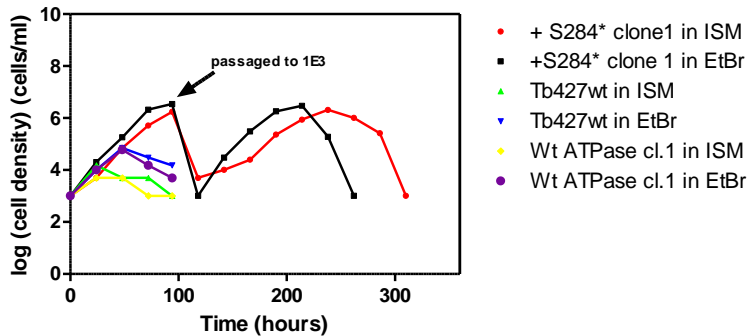
When the fluorescence microscopy images of DAPI stained cells were taken, it was found that the kinetoplasts were still intact. Hence, the compensating mutation we had introduced does not cause the spontaneous loss of the kinetoplast, i.e. without selective pressure.

5.3 Exposure of *Tb427* wt + S284* clones to Isometamidium or Ethidium

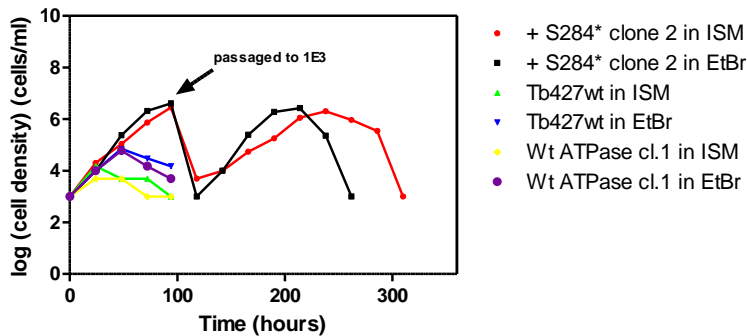
To demonstrate the selective advantage that possession of the compensating mutation confers on the trypanosomes, the *Tb427* wt + S284* clones were exposed at a density of 10^3 cells/ml to 20 nM ISM or Ethidium bromide (EtBr), with *Tb427*wt cells as control, to demonstrate their relative insensitivity to either ISM or ethidium bromide. Cell counts were also taken every 12 hours and plotted (figure 5.6). *Tb427* wt + S284* clones were all able to multiply in 20 nM ISM or ethidium bromide though they have no previous contact with either drug. *Tb427* wt cells were however unable to multiply in either ISM or ethidium bromide. This is direct evidence that the C851A mutation adapts the

parasites for survival under drug pressure and so this mutation confers a selective advantage to the trypanosomes for survival in ISM or ethidium bromide.

Tb427 wt + S284* ATPase gamma clone 1



Tb427 wt + S284* ATPase gamma clone 2



Tb427 wt + S284* ATPase gamma clone 3

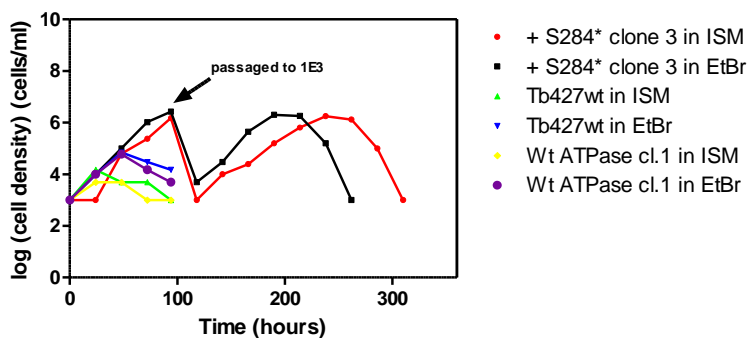


Figure 5.6 *In vitro* measurement of rate of multiplication of *Tb427* wt + S284* ATPase clones in ISM or EtBr. Assay was started with a 10^3 cells/ml seeding density for all cell lines, in the presence of 20 nM ISM or EtBr. Cell density was measured by counting on a haemocytometer once every 24 hours. All cell lines were sub-cultured to 10^3 cells/ml after the 4th day count.

5.3.1 In vitro measurement of resistance to trypanocides

Next was the re-assessment of the sensitivity to the trypanocides after incubation for a total of about 12 days in ISM or EtBr. The same protocol for modified alamar blue outlined in section 5.2 was used.

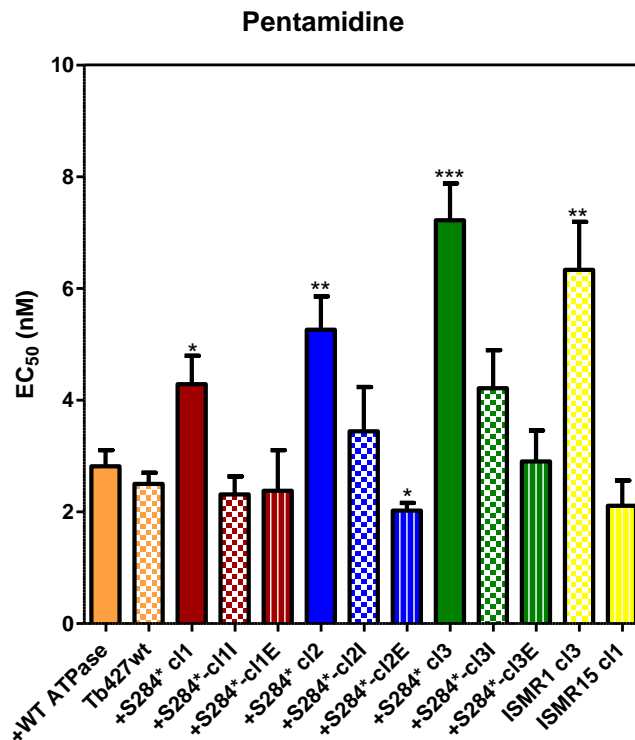


Figure 5.7 Cross-resistance to pentamidine in *Tb427* wt + *S284** ATPase clones before and after incubation in 20 nM ISM or EtBr. EC₅₀ values were determined by a modified alamar blue assay; plates were seeded with 5 x 10³ cells/ml density of all cell lines, incubated at 37°C and 5% CO₂ for 72 hours before addition of alamar blue dye. Fluorescence values were measured 18 hours after the addition of dye (details in section 2.2.3; ISMR clones were included for comparison). +WT ATPase = *Tb427* wt + wt ATPase γ ; +*S284** cl1I = *Tb427* wt + *S284** ATPase clone 1 cells after incubation in 20 nM ISM; +*S284** cl1E = *Tb427* wt + *S284** ATPase clone 1 cells after incubation in 20 nM EtBr; etc. *P < 0.05, **P < 0.01, ***P < 0.001, unpaired Student's t-test (n \geq 3). *Tb427* wt + *S284** ATPase clones were compared with *Tb427* wt + wt ATPase γ while the ISMR clones were compared with the untransformed *Tb427* wt.

Figure 5.7 shows that resistance to pentamidine was significant in all three *Tb427* wt + S284* ATPase γ clones before incubation in ISM or EtBr (figure 5.7, consistent with figure 5.2). This resistance was generally reduced after about 12 days incubation in ISM or pentamidine (*Tb427* wt + S284* ATPase γ clone 2E is actually significantly more sensitive to pentamidine than *Tb427* wt + wt ATPase!). The trend in figure 5.7 (also considering ISMR1 clone 3 and ISMR15 clone 1) when combined with data for resistance to ISM after ISM or EtBr incubation strongly suggests a reciprocal relationship between pentamidine and ISM resistance.

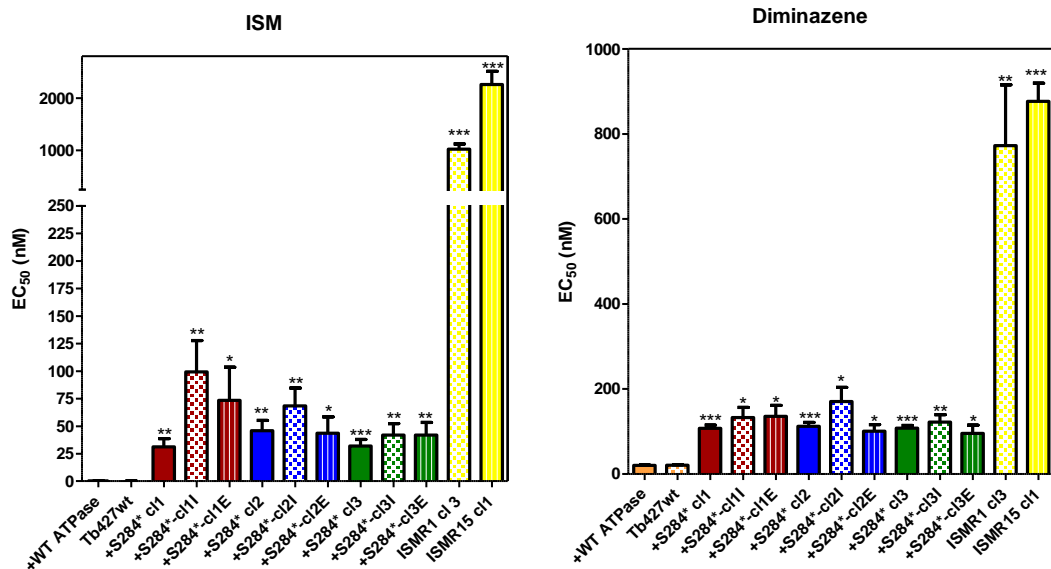


Figure 5.8 Resistance to ISM and cross-resistance diminazene in *Tb427* wt + S284* ATPase clones before and after incubation in 20 nM ISM or EtBr (experiment was performed as described in the legend to figure 5.7, ISMR clones were included for comparison). +WT ATPase = *Tb427* wt + wt ATPase γ ; +S284* c1I1 = *Tb427* wt + S284* ATPase clone 1 cells after incubation in 20 nM ISM; +S284* c1IE = *Tb427* wt + S284* ATPase clone 1 cells after incubation in 20 nM EtBr; etc. ***P<0.05, **P < 0.01, P < 0.001, unpaired Student's t-test (n \geq 3). *Tb427* wt + S284* ATPase clones were compared with *Tb427* wt + wt ATPase γ while the ISMR clones were compared with the untransformed *Tb427* wt.

Resistance to diminazene remained fairly constant across the clones after the incubation in ISM or EtBr. The point of interest however is that the large difference in level of resistance to either ISM or diminazene between the *Tb427* wt + S284* ATPase γ clones and the ISMR clones seems to suggest that there are other factors contributing to ISM and diminazene resistance in the drug-adapted clones ISMR1 and ISMR15 (difference in the rate of uptake and accumulation is in fact another important factor, which we have discussed in chapter 3). The reverse however seems to be the case for EtBr and oligomycin (figure 5.8). The similarity in the level of resistance to these two compounds in both the *Tb427* wt + S284* ATPase γ clones and the ISMR (drug-adapted) clones seems to suggest that the mechanism of resistance to oligomycin and EtBr depends on mutating the γ -subunit of the F_1F_0 -ATPase alone.

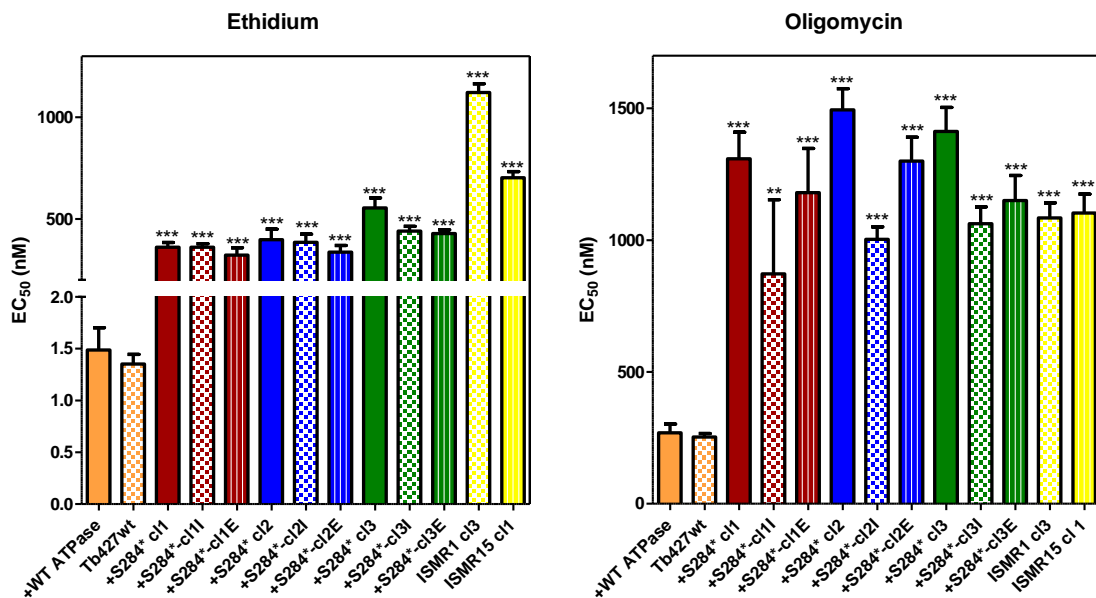


Figure 5.9 Cross-resistance to EtBr and oligomycin in *Tb427* wt + S284* clones before and after incubation in 20 nM ISM or EtBr (experiment was performed as described in the legend to figure 5.7, ISMR clones were included for comparison). +WT ATPase = *Tb427* wt + wt ATPase γ ; +S284* cl1I = *Tb427* wt + S284* ATPase γ clone 1 cells after incubation in 20 nM ISM; +S284* cl1E = *Tb427* wt + S284* ATPase γ clone 1 cells after incubation in 20 nM EtBr; etc. **P < 0.01, ***P < 0.001, one way ANOVA using Graphpad prism 5.0 (n \geq 3). *Tb427* wt + S284* ATPase γ clones were

compared with *Tb427* wt + wt ATPase γ while the ISMR clones were compared with the untransformed *Tb427* wt.

5.3.2 The mitochondrial membrane potential

The mitochondrial membrane potential (MMP) was further reduced in the *Tb427* wt + *S284** ATPase γ clones after they were incubated in ISM and EtBr (figure 5.10).

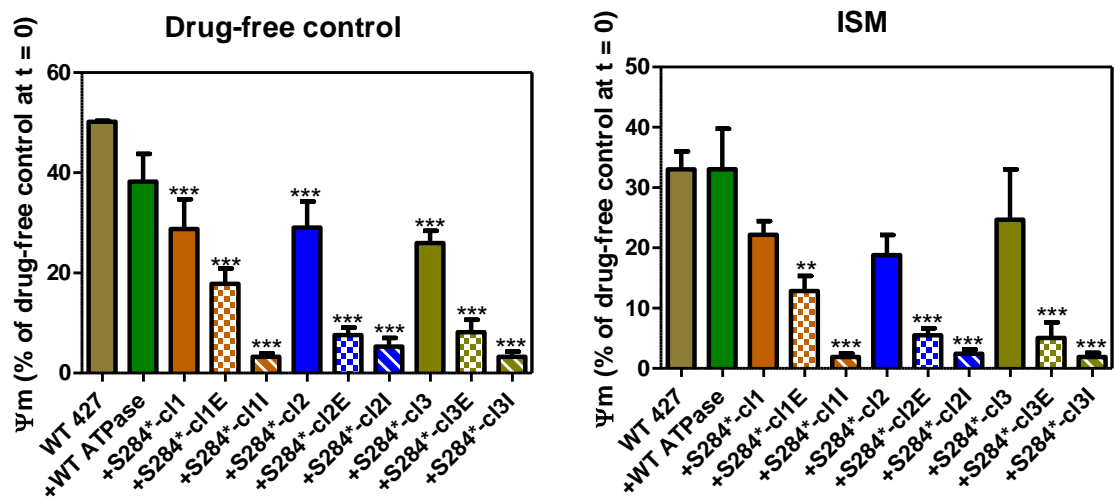


Figure 5.10 Mitochondrial membrane potential (MMP) of *Tb427* wt + *S284** ATPase clones, drug-free and after 1h incubation in 0.5 μ M ISM, to determine the effect of 72 hours incubation in 20nM ISM or EtBr on the MMP of mutant cells (experiment was performed as described in the legend to figure 5.4). +WT ATPase = *Tb427* wt + wt ATPase γ ; +*S284** cl1I = *Tb427* wt + *S284** ATPase γ clone 1 cells after incubation in 20 nM ISM; +*S284** cl1E = *Tb427* wt + *S284** ATPase γ clone 1 cells after incubation in 20 nM EtBr; etc. **P < 0.01, ***P < 0.001, one way ANOVA test using Graphpad prism 5.0.

Generally, for the three clones of *Tb427* wt + *S284** ATPase γ incubated for about 12 days in 20 nM ISM or EtBr, the trend in figure 5.10 suggests that incubation in 20 nM ISM seems to reduce the MMP more than 20 nM EtBr.

5.3.3 Fluorescent microscopy

Fluorescence microscopy of DAPI-stained cells showed that *Tb427* wt + S284* ATPase γ clones I and E may have lost their kinetoplasts in the 12 days of incubation in ISM or EtBr.

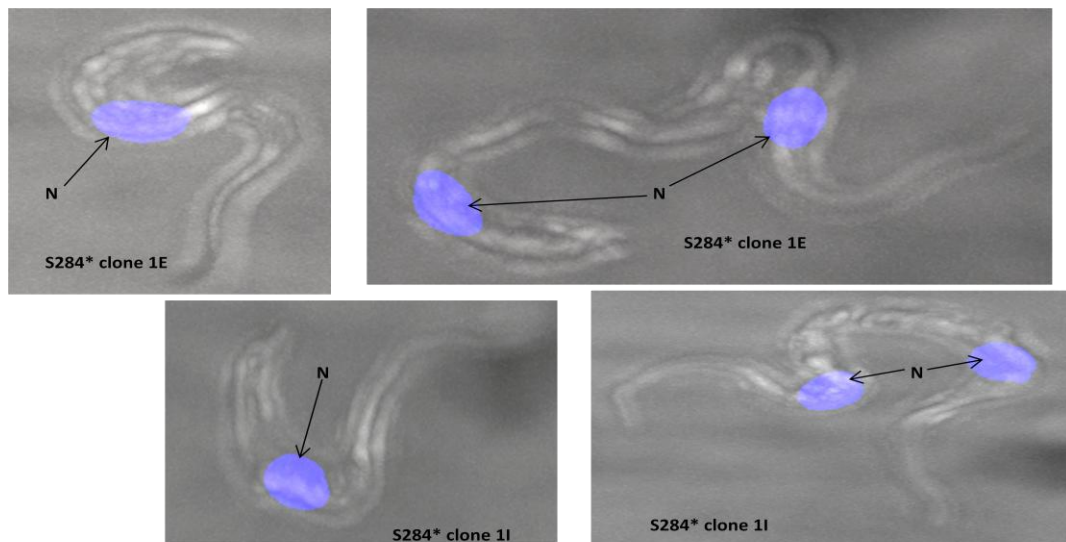


Figure 5.11 Fluorescent microscopy of DAPI-stained images of *Tb427* wt + S284* ATPase γ clones 1I and 1E, showing apparent loss of kinetoplast.

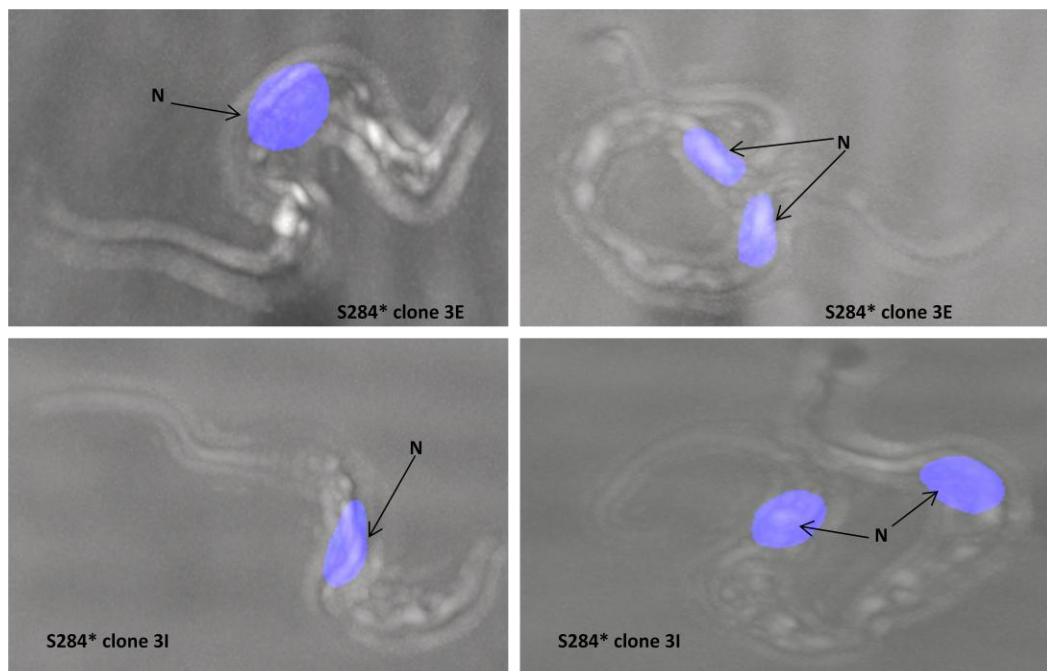


Figure 5.12 Fluorescent microscopy of DAPI-stained images of *Tb427* wt + S284* ATPase γ clones 3I and 3E, showing apparent loss of kinetoplast.

5.3.4 Loss of Kinetoplast PCR.

Considering that *Tb427* wt + S284* ATPase γ clone 1 was heterozygous for the mutation S284* before the incubation in ISM or EtBr (figure 5.1), we next used PCR to further ascertain if some or all the markers for the mitochondrial DNA was lost.

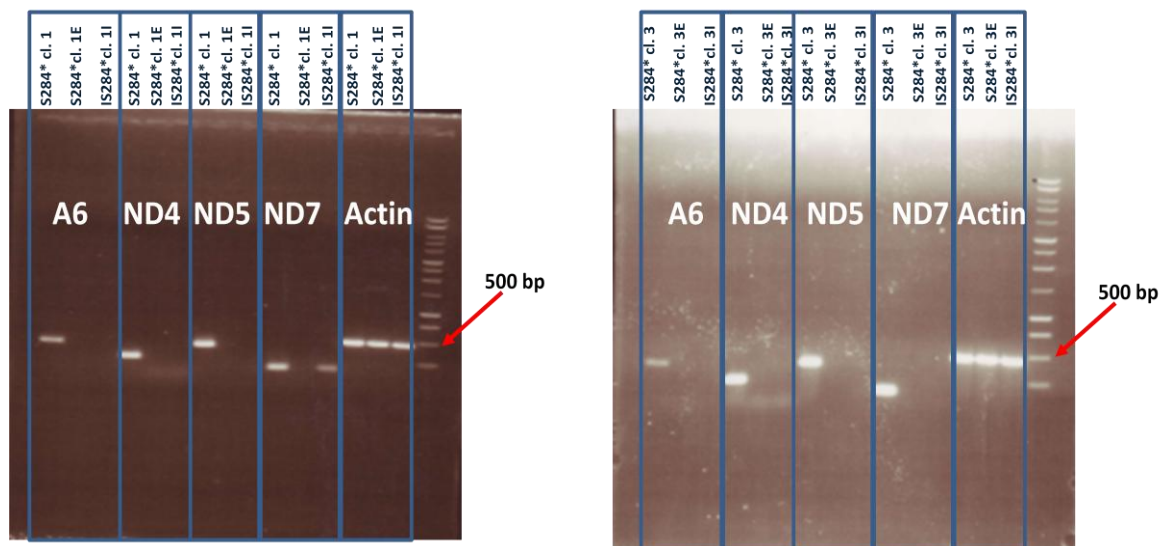


Figure 5.13 PCR showing the loss of maxi circle markers in *Tb427* wt + S284* ATPase γ clones 1E and I, and clones 3E and I. The nuclear-encoded gene Actin was included as a control. A6 = ATPase subunit 6; ND4, ND5, ND7 = NADH dehydrogenase subunits 4, 5 & 7 respectively.

The PCR of kinetoplast DNA indicates that the markers checked for were lost in *Tb427* wt + S284* ATPase γ clones 3E and 3I while *Tb427* wt + S284* ATPase γ clone 3, the unexposed mutant from which these clones were derived showed the presence of all the markers. On the other hand, *Tb427* wt + S284* clone 1I was found to have lost only some of the markers for mitochondrial genome while *Tb427* wt + S284* ATPase γ clones 1E seems to have lost all the markers. This would seem to suggest that the homozygous status of *Tb427* wt + S284* ATPase γ clone 3 with respect to the compensating mutation aided the loss of its kinetoplast on exposure to ISM or EtBr. *Tb427* wt + S284* ATPase γ clone 1 however being heterozygous with one wild-type unreplaced ATPase gamma gene

may have been slower to lose kinetoplast DNA. We conclude that the introduction of the S284* mutation (and thus truncating the gene for the γ -subunit of the F₁F₀-ATPase) rendered the mitochondrial genome non-essential under the experimental conditions, explaining the ease by which it is lost on exposure to EtBr (Lai *et al*, 2008;Chen & Clark-Walker, 1999). This is an indication of the efficiency with which EtBr (ISM) produces dyskinetoplastic trypanosomes once the mutation has been introduced in the γ -subunit of the F₁F₀-ATPase. The γ -subunit of the *Tb427* wt + S284* ATPase γ clones 1, 1E and 1I clones were re-sequenced to verify whether the heterozygous status of these *Tb427* wt + S284* clones 1 was retained after the incubation in ISM or EtBr.

5.4 Sequencing of *Tb427* wt + S284* clones 1I & 1E

ATPase gamma gene from *Tb427* wt + S284* ATPase γ clones 1, 1E and 1I was amplified by PCR using Taq polymerase, employing the primers for ATPase γ forward and reverse (table 2.1). PCR products were purified using the Macherey-Nagel Nucleospin gel and PCR clean-up kit, and sent for sequencing. The sequence results are presented below.



Figure 5.14 Sequence of the γ -subunit of the F₁F₀-ATPase from *Tb427* wt + S284* clone 1 showing the trace data. The trace data at the point of mutation (conflict) shows that the alleles of this gene in *Tb427* wt + S284* clone 1 are heterozygous for this mutation

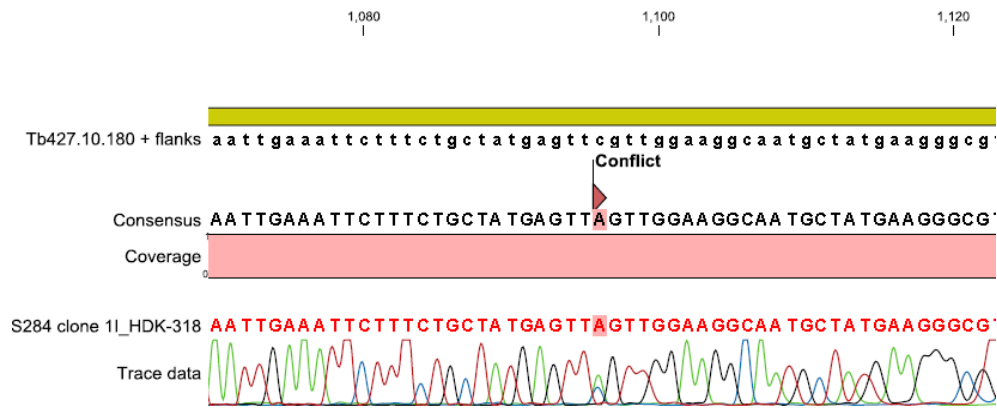


Figure 5.15 Sequence of the γ -subunit of the F_1F_0 -ATPase from *Tb427* wt + *S284** clone 1I showing the trace data. The trace data at the point of mutation (conflict) shows that the alleles of this gene in *Tb427* wt + *S284** clone 1I remained heterozygous for this mutation after 72 hours incubation in ISM.

Tb427 wt + *S284** ATPase γ clone 1 sequence (figure 5.14) shows a C to A mutation that is distinctively heterozygous from the trace data which at that point displays two clear peaks, a higher green peak (for Adenosine nucleotide) under which there is a clear smaller blue peak (for cytosine nucleotide).

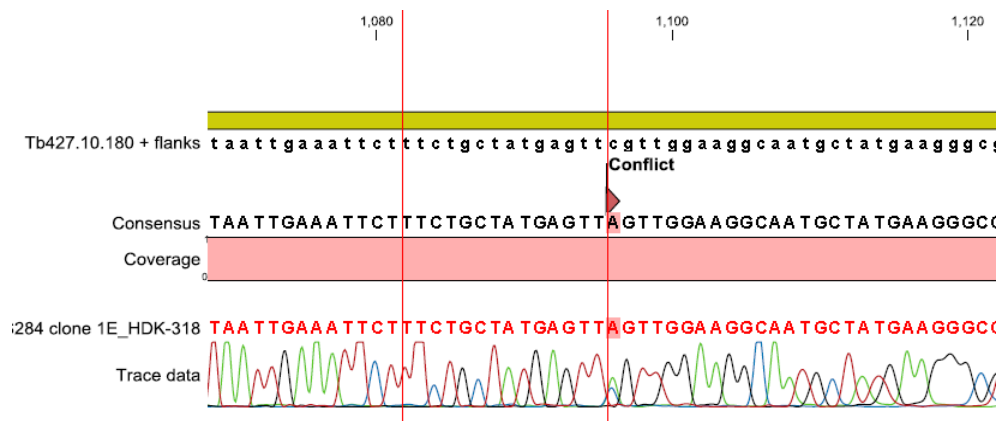


Figure 5.16 Sequence of the γ -subunit of the F_1F_0 -ATPase from *Tb427* wt + *S284** clone 1E showing the trace data. The trace data at the point of mutation (conflict) shows that the alleles of this gene in *Tb427* wt + *S284** clone 1E remained heterozygous for this mutation after 72 hours incubation in EtBr.

The trace data for *Tb427* wt + S284* clones 1I and 1E (figures 5.15 and 5.16) retained the double peak for cytosine and adenosine nucleotides, suggesting that the heterozygous status of both clones was not lost during the incubation in ISM or EtBr.

5.5 Infectivity of ISMR and S284* clones in mice

ISMR and S284* ATPase γ clones were used to infect mice to verify if these clones are still able to establish and sustain infection. *Tb427* wt was used as the positive control.

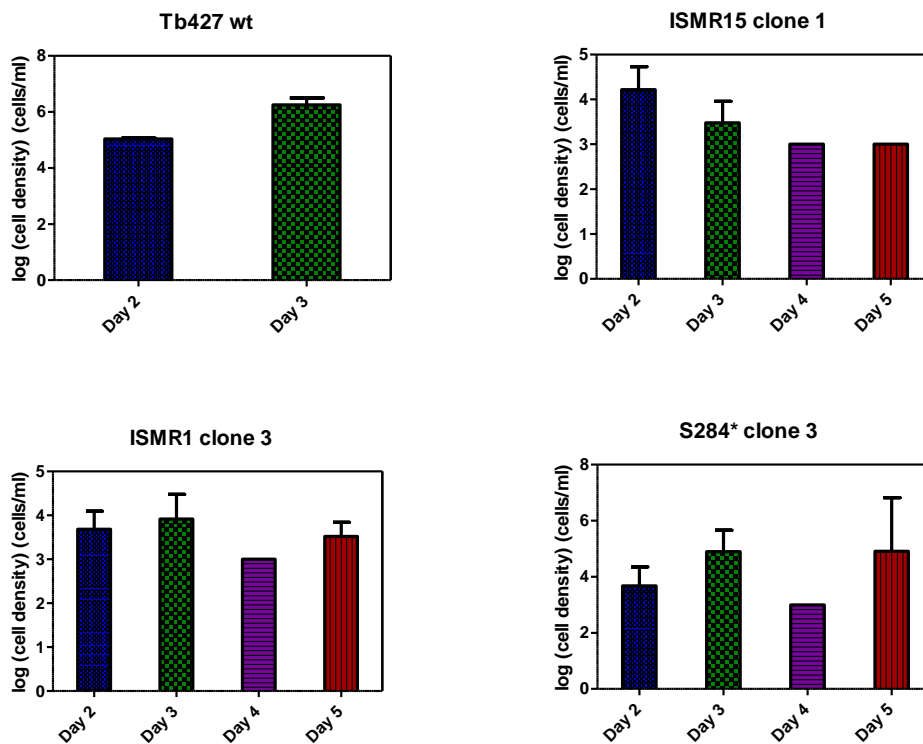


Figure 5.17 Study of infectivity of ISMR and S284* ATPase γ clones in mice; plot of logarithm of average cell density for each group. Each group consists of 5 mice, each of which was inoculated with 200,000 trypanosomes via the intraperitoneal route to start the experiment. Blood was drawn from tail puncture daily, starting after 24 hours, to monitor parasitemia. Each bar represents the average density of trypanosome per group per day and SEM. Experiment was terminated after the 5th day count.

Each group was composed of 5 mice. 100 % of the group inoculated with *Tb427* wt progressed to the terminal stage of the disease in 3 days while 60 % of the group infected with *Tb427* wt + S284* ATPase γ clone 3 reached the terminal stage in the same length of time and 80 % progressed to the terminal stage on the 4th day. The average plotted for *Tb427* wt + S284* ATPase γ clone 3 on the 5th day was for the two surviving mice. None of those inoculated with ISMR1 clone 3 or ISMR15 clone 1 reached the terminal stage of the disease within the duration of the experiment, and parasitaemia was much lower than in wild type controls, not exceeding 10^4 cells/ml compared to $> 10^6$ cells/ml in the wild type. The surviving mice were euthanized on the fifth day to end the experiment.

5.6 Discussions

The reconstruction of resistance phenotypes by transformation of the sensitive wild type cells has been emphasized as the most acceptable proof of the mechanism of resistance (Borst & Ouellette, 1995). Hence, the mechanism can only be considered as resolved if after the transformation, the wild type strain attains the same level of resistance as the resistant strain (Borst & Ouellette, 1995). We have reconstructed ISM resistance in wild type *Tb427* cells by transforming them with replacement plasmids bearing a mutated *Trypanosoma brucei brucei* ATPase gamma gene. Both alleles of this gene were replaced in *Tb427* wt + S284* ATPase γ clones 2 and 3 while only one was replaced in *Tb427* wt + S284* ATPase γ clone 1. However, this mutation proved to be a dominant mutation since the same level of phenotypic difference occurred in heterozygous (clone 1) and homozygous (clones 2 and 3) clones. Each clone was significantly more resistant ($p < 0.01$, unpaired student's t-test) than the control transformed the wild type ATPase gamma gene in the same vector (figure 5.2). The introduction of this mutation, though truncating the ATPase

gamma gene, did not cause a spontaneous loss of the kinetoplast in the transformed parasites (figure 5.5). However, the presence of this mutation seems to hasten the ease of loss of the kinetoplast, since the kinetoplast was found to have disappeared on only the 3rd day of incubation in 20 nM ISM or EtBr.

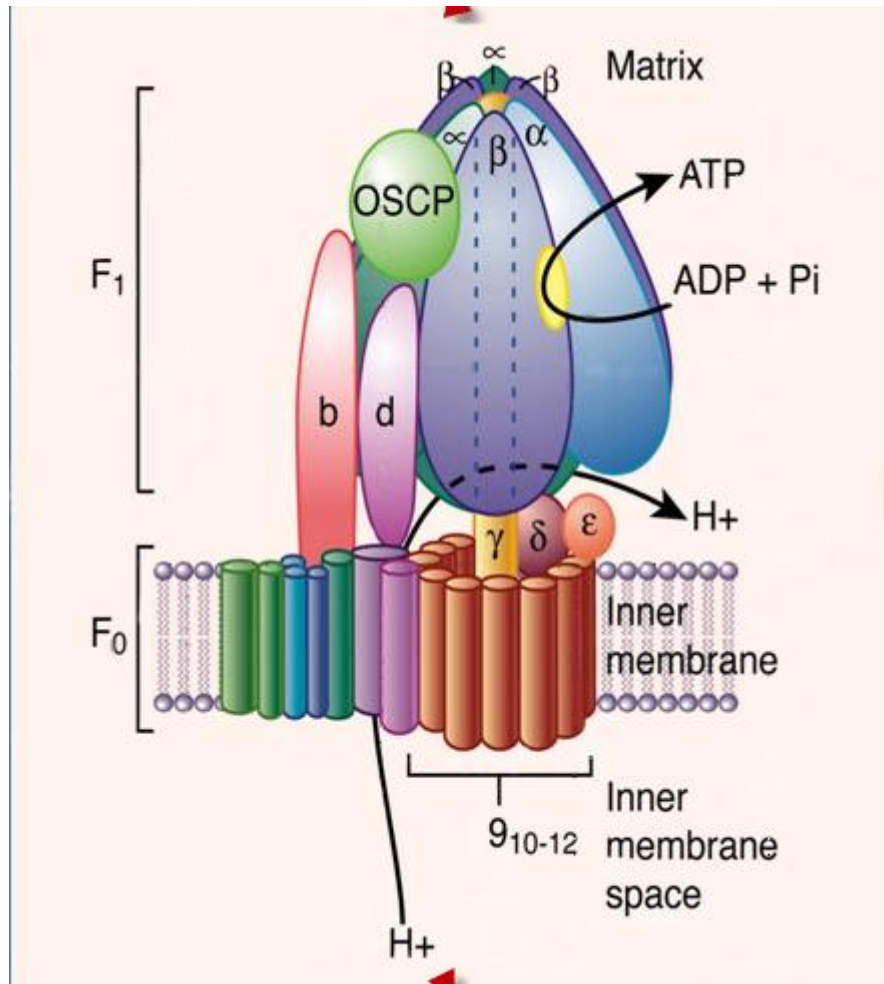


Figure 5.18 Diagram showing the two domains of the F₁F₀ ATPase and the position of the γ subunit in the oligomer Taken from <http://www.lycera.com/approach-bioenergetics.php>.

Similarly, the mitochondrial membrane potential of the transformed parasites, though significantly lower than the wild type potential ($p < 0.001$, one way ANOVA) was only lost after incubation in ISM or EtBr. The large difference in the resistance to ISM between the *Tb427* wt + S284* ATPase γ clones and the ISMR clones should be accounted for by the contribution made by reduced uptake to ISM resistance. The long adaptation to very high levels of ISM clearly

produced multi-factorial resistance. Hence, *Tb427* wt + S284* ATPase γ clones are at a lower level of resistance to ISM because only one mechanism of resistance operates in these parasites, namely S284* mutation of the ATPase gamma gene. In the case of resistance to EtBr and oligomycin acquired by transformation with the defective ATPase subunit (figure 5.9, figure 5.18) the ATPase gamma gene mutation is the sole mechanism of resistance to these drugs since the introduction of this mutation to the wild type *Tb427* was enough to bring them to the same level of resistance as the ISMR clones.

Maintenance of normal MMP seems to depend on the presence of a functional kinetoplast. Since the mitochondrial F_1F_0 -ATP synthase was found to be responsible for the maintenance of this potential (Nolan & Voorheis, 1992), and subunit A6, which is encoded by a maxicircle gene, is part of the F_0 component of this enzyme (Schnauffer *et al*, 2002). Hence the loss of kinetoplast DNA would be expected to deprive the cell of its usual mechanism of using an F_1F_0 -ATPase working in reverse to maintain its MMP (Schnauffer *et al*, 2005). This is consistent with our finding that the MMP of the S284* ATPase γ clones did not decrease to the level found in the ISMR clones until after the loss of their kinetoplasts (after incubation in ISM/ethidium bromide). Our finding that the loss of the kDNA is enhanced only in the presence of a compensating mutation (figures 5.6, 5.10 and 5.11) is consistent with earlier findings that suggest that the kinetoplast is essential to the bloodstream form *T. brucei* (Timms *et al*, 2002). Also, because of the essential requirement of the mitochondria for procyclic life, it is believed that Dk and Ak parasites may have lost the ability to survive as procyclics in the tsetse fly due to their inability to carry out oxidative phosphorylation (Schnauffer *et al*, 2002), and so these organisms may have gained the resistant phenotype at a great cost.

5.7 Conclusion

We can conclude at this point that S284* mutation of *Tb427* wt ATPase γ gene is a reproducible resistance marker in *T. b. brucei*. This mutation is dominant and is the only mechanism of resistance to EtBr and oligomycin. In ISM resistance however, this mutation is aided by a reduction in the uptake of the drug. Our findings also lead to the conclusion that loss of kinetoplast DNA correlates with, and coincides with, the loss of the MMP observed in our clones. Finally, resistance to ISM due to loss of MMP and ATPase γ -subunit mutations produces various levels of cross resistance to EtBr, diminazene, oligomycin and pentamidine. Resistance to pentamidine however seems to disappear as the level of resistance to ISM increases.

**6. Aquaporin-2 expression enhances
pentamidine but not ISM uptake: An
investigation into the genetic identity of the
High Affinity Pentamidine Transporter
(HAPT1).**

6.1. Introduction

The biggest problem facing chemotherapy as a means of control of African trypanosomiasis is the problem of resistance (Teka *et al*, 2011). Since an understanding of the mechanism of resistance is necessary for either the reversal or prevention of this problem, knowledge of the mechanisms of resistance is therefore as important as the development of new drugs (Bridges *et al*, 2007). Resistance to pentamidine can be attributed to changes in the intracellular drug target, reduced uptake of the drug or active extrusion from the cell by an ABC-type efflux pump (Bridges *et al*, 2007), though reduction in drug uptake seems to be the most important mechanism of arsenical and diamidine resistance in African trypanosomes. Indeed, the High Affinity Pentamidine Transporter, HAPT1 has been identified as the major determinant for high-level arsenical-diamidine cross-resistance in African trypanosomes (Bridges *et al*, 2007).

It has already been established that pentamidine is salvaged by three distinct transport activities in bloodstream trypanosomes, the P2 aminopurine transporter responsible for the adenosine sensitive uptake; the high-affinity pentamidine transporter (HAPT1) and the low-affinity pentamidine transporter (LAPT1) that both mediate adenosine-insensitive uptake (de Koning, 2001b; Matovu *et al*, 2003). It was also demonstrated that the TbAT1, an ENT gene expresses the P2 transporter (Mäser *et al*, 1999), but the gene responsible for either the HAPT1 or the LAPT1 is unknown. Since pentamidine is transported efficiently by bloodstream forms in the absence of P2, and the deletion of TbAT1 alone confers only a minimal level of resistance to pentamidine, it is therefore important to identify and characterize the non-P2-mediated uptake systems (Teka *et al*, 2011). This is even more important since it had been demonstrated

that *TbAT1*^(-/-) trypanosomes were still sensitive to diamidines at concentrations close to 1 μM *in vitro* (Matovu *et al*, 2003). Both the HAPT1 and the LAPT1 have been fully characterized biochemically in both the procyclic and the bloodstream forms of the trypanosomes (de Koning, 2001b). We attempt in this chapter to identify the gene responsible for the HAPT1 activity in bloodstream form *T. brucei brucei*. Very recently a further determinant for drug sensitivity/resistance in *T. brucei* was identified; using a fully validated RNAi library, a genome-wide screen for pentamidine resistance turned up fragments of the Aquaporin 2 (AQP2) gene (Alsford *et al*, 2012). We subsequently found that the wild type copy of this gene had been lost in our pentamidine-resistant line B48, which instead contained a novel chimeric gene consisting of parts of AQP2 and the adjacent gene AQP3, possibly arising from a cross-over event. B48 is a standardised cell line which has been shown to have lost both the HAPT1 and the P2 transporter, and so possesses only the LAPT1 activity. This strain did still contain wild-type copies of AQP1 and AQP3. In addition, we mentioned in chapter 3 that TbAT-E is the most closely related gene to TbAT1 and a likely candidate for the role of HAPT1 (de Koning *et al*, 2005). We therefore considered it necessary to assess the ability of both genes to take up pentamidine (when expressed in an appropriate *T. b. brucei* background or in a heterologous expression) and hence determine if either of them would display similar (or the same) kinetic parameters already published for HAPT1 (de Koning, 2001b). Therefore, the contributions of TbAT-E and TbAQP2 to pentamidine uptake and sensitivity were investigated and are reported here.

6.2. Uptake of [³H]-pentamidine by *Tb427 TbAT-E* dKO cells.

The deletion of both alleles of *TbAT-E* from *Tb427* wt was done by Dr. Jane Munday. The effect of this deletion on [³H]-pentamidine uptake was assessed and the result showed that the deletion of *TbAT-E* did not affect [³H]-pentamidine uptake (figure 6.1). HAPT1 (inhibited by propamidine) and LAPT1 activities (propamidine insensitive; approx. 20% of uptake) were both still present after *TbAT-E* deletion as shown in figure 6.1. This suggests that *TbAT-E* may not be responsible for the HAPT1 activity, or indeed for the LAPT1 activity.

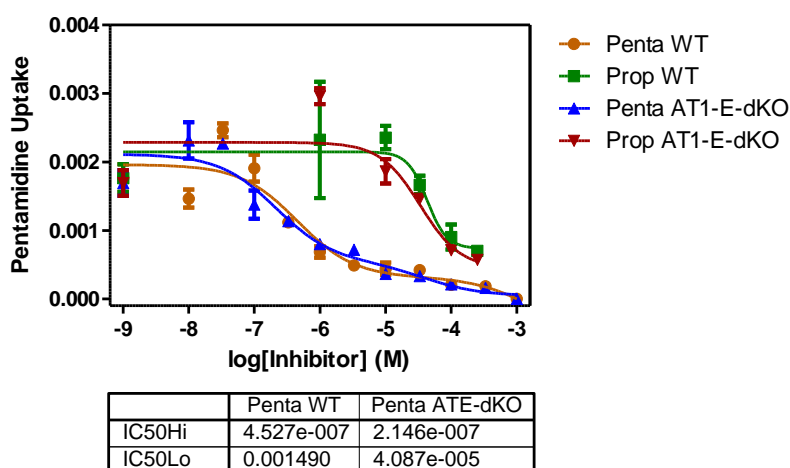


Figure 6.1 Uptake of 30 nM [³H]-pentamidine by *TbAT-E-dKO* in *Tb427* and *Tb427* wt control. Rate of uptake was determined by incubating ~ 10⁷ cells per experiment in the presence of 30 nM [³H]-labelled Pentamidine at room temperature (section 2.2.5). Experiment shown is representative of three identical but independent assays, each performed in triplicate and showing virtually identical outcomes.

6.3. Effect of *TbAT-E1* and *TbAQP2* expression on drug sensitivity in *T. b. brucei*.

TbAT-E1 and *TbAQP2* were cloned into pHD1336 and separately expressed in B48 cell line by Dr Jane Munday. Their sensitivity to some important trypanocides was tested, and the results presented in figure 6.2 and 6.3. B48

cells showed a much higher susceptibility to ISM, compared to the wild type *Tb427* (Figure 6.2). This is surprising, since the B48 cells have been characterised and found to have lost both the P2 and the HAPT1 transporters (Bridges *et al*, 2007) and indeed ISM uptake was significantly lower in this cell line than in the control wild-type strain (Figures 6.9 and 6.10; $P < 0.01$). This susceptibility is somewhat reduced by the expression of aquaporin 2 gene in the B48 cells (though this did not amount to statistical significance, figure 6.2); this again is an observation that is quite difficult to explain but certainly shows that ISM resistance is not solely the result of different uptake rates.

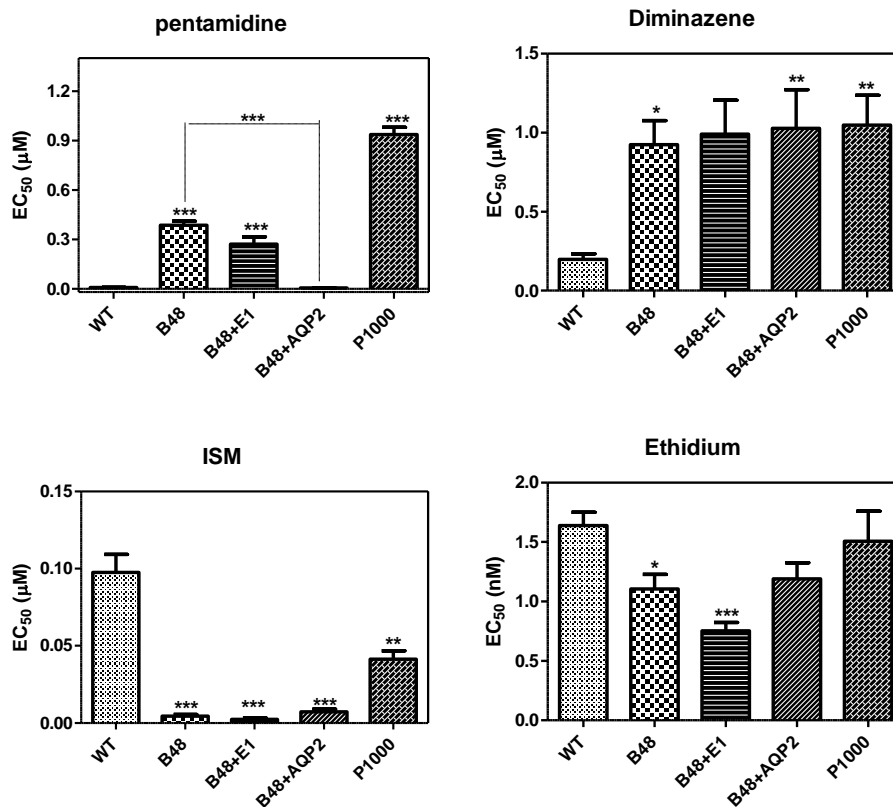


Figure 6.2 Overview of drug sensitivity in a few selected cell lines compared to *T. b. 427 wt.* Sensitivity was determined by alamar blue assay, using 10^5 cells/ml of each cell line, and incubating the assay at 37°C and 5% CO_2 for 48 hour before addition of alamar blue dye. Fluorescence was measured 24 hours after addition of dye. *** $P < 0.001$; ** $P < 0.01$; * $P < 0.05$ (One way ANOVA using Graph pad prism 5.0).

Expression of *TbAQP2* in B48 cells completely reversed the resistance of the B48 cells to pentamidine (figure 6.2) and cymelarsan (figure 6.3), returning the cells to wild type sensitivity to each drug. *TbAT-E1* expression in B48 on the other hand had no effect on pentamidine sensitivity (figure 6.2). It also could not reverse B48 resistance to cymelarsan (this assay was done only once, and is not shown on the graph).

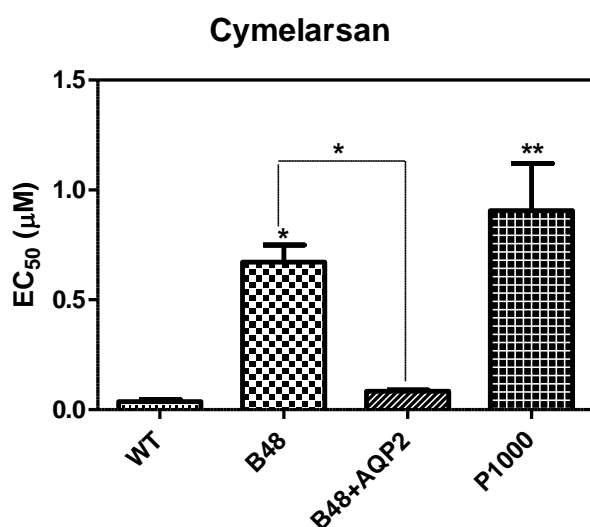


Figure 6.3 Effect of AQP2 expression on the sensitivity of B48 to cymelarsan. Sensitivity was determined by alamar blue assay, using 10⁵ cells/ml of each cell line, and incubating the assay at 37°C and 5% CO₂ for 48 hour before addition of alamar blue dye. Fluorescence was measured 24 hours after addition of dye. ** P < 0.01; * P < 0.05 (One way ANOVA using Graph pad prism 5.0).

6.4. [³H]-Pentamidine uptake by *TbAQP2* expression in B48.

TbAQP2 was sub-cloned into pHD1336 and expressed in B48 cells by Dr. Jane Munday. Uptake of 50 nM and 1 µM [³H]-pentamidine was subsequently assessed in the resultant clones with B48 as control. As stated earlier, B48 cells have lost both the P2 transport activity (which was deleted, since B48 was

derived from *TbAT1*^(-/-) and the HAPT1 but still has the low affinity pentamidine transport (LAPT1) activity. Hence our prediction was that the rate of LAPT1-mediated [³H]-pentamidine uptake would be similar in B48, *TbAT1*^(-/-) and B48 + AQP2 (figure 6.4).

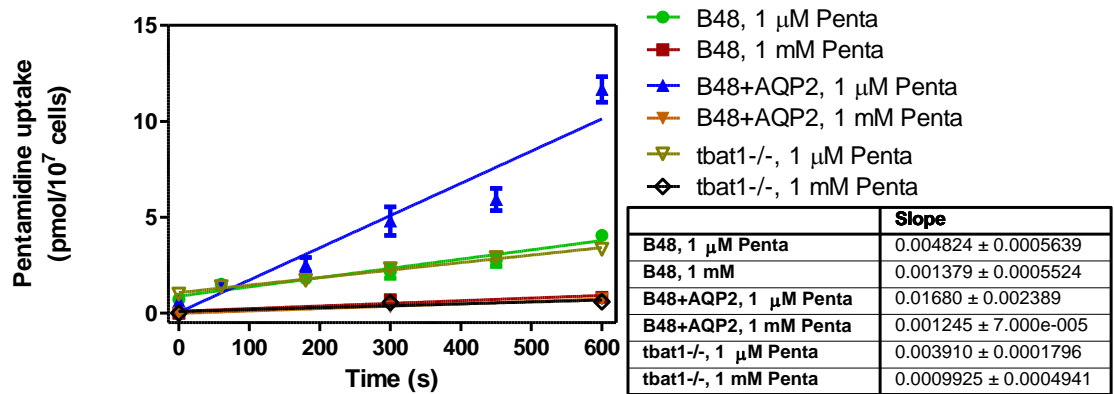


Figure 6.4 Low affinity [³H]-pentamidine timecourse uptake by *TbAQP2* expression in B48. Rate of uptake was determined by incubating ~ 10⁷ cells per experiment in the presence of 1 μM [³H]-labelled Pentamidine at room temperature (section 2.2.5). Saturability was verified in the presence of 1mM unlabelled permeant. Experiment shown is representative of three identical but independent assays, each performed in triplicate and showing virtually identical outcomes.

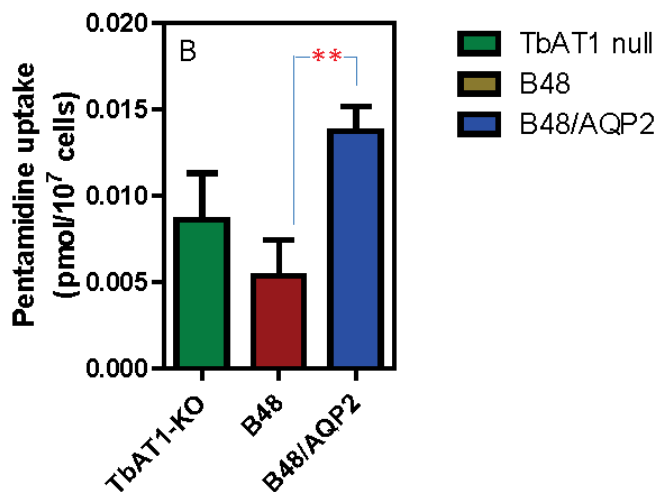


Figure 6.5 Summary of LAPT-mediated [³H]-Pentamidine uptake. Each bar is the average of 3 independent [³H]-Pentamidine uptake assays represented by figure 6.4, error bar is SEM. Data was analyzed with 1-way ANOVA/Tukey’s test using GraphPad Prism 5.0. **P<0.02.

However, the summary of pentamidine transport in these cell lines (figure 6.5) shows that the rate of 1 μM [^3H]-pentamidine uptake is significantly up-regulated in B48 + AQP2 ($P < 0.02$, 1 way ANOVA using the PRISM software) when compared to the B48. However, this increase in LAPT1 activity is not significant when compared to the *TbAT1*^(-/-) control (figure 6.5). While uptake of 1 μM labelled pentamidine is routinely used as a marker for low affinity pentamidine uptake, it does obviously contain within it the high affinity uptake component as well, though it saturates this activity. Thus, the results presented here do not necessarily indicate increased LAPT1 activity, but could also indicate a very substantial increase in HAPT1 activity.

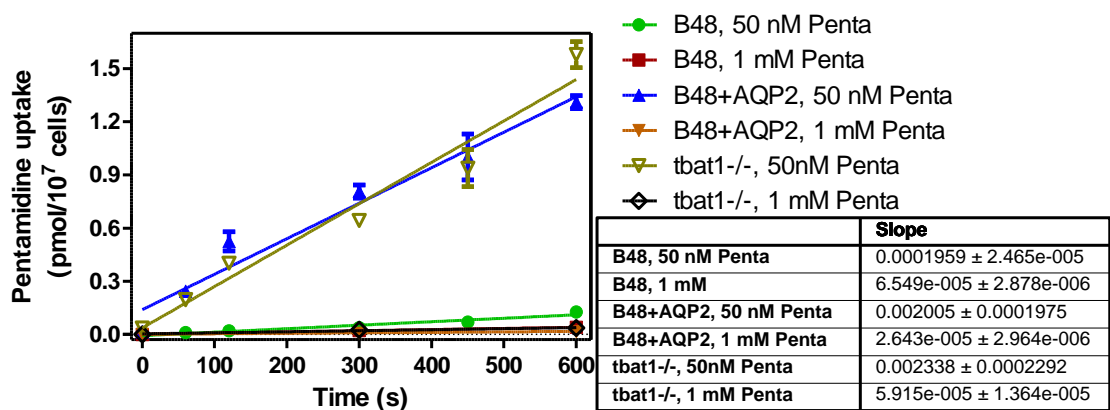


Figure 6.6 High affinity [^3H]-pentamidine timecourse uptake by *TbAQP2* expression in B48. Rate of uptake was determined by incubating $\sim 10^7$ cells per experiment in the presence of 50 nM [^3H]-labelled Pentamidine at room temperature (section 2.2.5). Saturability was verified in the presence of 1mM unlabelled permeant. Experiment shown is representative of three identical but independent assays, each performed in triplicate and showing virtually identical outcomes.

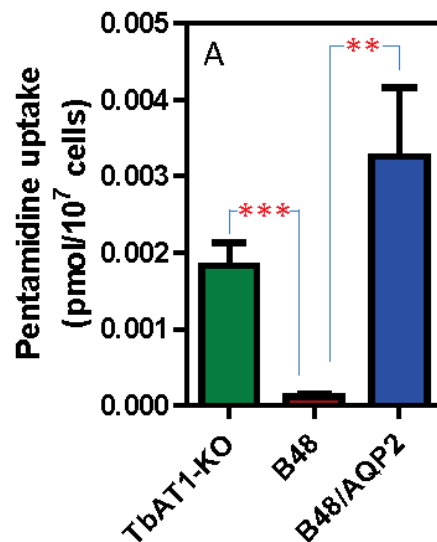


Figure 6.7 Summary of HAPT-mediated [³H]-Pentamidine uptake. Each bar is the average of 3 independent [³H]-Pentamidine uptake assays represented by figure 6.6, error bar is SEM. Data was analyzed with 1-way ANOVA/Tukey’s test using GraphPad Prism 5.0. **, P<0.02; ***, P<0.01

Indeed, the re-expression of *TbAQP2* in B48 seems to return the lost HAPT1 activity to this line (figures 6.6 & 6.7). A summary of the rate of high affinity pentamidine uptake shows that the rate in B48 + AQP2 is significantly higher than in B48 (P < 0.02, 1 way ANOVA using the PRISM software). This result is in agreement with the finding that *TbAQP2* expression in B48 increases the sensitivity to pentamidine of the B48 line to the level of the wild type trypanosomes (figure 6.8). B48 was significantly more resistant than the wild type control (p<0.01) while B48 + AQP2 was not significantly different from the control. A similar trend was observed when comparing the sensitivities of AQP2 KO (AQP2 deletion from 2T1) and AQP2+3 dKO (AQP2 and AQP3 deletion from 2T1) (Baker *et al*, 2012). Both AQP2 KO and AQP2+3 dKO were significantly more resistant to pentamidine than the parental 2T1 (p < 0.0001, unpaired Student’s t-test; figure 6.8). However, AQP2+3 dKO was not significantly more sensitive to pentamidine than AQP2 KO, indicating that the contribution of AQP3 to pentamidine sensitivity is minimal. Deletion of AQP3 alone was not done.

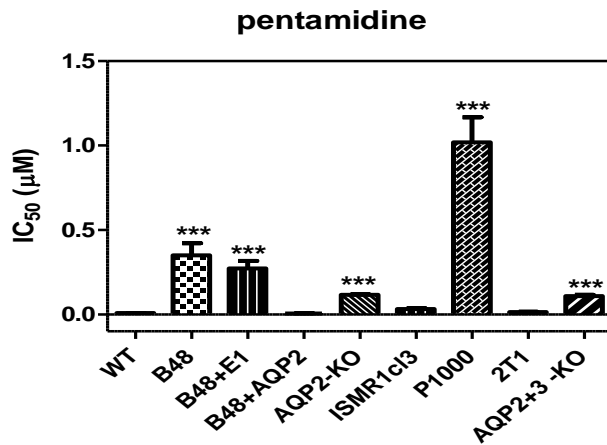


Figure 6.8 Effect of *TbAQP2* expression on pentamidine sensitivity. Sensitivity was determined by alamar blue assay, using 10^5 cells/ml of each cell line, and incubating the assay at 37°C and 5% CO₂ for 48 hour before addition of alamar blue dye. Fluorescence was measured 24 hours after addition of dye. Data was analyzed with unpaired Student’s t-test using GraphPad Prism 5.0. ***P<0.0001.

6.5. The contribution of the *TbAQP2* to ISM uptake in *T. b. brucei*

TbAT1 KO cells (*TbAT1*^(-/-)) were derived from *s427wt* by a deletion of the TbAT1 gene (Matovu *et al*, 2003). B48 cells were in turn derived from the TbAT1 KO cells by adapting them to higher levels of pentamidine resistance leading to the loss of the high affinity pentamidine transporter (HAPT1) activity in the B48 cells (Bridges *et al*, 2007). Hence B48 cells lack both the P2 and HAPT1 transport activities. We therefore expressed the AQP2 gene in B48 and studied ISM uptake in this cell line, compared with ISM uptake in the B48 line. Hence any difference in ISM uptake between them can be attributed to the activity of the protein expressed by the *TbAQP2* gene.

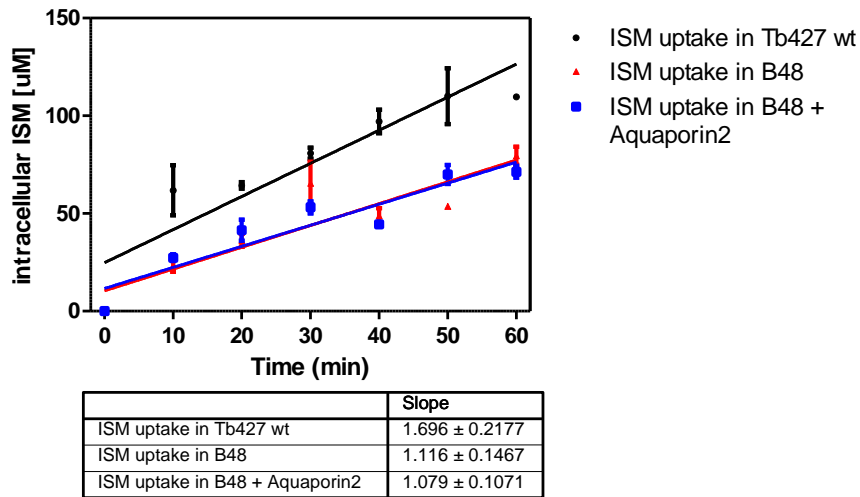


Figure 6.9 Timecourse uptake of ISM by some selected cell lines; $[\text{ISM}] = 10 \mu\text{M}$. Assay was performed in triplicate with $\sim 10^8$ cells/ml of each cell line in complete HMI-9 medium (+ 10% fetal bovine serum) at room temperature; $[\text{ISM}] = 10 \mu\text{M}$. ISM uptake was measured as described in section 2.2.5. The slope of each line represents the rate of uptake ($\mu\text{M}/\text{min}$). Experiment shown is representative of four identical but independent assays, each performed in triplicate and showing virtually identical outcomes.

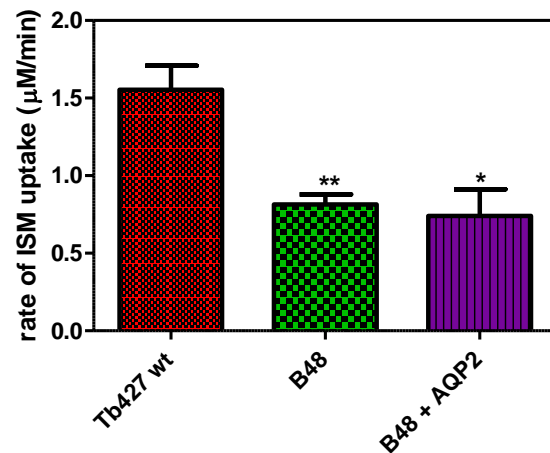


Figure 6.10 Summary of repeats for ISM uptake by some selected cell lines. Each bar is the average of 4 independent ISM uptake assays represented by figure 6.9; error bar is SEM. * $P < 0.05$, ** $P < 0.01$, one way ANOVA with Turkey's correction, using the Graphpad prism 5.0.

However, the expression of Aquaporin 2 in B48 cells did not increase the rate of ISM uptake (there was no significant difference between uptake rate in B48 and B48 + Aquaporin 2; figure 6.10).

6.6. Effect of *TbAQP2* expression on sensitivity to adenosine analogues

Sensitivity to adenosine analogues was determined to test the hypothesis that HAPT1 is an adenosine-insensitive route of uptake. This is to say that candidate genes for the HAPT1 should be those that their expression does not increase the uptake of adenosine and those compounds similar to it. Hence, AQP2 expression in B48 or its deletion from 2T1 should not affect the sensitivity to this class of drugs.

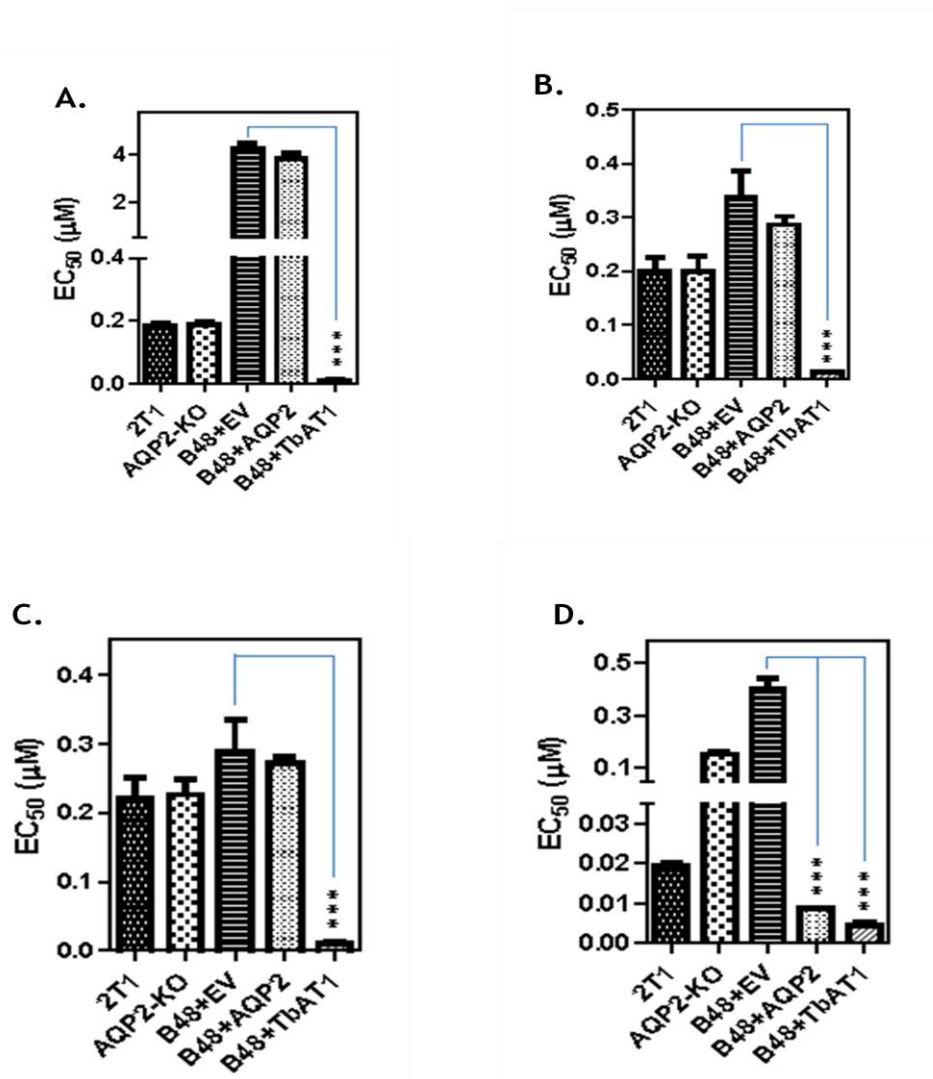


Figure 6.11 Sensitivity of various *T. b. brucei* lines to adenosine analogues. A: Tubercidin, B: Cordycepin, C: 5'-deoxyadenosine; Pentamidine (D) was used as a control. Sensitivity was determined by alamar blue assay, using 10^5 cells/ml of each cell line, and incubating the assay at 37°C and 5% CO₂ for 48 hour before addition of alamar blue dye. Fluorescence was measured 24 hours after addition of dye. All data shown are the average and SEM of at least three independent determinations. ***P<0.001, 1-way ANOVA/Tukey's test using GraphPad Prism 5.0.

Figure 6.11 shows that *aqp2* null cells have exactly the same sensitivity to tubercidin, cordycepin and 5'-deoxyadenosine as the 2T1 cells. This is the exact prediction for these drugs, since AQP2 is not their route of entry into the parasite, hence, AQP2 deletion should not affect their toxicity to the organism. The much higher resistance (which is uniform to that for B48 + EV) displayed by B48 + AQP2 is explained by the fact that AQP2 was derived from *TbAT1*^(-/-), and

hence has lost its P2 activity. Re-expression of TbAT1 in B48 (B48 + TbAT1) reverses this resistance completely and uniformly for all three drugs (figure 6.11).

6.7. ³H]-pentamidine uptake by 2T1 *TbAQP2* KO

The AQP2 gene was deleted from the 2T1 cell line to generate the *aqp2* null clones. Deletion was done by Dr Jane Munday while the [³H]-Pentamidine uptake was characterised by me.

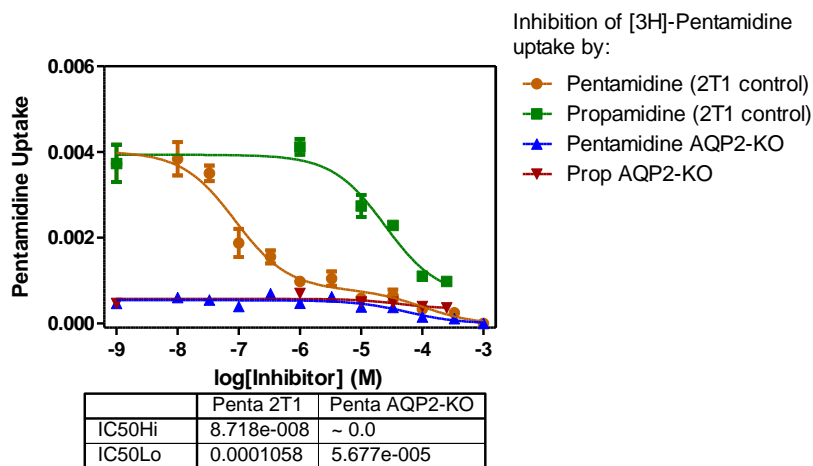


Figure 6.12 Uptake of 30 nM [³H]-pentamidine by *aqp2* null and wild-type control cells. Rate of uptake was determined by incubating ~ 10⁷ cells per experiment in the presence of 30 nM [³H]-labelled Pentamidine and different concentrations of unlabelled permeants at room temperature (section 2.2.5). Experiment shown is representative of four identical but independent assays, each performed in triplicate and showing virtually identical outcomes.

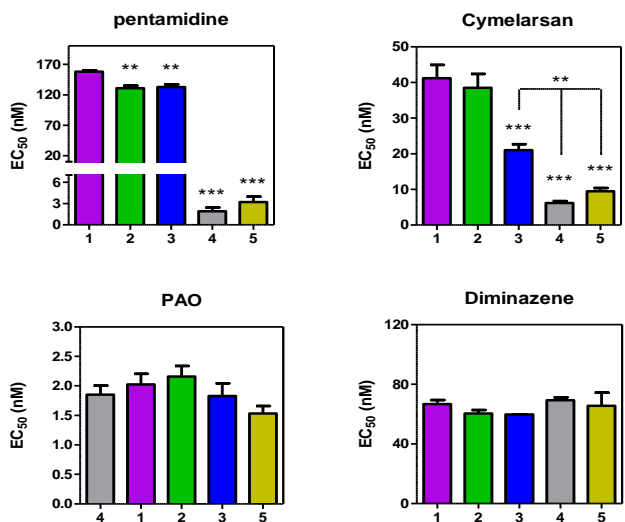
Figure 6.12 shows that *aqp2* null cells have lost their HAPT1 activity. This result is in agreement with our earlier results and strongly supports the theory that *TbAQP2* encodes the high affinity pentamidine transporter, HAPT1. Furthermore, AQP2 KO was significantly more resistant to pentamidine than the wild-type (P < 0.0001, unpaired t-test using GraphPad Prism 5.0; figure 6.8). This is also consistent with *TbAQP2* being the gene for HAPT1.

6.8. Expression of synthetic aquaporin constructs in bloodstream forms of the *aqp2/aqp3* double null line.

The sequence of the *AQP2* gene that was replaced with matching *AQP3* sequence in the crossover event that generated *AQP2/3* chimera contains most of the selectivity filter that is believed to be responsible for the distinct permeation profiles of aquaporins (Baker *et al*, 2012). As the chimeric aquaporin found in B48 did not appear to have the *TbAQP2* functionality with respect to pentamidine and melarsoprol sensitivity, we investigated whether the cross resistance between pentamidine and melarsoprol is determined principally by the few amino acids of the selectivity filter (structural element responsible for determining what passes through the channel). Synthetic genes of *AQP2/3* chimera and of *TbAQP3* were used, each with a *TbAQP2* selectivity filter (*chAQP2/3^{sf2}* and *AQP3^{sf2}*, respectively). These were cloned into the pRPa^{iGFPx} (Alsford & Horn, 2008) vector to allow expression analysis using the GFP-tag and expressed in the 2T1 *aqp2/aqp3* null cell line. Expression was induced by the addition of 1 µg/mL of tetracycline (TET) 24 h before setting up the plates for the assay, and each transformed cell line was tested in the presence and absence of TET.

Analysis of the drug sensitivity phenotype for the resultant lines showed that the transplantation of the amino acid residues likely to determine *AQP2* selectivity to *AQP3* did not result in an *AQP2*-type phenotype with respect to drug sensitivity: EC₅₀ values for cymelarsan, diminazene and PAO were all identical to the *aqp2/aqp3* null background in which the construct was expressed, but sensitivity to pentamidine was significantly increased from the *aqp2/aqp3* null background, though it was also significantly different from a line expressing WT *AQP2* in the same background (Figure 6.13). However, the TET-

induced cell line containing the *chAQP2/3^{sf2}* construct was significantly more sensitive to both pentamidine and cymelarsan than the non-induced control or the *aqp2/aqp3* null background, reaching wild-type sensitivity to cymelarsan. Similarly, the induction significantly increased its sensitivity to pentamidine compared to the *aqp2/aqp3* null background, but the level of sensitivity attained was still less than achieved with the TbaQP2 expression in the same background (Figure 6.13). This appears to indicate that the selectivity filter change alone was sufficient to produce the melaminophenyl arsenical (MPA) (Cymelarsan or Melarsoprol)-sensitizing phenotype in *chAQP2/3* but not in AQP3. Clearly, the selectivity filter helps to determine the highly unusual permeation phenotype of AQP2, but is not the sole structural determinant. Considering the relative size of pentamidine and MPAs compared to classical substrates of aquaglyceroporins (Baker *et al*, 2013), the pore size of the channel must be larger in *TbAQP2* than in *TbAQP3*.



1. *aqp2/aqp3* null
2. *aqp2/aqp3* null with *AQP3^{sf2}*
3. *aqp2/aqp3* null with *chAQP2/3^{sf2}*
4. *aqp2/aqp3* null with WT *AQP2*
5. 2T1 WT

Figure 6.13 Expression of synthetic aquaporin constructs in bloodstream forms of the *aqp2/aqp3* double null line. Sensitivity was determined by alamar blue assay, using 10^5 cells/ml of each cell line, and incubating the assay at 37°C and 5% CO₂ for 48 hour before addition of alamar blue dye. Fluorescence was measured 24 hours after addition of dye. All data are the average of at least 3 independent determinations; error bars are SEM. There were significant differences between

groups 4 and 5. Statistical significance was determined using a one-way ANOVA with Tukey's correction (Prism 5.0); **, P<0.02; ***, P<0.01

6.9. $[^3\text{H}]$ -pentamidine uptake by TbAQP2 expression in *Leishmania mexicana*.

TbAQP2 was sub-cloned into the pNUS-HcN expression vector by Becca Lee, an M.Res. student. The expression in *L. mexicana* and the subsequent characterization of the new phenotype were done by me. The expression of *TbAQP2* in *L. mexicana* resulted in a significant increase in the uptake of pentamidine ($p < 0.001$, one-way ANOVA; figure 6.16). Uptake was very rapid and linear, with a rate of $0.032 \pm 0.002 \text{ pmol}(10^7 \text{ cells})^{-1}\text{s}^{-1}$ in the first 15 seconds and ($r^2 = 0.98$, figure 6.15) equilibrating thereafter (figure 6.14). High affinity pentamidine transport was not detectable in *L. mexicana* promastigotes expressing either *TbAQP3* or empty pNUS vector (control) as shown by almost horizontal lines depicting uptake in these clones (figure 6.14). Hence, high affinity uptake of $[^3\text{H}]$ -pentamidine was not characterized further in these clones.

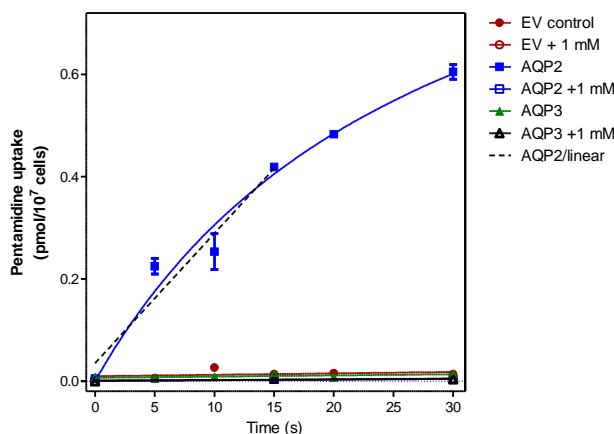


Figure 6.14 Timecourse uptake of 50 nM $[^3\text{H}]$ -pentamidine (HAPT1 uptake kinetics is studied below $1 \mu\text{M}$ pentamidine concentration), over 30 s, using *L. mexicana* promastigotes transformed with *TbAQP2*, *TbAQP3* and empty pNUS vector. Rate of uptake was determined by incubating -

10^7 cells per experiment in the presence of 50 nM [^3H]-labelled Pentamidine at room temperature (section 2.2.5). Saturability was verified in the presence of 1mM unlabelled permeant.

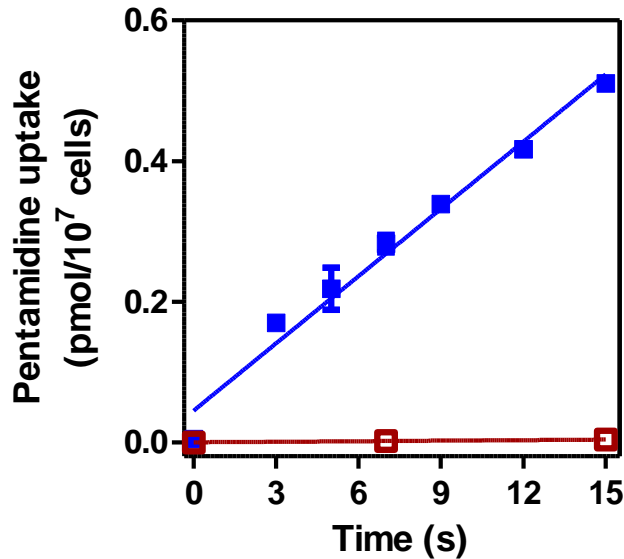


Figure 6.15 Timecourse uptake of 50 nM [^3H]-pentamidine (HAPT1 uptake kinetics is studied below 1 μM permeant concentration), over 15 s, using *L. mexicana* promastigotes transformed with *TbAQP2* in the presence (\square) and absence (\blacksquare) of 1 mM unlabelled pentamidine. Rate of uptake was determined by incubating $\sim 10^7$ cells per experiment in the presence of 50 nM [^3H]-labelled permeant at room temperature (section 2.2.5). Saturability was verified in the presence of 1mM unlabelled permeant. Uptake at 50 nM pentamidine was linear ($r^2 = 0.98$) and rapid, as shown by the rate of uptake, $0.032 \pm 0.002 \text{ pmol}(10^7 \text{ cells})^{-1}\text{s}^{-1}$, compared with $0.00026 \pm 1.8 \times 10^{-6} \text{ pmol}(10^7 \text{ cells})^{-1}\text{s}^{-1}$ in the presence of 1 mM pentamidine.

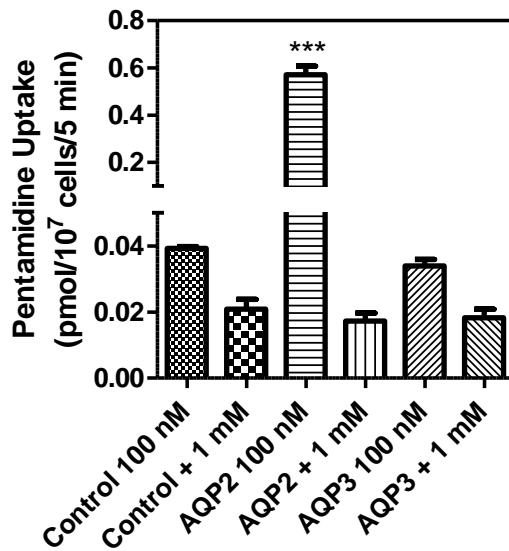


Figure 6.16 Specific uptake of 100 nM [³H]-pentamidine (HAPT1 uptake kinetics is studied below 1 μM pentamidine concentration) over 5 minutes in *L. mexicana* promastigotes transformed with empty pNUS vector (control); promastigotes transformed with *TbAQP2*; and with *TbAQP3*. In each case mediated uptake at 100 nM radiolabel was compared with total association of [³H]-pentamidine with the cell pellet in the presence of saturating (1 mM) unlabelled pentamidine. The data shown are the average of three independent assays done in triplicate, and SEM. ***, P<0.001 by 1-way ANOVA, compared to all other data sets.

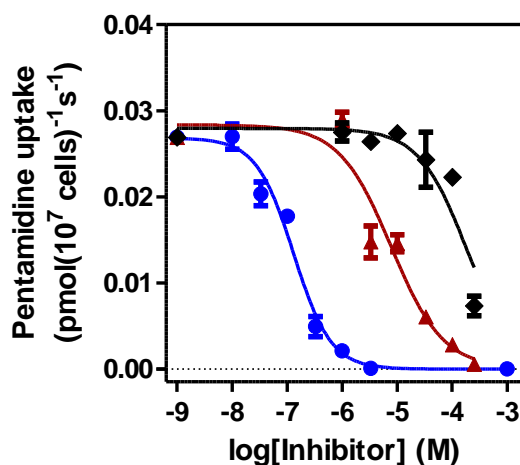


Figure 6.17 Characterization of 20 nM [³H]-pentamidine uptake in *L. mexicana* promastigotes expressing *TbAQP2*, in the presence of various concentrations of unlabelled inhibitor: pentamidine (●), propamidine (▲) and diminazene (◆). Rate of uptake was determined by

incubating $\sim 10^7$ cells per experiment in the presence of 20 nM [^3H]-labelled Pentamidine and different concentrations of unlabelled permeants (inhibitors) at room temperature (section 2.2.5). Experiment shown is representative of four identical but independent assays, each performed in triplicate and showing virtually identical outcomes.

Full characterization of the high affinity uptake was done on the uptake of 20 nM [^3H]-pentamidine in *L. mexicana* promastigotes expressing TbAQP2. K_m and V_{max} values of $0.055 \pm 0.004 \mu\text{M}$ and $0.123 \pm 0.025 \text{ pmol}/10^7 \text{ cells}/\text{s}$ respectively (figure 6.18) were found. Inhibition by unlabelled pentamidine, propamidine and diminazene was dose-dependent (Figure 6.17) and followed Michaelis-Menten kinetics. K_i values were also found to be equal to $8.1 \pm 0.8 \mu\text{M}$ and $100.47 \pm 20.87 \mu\text{M}$ for the inhibition of [^3H]-pentamidine uptake by propamidine and diminazene respectively.

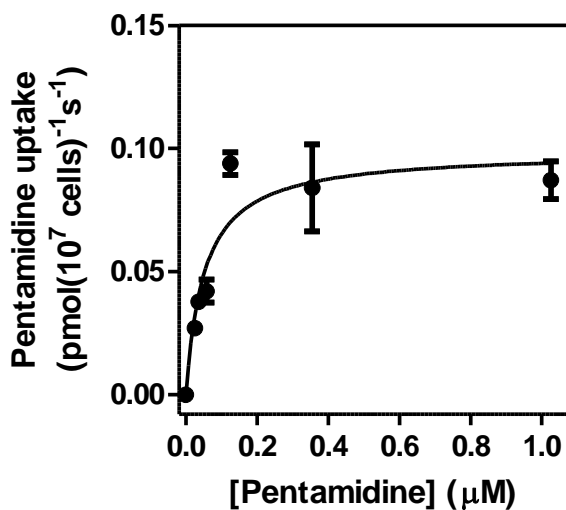


Figure 6.18 Michaelis-Menten saturation plot of 20 nM [^3H]-pentamidine uptake; conversion of pentamidine inhibition plot in figure 6.17.

6.9.1. Effect of expression of *T. brucei* aquaporins on drug sensitivity of *Leishmania mexicana*.

The effect of the expression of *TbAQP2* and *TbAQP3* on the sensitivity of *L. mexicana* promastigotes to pentamidine, cymelarsan and other trypanocides was assessed by the alamar blue assay, with empty pNUS vector expression in *L. mexicana* as control (figure 6.19). Both clones of *L. mexicana* + AQP2 showed a 40-fold increase in pentamidine sensitivity and more than 1000-fold increase in cymelarsan sensitivity in comparison to the empty vector control. There was also a 10-fold sensitization to diminazene (Fig. 6.19), but not to amphotericin B (figure 6.19), isometamidium, and ethidium (figure 6.20). Insensitivity of *L. mexicana* + AQP2 to ISM correlates with our earlier observation that AQP2 expression in B48 had no effect on the uptake of ISM in these cells (figure 6.9).

Expression of *TbAQP3* in two independent clones led to minor (1.5 - 3-fold) sensitization to pentamidine which amounted to statistical significance ($P < 0.001$, figure 6.19). This effect was far weaker than with *TbAQP2* and appears to indicate a small increase in the general permeability of the plasma membrane in the *TbAQP3*-expressing promastigotes, sufficient to lead to a small increase in pentamidine uptake over the 5 days of the Alamar blue assay used to determine IC_{50} values in these cells. This is in agreement with the observation that uptake of 100 nM [3H]-pentamidine in *TbAQP3*-transformed promastigotes was not different from control when measured over 5 minutes, whereas pentamidine uptake in *TbAQP2* expressing cells was increased almost 15-fold (figure 6.16). However, since *TbAQP3* was able to cause this small but significant sensitivity to pentamidine alone and at a relatively high concentration of this drug, we began to wonder if *TbAQP3* may turn out to be the gene encoding the LAPT1. This question will be addressed at the end of this chapter (Section 6. 12).

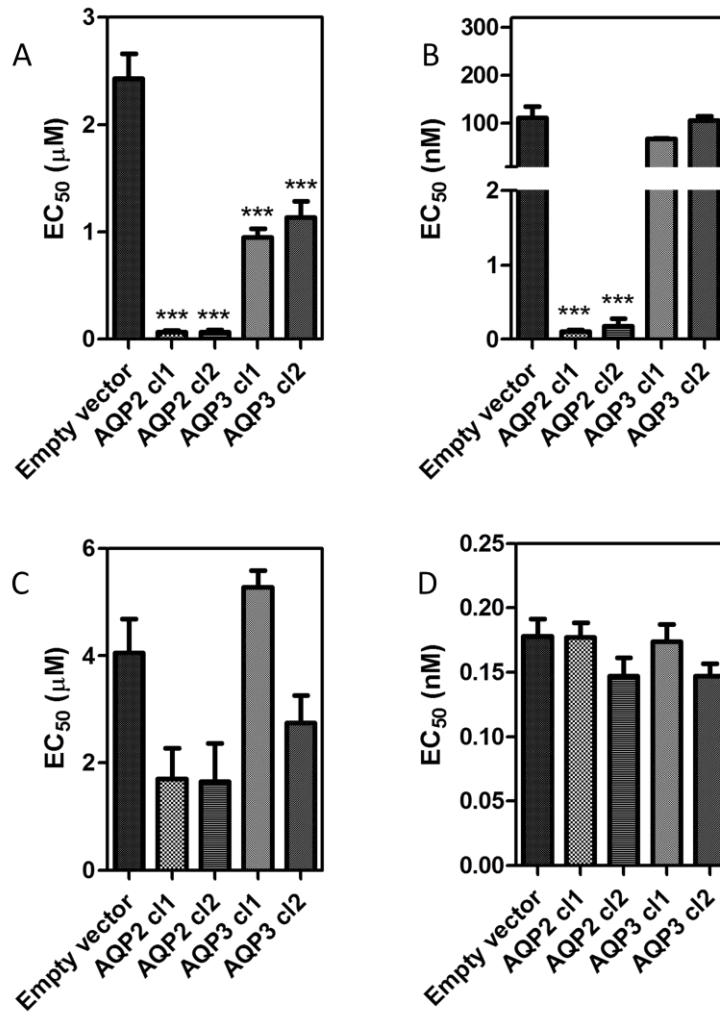


Figure 6.19 Effect of expression of *T. brucei* aquaporins on drug sensitivity of *Leishmania mexicana*. TbaQP2 and TbaQP3 were expressed in promastigotes using the pNUS vector. Two independent clones of each resulting cell line, and the promastigotes transfected with the ‘empty’ pNUS vector, were tested for sensitivity to (A) pentamidine, (B) cymelarsan, (C) diminazene, and (D) amphotericin B, using the Alamar blue fluorimetric assay. Bars are averages of 3 - 8 independent determinations; error bars are SEM. *P<0.05; **P<0.01; ***P<0.001 by one-way ANOVA with Tukey’s correction (Prism 5.0).

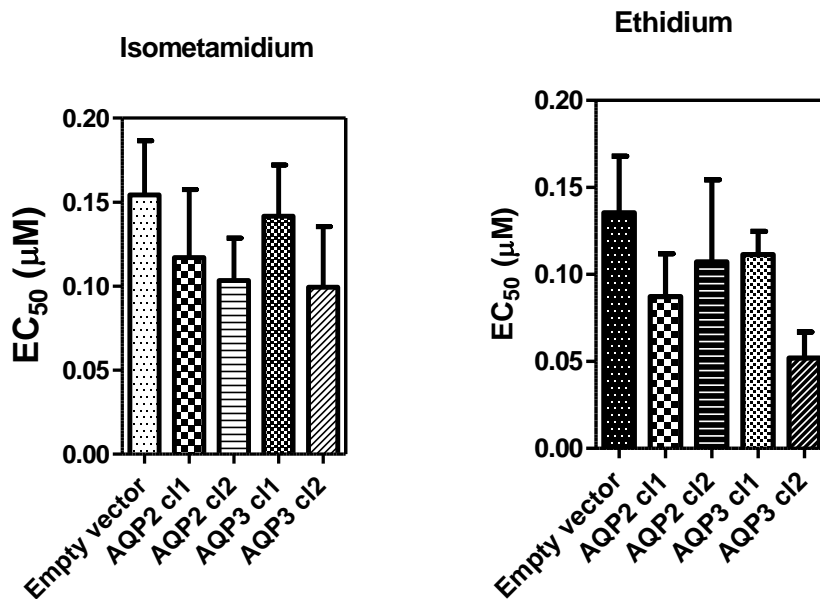


Figure 6.20 Effect of expression of *T. brucei* aquaporins on sensitivity to ISM and Ethidium bromide in *Leishmania mexicana*. Sensitivity was determined by alamar blue assay, using 10^6 cells/ml of each cell line, and incubating the assay at 27°C for 72 hour before addition of alamar blue dye. Fluorescence was measured 48 hours after addition of dye. Bars are averages of 5 - 8 independent determinations; error bars are SEM.

Finally, to buttress the point that only the expression of TbAQP2 is able to cause sensitivity to pentamidine at concentrations around 100 nM, we set up cultures of *L. mexicana* promastogotes expressing AQP2, AQP3, *TbAT-E1* or empty pNUS expression vector. Each cell line was cultured in fresh HOMEM media, starting at a uniform density of 10^4 cells/ml, in the presence and absence of 100 nM pentamidine. Only the *L. mexicana* cells expressing the AQP2 gene showed an observable difference between cells growing in pentamidine and those growing in free media (figure 6.21). In fact, the cell density of *L. mex.* + AQP2 cells growing in pentamidine was below 10^4 cells/ ml from the 2nd day to the 6th day of cell count.

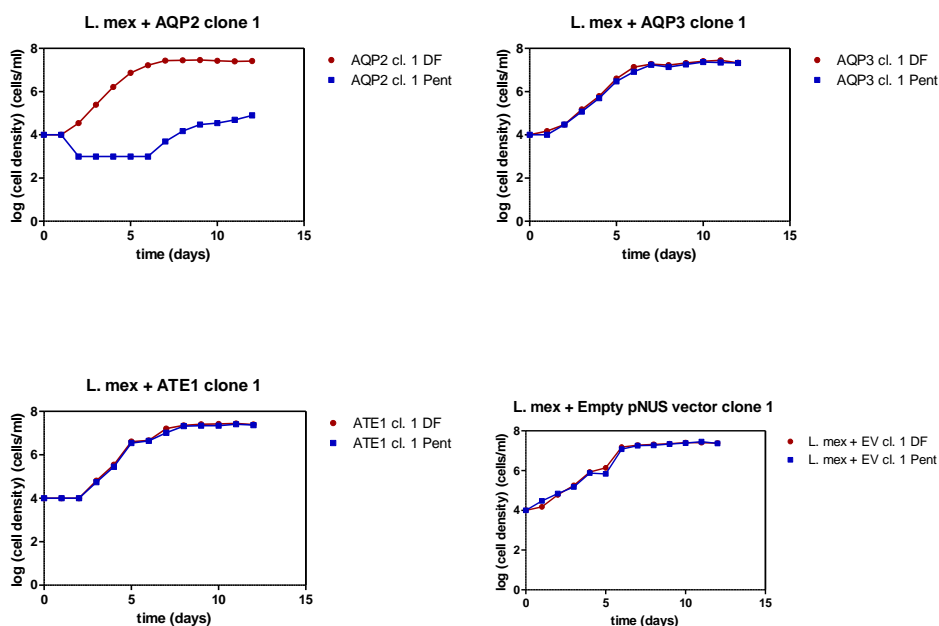


Figure 6.21 Demonstration of the effect of AQP genes on the sensitivity of *L. mexicana* to pentamidine. Rate of growth or increase in cell density was determined as a measure of sensitivity to Pentamidine. Assay was started with 10^4 cells/ml seeding density for all cell lines, in the presence (or absence) of 100 nM pentamidine. Cell density was measured by counting on a haemocytometer once every 24 hours.

6.10. Combination of Pentamidine and SHAM for synergistic studies.

Trypanosome alternative oxidase (TAO) is the sole terminal oxidase of the mitochondrial electron transport chain in the bloodstream forms of *T. brucei*; its function is to re-oxidize the reducing equivalents produced during glycolysis, transferring electrons from ubiquinol (the glycerol-3-phosphate/dihydroxyacetone phosphate shuttle) to oxygen, thus forming water (Chaudhuri *et al*, 2006). Hence, TAO activity is essential to the generation of ATP in bloodstream forms of *Trypanosoma brucei*. TAO inhibition by salicylhydroxamic acid (SHAM) creates an anaerobic-similar condition in which ATP production is halved with concomitant generation of equal amounts of pyruvate and glycerol (Chaudhuri *et al*, 2006).

We found our laboratory-generated B48 cell line to be significantly more sensitive to SHAM ($P < 0.02$, Student's t-test) than the wild type *T. b.427*. Furthermore, when SHAM IC_{50} values (from figure 6.22) are plotted on the same axis with pentamidine IC_{50} values (from figure 6.8), it was found that increase in resistance to pentamidine correlates with increase in sensitivity to SHAM (figure 6.23). We therefore studied the effect of combination of pentamidine and SHAM on our laboratory strains of *Trypanosoma brucei*. A case of synergy will present if a slight increase in pentamidine concentration reduces the SHAM IC_{50} significantly, while SHAM IC_{50} would be expected to remain relatively unchanging with slight increase in pentamidine concentration. Antagonism between the two compounds was not an expected possibility. A clear case of synergy between pentamidine and SHAM was found only in B48 + AQP2 (table 6.1). This finding is in complete agreement with the role of *TbAQP2* as the gene encoding the HAPT1, as the expression of this gene in B48 ensures that sub-nanomolar concentrations of pentamidine are taken up into the organism, where it acts on a different target from that acted on by SHAM, to produce synergy.

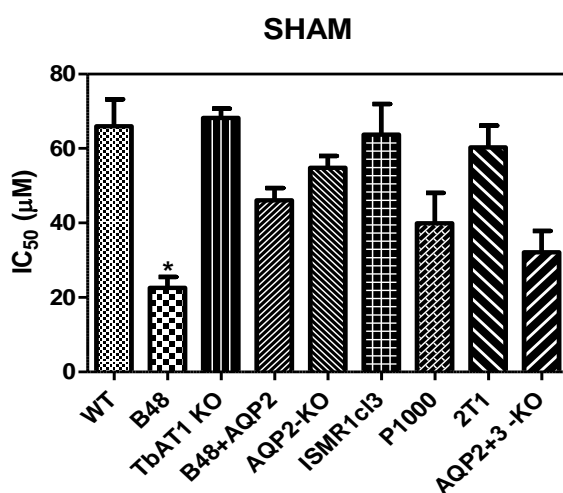


Figure 6.22 Sensitivity of selected cell lines to SHAM Sensitivity was determined by alamar blue assay, using 10^6 cells/ml of each cell line, and incubating the assay at $37^{\circ}C$ and 5% CO_2 for 48 hour before addition of alamar blue dye. Fluorescence was measured 24 hours after addition of

dye. Bars are averages of at least 3 independent determinations; error bars are SEM. *P < 0.02, unpaired Student's t-test

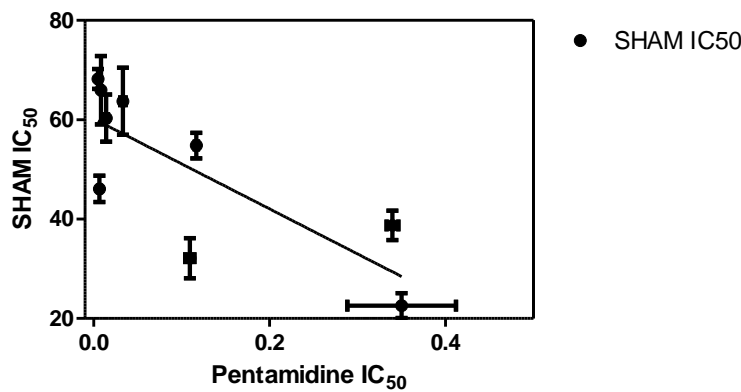


Figure 6.23 Correlation between SHAM and pentamidine IC₅₀ values. IC₅₀ values for SHAM from figure 6.22 were plotted against Pentamidine IC₅₀ values from figure 6.8 for all the cell lines represented. The higher the resistance level to pentamidine, the more susceptible the strain becomes to inhibition of alternative oxidase by SHAM.

WT						
Penta	SHAM IC50 (uM)				AVG	SE
[nM]	1	2	3	4		
0.3	58.1	107	57.25	57.84	70.0	10.7
0.9	48.44	79.6	55.4	61.43	61.2	5.8
3	39.48	71.1	58.25	61.7	57.6	5.7
9	16.48	40.8	71.64	73.01	50.5	11.7

B48

Penta	SHAM IC50 (uM)				AVG	SE
[nM]	1	2	3	4		
270	6.57	20.3	8.496		11.8	3.5
90	14.7	24.7	10.86		16.8	3.4
30	17.5	25.2	12.81		18.5	2.9
9	14.2	22.8	11.1		16.0	2.9

P1000

Penta	SHAM IC50 (uM)				AVG	SE
[nM]	1	2	3	4		
900			46.69		46.7	0.0
270	21.6	17.3	23.28		20.7	1.5
90	23.5	19.5	22.11		21.7	1.0

30	23.04	17.7	21.53	20.8	1.3
9	16.5	15.8	23.95	18.8	2.1

**TbAT1
KO**

Penta [nM]	SHAM IC50 (uM)				AVG	SE
	1	2	3	4		
0.3	44.9	41.5	47.32	25.49	31.85	3.7
0.9	38.9	35.9	52.39	24.23	29.94	4.3
3	33.9	23.04	39.29	20.13	23.52	3.3
9	8.4	0.73	32.72		14.0	7.9

B48 + AQP2						
Penta [nM]	SHAM IC50 (uM)				AVG	SE
	1	2	3	4		
0.3	18.5	26.46	23.85	20.66	22.4	1.5
0.9	11.9	24.6	23.63	21.12	20.3	2.5
3	5.8	10.55	14.46	5.984	9.2	1.8
9	0.82	1.055	2.709	0.9418	1.4	0.4

Table 6.1 SHAM IC₅₀ values in the presence of various concentrations of pentamidine; Doubling dilutions of SHAM (starting 780 μM) was employed in alamar blue assays in the presence of indicated pentamidine concentrations (constant pentamidine concentration per assay). Alamar blue dye was added as usual (after 48 hours incubation at 37°C and 5% CO₂), and fluorescence measured after subsequent incubation for 24 hours.

6.11. Sensitivity of High Affinity Pentamidine Uptake to inhibition by ionophores.

To further characterize the high affinity uptake of pentamidine in *Trypanosoma brucei*, uptake of 25 nM [³H]-pentamidine was measured in the presence of 1 mM adenosine (to block uptake of pentamidine through the P2 transporter). Uptake of [³H]-pentamidine was found to be sensitive to inhibition by specific ionophores known to dissipate plasma membrane proton gradient (CCCP, Nigericin; figure 6.25) but relatively insensitive to valinomycin known to specifically disrupt the mitochondrial membrane potential (figures 6.25 and 6.26) (Munday *et al*, submitted). These findings correlate with an earlier finding

that uptake of 12.5 nM [³H]-Pentamidine by HAPT1 in procyclic forms was similarly inhibited by CCCP, with 10 μM inhibiting >90% of the uptake (de Koning, 2001b)

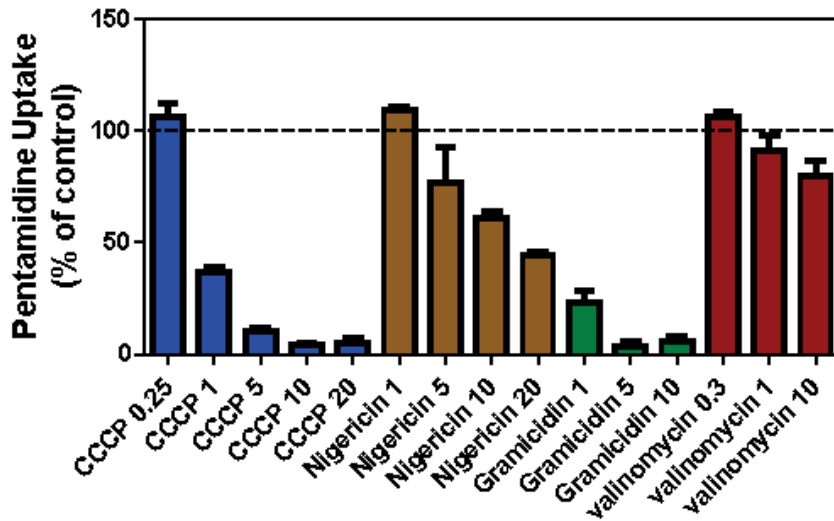


Figure 6.24 High affinity pentamidine uptake in *T. b. brucei* is sensitive to ionophores. Uptake of 25 nM [³H]-pentamidine in s427WT bloodstream forms was measured in the presence of various ionophores at the indicated concentrations in μM, over 5 min. Accumulation of radiolabel was expressed as a percentage of control, being a parallel incubation in the absence of any ionophore. Bars represent the average of 3 independent determinations, each performed in triplicate, and SEM.

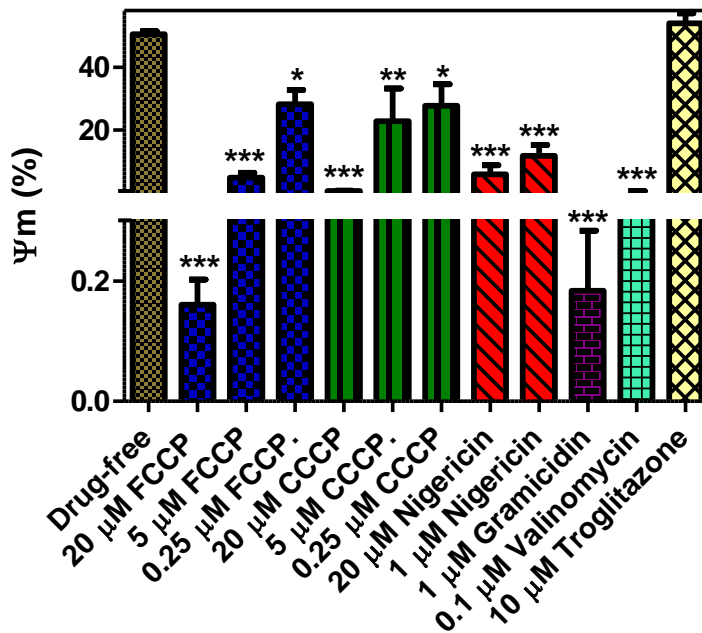


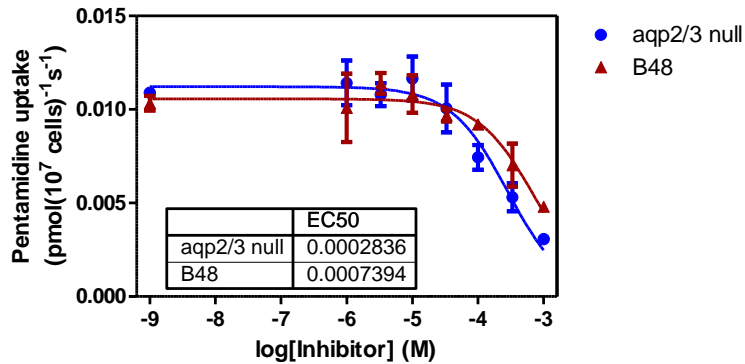
Figure 6.25 Effect of different concentrations of ionophores on the MMP in *T. b. brucei*. 10^6 *Tb427* wt cells were incubated in HMI-9(drug free control) and in the indicated concentrations of individual ionophores (in HMI-9 medium) at 37 °C and 5% CO₂ for 30 minutes before the MMP values were determined (details in section 2.2.9). Bars represent the average of 3 independent determinations and SEM. ***P<0.001; **P<0.01; *P<0.05 by one way ANOVA, compared to the drug-free control, using the Graphpad prism 5.0.

6.12. Does the TbAQP3 gene also express a pentamidine transporter?

It seems appropriate to end this chapter with an assessment of the transport capability of the *TbAQP3*. The expression of this gene in *L. mexicana* promastigotes increased pentamidine sensitivity by about 2-fold (p<0.001, one-way ANOVA using the Graphpad prism 5.0) (figure 6.19). We therefore measured [³H]-pentamidine uptake in *aqp2/aqp3* double null cells (in the presence of 1 mM adenosine) to determine whether the LAPT1 activity had been compromised (due to the additional deletion of AQP3, since *aqp2* null cells still have a functional

LAPT1; see figure 6.12). Figure 6.26 shows that *aqp2/3* double null cells still possess a functional LAPT1 activity, and this activity was found to be identical to the LAPT1 activity in B48 (figure 6.27).

Inhibition plot for uptake of [³H]-Penta in *aqp2/3* null and B48
³H]-Penta = 1 μM; incubation time = 120s.



Michaelis-Menten

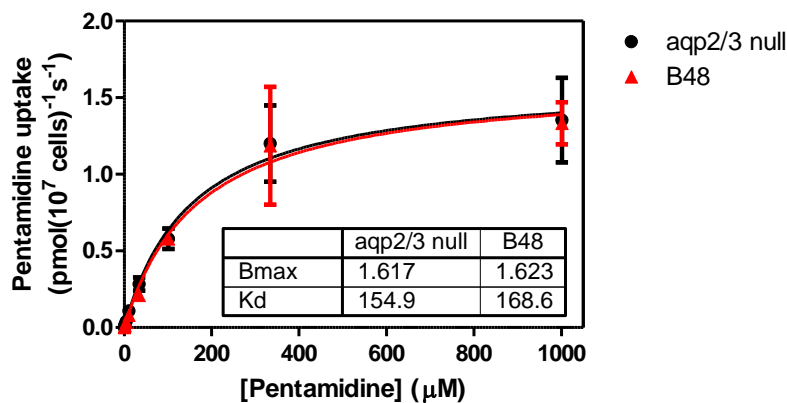


Figure 6.26 Inhibition and Michaelis-Menten plots for the Low affinity [³H]-Pentamidine uptake in *aqp2/3* double null and B48. Rate of uptake was determined by incubating ~ 10⁷ cells per experiment in the presence of 1 μM [³H]-labelled Pentamidine (HAPT1 is inhibited and LAPT1 kinetics are studied at 1 μM Pentamidine concentration) and different concentrations of unlabelled pentamidine at room temperature (section 2.2.5).

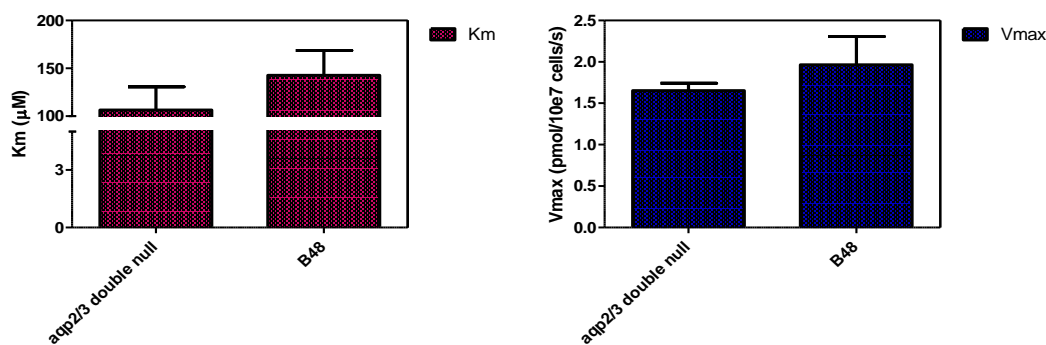


Figure 6.27 Summary of uptake kinetics for *aqp2/3* double null and B48. K_m and V_{max} were determined from the Michaelis Menten saturation curve for these cell lines (figure 6.26). Neither K_m nor V_{max} differed significantly between the two cell lines.

6.13. Discussion

We found that the deletion of both alleles of the *TbAT-E* from *Tb427* wt had no effect on the activity of HAPT1 in these cells (figure 6.1): a functional HAPT1 activity was still present in *TbAT-E* double knockout cells. Similarly, the expression of the *TbAT-E1* in B48 did not increase the sensitivity to pentamidine in this cell line as would be expected if *TbAT-E1* encodes HAPT1 (figure 6.2). These results suggest that the *TbAT-E* is not the gene that encodes for the HAPT1 activity in *Trypanosoma brucei*.

In contrast, *TbAQP2* was able to reverse the resistance to both pentamidine and cymelarsan in B48 (figures 6.2 and 6.3) when expressed in this cell line. In addition, a deletion of *TbAQP2* rendered wild type 2T1 cells significantly pentamidine resistant (figure 6.8). More important however is the fact that HAPT1 activity was not detectable in *aqp2* null cells (figure 6.12). Re-expression of *TbAQP2* in *aqp2/3* double null cell line reversed the resistance of this cell line to both pentamidine and cymelarsan completely, returning it to wild type sensitivity (figure 6.13). Adenosine analogues such as tubercidin, cordycepin and 5'-deoxyadenosine were not taken up through *TbAQP2*; B48 +

AQP2 cells were insensitive to these analogues since they lack the P2 transporter through which they could be taken up (figure 6.11). This finding indicates that *TbAQP2* is indeed a transporter with specificity for a range of ligands, and not just a non-saturable channel that is permeable to the diffusion of right sized molecules, as suggested recently (Bassarak *et al*, 2011). Also, a synergistic effect found for the combination of pentamidine and SHAM on B48 + AQP2 out of all cell lines tested (including *Tb427* wt; table 6.1) suggests that there is an enhanced uptake of pentamidine even at very low nanomolar concentrations (which can only be due to the activity of the HAPT1).

Furthermore, the heterologous expression of *TbAQP2* in *Leishmania mexicana* promastigotes resulted in a highly significant increase in sensitivity to both pentamidine and cymelarsan, compared to the control *L. mexicana* cells expressing the empty pNUS-HcN vector (figure 6.19). Again, the fact that inhibition studies carried out with pentamidine, propamidine and diminazene on the uptake of [³H]-pentamidine gave a kinetic profile that is fully consistent with the *T. b. brucei* HAPT1 activity (figure 6.17) was very important. This finding, in addition to the finding that HAPT1 activity in wild type *T. b. brucei* (which is lost on deletion of *TbAQP2* and is only present on the expression of wild type *TbAQP2* gene) is sensitive to agents such as CCCP and nigericin (figure 6.24) that are known to act by specifically dissipating the plasma membrane proton gradient, leads us to accept that *TbAQP2* indeed expresses the HAPT1 of bloodstream trypanosomes which uses the proton-motive force to drive pentamidine uptake.

6.14. Conclusion

We conclude, based on the findings presented in this chapter, that *TbAQP2* is responsible for the HAPT1 activity in bloodstream form *T. b. brucei*. Hence, kinetoplastid aquaporins have extended their traditional role of acting

only as bifunctional channels through which water and other uncharged solutes pass into the cell (Beitz, 2005), to the saturable transport of neutral and positively charged drugs with a substantially higher molecular weight.

**7. Test of a library of Bisphosphonium
compounds for inhibitors of the Low Affinity
Pentamidine Transporter (LAPT1).**

7.1. Introduction

The World Health Organisation puts the number of people at risk of being infected by the human African trypanosomiasis at above 60 million (W.H.O., 1998). While this figure is outrageous, the report claims that it may even be lower than the actual figure since less than 4 million people are under surveillance, and hence only 10% of new infections are diagnosed and treated (W.H.O., 1998). On the other hand, nagana which is caused by a wider range of trypanosome species is most always the greater epidemic across Africa and carries a more direct economic burden (Baral, 2010). One hundred years after this disease was first discovered, trypanosomiasis remains one of the major parasitic diseases for which control is not in sight (Baral, 2010). Control of both the human and animal trypanosomiasis relies heavily on chemotherapy, but with the few drugs currently available and the increasing reports of resistance to these few drugs, coupled with severe toxic effects of most HAT drugs, the need for new drugs cannot be over-emphasized (Baral, 2010). The currently available treatment schemes can however be made more effective if the mechanism of resistance could be elucidated so that future cases of resistance can easily be reversed and infections treated. Of all the proposed mechanisms of resistance, reduction of net drug uptake seems to be the most implicated with regards to trypanocidal resistance, and this mechanism most frequently implies mutations in transporters since most trypanocides are translocated across the plasma membrane by these transporters (Mäser *et al*, 2003). One approach to resolving the molecular mechanisms of trypanosomal drug resistance is therefore to identify candidate drug transporters and to investigate whether such transporters are mutated in drug-resistant trypanosomes (Mäser *et al*, 2003). HAPT1 and LAPT1 activities have both been identified and characterised in most

laboratory adapted cell lines of *T. b. brucei* (de Koning, 2001b; Matovu *et al*, 2003), and HAPT1 has been implicated in the uptake and resistance to diamidines and melaminophenyl arsenicals (Bridges *et al*, 2007). It was in fact demonstrated that loss of both TbAT1 and HAPT1 leads to high levels of cross resistance to pentamidine and melaminophenyl arsenicals (Bridges *et al*, 2007). Our recent demonstration that TbAQP2 encodes the HAPT1 (chapter 6) leaves us with only the LAPT1 as the major pentamidine transporter in *T. b. brucei* whose gene sequence is yet to be identified.

Preliminary work on the uptake of ISM, done in our group, before the start of my project, possibly implicated LAPT1 in the uptake of this drug in *Trypanosoma brucei brucei*. Our finding that the V_{\max} was significantly reduced ($P = 0.043$, unpaired student's t-test; chapter 4) in our ISM resistant clone, ISMR1 clone 3, is consistent with this. The problem however, is that a pentamidine concentration of about 1 mM is usually needed to completely inhibit this transporter and some other trypanocides, especially diminazene is not soluble in assay buffer at 1 mM (we usually prepare drugs for uptake initially at 4 times the final conc., that means that we make an initial 4 mM when the final conc. is 1 mM; diminazene cannot be dissolved at this conc.). Lack of specific inhibitors has been the biggest constraint to the study of this transporter and there is an urgent need to identify such inhibitors (250 μM maximum) so as to overcome this limitation on the study of the characteristics of LAPT1. We therefore screened a library of bisphosphonium compounds and drew up a short-list of LAPT1 inhibitors. We also tested (when possible) for selective inhibition of LAPT1 over HAPT1.

7.2. Bisphosphonium compounds as inhibitors of Pentamidine uptake through the LAPT1.

Phosphonium salts bearing hydrophobic functional groups are lipophilic cations with a delocalized charge, and this affords specific properties to these molecules such as the capacity to cross biological membranes driven by electrical potential (Taladriz *et al*, 2012). Bisphosphonium salts are therefore the symmetrical, higher molecular weight members of this group of compounds. They all tend to accumulate in organelles with high inside-negative membrane potential such as mitochondria, aided by their ability to cross the mitochondrial inner membrane without the assistance of ionophores or carrier proteins but solely driven by the MMP (Ross *et al*, 2005). On the contrary, hydrophilic inorganic or organic cations such as Na⁺ and pentamidine, respectively, cannot cross biological membranes except when facilitated by a transport protein (Ross *et al*, 2005). Since an increase in the level of lipophilic shielding around the phosphonium cation(s) correlates with increased levels of activity against *Trypanosoma* and *Leishmania* species, it was suggested that this class of compounds is most probably transported by diffusion into the parasites (Taladriz *et al*, 2012). This line of argument was supported by the fact that no correlation was found between the antiparasitic activity and inhibition of the known *T. brucei* transporters, namely, P2, HAPT1 and LAPT1 (Taladriz *et al*, 2012). Hence in tables 7.2, 7.3, and 7.4, there is no difference in the IC₅₀ values of these compounds for cells known to have lost one or two drug transporters, such as the *TbAT1*^(-/-) and the B48 cells respectively, when compared to the IC₅₀ for the wild type. Also, most of the bisphosphonium compounds were considered too large to be a substrate for these transporters (though they could still be good inhibitors, as suggested by their high affinities for HAPT1 and LAPT1, table 7.1 and figure

7.1) since their molecular weights range between 800 and 1300, compared to 340 for pentamidine (Taladriz *et al*, 2012).

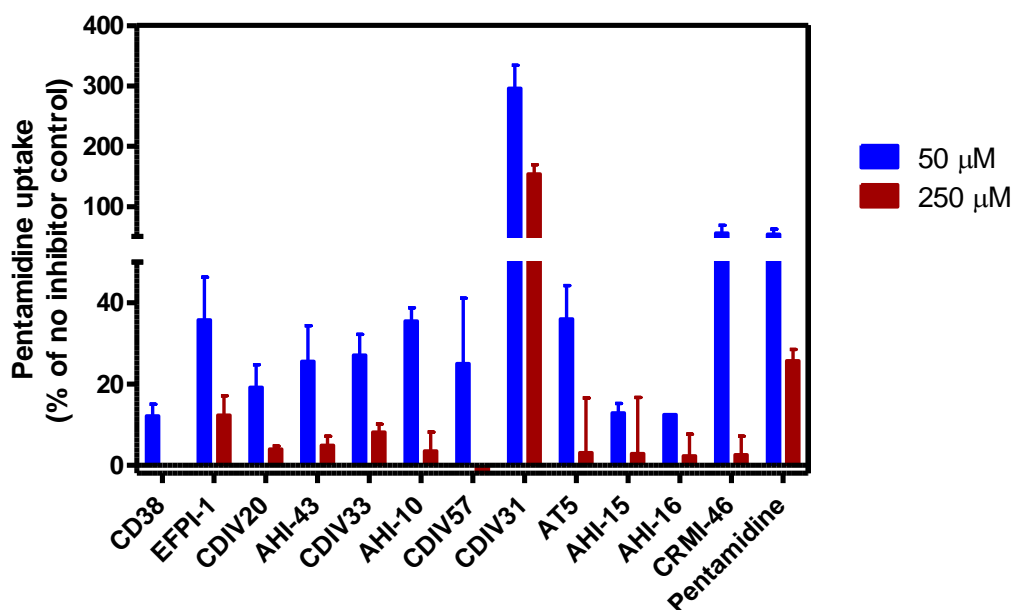


Figure 7.1 Percentage inhibition of 1 μM [³H]-pentamidine uptake by Tb427 wt in the presence of bisphosphonium compounds (synthesized by our collaborator, Dr Christophe Dardonville, Instituto de Quimica Medica, Madrid). Uptake was determined by incubating ~ 10⁷ cells per experiment in the presence of 1 μM [³H]-labelled Pentamidine (HAPT1 is inhibited and LAPT1 kinetics are studied at 1 μM Pentamidine concentration) and indicated concentrations of bisphosphonium compounds at room temperature (section 2.2.5).

The lack of correlation between antiparasitic activity and inhibition of the known *T. brucei* transporters confirms that these compounds are not dependent on the transporters for their antiparasitic action. Hence, these compounds bind to the transporters but may not be transported and so inhibit further transport activity. However, the data presented in tables 7.2, 7.3 and 7.4 is enough to rule out uptake of bisphosphonium compounds by either the P2 or the HAPT1, since the absence of either transporter did not affect sensitivity of trypanosomes to these compounds.

Compound	K _i HAPT1 (±SE) (μM)	K _i LAPT1 (±SE) (μM)
Pentamidine ¹	0.036 ± 0.006	56.2 ± 8.3
CDIV31 (18a)	>250	>250
CD38 (24a)	5.2 ± 0.9	2.2 ± 0.4
CRMI-46 (25a)	Not done	25 ± 6
AHI-16 (25b)	Not done	9.5 ± 0.5
AHI-15 (25c)	53 ± 13	7.2 ± 4.0
CDIV33 (26a)	Not done	39 ± 7.0
EFpl-1 (35a)	Not done	19 ± 6
CDIV20 (36a)	Not done	49 ± 6
AHI-10 (38b)	Not done	20 ± 4
AHI-43 (45e)	9.2 ± 1.3	3.6 ± 0.4
AT-5 (55)	Not done	25 ± 11

Table 7.1 Affinity of Selected Phosphonium compounds (synthesized by our collaborator, Dr Christophe Dardonville, Instituto de Quimica Medica, Madrid) on the HAPT1 and LAPT1 diamidine transporters of *T. b. brucei*. Affinity was determined by measuring the uptake of 30 nM (for HAPT1) or 1 μM (for LAPT1) concentration of [³H]-Pentamidine in the presence of different concentrations of each bisphosphonium compound. Each value is an average of at least 3 independent experiments, performed in triplicates (Assigned compound number in tables 7.2, 7.3 and 7.4 for each compound is in bracket). ¹Taken from De Koning (2001)

It may be argued that LAPT1 cannot transport bisphosphonium compounds because they are at least two times larger than pentamidine (Taladriz *et al*, 2012), the standard ligand for this transporter; however this argument is not completely persuasive. A similar argument was raised against the *TbAQP2* gene as a candidate for the gene encoding the HAPT1. Melarsoprol and pentamidine with molecular masses of 398 Da and 340 Da, respectively were considered

substantially larger than glycerol (the natural substrate of *TbAQP2*) at 92 Da, which led to the suggestion that AQP2 may indeed not transport these drugs directly but could indirectly regulate HAPT1 expression or function (Baker *et al*, 2013). However, it was earlier demonstrated that *Leishmania major* AQP1 transports trivalent arsenic and antimony (Figarella *et al*, 2007). In addition, we have been able to demonstrate that *TbAQP2* is indeed the long-sought HAPT1 (Chapter 6; manuscript accepted), and can directly transport pentamidine and cymelarsan (chapter 6). Therefore, data presented in tables 7.1 (low K_i values), 7.2, 7.3, 7.4 (corresponding low IC_{50} values) are in support of the LAPT1 being the route of entry for bisphosphonium compounds, perhaps alongside diffusion. Either way, these compounds are able to inhibit the transport of pentamidine through the LAPT1 as demonstrated by the low K_i values (concentration required to produce half maximum inhibition) found for most of these compounds (table 7.1). Also, the high K_i value found for CDIV31 (compound 18a) is quite consistent with the high EC_{50} presented for this compound in table 7.2. This suggests that CDIV31 is actually not a good substrate for the LAPT1.

Screening of this library of bisphosphonium compounds was done in order to select good inhibitors of LAPT1 that inhibit this transporter at lower concentrations than pentamidine. Interest in this class of compounds was awakened when the extensive trypanocidal activity of the lead bisphosphonium compound (CD-38 or compound 24a) was observed. CD-38 was initially followed up and screened as a trypanocidal drug candidate, but it was dropped after it was found to have a very low selectivity index (it was quite toxic to human cell lines, table 7.2). Subsequently, a library of bisphosphonium compounds was synthesized, patterned on CD-38 by altering functional groups or the linker group (figure 7.2).

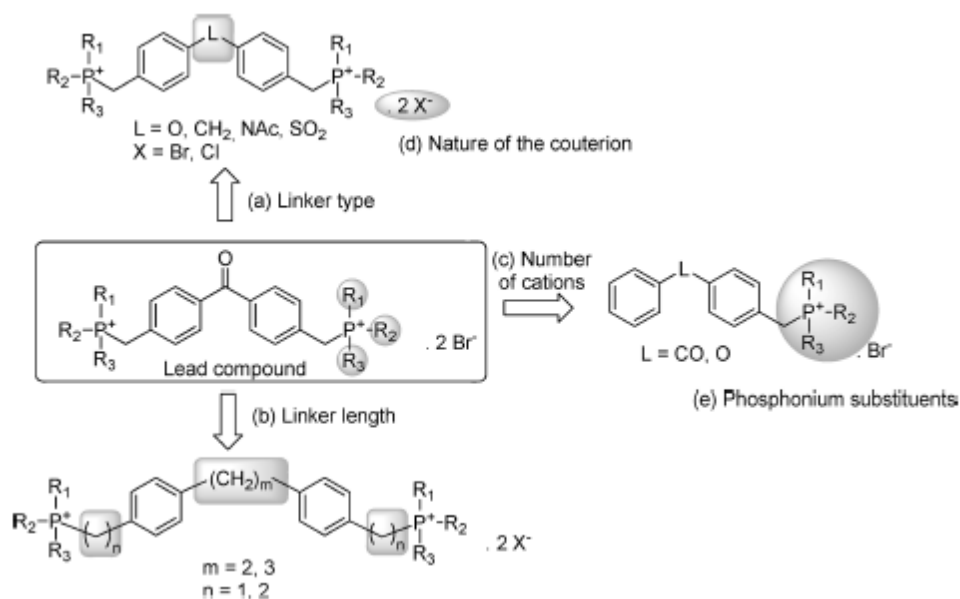


Figure 7.2 General structure of benzophenone-derived bisphosphonium salt derivatives with antileishmanial and antitrypanosomal activity. Taken from Taladriz *et al* (2012).

7.3. Time-dependent toxicity of selected bisphosphonium compounds to trypanosomes.

Since this is not a screen for potential drug candidates, we are not looking for compounds that will give the lowest EC_{50} ; rather we are interested in compounds with a low K_i for [3H]-pentamidine uptake by LAPT1 coupled with a relatively high EC_{50} for most of the trypanosome strains. The high EC_{50} values are important to avoid cell lysis or cell damage during the uptake assay time. Hence the compounds listed in table 7.1 were initially selected from the library of bisphosphonium compounds for having K_i values for LAPT1 that were less than $56.2 \pm 8.3 \mu M$ reported for pentamidine (de Koning, 2001b). Selected compounds were subsequently screened using propidium iodide real time assay. This assay measures fluorescence produced by propidium iodide on binding to nucleic acid; this binding is assumed to occur after cell lysis, or at least after the plasma membrane has ceased to be a barrier, as propidium iodide is otherwise unable to enter the cells. Hence, level of fluorescence is directly proportional to amount of nucleic acid available for binding, and also directly proportional to the number of dead cells. Fluorescence readings are taken for 8 hours, after cells are added at zero time. The next best inhibitor of LAPT1 after CD-38 is AHI-43 (compound 45e) with a K_i of $3.6 \pm 0.4 \mu M$ for LAPT1. This compound did not cause the lysis of trypanosomes within the first 15 minutes of incubation in $125 \mu M$ which is about 31 times the K_i (figure 7.4). AHI-43 was therefore selected as the best bisphosphonium inhibitor of LAPT1. However, the extraordinarily fast action on trypanosome viability and integrity makes these compounds less than perfect as pharmacological inhibitors of uptake of other drugs.

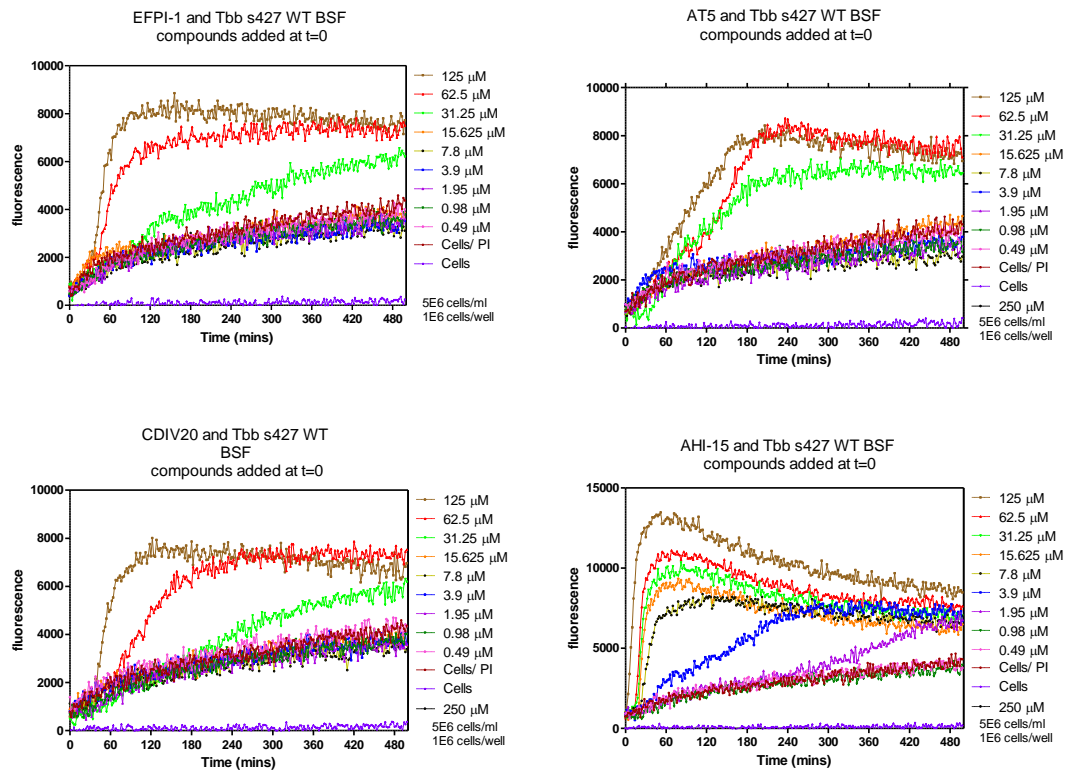


Figure 7.3 Propidium iodide real time assay showing the rate at which the selected bisphosphonium compounds kill trypanosomes. Assay was performed by incubating 5×10^5 trypanosomes in $9 \mu\text{M}$ propidium iodide at different concentrations (doubling dilutions) of each compound and at 37°C and $5\% \text{CO}_2$ for about 8 hours (250 cycles; with fluorescence being measured every 150 seconds in a FLUOstar OPTIMA fluorimeter. Note that AT5 is a monophosphonium compound.

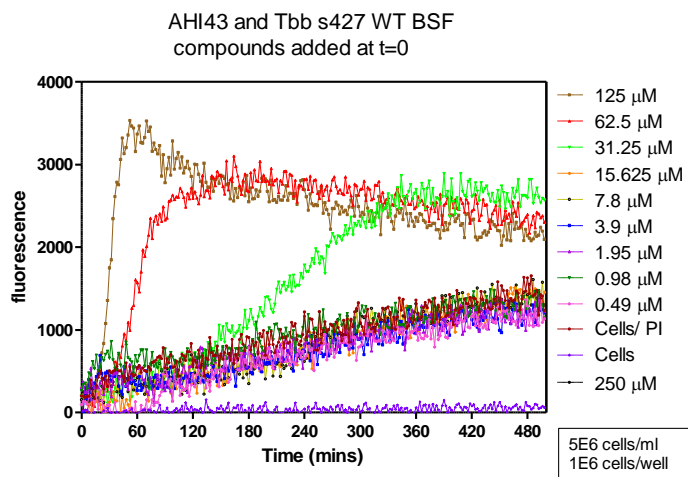
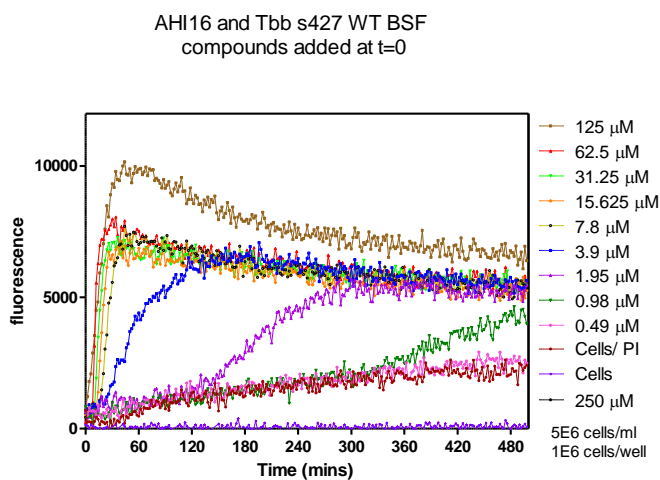
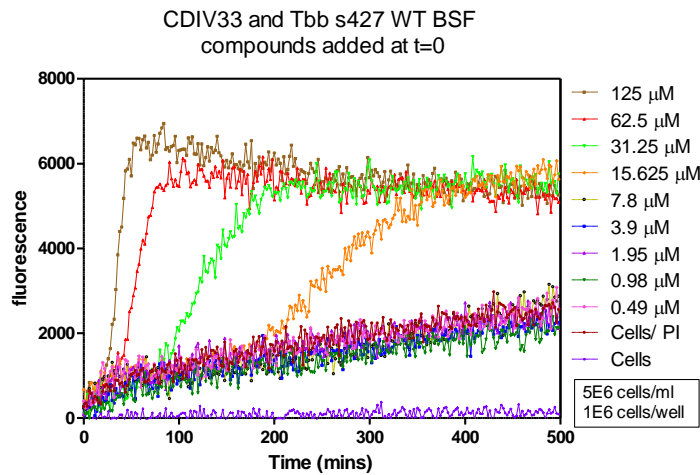


Figure 7.4 More propidium iodide real time assays, showing the rate at which selected bisphosphonium compounds kill trypanosomes. Assay was performed by incubating 5×10^5 trypanosomes in 9μ M propidium iodide at different concentrations (doubling dilutions) of each compound and at 37°C and $5\% \text{CO}_2$ for about 8 hours (250 cycles; with fluorescence being measured every 150 seconds in a FLUOstar OPTIMA fluorimeter).

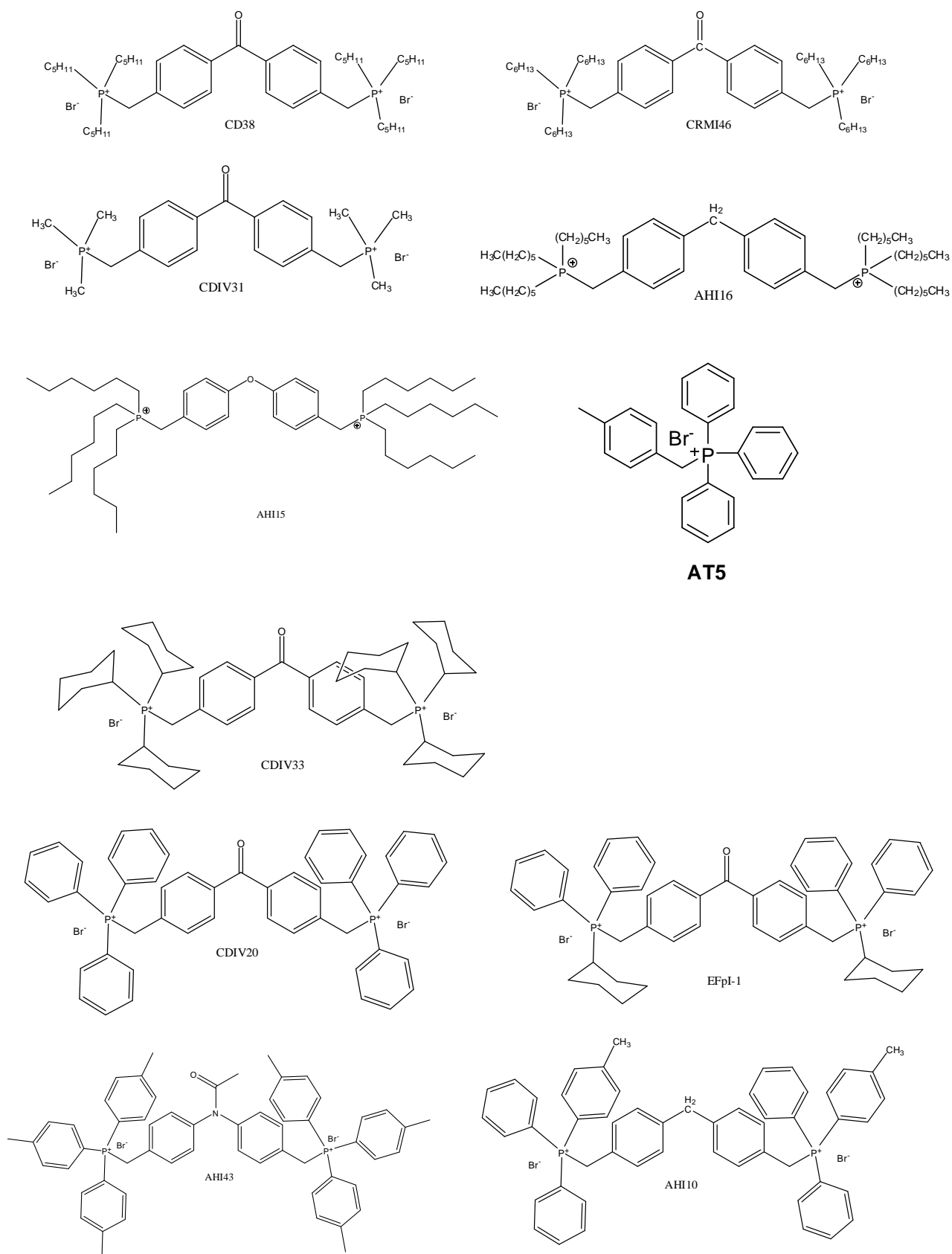
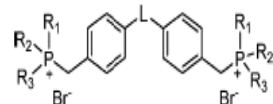


Figure 7.5 structures of selected bisphosphonium compounds.

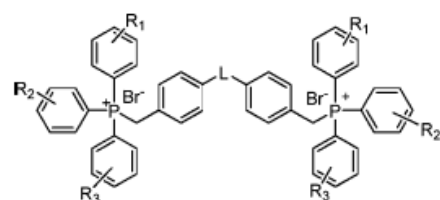
7.4. Discussion

LAPT1 is a high capacity transporter with a K_m of $56 \pm 8 \mu\text{M}$ for pentamidine uptake for which no practical inhibitors have been identified to date (de Koning, 2001b). LAPT1 and HAPT1 of the bloodstream forms of *T. b. brucei* were demonstrated to be kinetically identical to LAPT1 and HAPT1 of procyclic forms (Teka *et al*, 2011). Conclusive determination of the genetic identity of the two transporters is however necessary for a definitive proof that these transporters are identical in both lifecycle stages (Teka *et al*, 2011). We found recently that the HAPT1 is encoded by the AQP2 gene (Chapter 6; manuscript submitted). On the other hand, lack of specific inhibitors has hindered a thorough study of the kinetics and pharmacological importance of LAPT1. It takes about 1 mM of pentamidine to completely inhibit uptake through this transporter, yet no substrate or inhibitor with higher affinity than pentamidine has been identified for this transporter (Teka *et al*, 2011). We therefore tested a library of bisphosphonium compounds as possible inhibitors of this transporter.



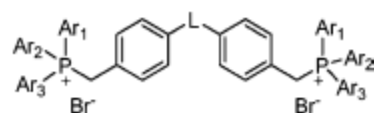
compd	L	R ₁	R ₂	R ₃	EC ₅₀ (μM) (selectivity index) ^f									
					<i>T. b. rhod.</i> ^a	cytox L6 ^b	<i>T. b. brucei</i> WT ^c	TbAT1-KO ^d	RP ^e	<i>T. b.</i> B48 ^f	RP ^e	cytox HEK ^g	SI ^h	
melarsoprol					0.0075									
podophyllotoxin						0.012								
pentamidine								0.008 ± 0.002	0.009 ± 0.003	1.1	0.567 ± 0.086	70.9		
diminazene								0.517 ± 0.132	2.39 ± 0.84	4.6	2.617 ± 0.714	5.1		
18a	CO	Me	Me	Me	127	>173	>100	>100		>100		nd ⁱ		
19a	CO	Et	Et	Et	77.8	>149	>100	>100		>100		>300		
19b	CH ₂	Et	Et	Et	18.7	48.3	21.5 ± 0.3	18.5 ± 0.4	0.9	19.3 ± 0.2	0.9	>300	>14	
19c	O	Et	Et	Et	31.9	101.6	36.5 ± 3.5	34.9 ± 0.2	1.0	36.6 ± 0.6	1.0	>300	>8	
20a	CO	<i>n</i> -Pr	<i>n</i> -Pr	<i>n</i> -Pr	8.5	>130	19.73 ± 4.11	27.15 ± 3.82	1.4	31.32 ± 4.15	1.6	nd		
21a	CO	ⁱ Pr	ⁱ Pr	ⁱ Pr	9.6	>130	20.55 ± 5.19	33.41 ± 6.20	1.6	38.82 ± 6.41	1.9	nd		
22a	CO	<i>n</i> -Bu	<i>n</i> -Bu	<i>n</i> -Bu	0.355 (315)	111.7	0.48 ± 0.11	1.32 ± 0.46	2.7	1.63 ± 0.46	3.4	>300	>620	
23a	CO	ⁱ Bu	ⁱ Bu	ⁱ Bu	1.46	>116	2.62 ± 0.69	8.34 ± 3.08	3.2	6.30 ± 1.39	2.4	>300	>110	
23b	CH ₂	ⁱ Bu	ⁱ Bu	ⁱ Bu	0.326 (141)	45.9	0.70 ± 0.03	0.88 ± 0.10	1.3	0.88 ± 0.06	1.3	>300	>429	
23c	O	ⁱ Bu	ⁱ Bu	ⁱ Bu	1.62	51.1	0.59 ± 0.06	0.80 ± 0.10	1.3	1.06 ± 0.34	1.8	>300	>507	
23d	SO ₂	ⁱ Bu	ⁱ Bu	ⁱ Bu	6.31	>111	16.7 ± 0.5	13.6 ± 2.2	0.8	13.3 ± 1.6	0.8	nd		
23e	NAc	ⁱ Bu	ⁱ Bu	ⁱ Bu	11.44	>112	nd	nd		nd		nd		
24a	CO	<i>n</i> -pentyl	<i>n</i> -pentyl	<i>n</i> -pentyl	0.289 (30)	8.7	0.20 ± 0.03	0.17 ± 0.01	0.8	0.18 ± 0.01	0.9	66.8 ± 4.9	338	
25a	CO	<i>n</i> -hex	<i>n</i> -hex	<i>n</i> -hex	0.112 (10)	1.11	0.038 ± 0.001	0.047 ± 0.007	1.2	0.035 ± 0.003	0.9	16.6 ± 0.7	438	
25b	CH ₂	<i>n</i> -hex	<i>n</i> -hex	<i>n</i> -hex	0.180 (5)	0.964	0.033 ± 0.006	0.033 ± 0.005	1.0	0.039 ± 0.002	1.2	18.1 ± 2.6	543	
25c	O	<i>n</i> -hex	<i>n</i> -hex	<i>n</i> -hex	0.109 (9)	1.03	0.037 ± 0.004	0.045 ± 0.005	1.2	0.041 ± 0.002	1.1	22.1 ± 1.1	593	
26a	CO	<i>c</i> -hex	<i>c</i> -hex	<i>c</i> -hex	0.197 (166)	32.7	0.14 ± 0.03	0.23 ± 0.05	1.6	0.25 ± 0.04	1.8	>300	>2100	
27a	CO	<i>n</i> -octyl	<i>n</i> -octyl	<i>n</i> -octyl	0.22 (5)	1.0	0.042 ± 0.002	0.061 ± 0.001	1.4	0.045 ± 0.001	1.1	27.0 ± 1.4	639	
28a	CO	Me	Me	Ph	8.8	>139	19.17 ± 7.17	28.77 ± 5.62	1.5	24.55 ± 4.75	1.3	nd		
28b	CH ₂	Me	Me	Ph	2.586	>142	5.45 ± 1.09	4.60 ± 0.80	0.8	3.84 ± 1.19	0.7	>300	>55	
28c	O	Me	Me	Ph	3.827	84.5	7.22 ± 0.16	6.52 ± 0.39	0.9	6.15 ± 0.89	0.9	>300	>40	
28f	(CH ₂) ₂	Me	Me	Ph	1.20 (40)	48.6	2.59 ± 0.64	2.62 ± 0.16	1.0	1.8 ± 0.58	0.5	>300	>110	
28g	(CH ₂) ₃	Me	Me	Ph	1.22 (49)	59.5	1.27 ± 0.33	1.37 ± 0.11	1.1	1.09 ± 0.38	0.9	>300	>230	
29a	CO	Et	Et	Ph	2.9	>128	8.59 ± 2.16	17.75 ± 2.03	2.1	15.17 ± 3.72	1.8	>300	>35	
30a	CO	<i>c</i> -hex	<i>c</i> -hex	Ph	0.32 (72)	22.9	0.24 ± 0.03	0.26 ± 0.04	1.1	0.29 ± 0.03	1.2	>300	>1270	
31a	CO	Me	Ph	Ph	0.656 (177)	115.9	1.53 ± 0.38	2.08 ± 0.63	1.4	2.05 ± 0.38	1.3	>300	>200	
32a	CO	Et	Ph	Ph	0.554 (>204)	>113	0.97 ± 0.27	2.10 ± 0.54	2.2	1.76 ± 0.30	1.8	>300	>300	
33b	CH ₂	<i>n</i> -Pr	Ph	Ph	0.799 (4.1)	3.27	0.373 ± 0.003	0.40 ± 0.01	1.1	0.43 ± 0.08	1.1	>300	>800	
33c	O	<i>n</i> -Pr	Ph	Ph	0.567 (5)	2.9	0.25 ± 0.03	0.28 ± 0.01	1.1	0.3 ± 0.01	1.2	233 ± 31	914	
34b	CH ₂	ⁱ Pr	Ph	Ph	0.534 (6.4)	3.44	0.44 ± 0.04	0.40 ± 0.03	0.9	0.43 ± 0.09	1.0	>300	>680	
34c	O	ⁱ Pr	Ph	Ph	0.585 (8.6)	5.0	0.33 ± 0.02	0.33 ± 0.01	1.0	0.33 ± 0.01	1.0	>300	>900	
35a	CO	<i>c</i> -hex	Ph	Ph	0.43 (155)	65.8	0.30 ± 0.03	0.41 ± 0.01	1.4	0.33 ± 0.03	1.1	>300	>1000	

Table 7.2 Antitrypanosomal activity of bisphosphonium salts having aliphatic and phenyl substituents (18a = CDIV31, 24a = CD38, 25a = CRMI-46, 25b = AHI-16, 25c = AHI-15, 26a = CDIV33, 35a = EFPI-1). Taken from Taladriz *et al* (2012). ^a*T. b. rhodesiense* STIB900 trypomastigotes. ^bRat skeletal myoblast L6 cells. ^c*T. b. brucei* s427 trypomastigotes. ^d*T. b. brucei* knockout strain lacking a functional P2-transporter and resistant to diminazene aceturate. ^eResistance factor compared to WT. ^fThe B48 strain is a mutant, derived from the TbAT1-KO strain, with a nonfunctional high affinity pentamidine transporter (HAPT). This strain is resistant to diminazene, pentamidine and melaminophenyl arsenicals. ^gHuman embryonic kidney (HEK) cells. ^hSelectivity index = [EC₅₀(HEK cells)/EC₅₀(*T. b. brucei* WT)]. ⁱSelectivity index = [EC₅₀(L6-cells)/EC₅₀(*T. b. rhodesiense*)]. ^jNot determined.



compd	L	R ₁	R ₂	R ₃	EC ₅₀ (μM) (selectivity index) ^f								
					<i>T. b. rhod</i> ^a	cytox L6 ^b	<i>T. b. brucei</i> WT ^c	TbAT1-KO ^d	RP ^e	<i>T. b.</i> B48 ^f	RP ^e	cytox HEK ^g	SI ^h
36a	CO	H	H	H	0.260 (282)	73.3	0.24 ± 0.07	0.36 ± 0.07	1.5	0.38 ± 0.06	1.6	>300	>1250
37a	CO	H	H	2-Me	0.16 (88)	14.0	0.20 ± 0.01	0.24 ± 0.03	1.2	0.22 ± 0.02	1.1	214.3 ± 9.5	1098
38a	CO	H	H	4-Me	0.26 (62)	16.3	0.180 ± 0.002	0.182 ± 0.006	1.0	0.183 ± 0.005	1.0	261.3 ± 24.3	1449
38b	CH ₂	H	H	4-Me	0.200 (22)	4.47	0.24 ± 0.04	0.19 ± 0.03	0.8	0.18 ± 0.02	0.7	>300	>1250
38c	O	H	H	4-Me	0.142 (23)	3.34	0.082 ± 0.014	0.077 ± 0.002	0.9	0.064 ± 0.009	0.8	240.3 ± 6.7	2930
39a	CO	4-Cl	4-Cl	4-Cl	0.41 (18)	7.2	0.94 ± 0.14	1.37 ± 0.02	1.5	0.95 ± 0.13	1.0	63 ± 8	67
40a	CO	4-F	4-F	4-F	0.45 (172)	77.4	0.85 ± 0.17	2.10 ± 0.03	2.5	1.24 ± 0.14	1.5	>300	>350
41a	CO	4-OMe	4-OMe	4-OMe	0.29 (40)	11.8	0.32 ± 0.07	0.52 ± 0.02	1.6	0.23 ± 0.04	0.7	172 ± 7	529
42a	CO	2-OMe	2-OMe	H	0.23 (28)	6.4	0.24 ± 0.04	0.32 ± 0.02	1.3	0.19 ± 0.04	0.8	107 ± 15	438
43a	CO	2-OMe	2-OMe	2-OMe	0.20 (45)	9.0	0.11 ± 0.02	0.16 ± 0.01	1.5	0.08 ± 0.02	0.7	131 ± 17	1175
43b	CH ₂	2-OMe	2-OMe	2-OMe	0.209 (5)	1.08	0.080 ± 0.004	0.074 ± 0.003	0.9	0.066 ± 0.002	0.8	204 ± 13	2561
43c	O	2-OMe	2-OMe	2-OMe	0.153 (8)	1.27	0.056 ± 0.011	0.057 ± 0.008	1.0	0.045 ± 0.004	0.8	141 ± 5	2518
44a	CO	4-CF ₃	4-CF ₃	4-CF ₃	16.4	25.0	5.05 ± 1.84	8.51 ± 1.98	1.7	2.73 ± 0.76	0.5	>300	>60
44b	CH ₂	4-CF ₃	4-CF ₃	4-CF ₃	1.72	7.52	0.23 ± 0.06	0.37 ± 0.09	1.6	0.28 ± 0.04	1.2	77.1 ± 8.6	338
44c	O	4-CF ₃	4-CF ₃	4-CF ₃	5.26	9.93	0.24 ± 0.06	0.32 ± 0.05	1.3	0.28 ± 0.05	1.2	174 ± 23	723
45a	CO	4-Me	4-Me	4-Me	0.22 (49)	10.8	0.11 ± 0.02	0.018 ± 0.01	1.6	0.09 ± 0.02	0.8	141 ± 10	1266
45a (Cl ⁻ salt)	CO	4-Me	4-Me	4-Me	0.084 (14.5)	1.22	0.094 ± 0.023	0.065 ± 0.002	0.7	0.073 ± 0.025	0.8	24 ± 1.2	254
45b	CH ₂	4-Me	4-Me	4-Me	0.099 (24)	2.33	0.080 ± 0.002	0.080 ± 0.003	1.0	0.074 ± 0.001	0.9	233 ± 14	2905
45f	(CH ₂) ₂	4-Me	4-Me	4-Me	0.084 (7.8)	0.656	0.15 ± 0.06	0.15 ± 0.02	1.0	0.15 ± 0.06	1.0	32.4 ± 2.4	213
45f (Cl ⁻ salt)	(CH ₂) ₂	4-Me	4-Me	4-Me	0.050 (33.8)	1.69	0.058 ± 0.026	0.030 ± 0.008	0.5	0.045 ± 0.018	0.8	23.3 ± 0.4	404
45g	(CH ₂) ₃	4-Me	4-Me	4-Me	0.081 (22)	1.80	0.029 ± 0.005	0.049 ± 0.007	1.7	0.053 ± 0.003	1.8	25.8 ± 1.7	897
45g (Cl ⁻ salt)	(CH ₂) ₃	4-Me	4-Me	4-Me	0.063 (27.3)	1.72	0.100 ± 0.034	0.066 ± 0.005	0.7	0.062 ± 0.004	0.6	12.7 ± 0.5	127
45c	O	4-Me	4-Me	4-Me	0.170 (14)	2.34	0.024 ± 0.005	0.025 ± 0.004	1.0	0.021 ± 0.001	0.8	85.7 ± 6.4	3567
45d	SO ₂	4-Me	4-Me	4-Me	0.173 (127)	22.0	0.23 ± 0.01	0.253 ± 0.002	1.1	0.27 ± 0.01	1.2	>300	>1300
45e	NAc	4-Me	4-Me	4-Me	0.159 (137)	21.8	0.32 ± 0.01	0.30 ± 0.01	0.9	0.29 ± 0.01	0.9	>300	>930
46b	CH ₂	3-Me	3-Me	3-Me	0.231 (4)	0.939	0.14 ± 0.02	0.14 ± 0.01	1.0	0.13 ± 0.02	0.9	72.6 ± 7.1	524
46c	O	3-Me	3-Me	3-Me	0.488 (1.9)	0.942	0.057 ± 0.013	0.043 ± 0.004	0.7	0.088 ± 0.024	1.5	45.4 ± 12.4	792

Table 7.3 Antitrypanosomal activity of bisphosphonium salts having substituted phenyl substituents (36a = CDIV20, 38b = AHI-10, 45e = AHI-43). Taken from Taladriz *et al* (2012). ^aT. b. rhodesiense STIB900 trypomastigotes. ^bRat skeletal myoblast L6 cells. ^cT. b. brucei s427 trypomastigotes. ^dT. b. brucei knockout strain lacking a functional P2-transporter and resistant to diminazene aceturate. ^eResistance factor compared to WT. ^fThe B48 strain is a mutant, derived from the TbAT1-KO strain, with a nonfunctional high affinity pentamidine transporter (HAPT). This strain is resistant to diminazene, pentamidine and melaminophenyl arsenicals. ^gHuman embryonic kidney (HEK) cells. ^hSelectivity index = $[EC_{50}(\text{HEK cells})/EC_{50}(\text{T. b. brucei WT})]$. ⁱSelectivity index = $[EC_{50}(\text{L6-cells})/EC_{50}(\text{T. b. rhodesiense})]$.



EC₅₀ (μM) (selectivity index)^f

compd	L	Ar ₁	Ar ₂	Ar ₃	EC ₅₀ (μM) (selectivity index) ^f								
					<i>T. b. rhod.</i> ^a	cytox L6 ^b	<i>T. b. brucei</i> WT ^c	TbAT1-KO ^d	RP ^e	<i>T. b.</i> B48 ^f	RP ^e	cytox HEK ^g	SI ^h
36a	CO	Ph	Ph	Ph	0.260 (282)	73.3	0.24 ± 0.07	0.36 ± 0.07	1.5	0.38 ± 0.06	1.6	>300	>1250
47a	CO	2-thienyl	2-thienyl	2-thienyl	0.29 (58)	16.6	0.33 ± 0.06	0.52 ± 0.03	1.6	0.33 ± 0.05	1.0	260 ± 21	785
48a	CO	2-furanyl	2-furanyl	2-furanyl	13.81	86.0	36.9 ± 1.2	33.8 ± 1.2	0.9	21.7 ± 1.2	0.6	nd ^k	
49a	CO	Ph	Ph	2-pyridyl	0.607 (24)	14.6	0.70 ± 0.24	1.43 ± 0.41	2.0	1.33 ± 0.26	1.9	>300	>400
50a	CO	Bn	Ph	Ph	0.48 (67)	32.0	0.81 ± 0.12	1.02 ± 0.02	1.3	1.03 ± 0.22	1.3	>300	>370
51b	CH ₂	Ph	Ph	C ₆ F ₅	16.0	P ^j	2.68 ± 0.05	3.79 ± 0.09	1.4	2.74 ± 0.02	1.0	>300	>110
51c	O	Ph	Ph	C ₆ F ₅	12.8	5.35	23.2 ± 3.1	9.9 ± 1.9	0.4	6.68 ± 1.65	0.3	>300	>10
52b	CH ₂	Ph	Ph	3-(SO ₃ Na)Ph	>92	>92	>100	>100		>100		>300	
52c	O	Ph	Ph	3-(SO ₃ Na)Ph	>92	90.5	>100	>100		>100		>300	
53a	CO	1-naphthyl	1-naphthyl	1-naphthyl	0.40 (12)	4.9	0.18 ± 0.04	0.339 ± 0.005	1.8	0.18 ± 0.04	1.0	92 ± 4.0	502
53b	CH ₂	1-naphthyl	1-naphthyl	1-naphthyl	0.299 (12)	3.43	0.14 ± 0.02	0.17 ± 0.04	1.3	0.14 ± 0.01	1.0	163 ± 19	1207
53c	O	1-naphthyl	1-naphthyl	1-naphthyl	0.384 (9)	3.45	0.16 ± 0.01	0.14 ± 0.01	0.9	0.128 ± 0.002	0.8	114 ± 16	722

Table 7.4 Antitrypanosomal activity of monophosphonium salts (55 = AT-5). Taken from Taladriz *et al* (2012). ^a*T. b. rhodesiense* STIB900 trypomastigotes. ^bRat skeletal myoblast L6 cells. ^c*T. b. brucei* s427 trypomastigotes. ^d*T. b. brucei* knockout strain lacking a functional P2-transporter and resistant to diminazene aceturate. ^eResistance factor compared to WT. ^fThe B48 strain is a mutant, derived from the TbAT1-KO strain, with a nonfunctional high affinity pentamidine transporter (HAPT). This strain is resistant to diminazene, pentamidine and melaminophenyl arsenicals. ^gHuman embryonic kidney (HEK) cells. ^hSelectivity index = $[EC_{50}(\text{HEK cells})/EC_{50}(\textit{T. b. brucei} \text{ WT})]$. ⁱSelectivity index = $[EC_{50}(\text{L6-cells})/EC_{50}(\textit{T. b. rhodesiense})]$.

Most of the compounds presented in table 7.1 are better inhibitors of the LAPT1 than pentamidine, and therefore most likely to be transported by this transporter. Our finding that AQP2 can transport pentamidine irrespective of the large difference in size between pentamidine and other ligands transported through this transporter suggests that, in some cases, molecular size may be of secondary importance when considering their suitability to be transported by a particular transporter; this is especially true when screening for inhibitors rather than substrates. Though most of the bisphosphonium compounds are much larger molecules than pentamidine, which is the only known substrate for this transporter, the low K_i values found for the inhibition of pentamidine uptake by these compounds coupled with their equally low EC_{50} values for all trypanosome strains that have the LAPT1 leads us to conclude that these compounds could indeed be good substrates for the LAPT1. However, a plot of K_i (LAPT) against *Tb427* wt EC_{50} values gave an R^2 (correlation coefficient) value of 0.16, indicating a lack of correlation. Hence, these bisphosphonium compounds may be inhibiting the uptake of [3 H]-pentamidine, without being transported, by the LAPT1. It had been demonstrated that good inhibitors of transporters do not always turn out to be good substrates, and may even not be transported at all. Compounds that were good inhibitors of adenosine uptake through the P2 transporter were found to still be effective against *TbAT1*-null trypanosomes that lack the P2 transporter (Stewart *et al*, 2004), thus suggesting that uptake through the P2 transporter is not taking place at all or is not important to their activity against trypanosomes. Finally, apart from compound 35a that gave an EC_{50} value of 65.8 μ M with rat skeletal myoblast L6 cells, most of the selected bisphosphonium compounds gave EC_{50} values of less than 10 μ M with the same skeletal myoblast L6 cells (tables 7.2 and 7.3), indicating that these compounds are not only toxic to the trypanosomes but can also be toxic to the tissues.

Tissue toxicity is an unwanted attribute of any agent being considered for use as a pharmacological tool, hence these bisphosphonium compounds may not be very useful drug candidates against trypanosomes.

8. General Discussion

Control of veterinary trypanosomiasis in poor rural African communities relies heavily on the use of trypanocidal compounds such as ISM and diminazene (Delespaux *et al*, 2008). Diminazene serves mostly for chemotherapy while ISM is used mainly as a prophylactic agent, providing an average of 3 months' protection against trypanosome infection (Delespaux *et al*, 2008). Since the value of the African veterinary trypanocide market is considered too low to attract pharmaceutical companies' investment in new drugs, the only option left is to make the best use of the available drugs (Delespaux *et al*, 2008). The major factor militating against the continued use of these few existing trypanocides is the development of resistance to these drugs in trypanosomes. Though the development of resistance to a drug can be prevented or the rate reduced by strict control of drug usage (not practicable in rural central Africa), a reversal of resistance would normally require a complete understanding of the mechanism involved in the development of resistance. In addition, A PCR-based test could be developed as a convenient tool for fast, large-scale testing of livestock for resistant trypanosomes. Development of such a test requires the identification of genetic markers for isometamidium chloride resistance in livestock-infective trypanosomes (Delespaux *et al*, 2005). One of such resistance markers was a GAA codon insertion (coding for an extra lysine) in the gene for a putative ABC transporter in resistant clones of *Trypanosoma congolense* (Delespaux *et al*, 2005). However, the non-universality of this ISM resistance marker was indicated by the presence of five resistant isolates not possessing the GAA insertion, though all the sensitive strains characterised in the study were found to be GAA positive (Delespaux *et al*, 2005). Recently, and in support of the above finding, is the hypothesis that inhibitors of ABC transport could reverse resistance to ISM in *Trypanosoma congolense*; tetracycline and oxy-tetracycline were able to

significantly re-sensitize ISM resistant trypanosomes (*T. congolense*) to ISM (Delespaux *et al*, 2010). Our findings presented in chapter 3 however suggest that ABC transport activities do not contribute to ISM resistance in *Trypanosoma brucei brucei*, that efflux of ISM could not be inhibited by any of the established inhibitors of ABC transport, and the effect of ISM on ISM-resistant trypanosomes was not potentiated by any of such inhibitors.

This does not necessarily disprove the *T. congolense* hypothesis, however. It is rapidly becoming clear that drug transport in *T. brucei* spp and in *T. congolense* is very different. We recently published a study proving that *T. congolense* does not have an equivalent of TbAT1/P2 (Munday *et al*, 2013). In addition, *T. congolense* does not have an equivalent of HAPT1 either (Munday and De Koning, unpublished observations). We therefore have to conclude that it is far from certain that ISM uptake, efflux and resistance models of either trypanosome species will be predictive for the other.

Pentamidine, diminazene, ISM and EtBr have all been reported to act on the kinetoplast DNA (kDNA) by inhibiting the trypanosomal topoisomerase II, thereby creating linearized minicircle DNA in *Trypanosoma equiperdum*, leading to the disruption of the kDNA structure and, potentially, to the generation of dyskinetoplastic trypanosomes (Shapiro & Englund, 1990). However, it is important to note that actual loss of kinetoplast has only been demonstrated in *T. equiperdum*, after *in vivo* treatment with ethidium bromide or acriflavine (Riou *et al*, 1980). However, it was subsequently reported that dyskinetoplastic *T. evansi* and *T. equiperdum* display identical sensitivity to isometamidium as kinetoplastid clones of the same species (Kaminsky *et al*, 1997). Moreover, the dyskinetoplastic trypanosomes did not lose infectivity or viability (Riou *et al*, 1980). Yet, it has been amply demonstrated by fluorescence microscopy that

isometamidium predominantly accumulates in, and associates with, the kinetoplast (Wilkes *et al*, 1995; Ardelli & Woo, 2001; Boibessot *et al*, 2002).

A subsequent report upholds the accumulation of ISM in the kinetoplast, and in addition proposes that resistance to ISM is a function of reduced mitochondrial membrane potential; however this report found no link between ISM resistance and ABC transport activities (Wilkes *et al*, 1997). We also found that ISM exposure leads to the generation of dyskinetoplastic trypanosomes. In fact, ISM-resistant clones of *T. b. brucei* generated in our laboratory had lost their kDNA as well as their mitochondrial membrane potential (MMP). We linked this loss of MMP to the F_1F_0 -ATPase, and demonstrated that the kDNA loss was enabled by two distinct point mutations on the nuclearly-encoded γ -subunit of the F_0F_1 -ATPase. One of the two point mutations was characterised. It changed a serine residue to a stop codon, hence truncating the gene sequence at the point C851A (S284*). This mutation was found to be dominant when it was introduced into the wild type *Trypanosoma brucei brucei*; the introduction of this mutation made the wild type trypanosomes significantly resistant to ISM (>80 folds) and significantly cross resistant to EtBr (>250 folds), diminazene (about 5 folds) and oligomycin (6.8 folds), indicating that the effect of this mutation is fully reproducible. Since the S284* mutant has not lost its kDNA until after exposure to phenanthridines, these observations seem to prove that it is the mutation in the γ -subunit of the F_1F_0 -ATPase, and the resultant loss in mitochondrial membrane potential (MMP) that is responsible for the phenanthridine resistance, rather than the loss of kDNA per se. However, in trypanosomes carrying the γ -subunit mutation the kDNA is no longer essential and thus rapidly lost under (further) selective pressure with isometamidium. This conclusion is completely in agreement with previously reports that ISM elicits its linearizing effects on

minicircles through inhibition of mitochondrial Topoisomerase II (Shapiro & Englund, 1990; Shapiro, 1993). Indeed, Delespaux et al (Delespaux *et al*, 2007) could find no evidence that point mutations in *T. congolense* topoisomerases are involved in isometamidium resistance - all indicating that the loss of kinetoplast DNA is not critical for (but a by-product) of ISM resistance.

We found that our ISM-resistant *T. b. brucei* clones displayed a reduced ISM accumulation. This reduction was earlier attributed to the reduction in MMP (Wilkes *et al*, 1997). We were also able to demonstrate that although the mutation of the γ -ATPase was sufficient to make the wild type trypanosomes significantly resistant to ISM, exposure to ISM (or EtBr) is necessary for the loss of the kDNA and the MMP. Exposure to 20 nM ISM or EtBr for 72 hours was all that was required for mutant trypanosomes (trypanosomes transfected with replacement plasmids bearing C851A γ -ATPase) to lose their kDNA. Wild type trypanosomes (and wild type clones transfected with plasmids bearing wild type γ -ATPase) did not survive this exposure at the concentration stated. Thus, the expression of the compensating mutation clearly enables the loss of kDNA. Considering the speed at which kDNA is lost under in vitro drug pressure of trypanosomes with the enabling mutation, this is highly likely to give these trypanosomes an enhanced survival or growth rates compared to trypanosomes that continue to carry the full kDNA complement. We speculate that the binding of isometamidium to kDNA continues to drive uptake of the drug into mitochondria, even with a much-reduced membrane potential. Thus, the loss of kDNA removes the last driving force that enabled mitochondrial uptake, and leaves isometamidium free in the cytoplasm, from which it is available for efflux.

We also found a >35-fold cross resistance and about 5.5 fold cross resistance to diminazene in our ISM-resistant clones and in our γ -ATPase mutant clones respectively. A similar pattern of cross resistance between ISM and diminazene was earlier reported in the field (Sinyangwe *et al*, 2004;McDermott *et al*, 2003;Clausen *et al*, 1992). However, cross resistance to ethidium bromide in ISM resistance seems to be more wide-spread (Peregrine *et al*, 1997;Schonefeld *et al*, 1987;Codjia *et al*, 1993;Gray & Peregrine, 1993), and this correlates with at least 540-fold cross resistance to EtBr found in our ISM resistant clones and at least 270-fold cross resistance to EtBr in our S284* γ -ATPase strains. This trend seems to suggest that EtBr resistance in *T. brucei brucei* is controlled solely by the γ -ATPase mutation while ISM resistance is multifactorial.

At the start of my project, ISM uptake was attributed to the P2 transporter and resistance to ISM was found to correlate with the presence of six point mutations on the TbAT1 sequence (Afework *et al*, 2006). These point mutations were however absent from our ISM resistant clones, though we found some reduction in uptake of ISM in *T. b. brucei* cells expressing RNAi of *TbAT1* and in the TbAT1 KO cells. Also, the expression of *TbAT1* in yeast increased ISM uptake significantly, compared to the yeast expression of the empty pDR195 vector. In addition, ISMR1 clone 3 displayed a significant cross resistance to tubercidin, compared to parental *Tb427* wt. This resistance to tubercidin strongly suggests the involvement of the P2 transporter in ISM uptake. We were however unable to compare P2 activity in our ISM resistant clones (by means of [³H]-Adenosine uptake) with that in *Tb427* wt because though P2 activity was greatly reduced in our ISM resistant clones, the same activity was also low in the wild type cells. This low activity was attributed to the low level of *TbAT1*

expression by *Tb427* wt when grown in culture. We therefore passaged both the *Tb427* wt and our ISM resistant clones in rats. However, though both the wild type cells and the resistant clones were both able to establish infection in rats (confirmed by microscopy), only *Tb427* wt was able to sustain infection. This line of investigation was therefore inconclusive, although the balance of evidence suggests that P2 does mediate part of the isometamidium flux, and its loss can contribute to high-level multi-factorial resistance. This is consistent with the high affinity of P2 for isometamidium, for which it displays a K_i value of just $0.22 \pm 0.05 \mu\text{M}$ (de Koning, 2001a).

Other AT-like transporters, TbATE and TbATA (de Koning *et al*, 2005) were also assessed for the ability to mediate ISM uptake. TbATE and TbATA were named TbNT12.1 and TbNT11.1, respectively, by the Landfear group, and their characterization after expression in *Xenopus oocytes* showed that both transporters were capable of mediating pentamidine uptake (Ortiz *et al*, 2009). However, neither transporter significantly increased sensitivity to pentamidine when expressed in *Leishmania mexicana* (Chapter 3). Also expression of TbATE in B48 cells did not increase pentamidine sensitivity significantly compared to the empty vector expression. On the other hand, TbATE1 expression in yeast increased ISM uptake significantly, and the expression of TbATE1 in *L. mexicana* also increased sensitivity to ISM significantly. In addition, RNAi of ATE in 2T1 caused a reduction in ISM uptake (although this did not amount to statistical significance). These findings together suggest strongly that TbATE1 expression mediates ISM uptake in *T. brucei brucei*. A re-expression of TbATE1 in B48 did not increase ISM uptake (assay done once and not shown). This may be because TbATE1 was not first deleted before the re-expression was done; moreover, the level of AT-E1 over-expression in these cells was not known. Similarly, the

expression of TbATA in yeast was assessed for the ability to mediate ISM uptake. Only the expression of TbATA1 in yeast was able to increase ISM uptake significantly; however TbATA1 expression in *Leishmania mexicana* did not cause a significant sensitization to ISM. Finally, we observed a significantly reduced average V_{\max} for LAPT1 activity in ISMR1 clone 3 (0.32 ± 0.06) compared to *Tb427* wt (0.85 ± 0.15). V_{\max} reduction could be the result of a down-regulation of expression of the gene that encodes this protein. We were however unable to check expression levels of the LAPT1 because we do not know the gene involved.

Also at the start of my project, the only pentamidine transporter that was characterized at both the biochemical and molecular level was the P2 aminopurine transporter (Mäser *et al*, 1999;Barrett & Fairlamb, 1999;Carter *et al*, 1995), encoded by the TbAT1 gene. The gene responsible for either the HAPT1 or the LAPT1 was unknown. We found that the AQP2 gene is responsible for the HAPT1 activity in *Trypanosoma brucei brucei*. This finding correlates with recent findings that describe aquaporins as conduits for drugs, such as arsenic and antimony, and other metabolites such as lactate (Sanders *et al*, 1997;Liu *et al*, 2002;Gourbal *et al*, 2004b;Tsukaguchi *et al*, 1998). These reports are together unique because they define new roles for aquaporins that differ from their original function as transmembrane proteins that act as pores for the movement of water, glycerol, urea (and in some cases, glycine) in and out of cells (Gonen & Walz, 2006). The identification of AQP2 as the genetic basis for the HAPT1 opens the door for the study of the actual contribution of this transporter to pentamidine and diamidine resistance in trypanosomes, especially in the field. Hence, the function and the presence of this gene in other trypanosome species can now be checked to see if this gene is universally present in other *Trypanosoma* species and to find out if their expression is also

responsible for a HAPT1 (or similar) activity. It will also be interesting to study the functions of aquaporins in other members of the Kinetoplastida, since comparing them to the function of aquaporins in trypanosomes will certainly help in the understanding of how the sequence and other structural variations that occur in this ubiquitous protein across species and genera have come to shape its function. Also, the presence (absence or alteration) of this gene in resistance or susceptibility can now be studied in field isolates from different locations to further confirm (or contradict) the earlier assigned roles of HAPT1 in trypanocide resistance (Teka *et al*, 2011;Matovu *et al*, 2003). Indeed, very recent results from the Mäser group at the Swiss Tropical Institute confirm genetic changes in the TbAQP2 locus of melarsoprol-resistant *T. b. gambiense* isolates (Graf *et al.*, manuscript submitted). Thus, simple tests to show the presence or absence of the wild type AQP2 gene can now be designed for use in the field as a tool for the detection of pentamidine and melarsoprol resistance, allowing the presence or absence of pentamidine resistant trypanosomes to be established before commencement of treatment.

We were also able to demonstrate that HAPT1 (AQP2) activity depends on the plasma membrane proton gradient, since HAPT1 activity was found to be abolished by agents that dissipate the plasma membrane proton gradient but insensitive to ionophores specific for disruption of the mitochondrial membrane potential. This finding suggests that pentamidine uptake through the HAPT1 is driven by proton motive force (PMF). And this correlates with other transport systems described earlier (de Koning & Jarvis, 1997b;Hasne & Barrett, 2000). The HAPT1 in this regard is therefore an expression of a most unique aquaporin since one of the fundamental properties of aquaporins is that they strictly prevent the conduction of protons (Gonen & Walz, 2006), exactly to prevent the

dissipation of proton gradients. An alternative interpretation of the ionophore data is that these reagents not only reduce the PMF but, equally, the plasma membrane potential that forms a large part of the PMF, especially in bloodstream trypanosomes (De Koning et al., 1998). Even, if the HAPT1/AQP2 transporter is not acting as a proton symporter, the depolarisation of the negative-inside plasma membrane potential removes much of the driving force for the rapid entry of the dicationic pentamidine.

Appendices

Appendix A: General buffers, solutions and media

Assay buffer (pH 7.3)

D-Glucose	2.53g
HEPES	8.0g
MOPS	5.0g
NaHCO ₃	2.0g
KCl	347.5mg
MgCl ₂ .6H ₂ O	62.5mg
NaH ₂ PO ₄ .2H ₂ O	913.5mg
CaCl ₂ .2H ₂ O	40.7mg
MgSO ₄ .7H ₂ O	19.9mg
NaCl	5.7g

These were dissolved in 1 litre of ddH₂O, allowed to stir for 2 hours before the pH was adjusted to 7.3 and the buffer stored at 4 °C.

2% SDS

10g of sodium dodecyl sulphate (SDS) was weighed out and dissolved in 500ml of distilled water.

Oil mixture

50 ml of mineral oil was mixed with 350 ml di-n-butyl phthalate.

Alamar blue solution

12.5mg resazurin sodium salt was weighed and dissolved in 100 ml of PBS. The solution was stirred for about 2 hours while wrapped in aluminium foil. It was then filter-sterilized, stored at -20 °C and away from light.

Tb-BSF-buffer

Stock solutions include 0.5M Na-PO₄, pH 7.3 (77.4 ml of 0.5M Na₂HPO₄ + 22.6 ml of 0.5M NaH₂PO₄; pH adjusted with pH-metre), 0.3M KCl, 0.5M HEPES (pH 7.3; adjusted with KOH) and 50 mM CaCl₂.

To prepare *Tb*-BSF-buffer, 1.8 ml of Na-PO₄, 1.66 µl of KCl, 1ml of HEPES and 30 µl of CaCl₂ were added to 7 ml of ddH₂O, giving a final concentration of 90 mM, 5 mM, 50 mM and 0.15 mM respectively. The buffer was stored at 4 °C.

Acidified Methanol (lysis buffer for ISM uptake)

0.1 N HCl	50 ml
Methanol	400 ml

Lysis buffer was stored at room temperature.

HMI-9 media (+ 5 % FCS)

A pack of HMI-9 powder was emptied into a 5-litre capacity beaker, followed by 4.5 litres of ddH₂O and 15g of NaHCO₃. After stirring for some time on a magnetic stirrer (about an hour), 500ml of FCS and 71.5 µl of β-mercaptoethanol were added and the solution left to stir overnight at 4 °C. The pH was adjusted to 7.4 the next day, and the media filtered into 10 sterile 500 ml reagent bottles and stored at 4 °C.

LB (Luria Bertani) broth and LB agar

10 g of LB powder was used to prepare 400 ml of LB media while 14 g of LB agar powder was used to prepare 400 ml of LB agar. In each case, the appropriate amount of powder was added to 400 ml of ddH₂O in 500 ml capacity reagent bottles, swirled to mix and autoclaved. After autoclaving, LB media was stored at room temperature. LB agar was however cooled down midway before 400 µl of 100 mg/ml ampicillin was added, swirled to mix and 20 ml was pipetted into petri dishes for storage at 4 °C until when needed.

Synthetic complete medium minus uracil (SC-URA).

Synthetic complete drop out mix was first prepared from the following components in the proportions shown:

Adenine hemisulphate	2 g
Arginine HCl	2 g
Histidine HCl	2 g
Isoleucine	2 g
Leucine	4 g
Lysine HCl	2 g
Methionine	2 g
Phenylalanine	3 g
Homoserine	6 g
Tryptophan	3 g
Tyrosine	2 g
Valine	9 g

Then, SC-URA was prepared by dissolving 4 g of yeast nitrogen base without amino acids, 12 g of glucose and 0.5 g of the synthetic complete drop out mix in 600 ml of ddH₂O and the pH adjusted to 5.6 with 10 M NaOH. 10 g of bacto-agar is added if solid medium is required and the medium is sterilized by autoclaving.

Yeast Extract-Peptone-Dextrose and Adenine (YPD) Medium

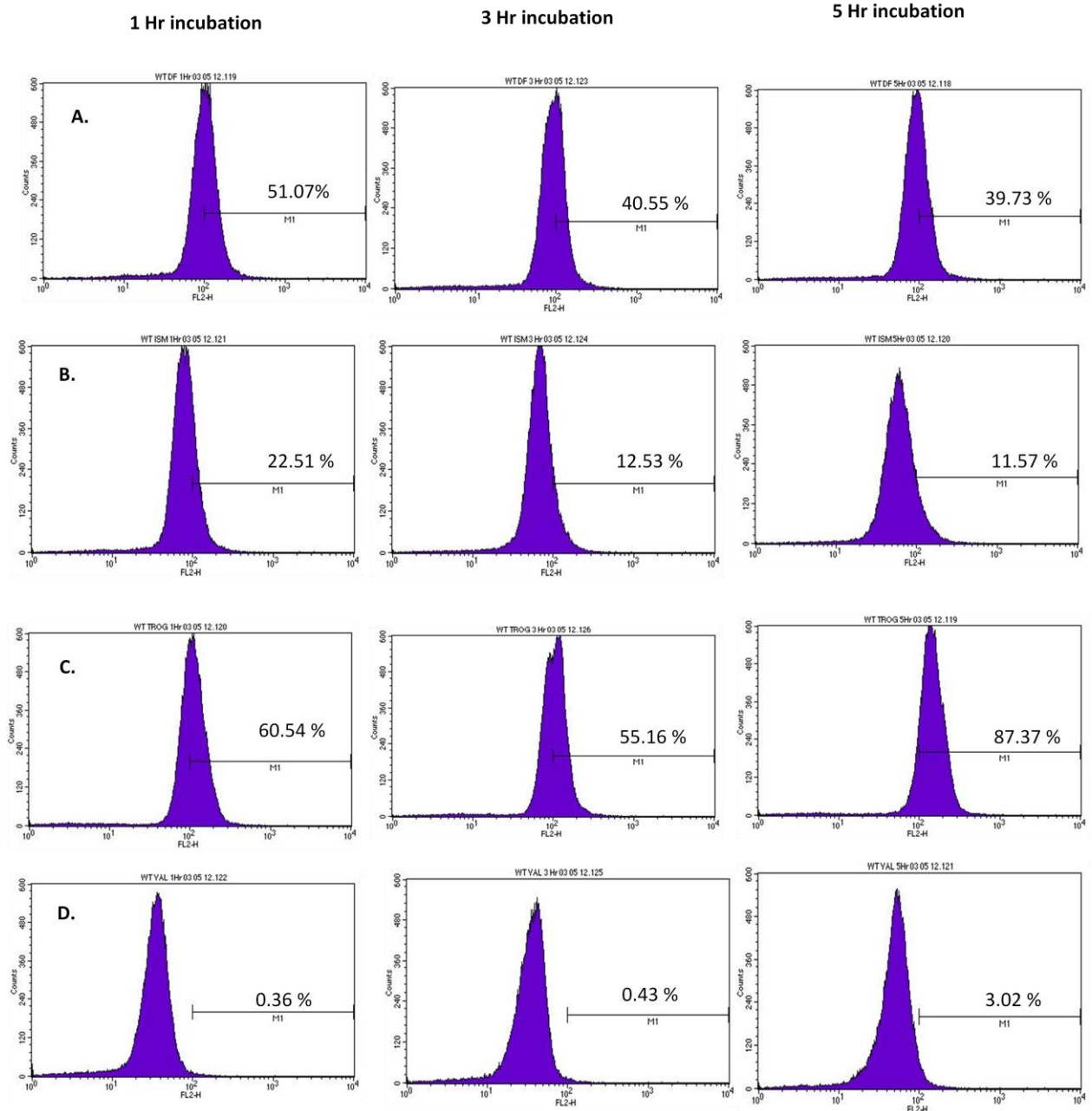
YPD medium was prepared by dissolving 6 g of yeast extract, 12 g of peptone, 12 g of glucose and 60 mg of adenine hemisulphate (10 g of bacto-agar if solid medium is desired) in 600 ml of ddH₂O and adjusting the pH to 6.0 before autoclaving and subsequent storage at 4 °C.

TE/LiAc and PEG/LiAc/TE was each prepared from 50% PEG (w/v; Polyethylene glycol) solution, 10 X TE (Tris-EDTA; 0.1 M Tris-HCl + 0.01 M EDTA, pH 7.5) and 10 X LiAc (1M LiAc, pH adjusted to 7.5 with dilute acetic acid).

1 X TE/LiAc was therefore prepared by adding 1 ml of 10 X TE and 1 ml of 10 X LiAc to 8 ml of ddH₂O, while PEG/LiAc/TE contained 40% PEG in 1 X TE and 1 X LiAc.

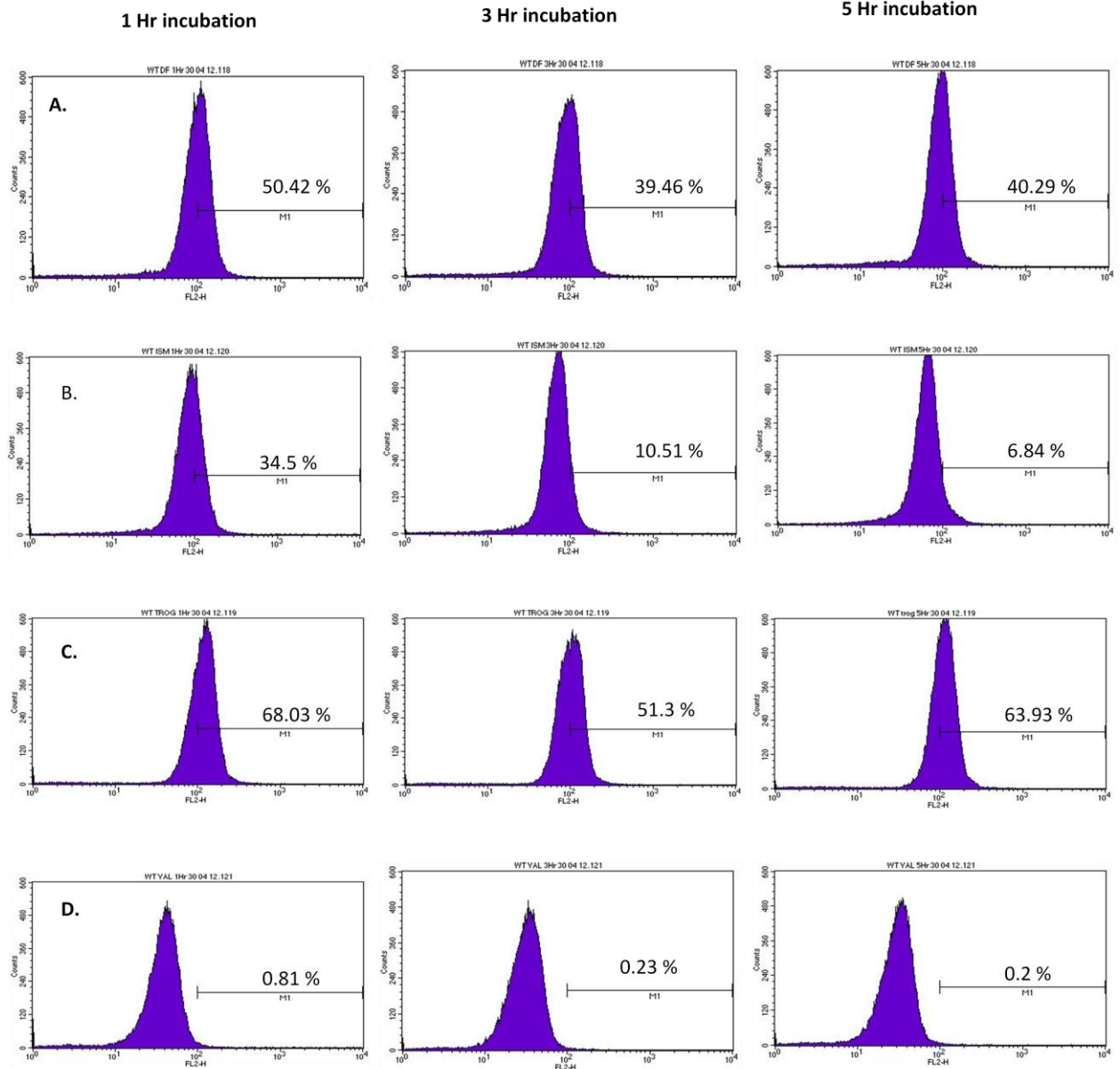
Appendix B: Mitochondrial membrane potential graphics.

MMP Graphics for Tb427 wt.



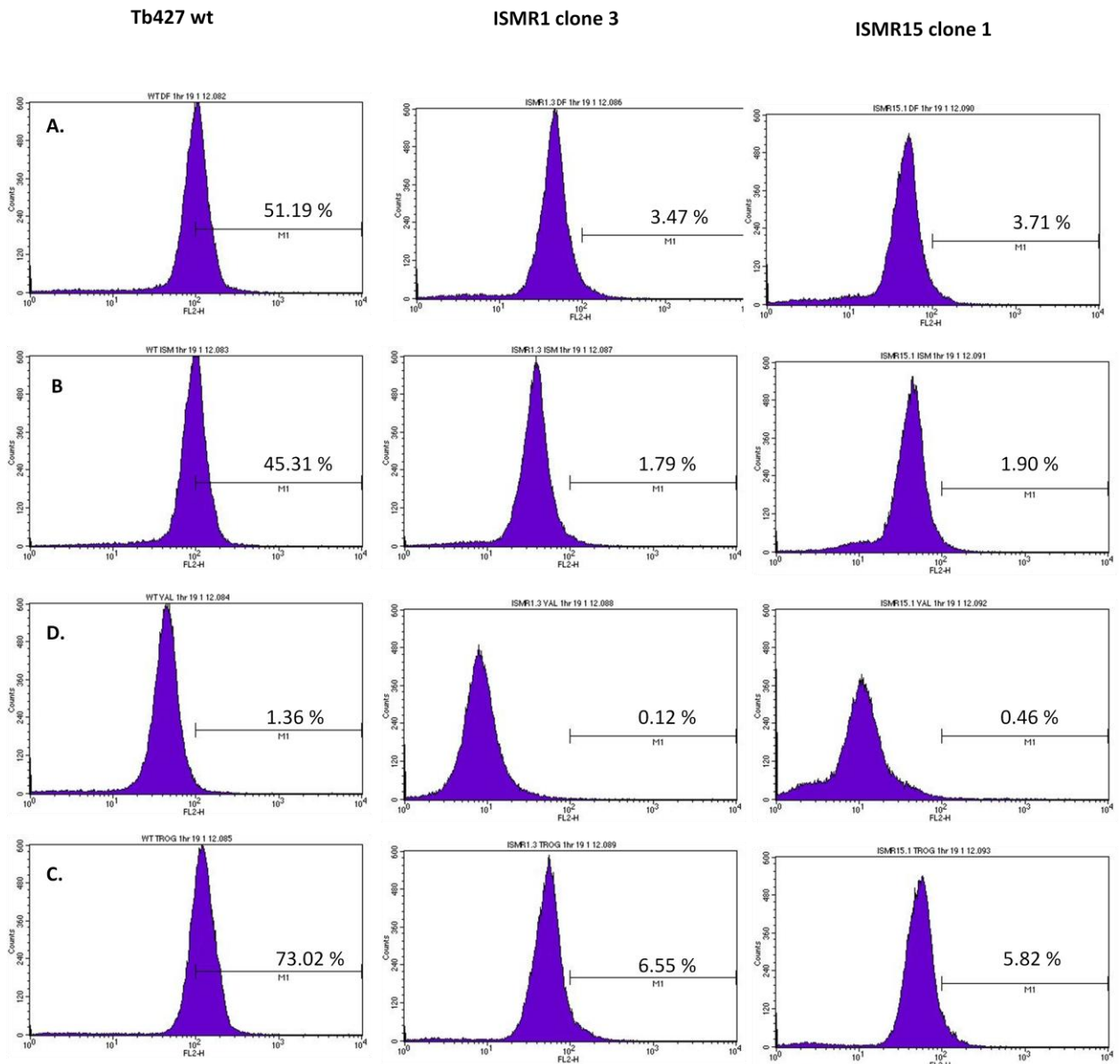
A. = Drug-free, B. = ISM-treated, C. = Troglitazone- treated, D. = Valinomycin-treated

MMP Graphics for Tb427 wt.



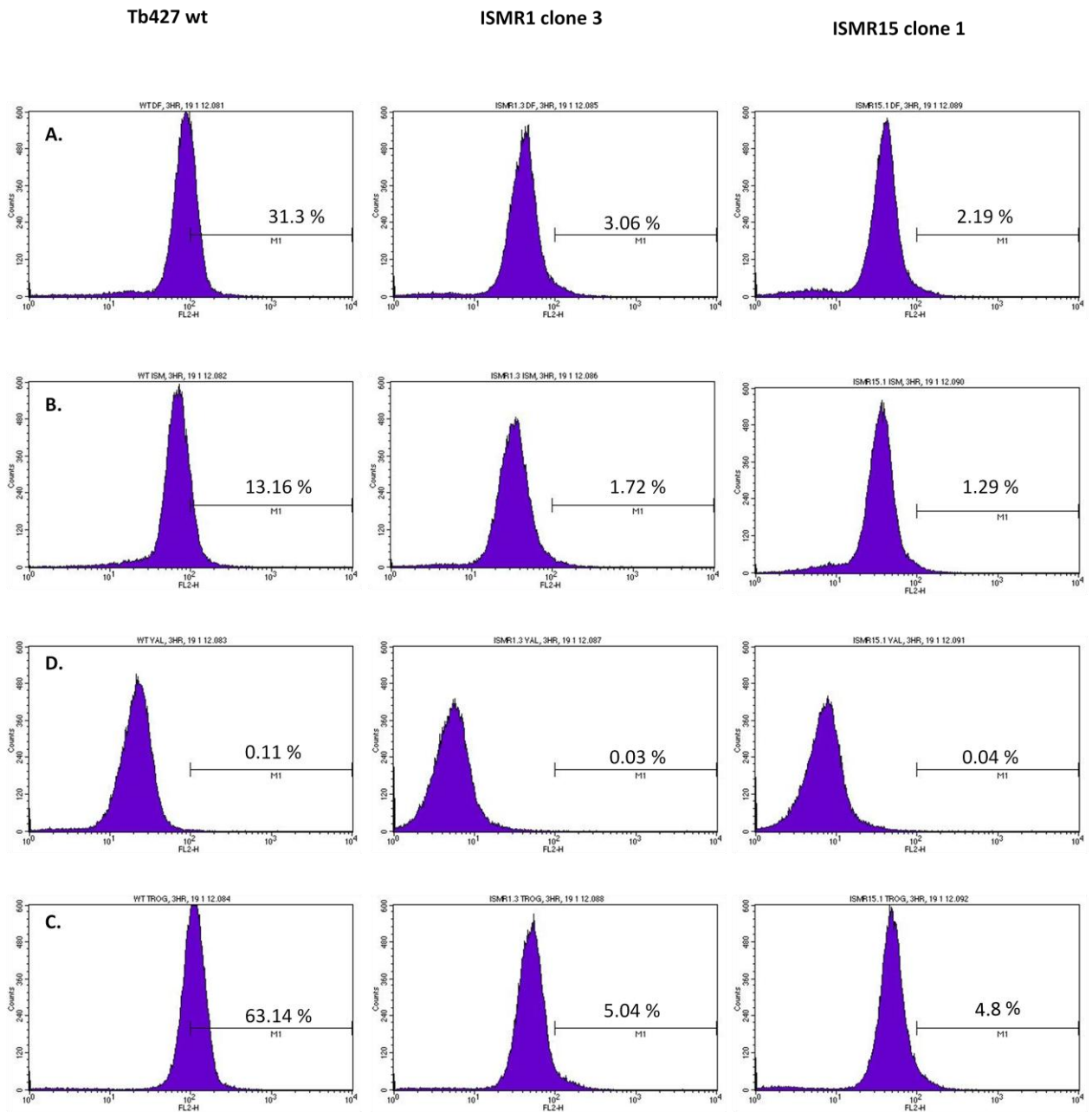
A. = Drug-free, B. = ISM-treated, C. = Troglitazone- treated, D. = Valinomycin-treated

MMP Graphics for Tb427 wt, ISMRI clone 3 & ISMR15 clone 1; 1 Hour incubation in ISM.



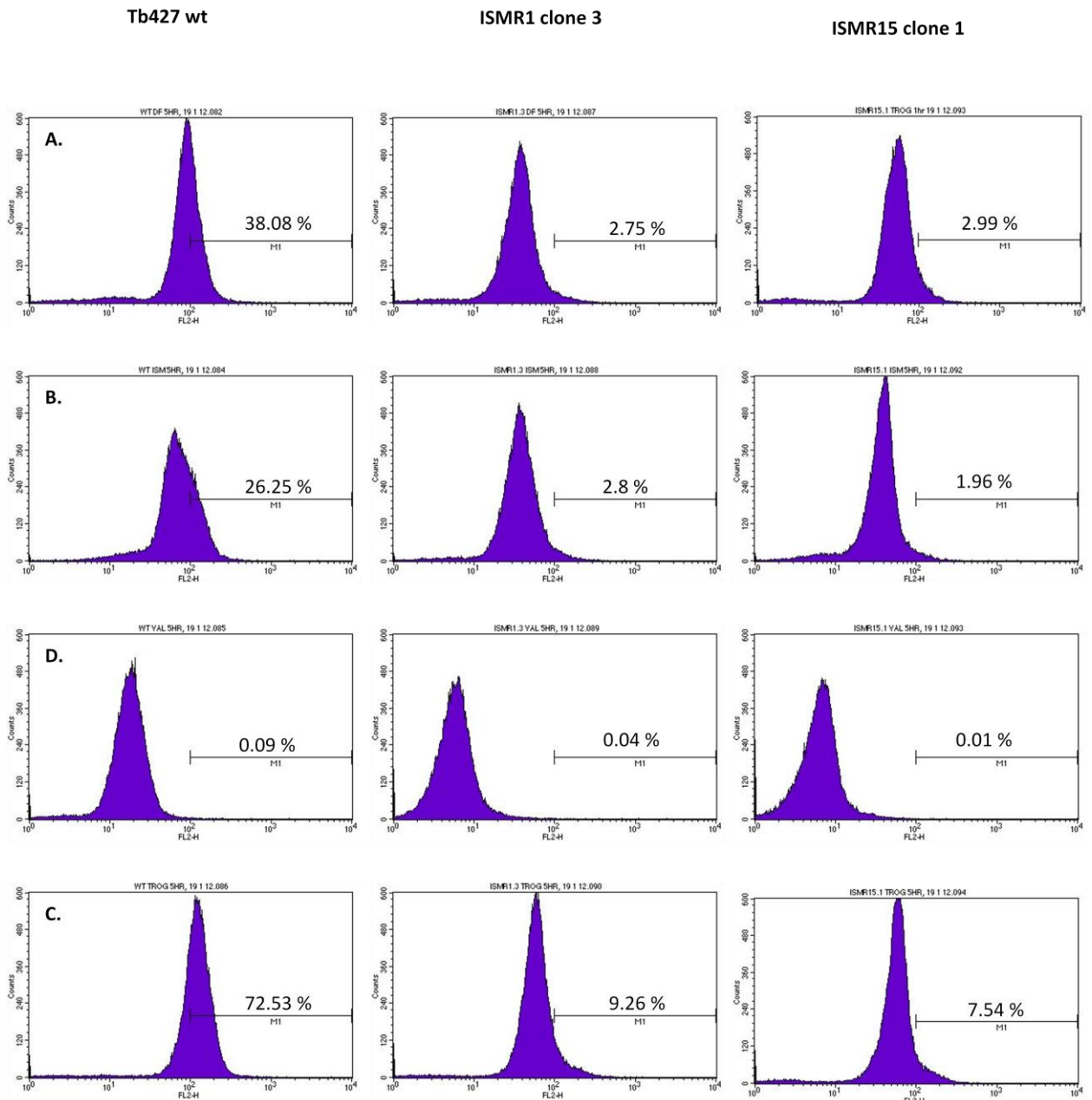
A. = Drug-free, B. = ISM-treated, C. = Troglitazone- treated, D. = Valinomycin-treated

MMP Graphics for Tb427 wt, ISMRI clone 3 & ISMR15 clone 1; 3 Hour incubation in ISM.



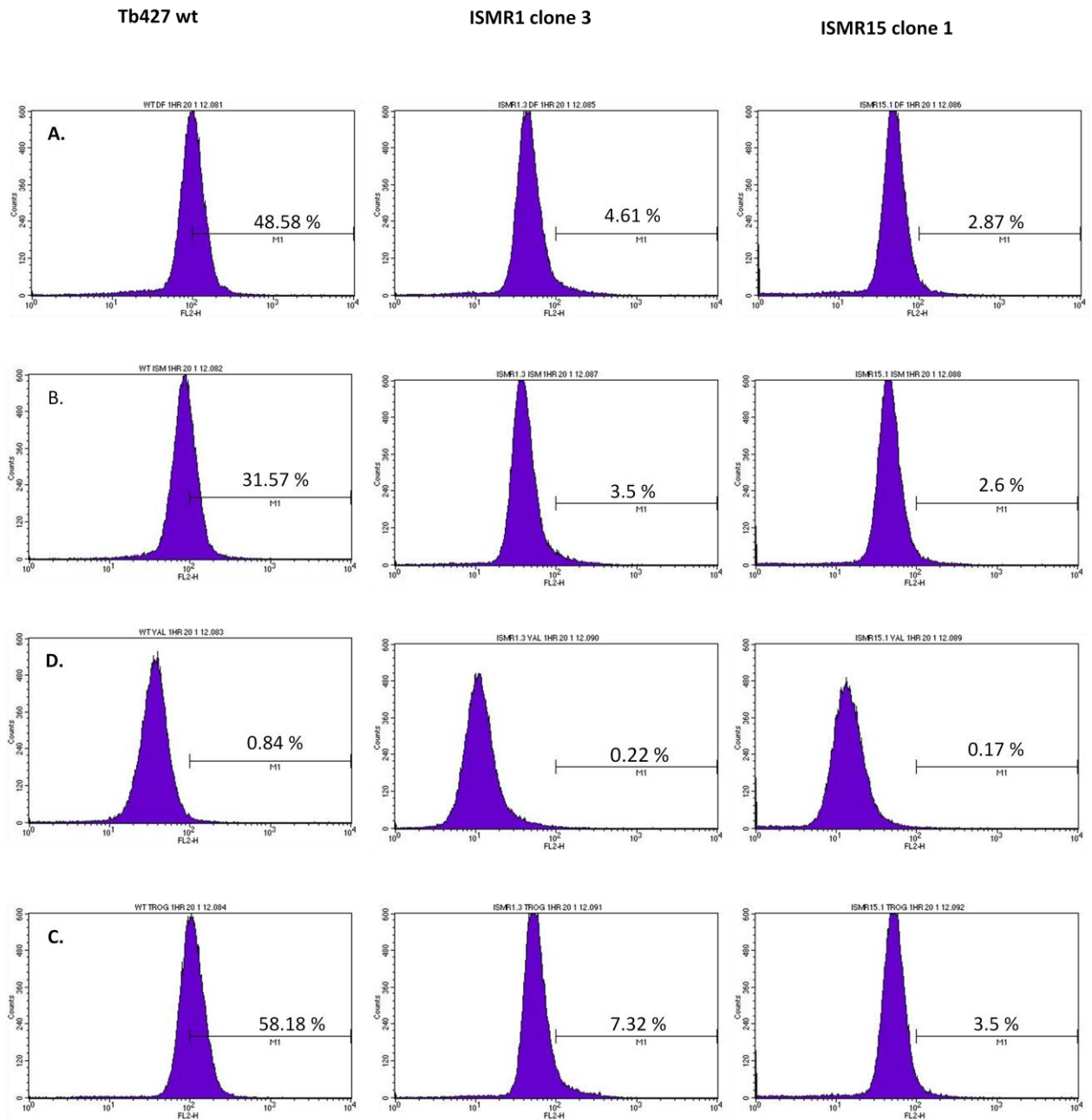
A. = Drug-free, B. = ISM-treated, C. = Troglitazone- treated, D. = Valinomycin-treated

MMP Graphics for Tb427 wt, ISMRI clone 3 & ISMR15 clone 1; 5 Hour incubation in ISM.



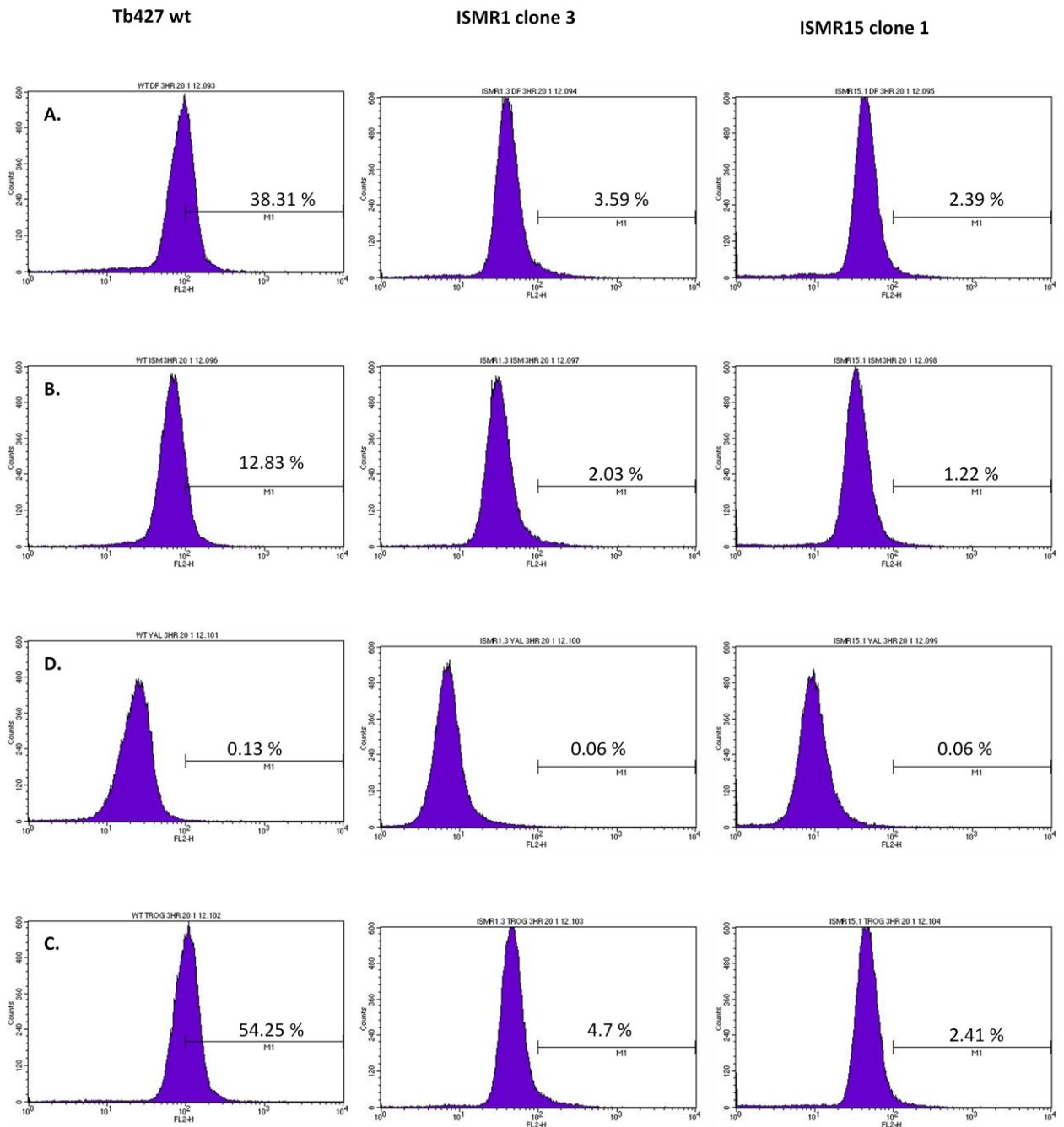
A. = Drug-free, B. = ISM-treated, C. = Troglitazone- treated, D. = Valinomycin-treated

MMP Graphics for Tb427 wt, ISMR1 clone 3 & ISMR15 clone 1; 1 Hour incubation in ISM.



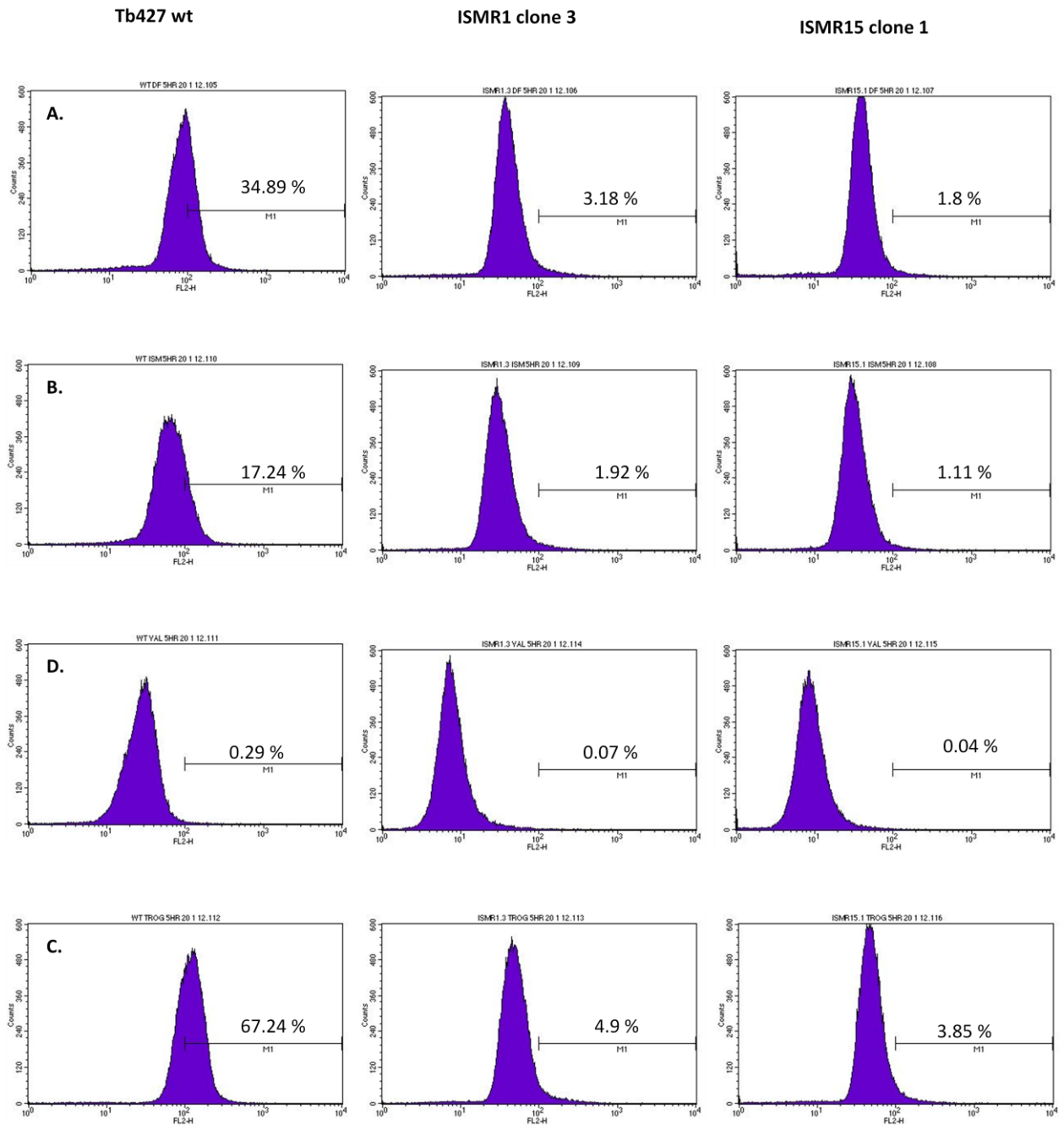
A. = Drug-free, B. = ISM-treated, C. = Troglitazone- treated, D. = Valinomycin-treated

MMP Graphics for Tb427 wt, ISMRI clone 3 & ISMR15 clone 1; 3 Hour incubation in ISM.



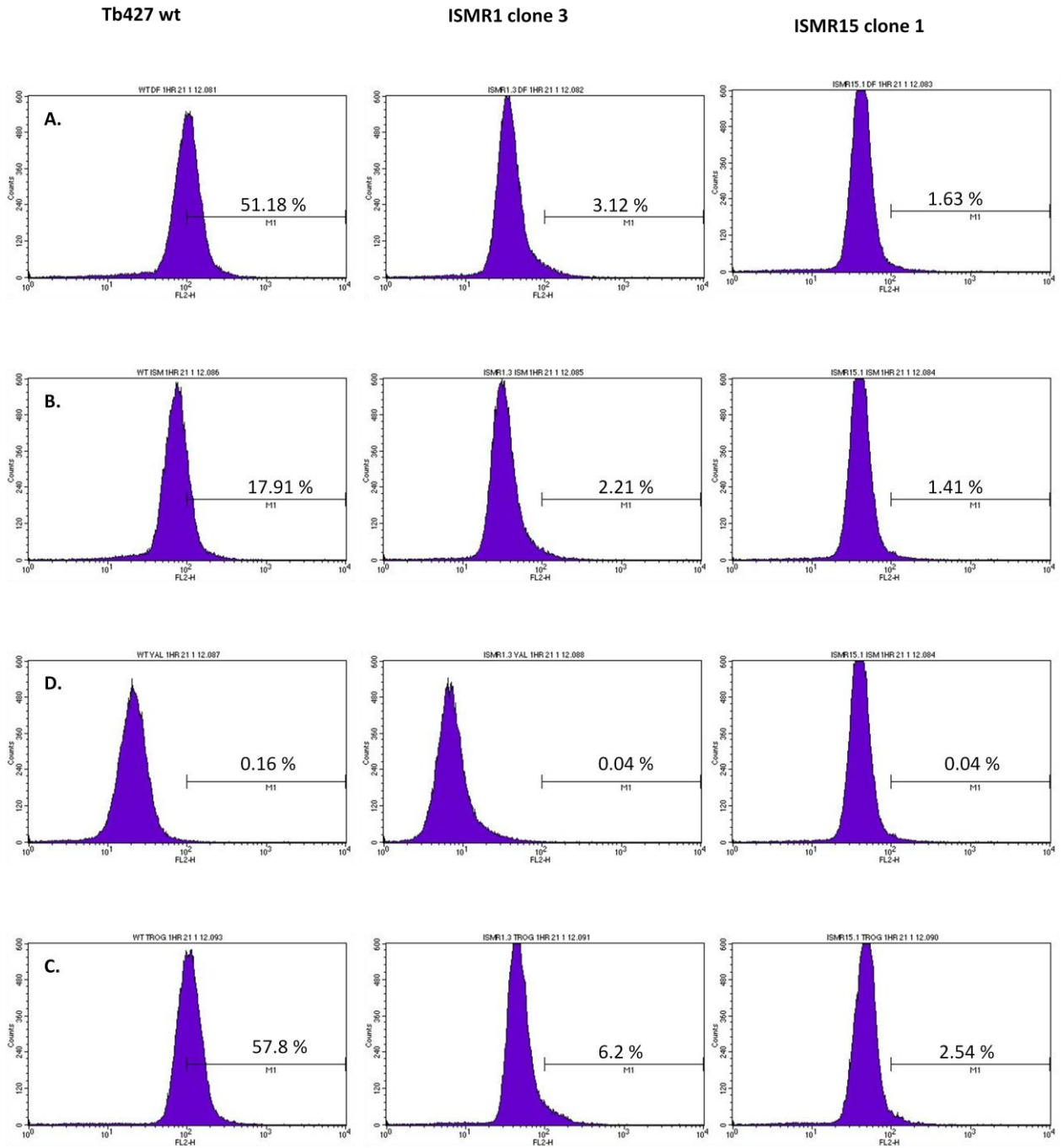
A. = Drug-free, B. = ISM-treated, C. = Troglitazone- treated, D. = Valinomycin-treated

MMP Graphics for Tb427 wt, ISMR1 clone 3 & ISMR15 clone 1; 5 Hour incubation in ISM.



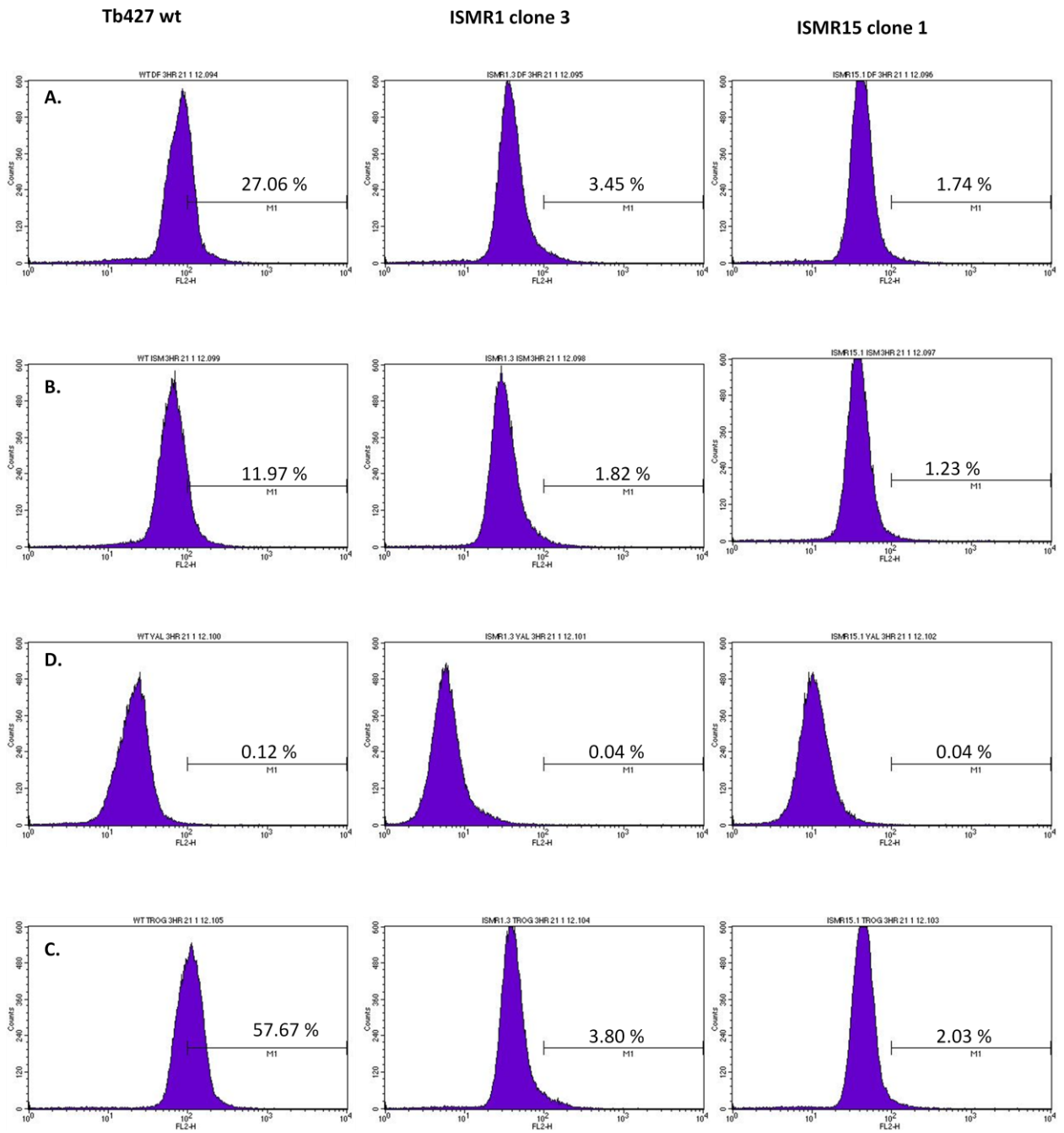
A. = Drug-free, B. = ISM-treated, C. = Troglitazone- treated, D. = Valinomycin-treated

MMP Graphics for Tb427 wt, ISMR1 clone 3 & ISMR15 clone 1; 1 Hour incubation in ISM.



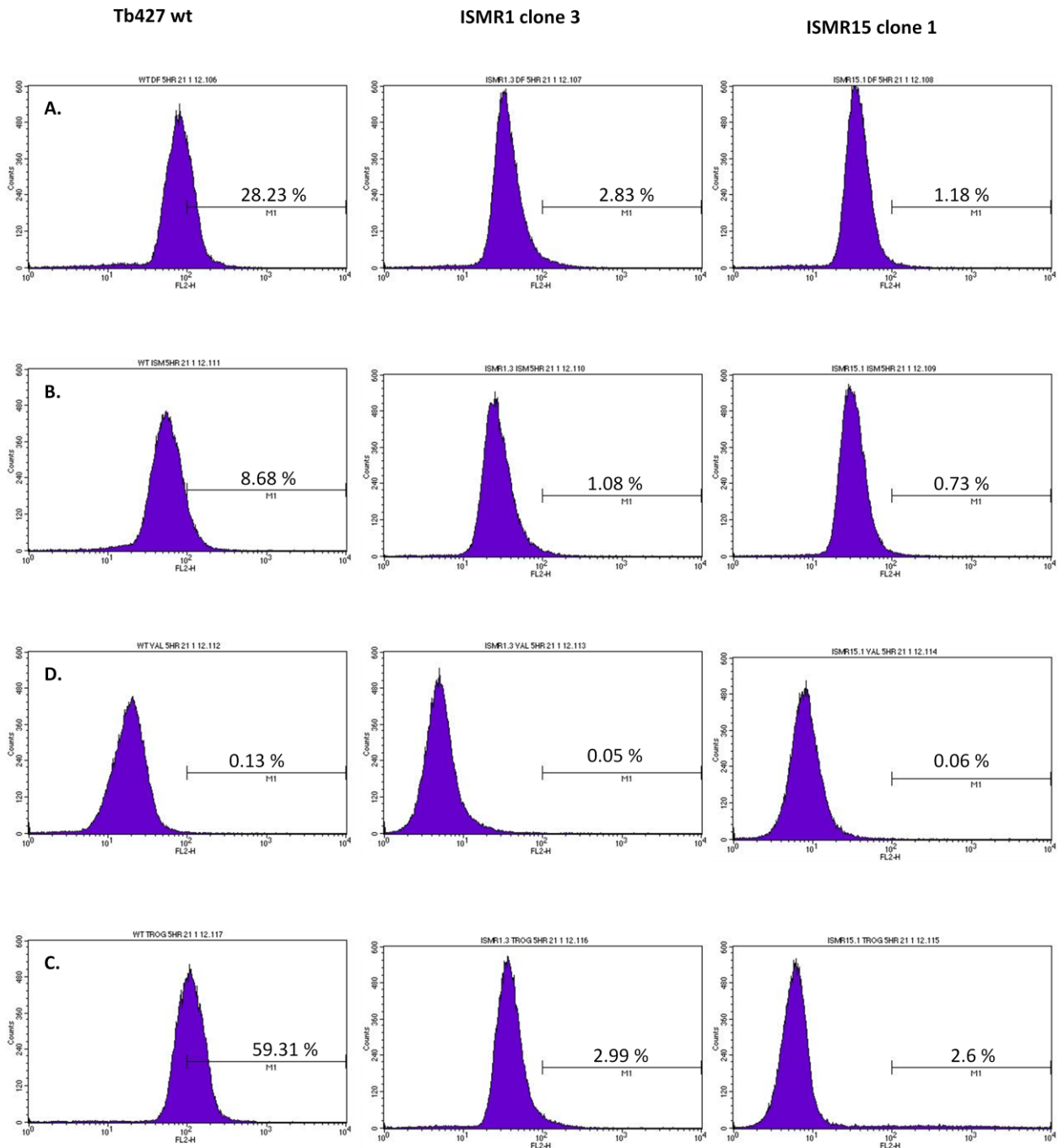
A. = Drug-free, B. = ISM-treated, C. = Troglitazone- treated, D. = Valinomycin-treated

MMP Graphics for Tb427 wt, ISMRI clone 3 & ISMR15 clone 1; 3 Hour incubation in ISM.



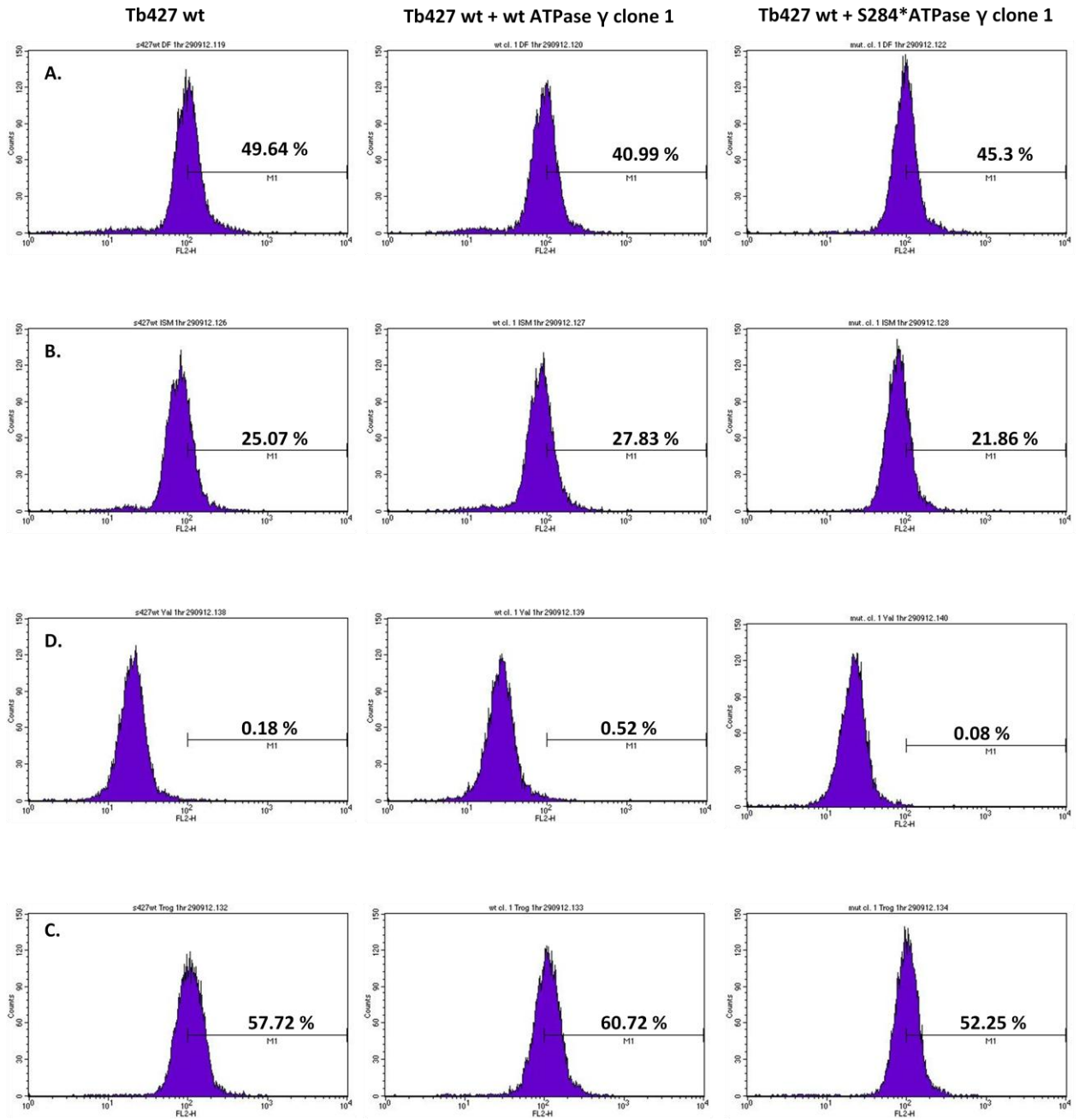
A. = Drug-free, B. = ISM-treated, C. = Troglitazone- treated, D. = Valinomycin-treated

MMP Graphics for Tb427 wt, ISMRI clone 3 & ISMR15 clone 1; 5 Hour incubation in ISM.



A. = Drug-free, B. = ISM-treated, C. = Troglitazone- treated, D. = Valinomycin-treated

MMP Graphics for Tb427 wt, + wt ATPase γ clone 1, + S284* ATPase γ clones 1, 2 & 3; 1 Hour incubation in ISM.

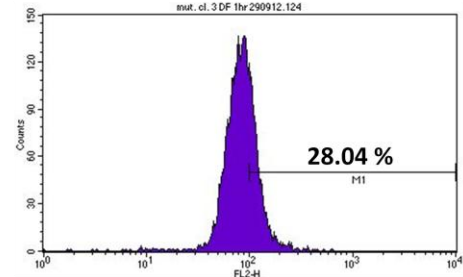
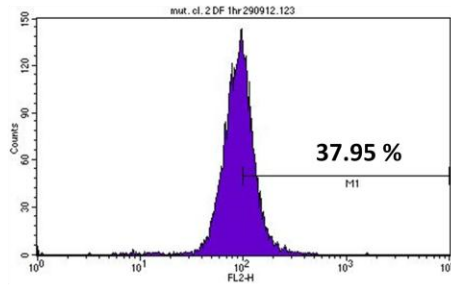


A. = Drug-free, B. = ISM-treated, C. = Troglitazone- treated, D. = Valinomycin-treated

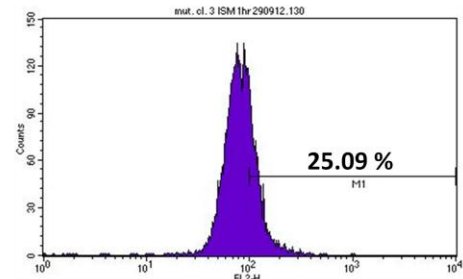
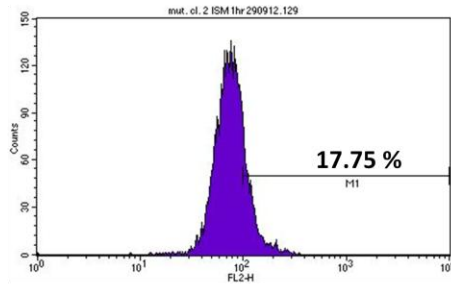
Tb427 wt + S284* ATPase γ clone 2

Tb427 wt + S284* ATPase γ clone 3

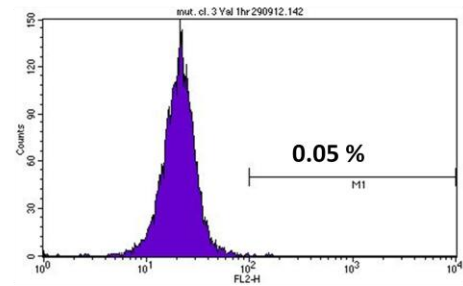
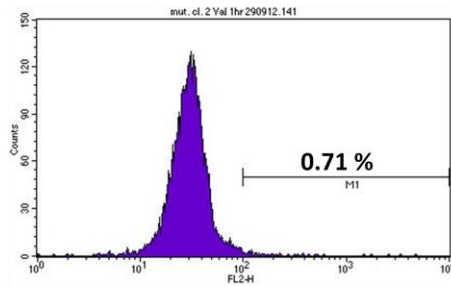
A.



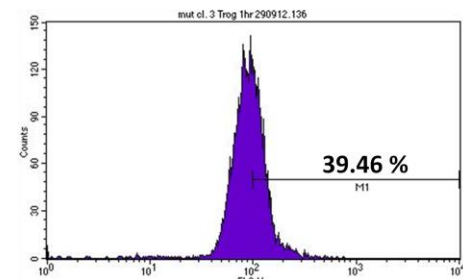
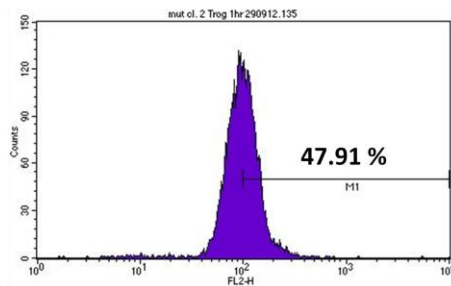
B.



D.

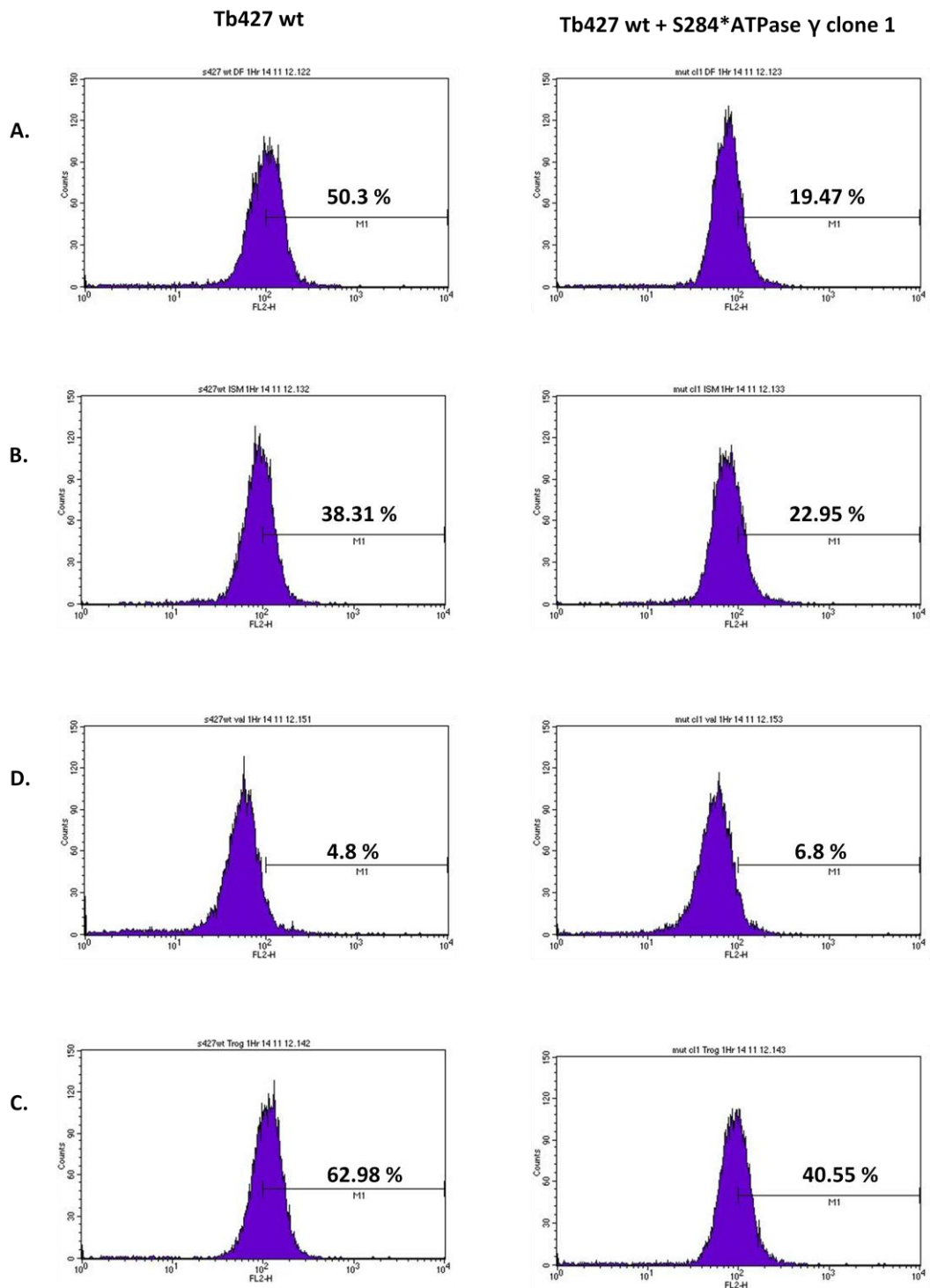


C.



A. = Drug-free, B. = ISM-treated, C. = Troglitazone- treated, D. = Valinomycin-treated

MMP Graphics for Tb427 wt, + S284* ATPase γ clones 1, 2 & 3; 1 Hour incubation in ISM.

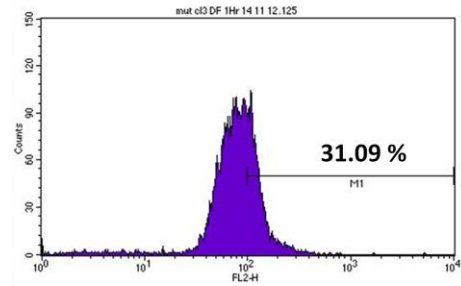
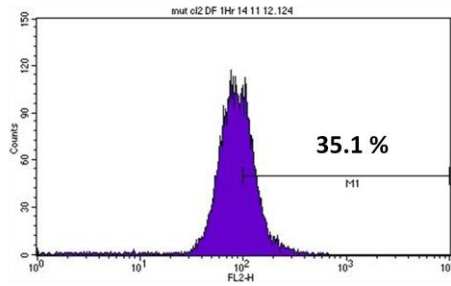


A. = Drug-free, B. = ISM-treated, C. = Troglitazone- treated, D. = Valinomycin-treated

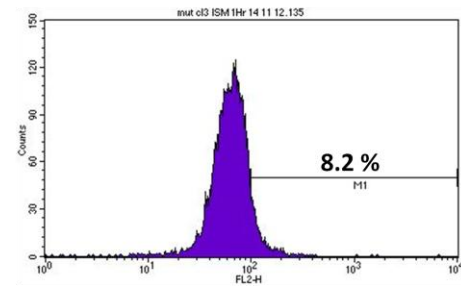
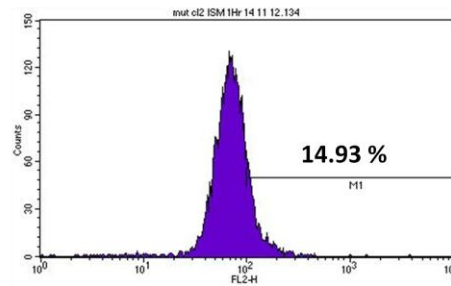
Tb427 wt + S284* ATPase γ clone 2

Tb427 wt + S284*ATPase γ clone 3

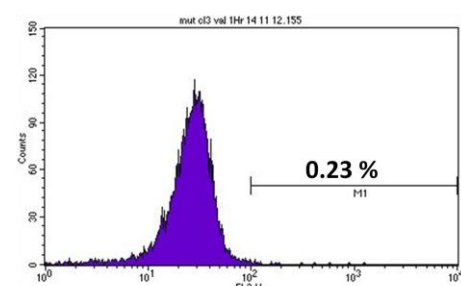
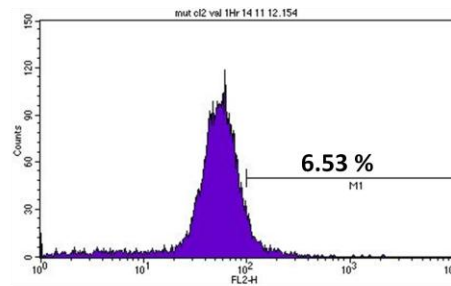
A.



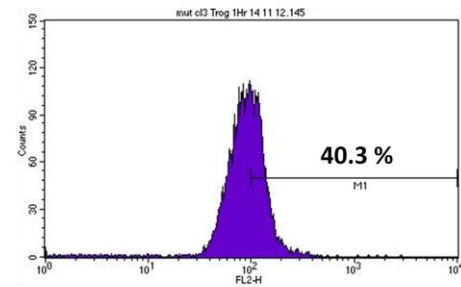
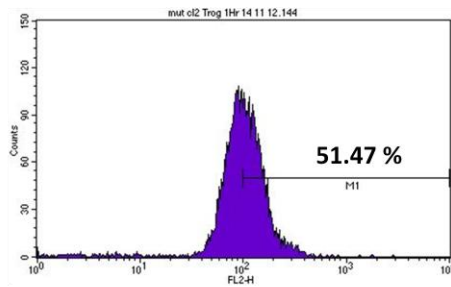
B.



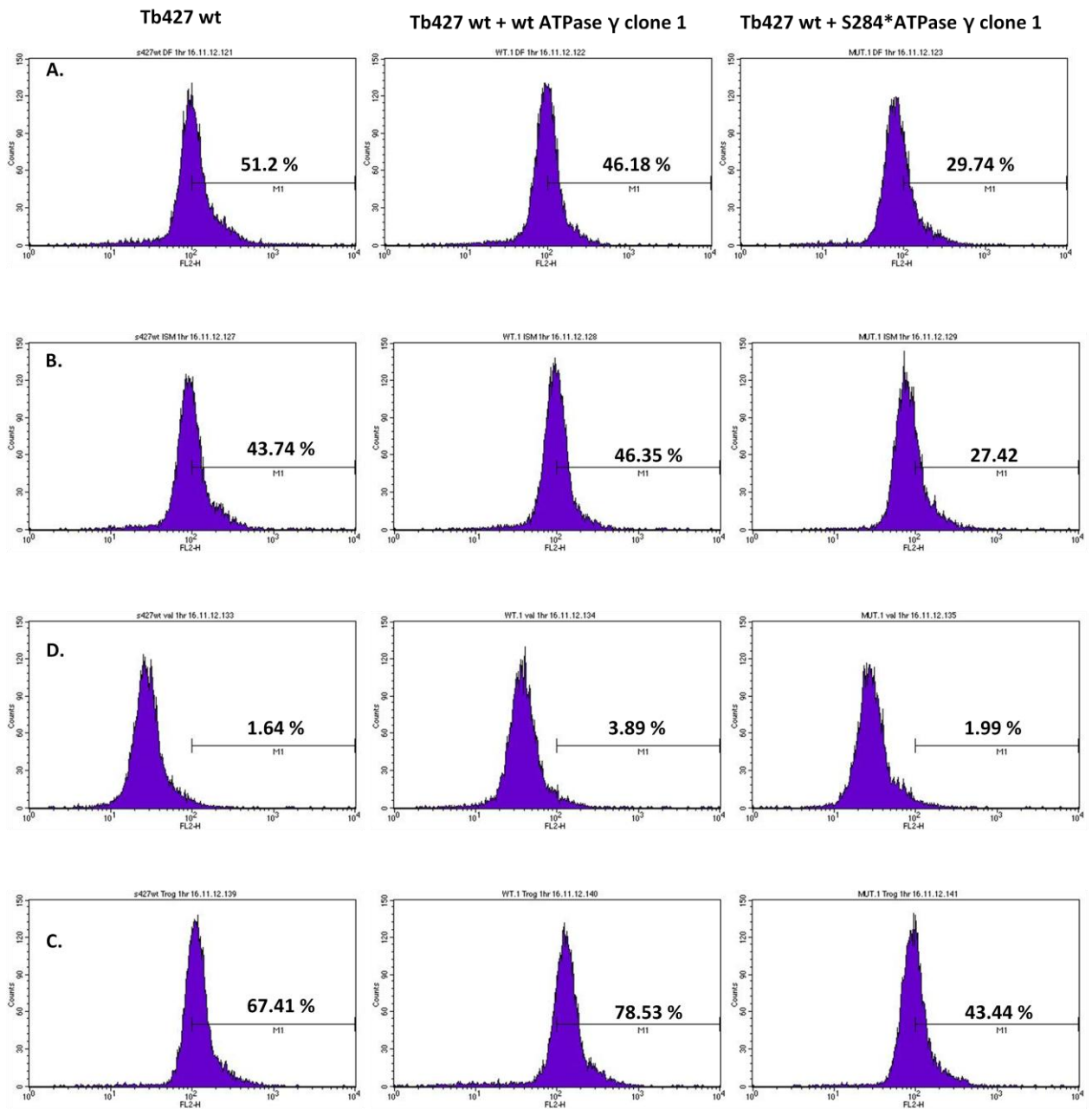
D.



C.



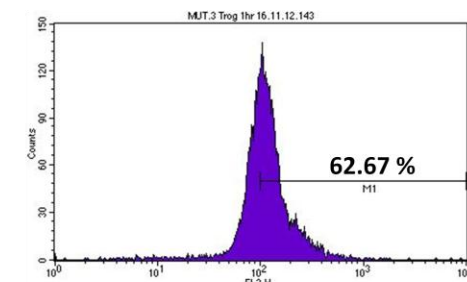
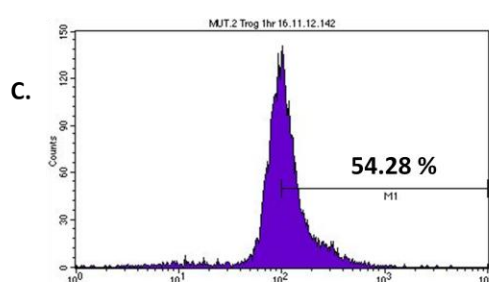
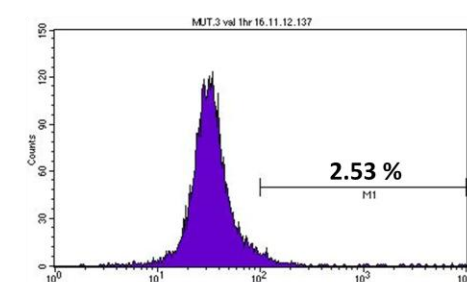
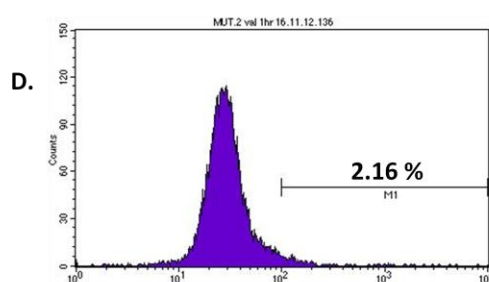
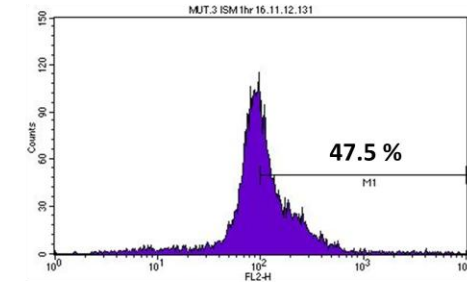
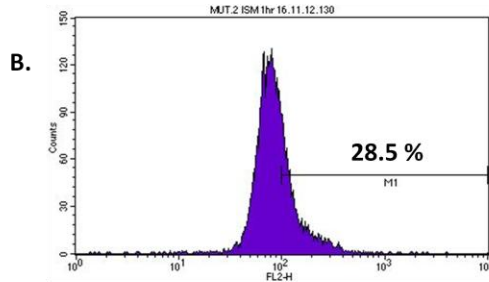
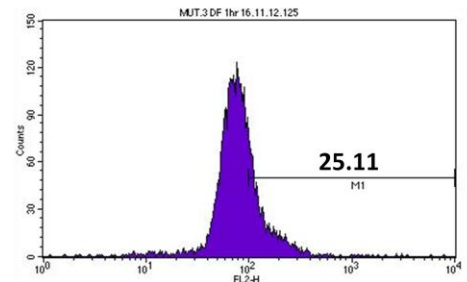
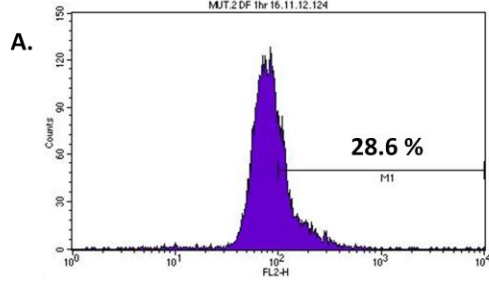
A. = Drug-free, B. = ISM-treated, C. = Troglitazone- treated, D. = Valinomycin-treated



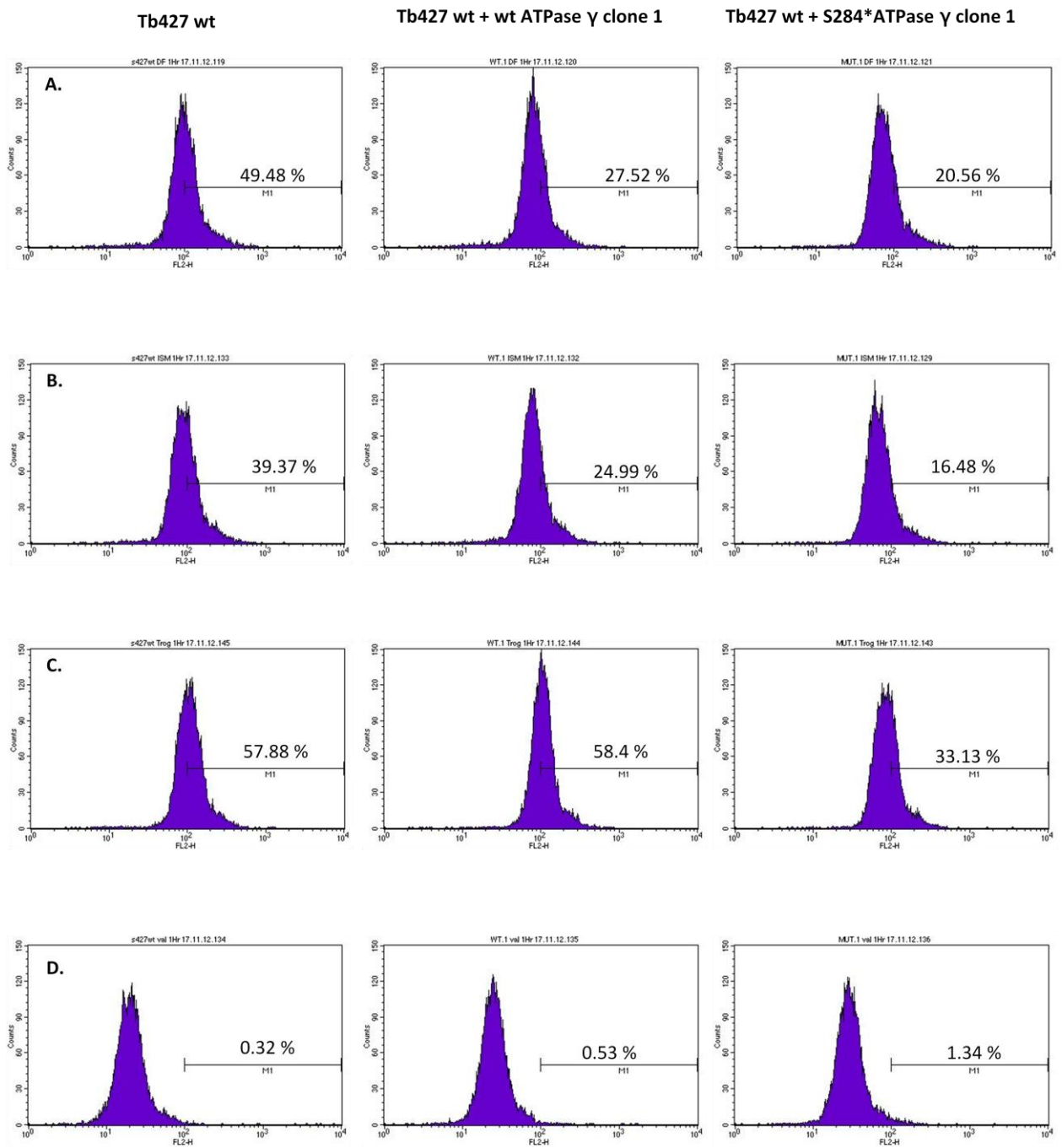
A. = Drug-free, B. = ISM-treated, C. = Troglitazone- treated, D. = Valinomycin-treated

Tb427 wt + S284*ATPase γ clone 2

Tb427 wt + S284*ATPase γ clone 3



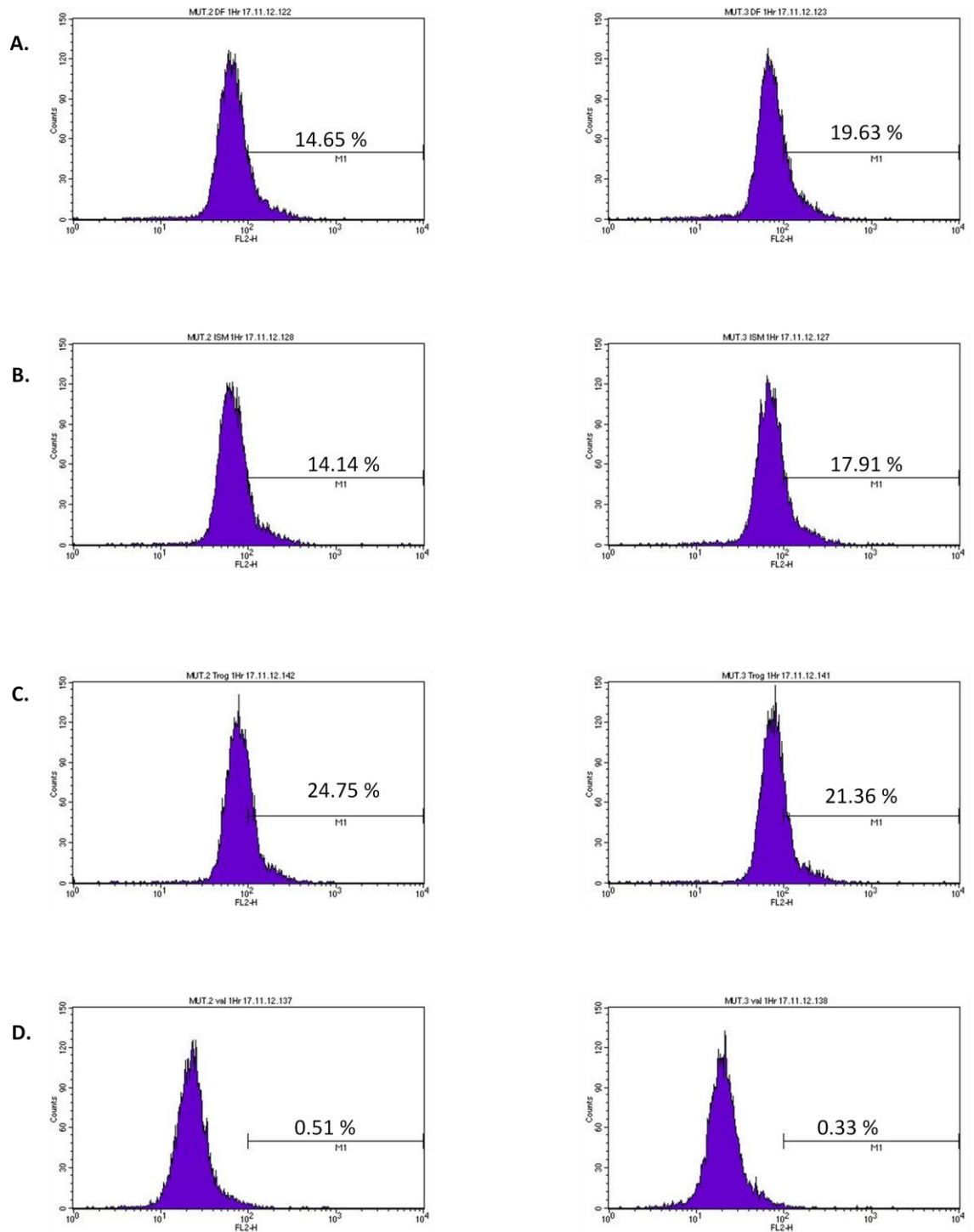
A. = Drug-free, B. = ISM-treated, C. = Troglitazone- treated, D. = Valinomycin-treated



A. = Drug-free, B. = ISM-treated, C. = Troglitazone- treated, D. = Valinomycin-treated

Tb427 wt + S284*ATPase γ clone 2

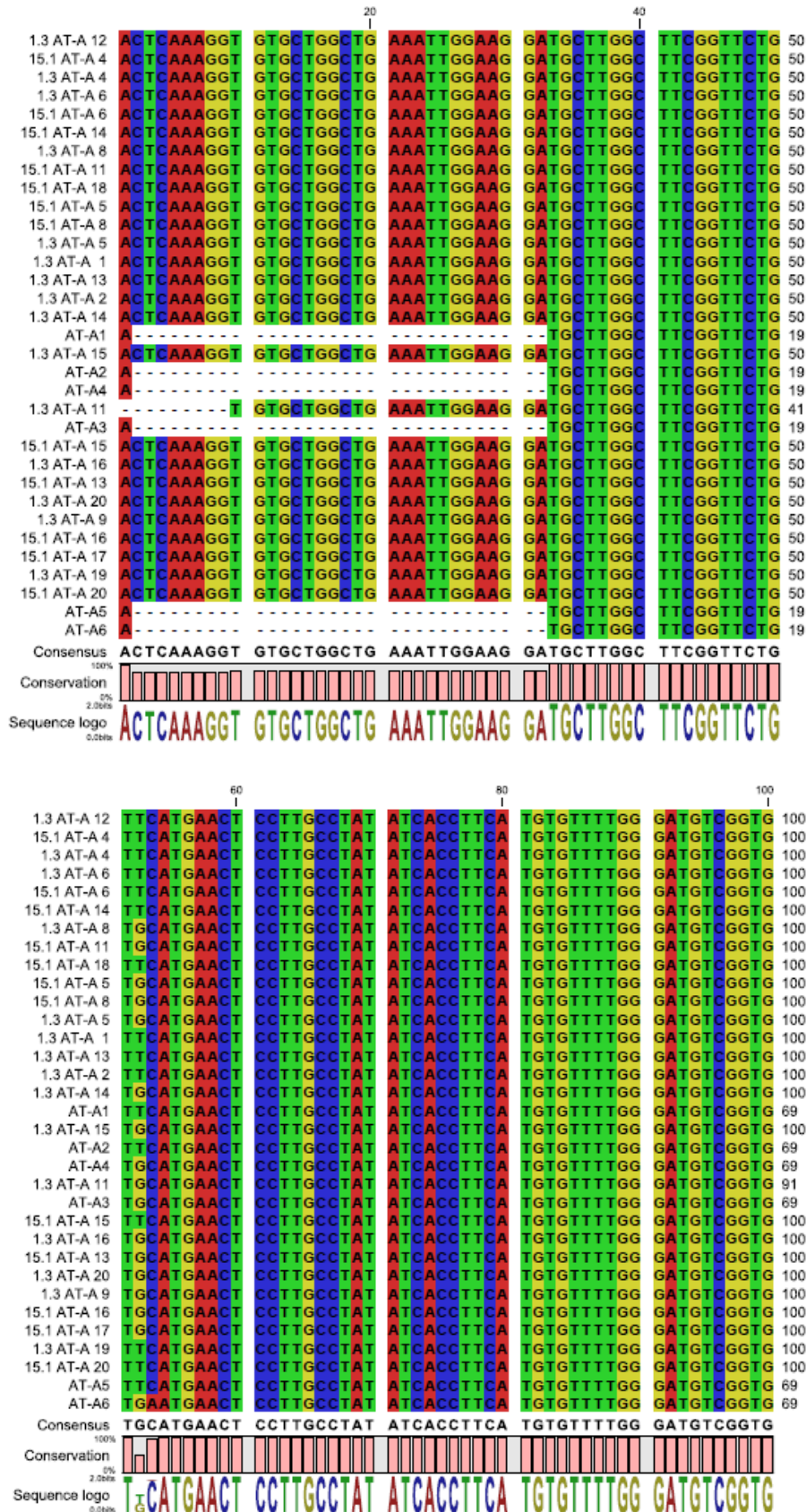
Tb427 wt + S284*ATPase γ clone 3

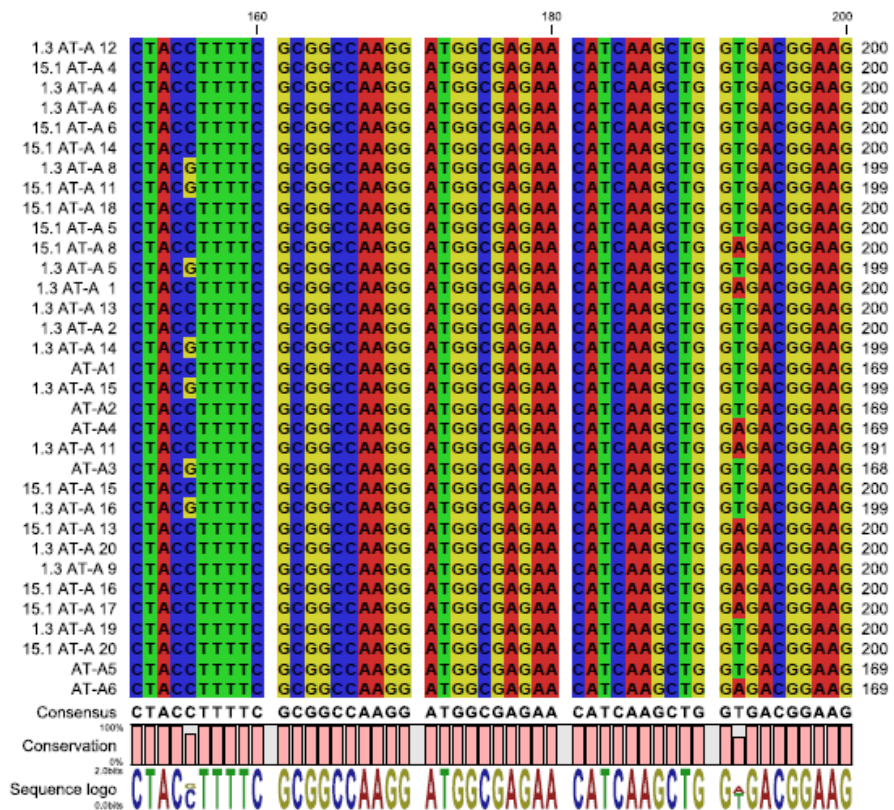
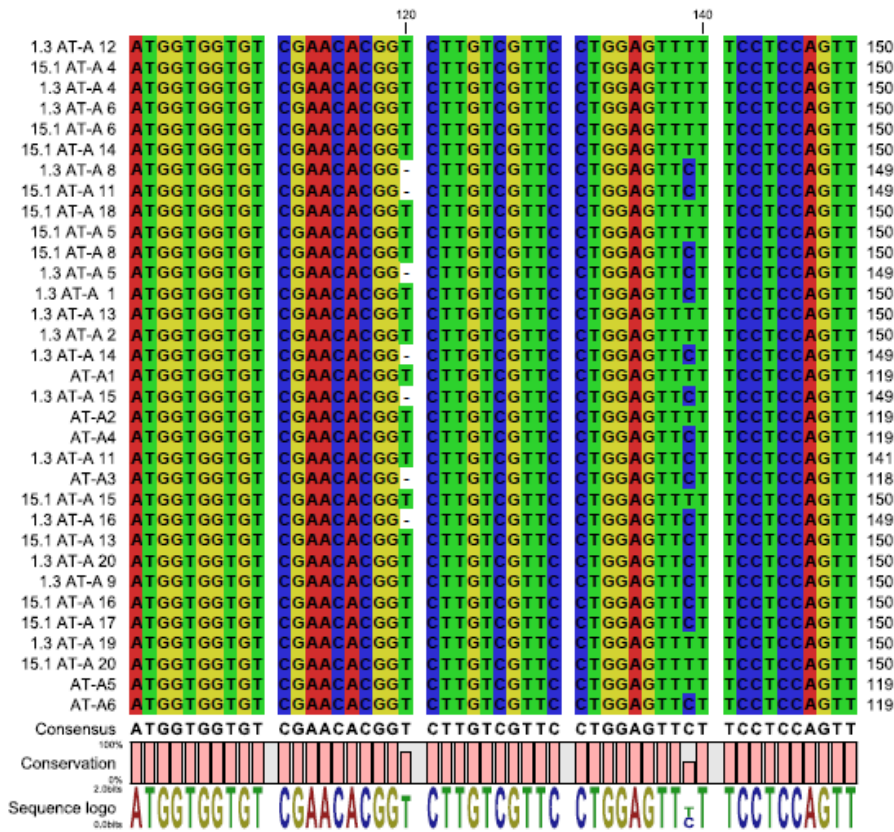


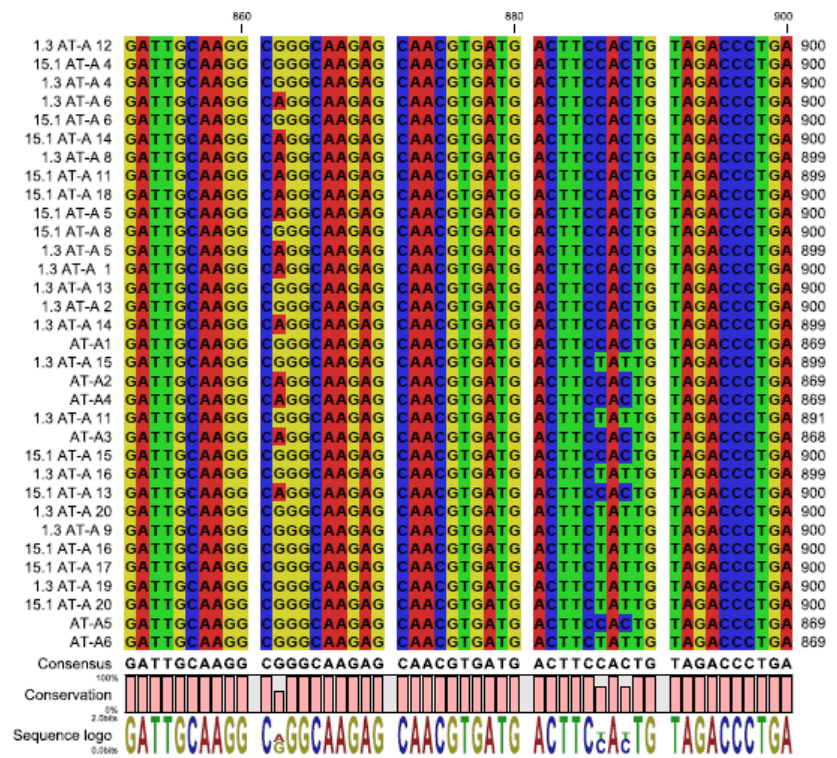
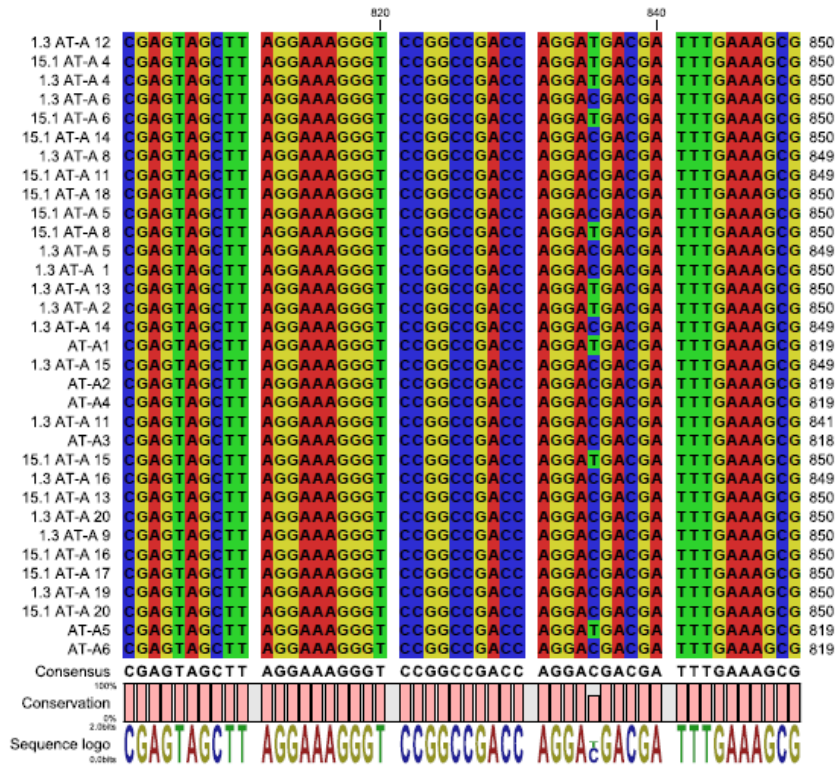
A. = Drug-free, B. = ISM-treated, C. = Troglitazone- treated, D. = Valinomycin-treated

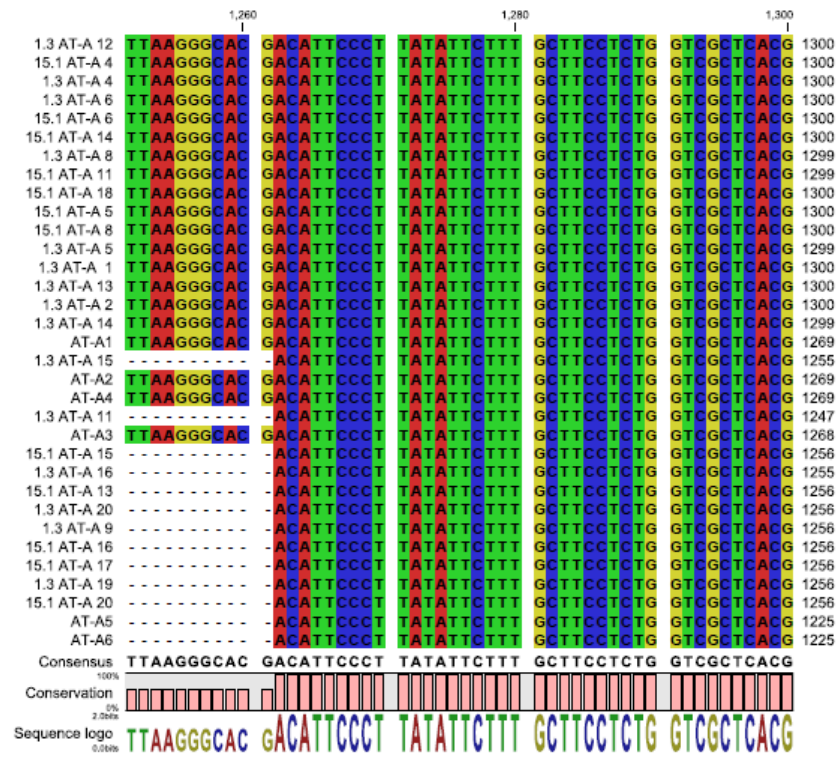
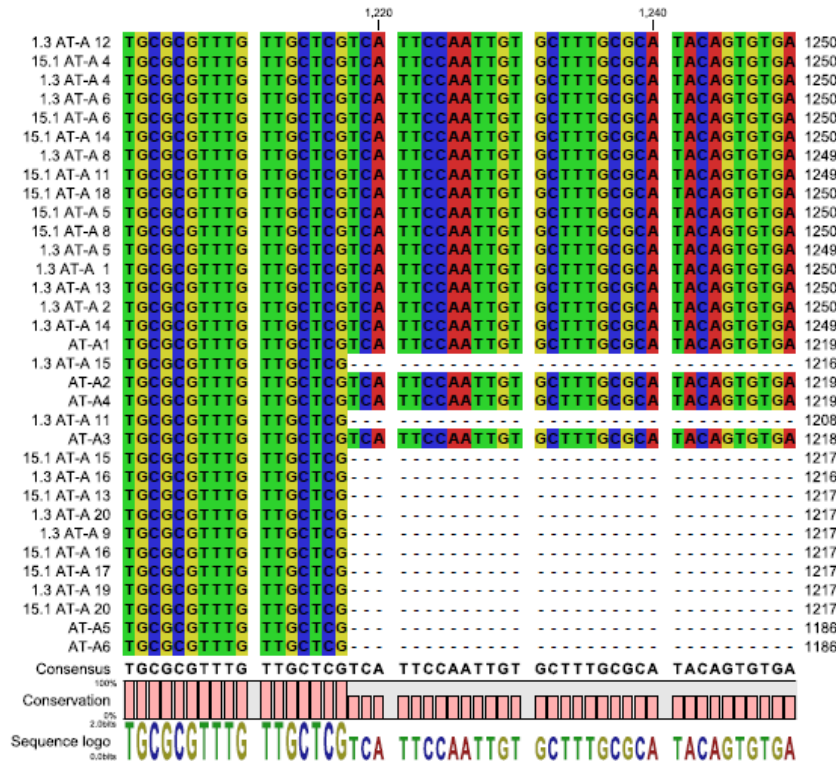
Appendix C: DNA sequencing alignment of *TbAT-A*, *TbAT-E*, *TbAT1* and ATPase γ from ISMR clones.

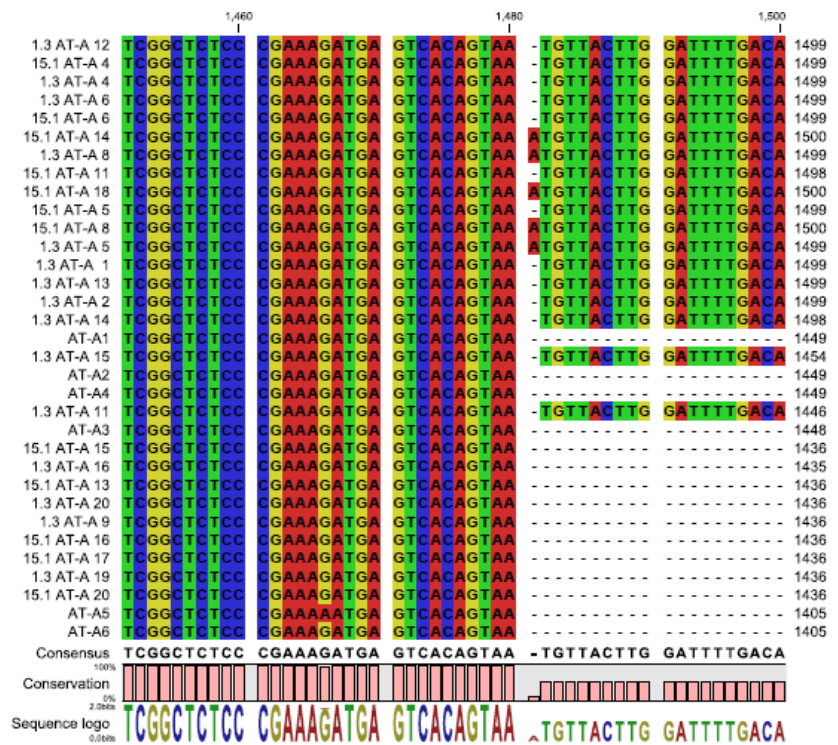
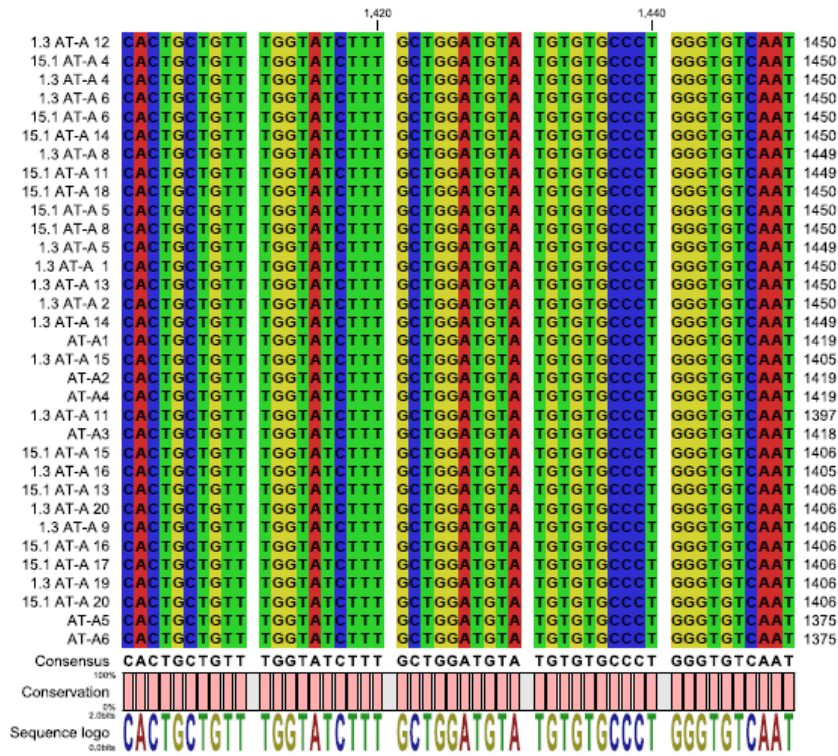
TbAT-A sequences from ISMR1 clone 3 and ISMR15 clone 1.

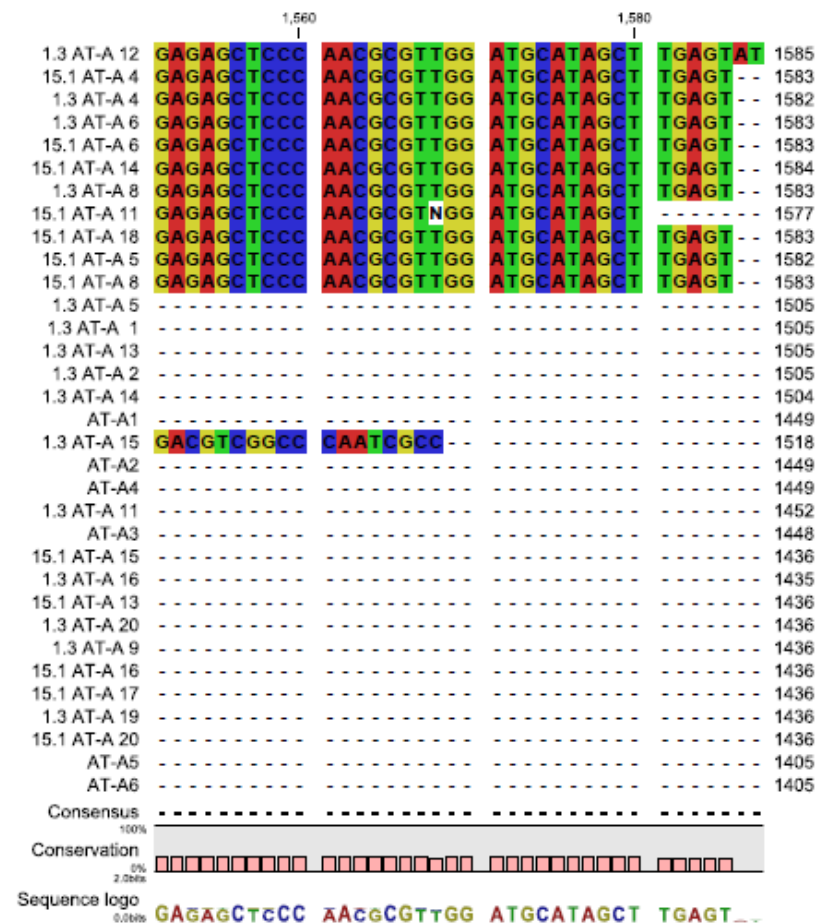
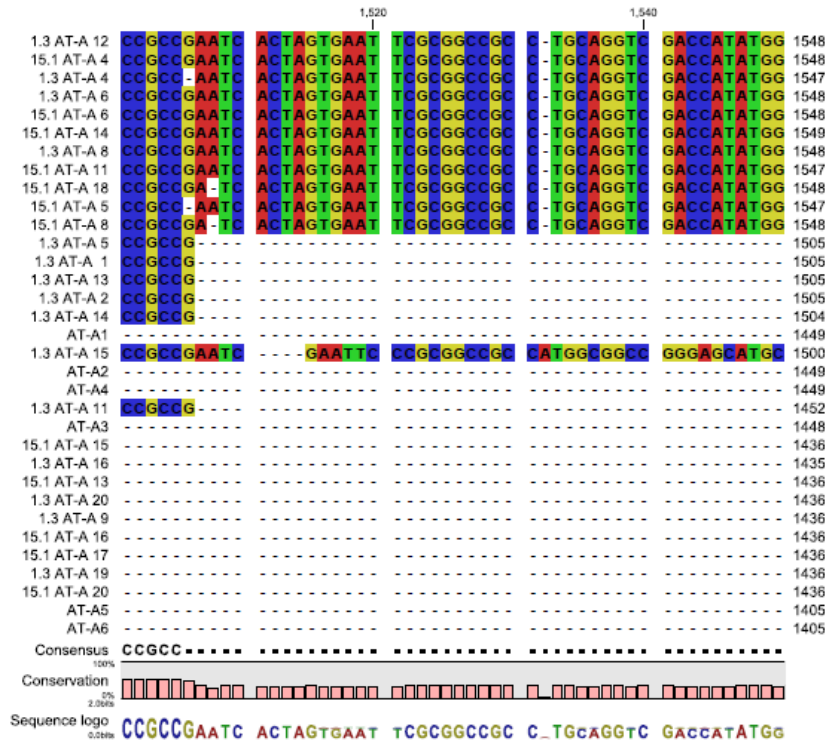


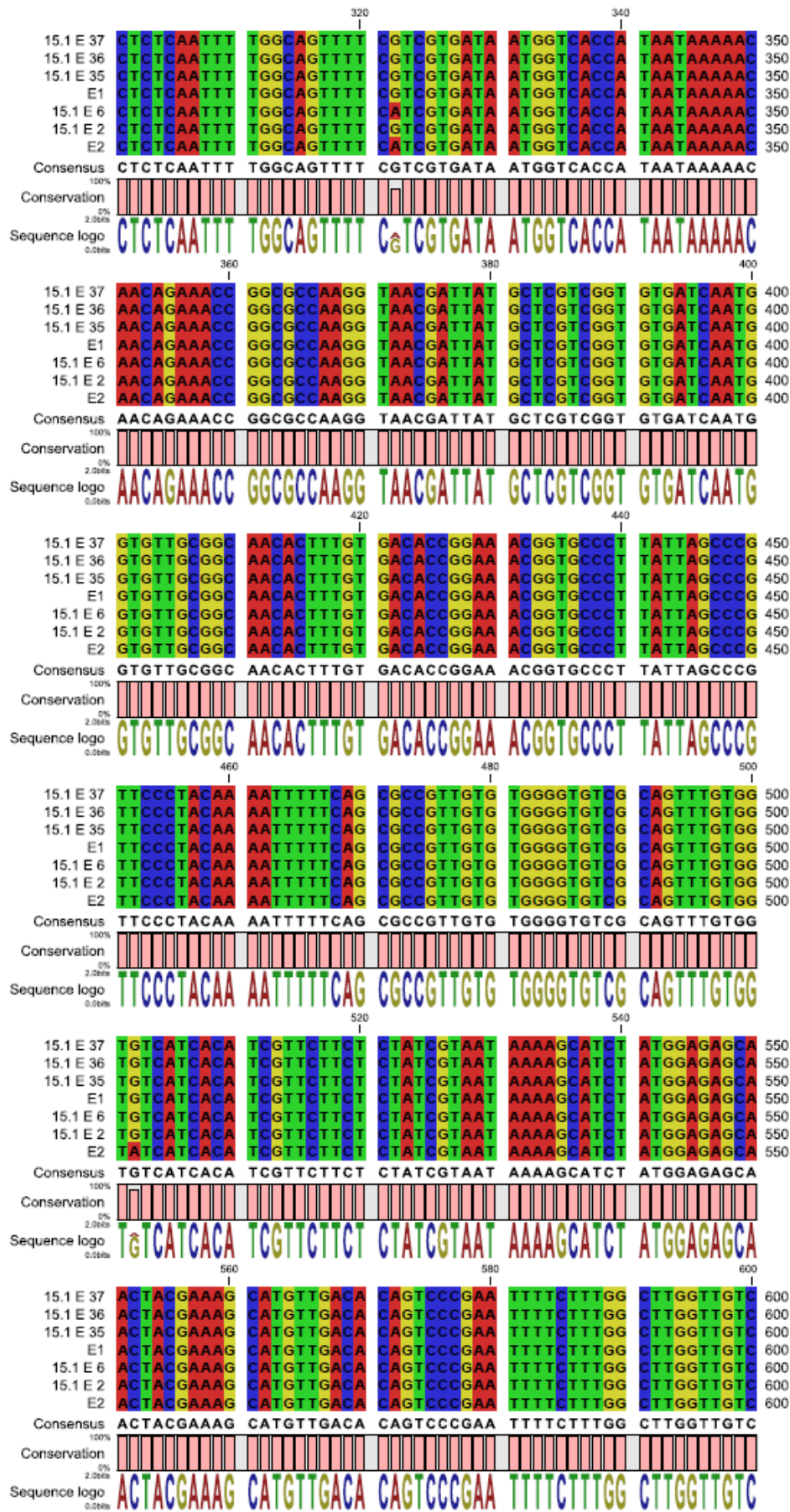


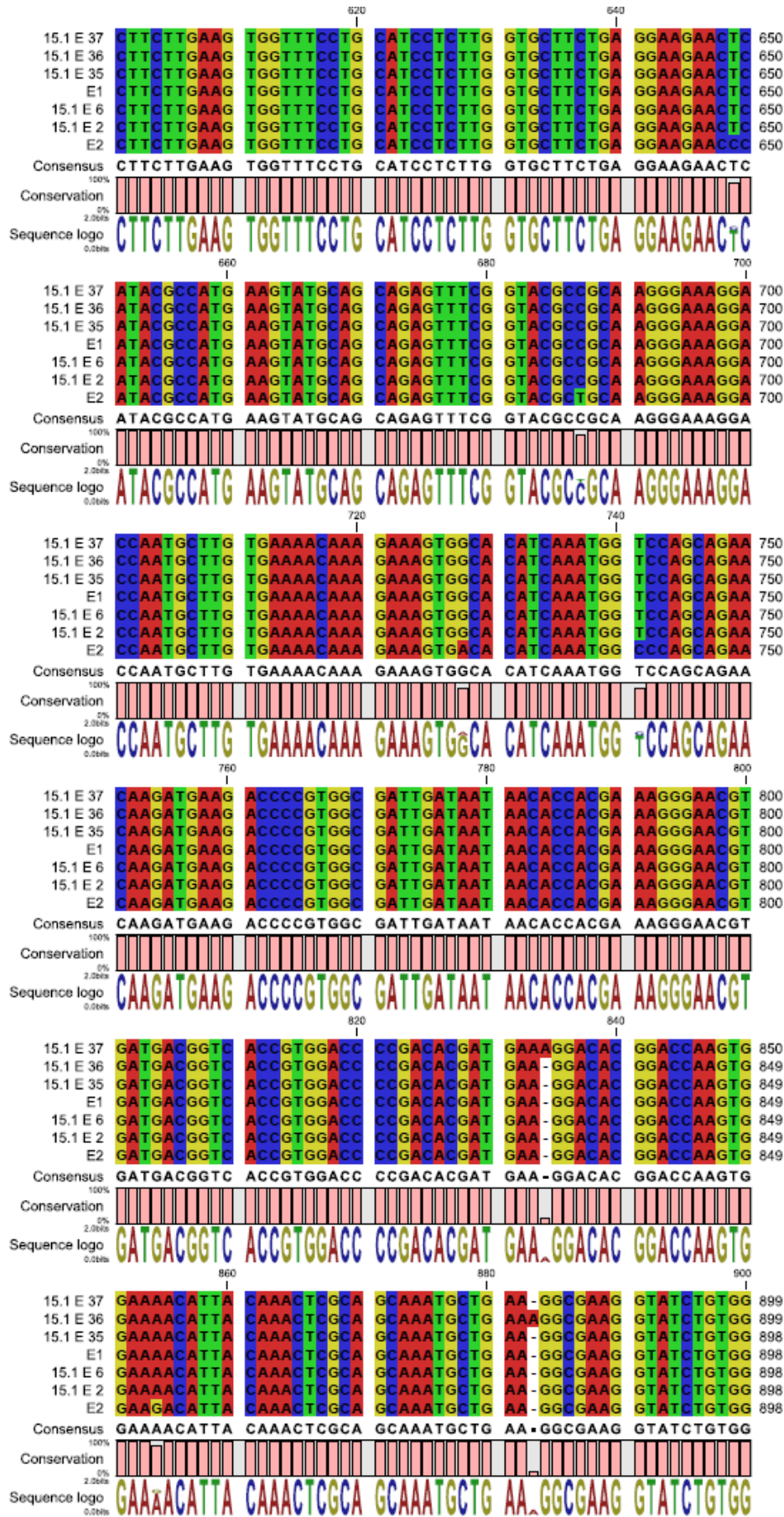


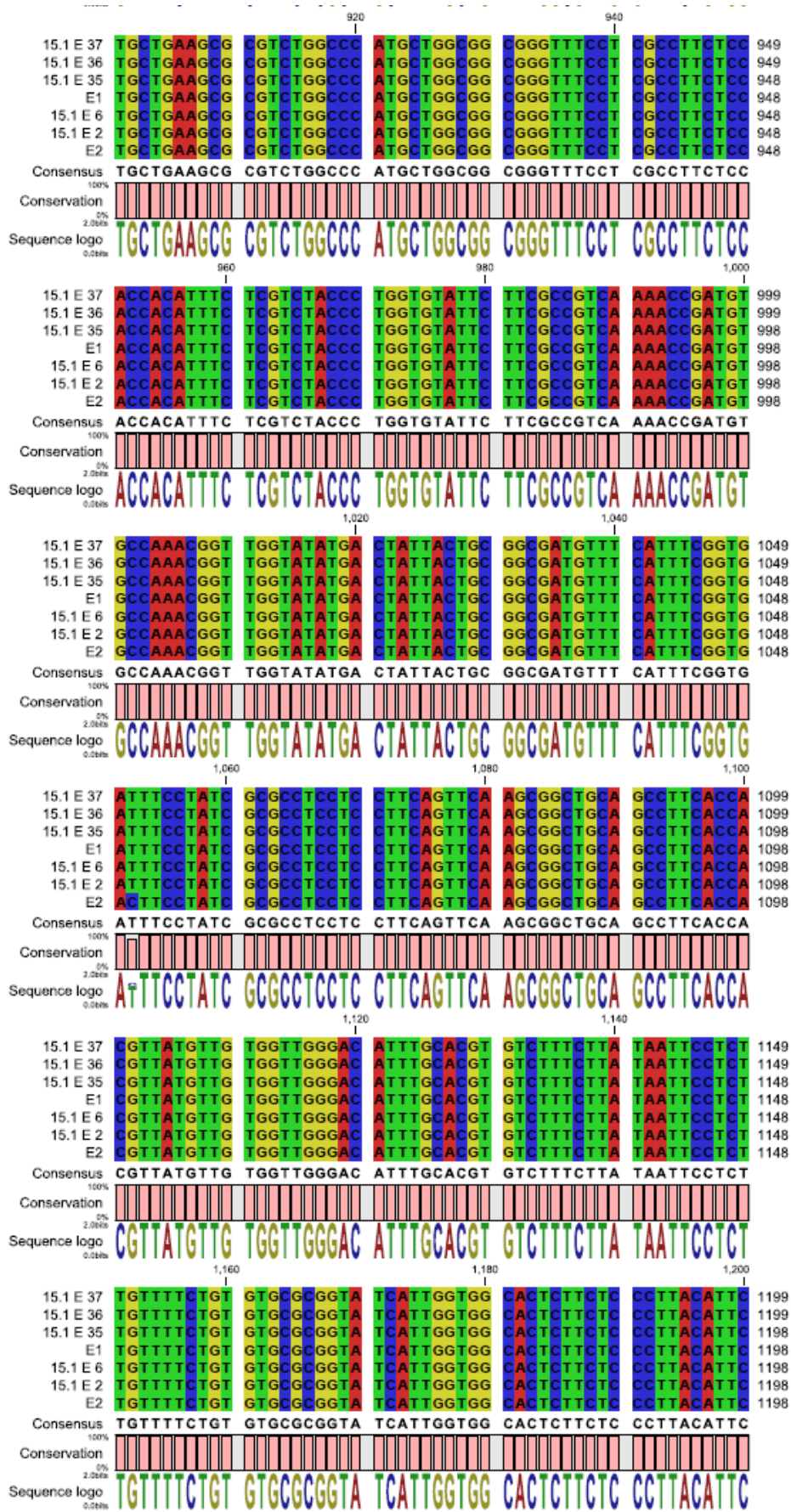


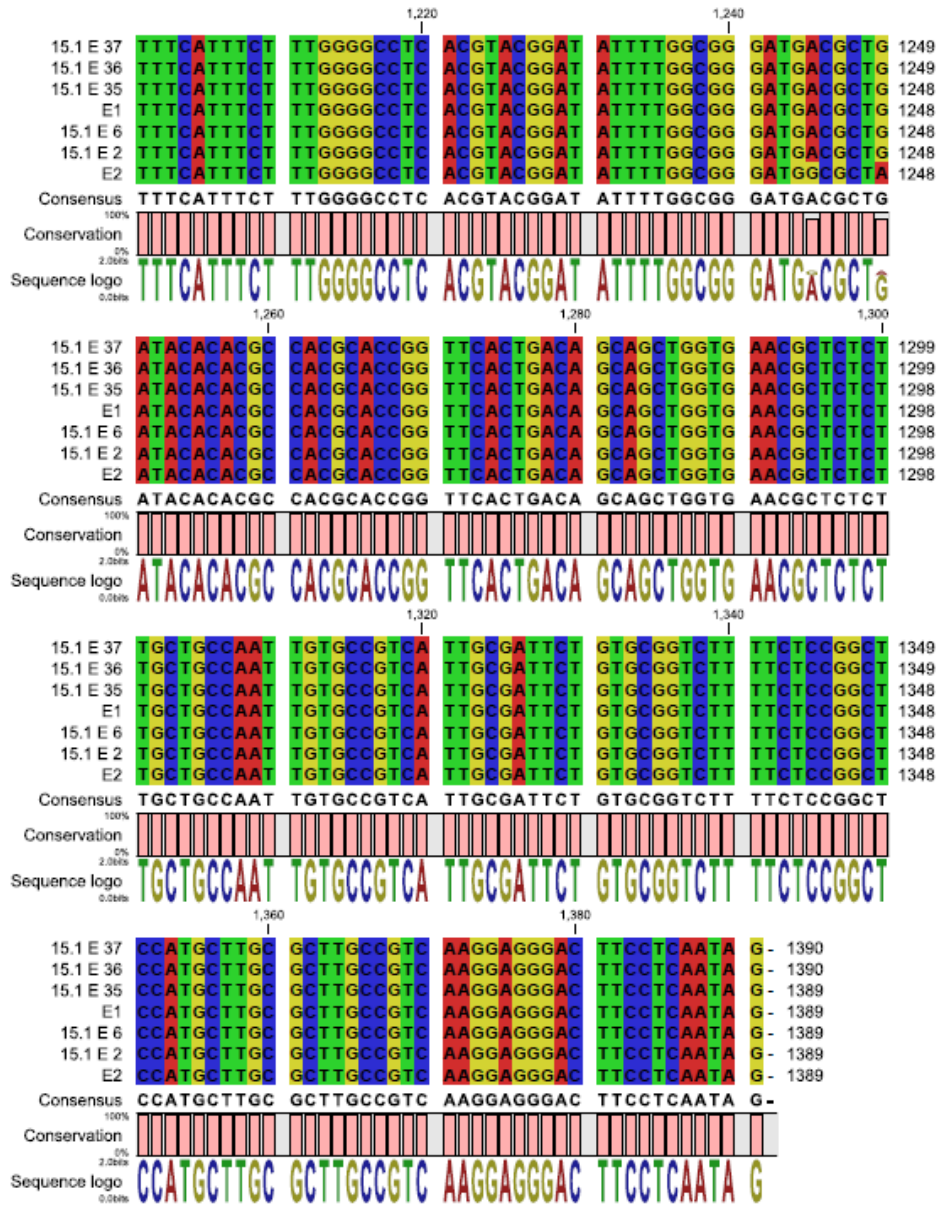




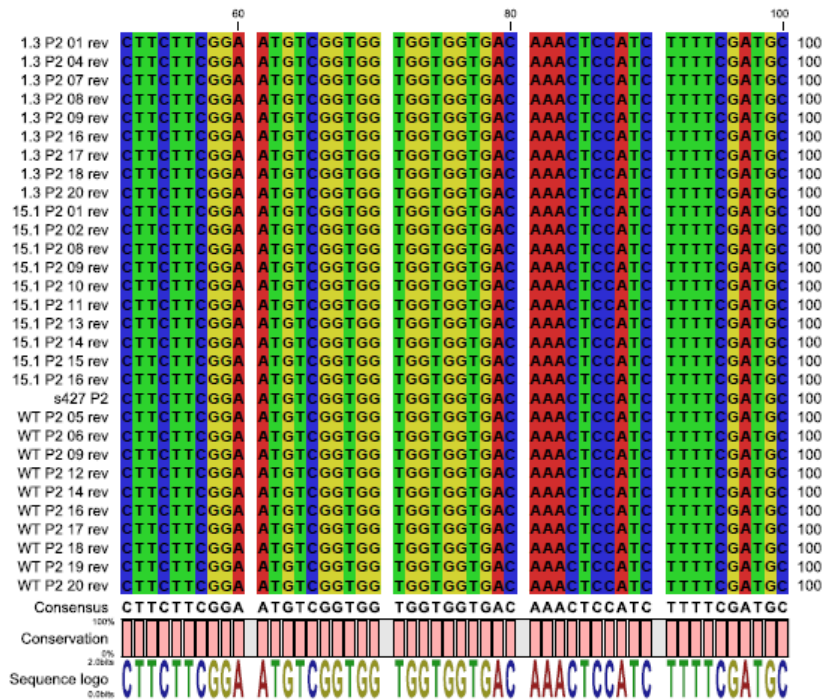
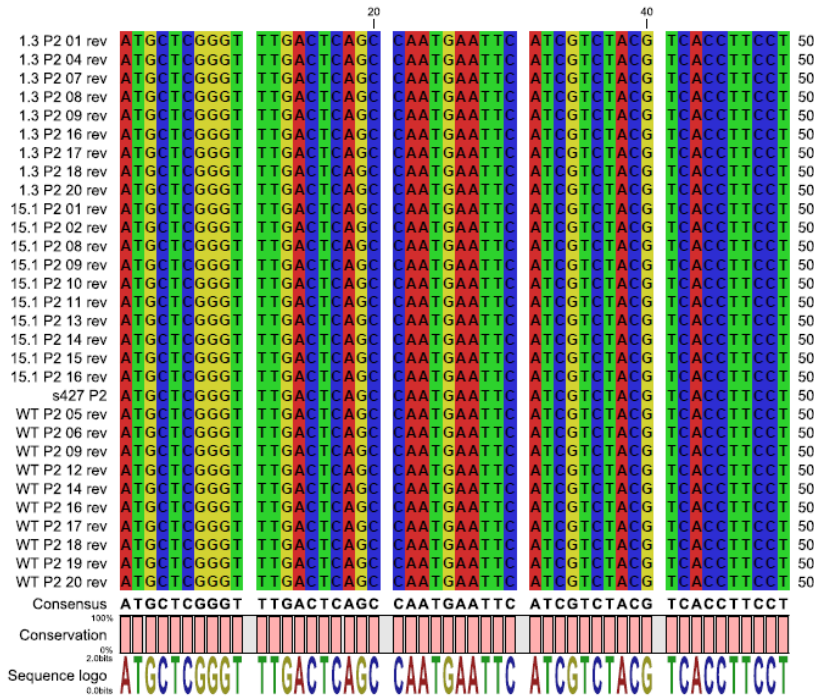




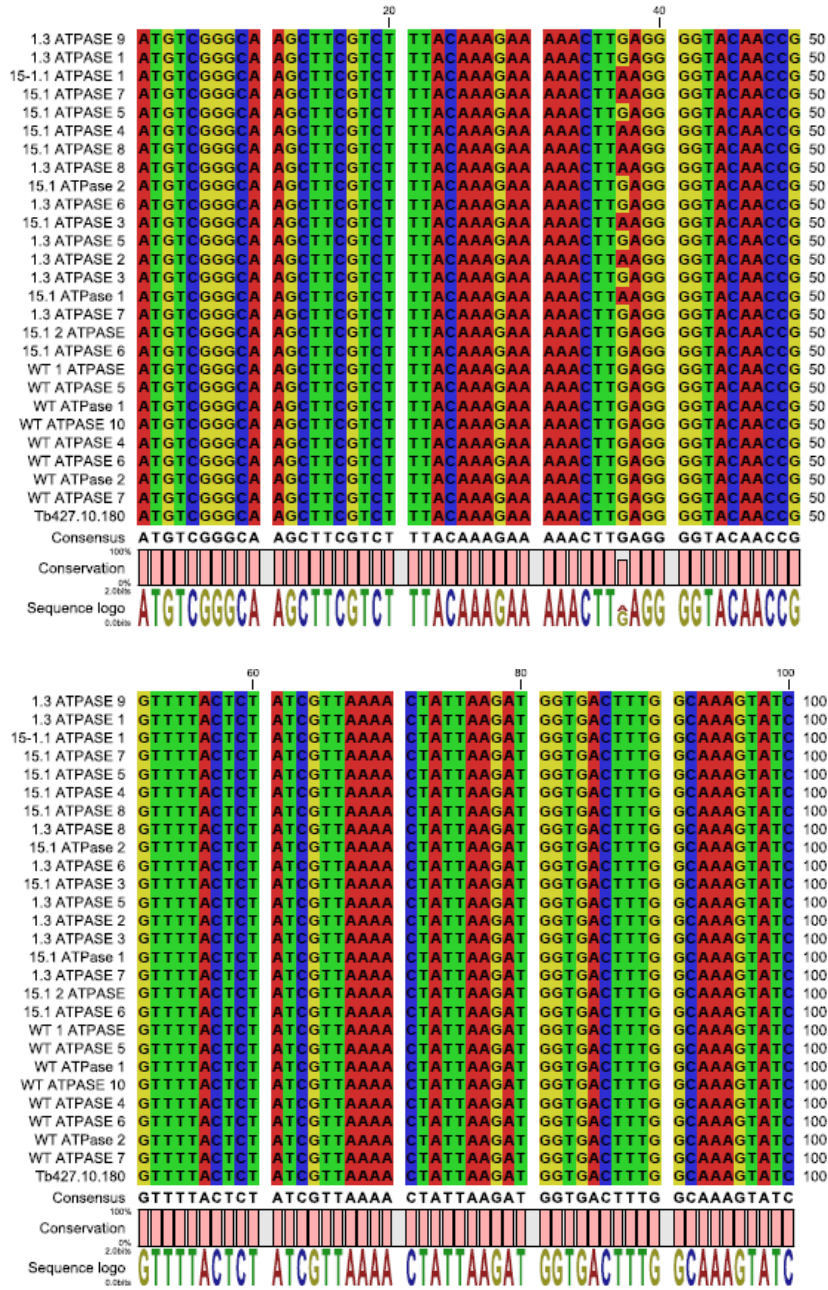


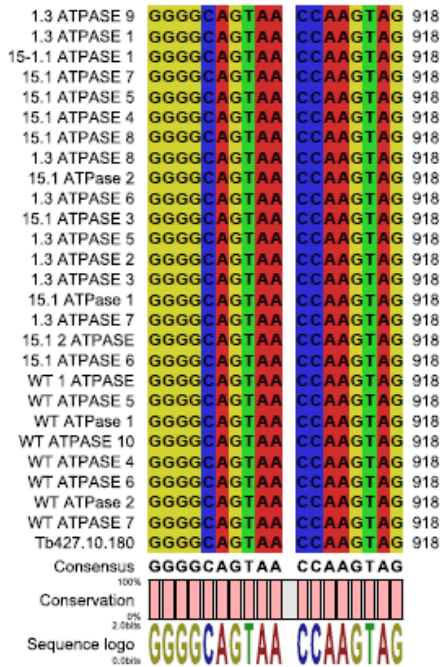
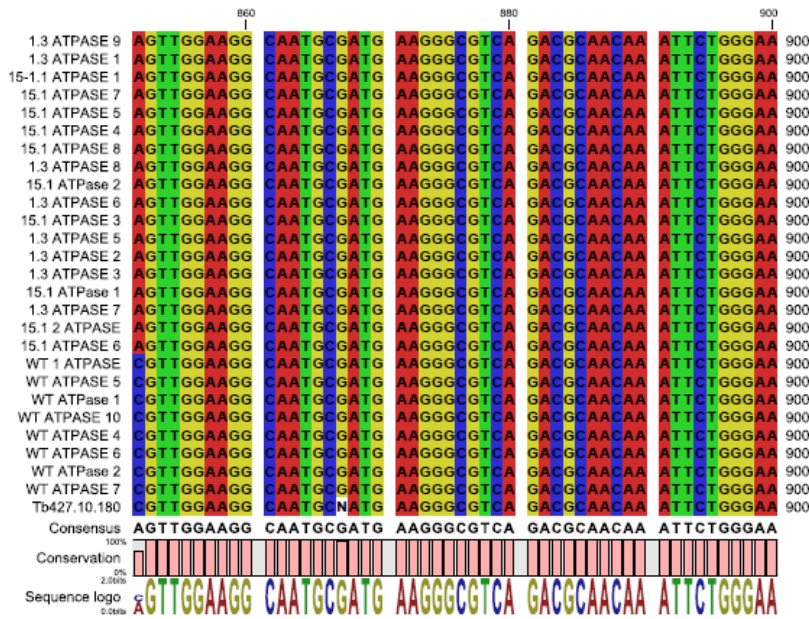


TbAT1 sequences from ISMR1 clone 3, ISMR15 clone 1 and *Tb427* wt.



ATPase γ sequences from ISMR1 clone 3, ISMR15 clone 1 and *Tb427*wt.





References

- Afework,Y., Maser,P., Etschmann,B., von Samson-Himmelstjerna,G., Zessin,K.H., & Clausen,P.H. (2006) Rapid identification of isometamidium-resistant stocks of *Trypanosoma b. brucei* by PCR-RFLP. *Parasitol.Res.*, **99**, 253-261.
- Agabian,N. (1990) Trans splicing of nuclear pre-mRNAs. *Cell*, **61**, 1157-1160.
- Alsford,N.S., Navarro,M., Jamnadass,H.R., Dunbar,H., Ackroyd,M., Murphy,N.B., Gull,K., & Ersfeld,K. (2003) The identification of circular extrachromosomal DNA in the nuclear genome of *Trypanosoma brucei*. *Molecular Microbiology*, **47**, 277-289.
- Alsford,S. & Horn,D. (2008) Single-locus targeting constructs for reliable regulated RNAi and transgene expression in *Trypanosoma brucei*. *Mol Biochem Parasitol.*, **161**, 76-79.
- Alsford,S., Eckert,S., Baker,N., Glover,L., Sanchez-Flores,A., Leung,K.F., Turner,D.J., Field,M.C., Berriman,M., & Horn,D. (2012) High-throughput decoding of antitrypanosomal drug efficacy and resistance. *Nature*, **482**, 232-236.
- Alsford,S., Kawahara,T., Glover,L., & Horn,D. (2005) Tagging a *T. brucei* rRNA locus improves stable transfection efficiency and circumvents inducible expression position effects. *Molecular and Biochemical Parasitology*, **144**, 142-148.
- Anene,B.M., Onah,D.N., & Nawa,Y. (2001) Drug resistance in pathogenic African trypanosomes: what hopes for the future? *Vet.Parasitol.*, **96**, 83-100.
- Angelopoulos,E. (1970) Pellicular microtubules in the family Trypanosomatidae. *J Protozool.*, **17**, 39-51.
- Ardelli,B.F. & Woo,P.T. (2001) The in vitro effects of isometamidium chloride (Samorin) on the piscine hemoflagellate *Cryptobia salmositica* (Kinetoplastida, Bodonina). *J Parasitol.*, **87**, 194-202.
- Atwal,K.S., Wang,P., Rogers,W.L., Sleph,P., Monshizadegan,H., Ferrara,F.N., Traeger,S., Green,D.W., & Grover,G.J. (2004) Small molecule mitochondrial F₁F₀ ATPase hydrolase inhibitors as cardioprotective agents. Identification of 4-(N-arylimidazole)-substituted benzopyran derivatives as selective hydrolase inhibitors. *J Med Chem.*, **47**, 1081-1084.
- Baker,N., Glover,L., Munday,J.C., Aguinaga,A.D., Barrett,M.P., de Koning,H.P., & Horn,D. (2012) Aquaglyceroporin 2 controls susceptibility to melarsoprol and pentamidine in African trypanosomes. *Proc.Natl.Acad.Sci U.S.A*, **109**, 10996-11001.

- Baker, N., de Koning, H.P., Maser, P., & Horn, D. (2013) Drug resistance in African trypanosomiasis: the melarsoprol and pentamidine story. *Trends in Parasitology*, **29**, 110-118.
- Baral, T.N. (2010) Immunobiology of African trypanosomes: need of alternative interventions. *J Biomed. Biotechnol.*, **2010**, 389153.
- Bargues, M.D., Klisiowicz, D.R., Panzera, F., Noireau, F., Marcilla, A., Perez, R., Rojas, M.G., O'Connor, J.E., Gonzalez-Candelas, F., Galvao, C., Jurberg, J., Carcavallo, R.U., Dujardin, J.P. & Mas-Coma, S. (2006) Origin of phylogeography of the Chagas disease main vector *Triatoma infectans* based on nuclear rDNA sequences and genome size. *Infect. Genet. Evol.*, **6**, 46-62.
- Barrett, M.P. (2000) Problems for the chemotherapy of human African trypanosomiasis. *Curr. Opin. Infect. Dis.*, **13**, 647-651.
- Barrett, M.P. & Fairlamb, A.H. (1999) The biochemical basis of arsenical-diamidine crossresistance in African trypanosomes. *Parasitol. Today*, **15**, 136-140.
- Barrett, M.P. & Gilbert, I.H. (2006) Targeting of toxic compounds to the trypanosome's interior. *Adv. Parasitol.*, **63**, 125-183.
- Barrett, M.P., Zhang, Z.Q., Denise, H., Giroud, C., & Baltz, T. (1995) A diamidine-resistant *Trypanosoma equiperdum* clone contains a P2 purine transporter with reduced substrate affinity. *Mol Biochem Parasitol.*, **73**, 223-229.
- Barrett, M.P., Fairlamb, A.H., Rousseau, B., Chauvière, G., & Peris, J. (2000) Uptake of the nitroimidazole drug meglumine by African trypanosomes. *Biochemical Pharmacology*, **59**, 615-620.
- Bassarak, B., Uzcategui, N.L., Schonfeld, C., & Duszenko, M. (2011) Functional characterization of three aquaglyceroporins from *Trypanosoma brucei* in osmoregulation and glycerol transport. *Cell Physiol Biochem*, **27**, 411-420.
- Basselin, M., Denise, H., Coombs, G.H., & Barrett, M.P. (2002) Resistance to pentamidine in *Leishmania mexicana* involves exclusion of the drug from the mitochondrion. *Antimicrobial Agents and Chemotherapy*, **46**, 3731-3738.
- Beitz, E. (2005) Aquaporins from pathogenic protozoan parasites: structure, function and potential for chemotherapy. *Biol. Cell*, **97**, 373-383.
- Bellofatto, V., Fairlamb, A.H., Henderson, G.B., & Cross, G.A. (1987) Biochemical changes associated with alpha-difluoromethylornithine uptake and resistance in *Trypanosoma brucei*. *Mol. Biochem Parasitol.*, **25**, 227-238.

- Benz,R. & McLaughlin,S. (1983) The molecular mechanism of action of the proton ionophore FCCP (carbonylcyanide p-trifluoromethoxyphenylhydrazone). *Biophys.J*, **41**, 381-398.
- Bertrand,K.I. & Hajduk,S.L. (2000) Import of a constitutively expressed protein into mitochondria from procyclic and bloodstream forms of *Trypanosoma brucei*. *Molecular and Biochemical Parasitology*, **106**, 249-260.
- Bhat,G.J., Koslowsky,D.J., Feagin,J.E., Smiley,B.L., & Stuart,K. (1990) An extensively edited mitochondrial transcript in kinetoplastids encodes a protein homologous to ATPase subunit 6. *Cell*, **61**, 885-894.
- Bienen,E.J. & Shaw,M.K. (1991) Differential expression of the oligomycin-sensitive ATPase in bloodstream forms of *Trypanosoma brucei brucei*. *Molecular and Biochemical Parasitology*, **48**, 59-66.
- Biteau,N., Bringaud,F., Gibson,W., Truc,P., & Baltz,T. (2000) Characterization of Trypanozoon isolates using a repeated coding sequence and microsatellite markers. *Mol Biochem Parasitol.*, **105**, 187-202.
- Bitonti,A.J., Bacchi,C.J., McCann,P.P., & Sjoerdsma,A. (1986) Uptake of [alpha]-difluoromethylornithine by *Trypanosoma brucei brucei*. *Biochemical Pharmacology*, **35**, 351-354.
- Boibessot,I., Tettey,J.N., Skellern,G.G., Watson,D.G., & Grant,M.H. (2006) Metabolism of isometamidium in hepatocytes isolated from control and inducer-treated rats. *J Vet.Pharmacol.Ther.*, **29**, 547-553.
- Boibessot,I., Turner,C.M., Watson,D.G., Goldie,E., Connel,G., McIntosh,A., Grant,M.H., & Skellern,G.G. (2002) Metabolism and distribution of phenanthridine trypanocides in *Trypanosoma brucei*. *Acta Trop.*, **84**, 219-228.
- Borst,P. & Ouellette,M. (1995) New mechanisms of drug resistance in parasitic protozoa. *Annu.Rev Microbiol.*, **49**, 427-460.
- Bray,P.G., Barrett,M.P., Ward,S.A., & de Koning,H.P. (2003) Pentamidine uptake and resistance in pathogenic protozoa: past, present and future. *Trends Parasitol.*, **19**, 232-239.
- Bridges,D.J., Gould,M.K., Nerima,B., Maser,P., Burchmore,R.J.S., & de Koning,H.P. (2007) Loss of the High-Affinity Pentamidine Transporter Is Responsible for High Levels of Cross-Resistance between Arsenical and Diamidine Drugs in African Trypanosomes. *Molecular Pharmacology*, **71**, 1098-1108.
- Bringaud,F. & Baltz,T. (1993) Differential regulation of two distinct families of glucose transporter genes in *Trypanosoma brucei*. *Molecular and Cellular Biology*, **13**, 1146-1154.

- Brown,S.V., Hosking,P., Li,J., & Williams,N. (2006) ATP Synthase Is Responsible for Maintaining Mitochondrial Membrane Potential in Bloodstream Form *Trypanosoma brucei*. *Eukaryotic Cell*, **5**, 45-53.
- Brun,R., Hecker,H., & Lun,Z.R. (1998) *Trypanosoma evansi* and *T. equiperdum*: distribution, biology, treatment and phylogenetic relationship (a review). *Vet.Parasitol.*, **79**, 95-107.
- Burchmore,R.J.S., Wallace,L.J.M., Candlish,D., Al-Salabi,M.I., Beal,P.R., Barrett,M.P., Baldwin,S.A., & de Koning,H.P. (2003) Cloning, heterologous expression, and in situ characterization of the first high affinity nucleobase transporter from a protozoan. *Journal of Biological Chemistry*, **278**, 23502-23507.
- Burri,C., Baltz,T., Giroud,C., Doua,F., Welker,H.A., & Brun,R. (1993) Pharmacokinetic properties of the trypanocidal drug melarsoprol. *Chemotherapy*, **39**, 225-234.
- Caffrey,C.R. & Steverding,D. (2009) Kinetoplastid papain-like cysteine peptidases. *Molecular and Biochemical Parasitology*, **167**, 12-19.
- Carter,N.S., Berger,B.J., & Fairlamb,A.H. (1995) Uptake of diamidine drugs by the P2 nucleoside transporter in melarsen-sensitive and -resistant *Trypanosoma brucei brucei*. *J Biol.Chem.*, **270**, 28153-28157.
- Carter,N.S. & Fairlamb,A.H. (1993) Arsenical-resistant trypanosomes lack an unusual adenosine transporter. *Nature*, **361**, 173-176.
- Chappuis,F., Loutan,L., Simarro,P., Lejon,V., & Buscher,P. (2005) Options for field diagnosis of human african trypanosomiasis. *Clin Microbiol.Rev.*, **18**, 133-146.
- Chaudhuri,M., Ott,R.D., & Hill,G.C. (2006) Trypanosome alternative oxidase: from molecule to function. *Trends in Parasitology*, **22**, 484-491.
- Chen,X.J. & Clark-Walker,G.D. (1999) The Petite Mutation in Yeasts: 50 Years On. *International Review of Cytology* (ed. by W. J. Kwang), pp. 197-238. Academic Press.
- Chopra,I. & Roberts,M. (2001) Tetracycline Antibiotics: Mode of Action, Applications, Molecular Biology, and Epidemiology of Bacterial Resistance. *Microbiology and Molecular Biology Reviews*, **65**, 232-260.
- Claes,F., Buscher,P., Touratier,L., & Goddeeris,B.M. (2005) *Trypanosoma equiperdum*: master of disguise or historical mistake? *Trends Parasitol.*, **21**, 316-321.

- Clarkson,A.B., Jr. & Brohn,F.H. (1976) Trypanosomiasis: an approach to chemotherapy by the inhibition of carbohydrate catabolism. *Science*, **194**, 204-206.
- Clarkson,J., Bienen,E.J., Pollakis,G., & Grady,R.W. (1989) Respiration of bloodstream forms of the parasite *Trypanosoma brucei brucei* is dependent on a plant-like alternative oxidase. *Journal of Biological Chemistry*, **264**, 17770-17776.
- Clausen,P.H., Sidibe,I., Kabore,I., & Bauer,B. (1992) Development of multiple drug resistance of *Trypanosoma congolense* in Zebu cattle under high natural tsetse fly challenge in the pastoral zone of Samorogouan, Burkina Faso. *Acta Trop.*, **51**, 229-236.
- Claverol,S., Burlet-Schiltz,O., Girbal-Neuhauser,E., Gairin,J.E., & Monsarrat,B. (2002) Mapping and Structural Dissection of Human 20 S Proteasome Using Proteomic Approaches. *Molecular Cellular Proteomics*, **1**, 567-578.
- Clayton,C.E. & Michels,P. (1996) Metabolic compartmentation in African trypanosomes. *Parasitol.Today*, **12**, 465-471.
- Clayton,C.E. (2002) Life without transcriptional control? From fly to man and back again. *EMBO J*, **21**, 1881-1888.
- Codjia,V., Mulatu,W., Majiwa,P.A., Leak,S.G., Rowlands,G.J., Authie,E., d'Ieteren,G.D., & Peregrine,A.S. (1993) Epidemiology of bovine trypanosomiasis in the Ghibe valley, southwest Ethiopia. 3. Occurrence of populations of *Trypanosoma congolense* resistant to diminazene, isometamidium and homidium. *Acta Trop.*, **53**, 151-163.
- Coley,A.F., Dodson,H.C., Morris,M.T., & Morris,J.C. (2011) Glycolysis in the african trypanosome: targeting enzymes and their subcellular compartments for therapeutic development. *Mol Biol.Int.*, **2011**, 123702.
- Coppens,I. & Courtoy,P.J. (2000) The adaptative mechanisms of *Trypanosoma brucei* for sterol homeostasis in its different life-cycle environments. *Annual Review of Microbiology*, **54**, 129-156.
- Coustou,V., Besteiro,S., Biran,M., Diolez,P., Bouchaud,V., Voisin,P., Michels,P.A., Canioni,P., Baltz,T., & Bringaud,F. (2003a) ATP generation in the *Trypanosoma brucei* procyclic form: cytosolic substrate level is essential, but not oxidative phosphorylation. *J Biol.Chem.*, **278**, 49625-49635.
- Coustou,V., Besteiro,S., Biran,M., Diolez,P., Bouchaud,V., Voisin,P., Michels,P.A.M., Canioni,P., Baltz,T., & Bringaud,F. (2003b) ATP Generation in the *Trypanosoma brucei* Procyclic Form: cytosolic substrate level phosphorylation is essential, but not oxidative phosphorylation. *Journal of Biological Chemistry*, **278**, 49625-49635.

- Coux,O., Tanaka,K., & Goldberg,A.L. (1996) Structure and Functions of the 20S and 26S Proteasomes. *Annual Review of Biochemistry*, **65**, 801-847.
- Cox,F.E. (2004) History of sleeping sickness (African trypanosomiasis). *Infect.Dis.Clin North Am.*, **18**, 231-245.
- Czichos,J., Nonnengaesser,C., & Overath,P. (1986) Trypanosoma brucei: cis-Aconitate and temperature reduction as triggers of synchronous transformation of bloodstream to procyclic trypomastigotes in vitro. *Experimental Parasitology*, **62**, 283-291.
- de Koning,H.P. (2001a) Transporters in African trypanosomes: role in drug action and resistance. *Int.J Parasitol.*, **31**, 512-522.
- de Koning,H.P. (2001b) Uptake of pentamidine in Trypanosoma brucei brucei is mediated by three distinct transporters: implications for cross-resistance with arsenicals. *Mol.Pharmacol.*, **59**, 586-592.
- de Koning,H.P. (2008) Ever-increasing complexities of diamidine and arsenical crossresistance in African trypanosomes. *Trends Parasitol.*, **24**, 345-349.
- de Koning,H.P., Anderson,L.F., Stewart,M., Burchmore,R.J., Wallace,L.J., & Barrett,M.P. (2004) The trypanocide diminazene aceturate is accumulated predominantly through the TbAT1 purine transporter: additional insights on diamidine resistance in african trypanosomes. *Antimicrobial Agents and Chemotherapy*, **48**, 1515-1519.
- de Koning,H.P. & Jarvis,S.M. (1997a) Hypoxanthine uptake through a purine-selective nucleobase transporter in Trypanosoma brucei brucei procyclic cells is driven by protonmotive force. *Eur.J Biochem*, **247**, 1102-1110.
- de Koning,H.P. & Jarvis,S.M. (1997b) Purine nucleobase transport in bloodstream forms of Trypanosoma brucei is mediated by two novel transporters. *Mol.Biochem Parasitol.*, **89**, 245-258.
- de Koning,H.P. & Jarvis,S.M. (1999) Adenosine transporters in bloodstream forms of Trypanosoma brucei brucei: substrate recognition motifs and affinity for trypanocidal drugs. *Mol.Pharmacol.*, **56**, 1162-1170.
- de Koning,H.P., Bridges,D.J., & Burchmore,R.J.S. (2005) Purine and pyrimidine transport in pathogenic protozoa: From biology to therapy. *FEMS Microbiology Reviews*, **29**, 987-1020.
- De Raadt,P. (2005) The history of sleeping sickness. *W.H.O.*, Fourth International Cours on African Trypanosomoses.
http://www.who.int/trypanosomiasis_african/country/history/en/print.html.

- Deeley,R.G., Westlake,C., & Cole,S.P.C. (2006) Transmembrane Transport of Endo- and Xenobiotics by Mammalian ATP-Binding Cassette Multidrug Resistance Proteins. *Physiological Reviews*, **86**, 849-899.
- Delespaux,V. & de Koning,H.P. (2007) Drugs and drug resistance in African trypanosomiasis. *Drug Resist.Updat.*, **10**, 30-50.
- Delespaux,V., Geysen,D., & Geerts,A.S. (2007) Point mutations in mitochondrial topoisomerase enzymes of *Trypanosoma congolense* are not involved in isometamidium resistance. *Molecular and Biochemical Parasitology*, **151**, 137-140.
- Delespaux,V., Geysen,D., Majiwa,P.A., & Geerts,S. (2005) Identification of a genetic marker for isometamidium chloride resistance in *Trypanosoma congolense*. *Int.J Parasitol.*, **35**, 235-243.
- Delespaux,V., Geysen,D., Van den Bossche,P., & Geerts,S. (2008) Molecular tools for the rapid detection of drug resistance in animal trypanosomes. *Trends Parasitol.*, **24**, 236-242.
- Delespaux,V., Vitouley,H.S., Marcotty,T., Speybroeck,N., Berkvens,D., Roy,K., Geerts,S., & Van den Bossche,P. (2010) Chemosensitization of *Trypanosoma congolense* strains resistant to isometamidium chloride by tetracyclines and enrofloxacin. *PLoS.Negl.Trop.Dis.*, **4**, e828.
- Denninger,V., Figarella,K., Schonfeld,C., Brems,S., Busold,C., Lang,F., Hoheisel,J., & Duzsenko,M. (2007) Troglitazone induces differentiation in *Trypanosoma brucei*. *Exp.Cell Res.*, **313**, 1805-1819.
- Desquesnes,M. & Davila,A.M. (2002) Applications of PCR-based tools for detection and identification of animal trypanosomes: a review and perspectives. *Vet.Parasitol.*, **109**, 213-231.
- Docampo,R., Moreno,S.N., Stoppani,A.O., Leon,W., Cruz,F.S., Villalta,F., & Muniz,R.F. (1981) Mechanism of nifurtimox toxicity in different forms of *Trypanosoma cruzi*. *Biochem Pharmacol.*, **30**, 1947-1951.
- Doering,T.L., Raper,J., Buxbaum,L.U., Adams,S.P., Gordon,J.I., Hart,G.W., & Englund,P.T. (1991) An analog of myristic acid with selective toxicity for African trypanosomes. *Science*, **252**, 1851-1854.
- Donelson,J.E. & Rice-Ficht,A.C. (1985) Molecular biology of trypanosome antigenic variation. *Microbiology and Molecular Biology Reviews*, **49**, 107-125.
- Dressel,J.R.E.O. (1961) The discovery of Germanin by Oskar Dressel and Richard Kothe. *Journal of Chemical Education*, **38**, 620.

- Eisenthal,R., Game,S., & Holman,G.D. (1989) Specificity and kinetics of hexose transport in *Trypanosoma brucei*. *Biochimica et Biophysica Acta (BBA) - Biomembranes*, **985**, 81-89.
- El Kouni,M.H. (2003) Potential chemotherapeutic targets in the purine metabolism of parasites. *Pharmacol.Ther.*, **99**, 283-309.
- Enanga,B., Keita,M., Chauviere,G., Dumas,M., & Bouteille,B. (1998) Megazol combined with suramin: a chemotherapy regimen which reversed the CNS pathology in a model of human African trypanosomiasis in mice. *Trop.Med Int.Health*, **3**, 736-741.
- Fairlamb,A.H. (2003) Chemotherapy of human African trypanosomiasis: current and future prospects. *Trends Parasitol.*, **19**, 488-494.
- Fairlamb,A.H. & Bowman,I.B.R. (1980) *Trypanosoma brucei*: Maintenance of concentrated suspensions of bloodstream trypomastigotes in vitro using continuous dialysis for measurement of endocytosis. *Experimental Parasitology*, **49**, 366-380.
- Fairlamb,A.H., Henderson,G.B., Bacchi,C.J., & Cerami,A. (1987) In vivo effects of difluoromethylornithine on trypanothione and polyamine levels in bloodstream forms of *Trypanosoma brucei*. *Mol.Biochem Parasitol.*, **24**, 185-191.
- Fairlamb,A.H., Henderson,G.B., & Cerami,A. (1989) Trypanothione is the primary target for arsenical drugs against African trypanosomes. *Proc.Natl.Acad.Sci U.S.A*, **86**, 2607-2611.
- Fairlamb,A.H., Opperdoes,F.R., & Borst,P. (1977) New approach to screening drugs for activity against African trypanosomes. *Nature*, **265**, 270-271.
- Fairlamb,A.H. (2012) Infectious disease: Genomics decodes drug action. *Nature*, **482**, 167-169.
- Ferguson,M.A.J. & Cross,G.A.M. (1984) Myristylation of the Membrane Form of A *Trypanosoma-Brucei* Variant Surface Glycoprotein. *Journal of Biological Chemistry*, **259**, 3011-3015.
- Fevre,E.M., Picozzi,K., Jannin,J., Welburn,S.C., & Maudlin,I. (2006) Human African trypanosomiasis: Epidemiology and control. *Adv.Parasitol.*, **61**, 167-221.
- Figurella,K., Uzcategui,N.L., Zhou,Y., LeFurgey,A., Ouellette,M., Bhattacharjee,H., & Mukhopadhyay,R. (2007) Biochemical characterization of *Leishmania major* aquaglyceroporin LmAQP1: Possible role in volume regulation and osmotaxis. *Molecular Microbiology*, **65**, 1006-1017.

- Filardi, L.S. & Brener, Z. (1982) A nitroimidazole-thiadiazole derivative with curative action in experimental *Trypanosoma cruzi* infections. *Ann. Trop. Med Parasitol.*, **76**, 293-297.
- Galarreta, B.C., Sifuentes, R., Carrillo, A.K., Sanchez, L., Amado, M.R., & Maruenda, H. (2008) The use of natural product scaffolds as leads in the search for trypanothione reductase inhibitors. *Bioorg. Med. Chem.*, **16**, 6689-6695.
- Geerts, S. (2011) The struggle against tsetse flies and animal trypanosomiasis in Africa. [http://www.kaowarsom.be/documents/57-58\(2011-2012\)/GEERTS.pdf](http://www.kaowarsom.be/documents/57-58(2011-2012)/GEERTS.pdf).
- Geerts, S., Holmes, P.H., Eisler, M.C., & Diall, O. (2001) African bovine trypanosomiasis: the problem of drug resistance. *Trends Parasitol.*, **17**, 25-28.
- Geiser, F., Luscher, A., de Koning, H.P., Seebeck, T., & Maser, P. (2005) Molecular Pharmacology of Adenosine Transport in *Trypanosoma brucei*: P1/P2 Revisited. *Molecular Pharmacology*, **68**, 589-595.
- Gillissen, B., Burkle, L., Andre, B., Kuhn, C., Rentsch, D., Brandl, B., & Frommer, W.B. (2000) A new family of high-affinity transporters for adenine, cytosine, and purine derivatives in Arabidopsis. *Plant Cell*, **12**, 291-300.
- Glenn, R.J., Pemberton, A.J., Royle, H.J., Spackman, R.W., Smith, E., Jennifer Rivett, A., & Steverding, D. (2004) Trypanocidal effect of [α],[β]-epoxyketones indicates that trypanosomes are particularly sensitive to inhibitors of proteasome trypsin-like activity. *International Journal of Antimicrobial Agents*, **24**, 286-289.
- Godfrey, D.G., Scott, C.M., Gibson, W.C., Mehlitz, D., & Zillmann, U. (1987) Enzyme polymorphism and the identity of *Trypanosoma brucei gambiense*. *Parasitology*, **94 (Pt 2)**, 337-347.
- Gonen, T. & Walz, T. (2006) The structure of aquaporins. *Q. Rev Biophys.*, **39**, 361-396.
- Gourbal, B., Sonuc, N., Bhattacharjee, H., Legare, D., Sundar, S., Ouellette, M., Rosen, B.P., & Mukhopadhyay, R. (2004) Drug uptake and modulation of drug resistance in *Leishmania* by an aquaglyceroporin. *J Biol. Chem.*, **279**, 31010-31017.
- Grant, I.F. (2001) Insecticides for tsetse and trypanosomiasis control: is the environmental risk acceptable? *Trends Parasitol.*, **17**, 10-14.
- Gray, M.A. & Peregrine, A.S. (1993) An in vitro assay for drug sensitivity of *Trypanosoma congolense* using in vitro-derived metacyclic trypanosomes. *Acta Trop.*, **54**, 291-300.

- Gruenberg, J., Sharma, P.R., & Deshusses, J. (1978) D-Glucose transport in *Trypanosoma brucei*. D-Glucose transport is the rate-limiting step of its metabolism. *Eur. J Biochem*, **89**, 461-469.
- Gunzl, A., Bruderer, T., Laufer, G., Schimanski, B., Tu, L.C., Chung, H.M., Lee, P.T., & Lee, M.G. (2003) RNA polymerase I transcribes procyclin genes and variant surface glycoprotein gene expression sites in *Trypanosoma brucei*. *Eukaryot. Cell*, **2**, 542-551.
- Haanstra, J.R., van Tuijl, A., Kessler, P., Reijnders, W., Michels, P.A.M., Westerhoff, H.V., Parsons, M., & Bakker, B.M. (2008) Compartmentation prevents a lethal turbo-explosion of glycolysis in trypanosomes. *Proceedings of the National Academy of Sciences*, **105**, 17718-17723.
- Hasne, M.P. & Barrett, M.P. (2000) Transport of methionine in *Trypanosoma brucei brucei*. *Mol Biochem Parasitol.*, **111**, 299-307.
- Helfert, S., Estevez, A.M., Bakker, B., Michels, P., & Clayton, C. (2001) Roles of triosephosphate isomerase and aerobic metabolism in *Trypanosoma brucei*. *Biochemical Journal*, **357**, 117-125.
- Herman, M., Perez-Morga, D., Shtickzelle, N., & Michels, P.A.M. (2008) Turnover of glycosomes during life-cycle differentiation of *Trypanosoma brucei*. *Autophagy*, **4**, 294-308.
- Hide, G., Welburn, S.C., Tait, A., & Maudlin, I. (1994) Epidemiological relationships of *Trypanosoma brucei* stocks from south east Uganda: evidence for different population structures in human infective and non-human infective isolates. *Parasitology*, **109 (Pt 1)**, 95-111.
- Hide, G. (1999) History of Sleeping Sickness in East Africa. *Clinical Microbiology Reviews*, **12**, 112-125.
- Hinshaw, J.C., Suh, D.Y., Garnier, P., Buckner, F.S., Eastman, R.T., Matsuda, S.P.T., Joubert, B.M., Coppens, I., Joiner, K.A., Merali, S., Nash, T.E., & Prestwich, G.D. (2003) Oxidosqualene Cyclase Inhibitors as Antimicrobial Agents. *Journal of Medicinal Chemistry*, **46**, 4240-4243.
- Hirumi, H. & Hirumi, K. (1989) Continuous cultivation of *Trypanosoma brucei* blood stream forms in a medium containing a low concentration of serum protein without feeder cell layers. *J Parasitol.*, **75**, 985-989.
- Hua, S.b., To, W.Y., Nguyen, T.T., Wong, M.L., & Wang, C.C. (1996) Purification and characterization of proteasomes from *Trypanosoma brucei*. *Molecular and Biochemical Parasitology*, **78**, 33-46.
- Hursey, B.S. (2001) The programme against African trypanosomiasis: aims, objectives and achievements. *Trends in Parasitology*, **17**, 2-3.

- Ibrahim,H.M.S., Al-Salabi,M.I., El Sabbagh,N., Quashie,N.B., Alkhaldi,A.A.M., Escale,R., Smith,T.K., Vial,H.J., & de Koning,H.P. (2011) Symmetrical choline-derived dications display strong anti-kinetoplastid activity. *Journal of Antimicrobial Chemotherapy*, **66**, 111-125.
- Iten,M., Mett,H., Evans,A., Enyaru,J.C., Brun,R., & Kaminsky,R. (1997) Alterations in ornithine decarboxylase characteristics account for tolerance of *Trypanosoma brucei rhodesiense* to D,L-alpha- difluoromethylornithine. *Antimicrobial Agents and Chemotherapy*, **41**, 1922-1925.
- Jacobs,W.A. & Heidelberger,M. (1919) Aromatic arsenic compounds. V. N-substituted glycyarsanilic acids. *Journal of the American Chemical Society*, **41**, 1809-1821.
- Jamal,S., Sigauque,I., Macuamule,C., Neves,L., Penzhorn,B.L., Marcotty,T., & Van Den Bossche,P. (2005) The susceptibility of *Trypanosoma congolense* isolated in Zambezia Province, Mozambique, to isometamidium chloride, diminazene aceturate and homidium chloride. *Onderstepoort J Vet.Res.*, **72**, 333-338.
- Jensen,R.E., Simpson,L., & Englund,P.T. (2008) What happens when *Trypanosoma brucei* leaves Africa. *Trends in Parasitology*, **24**, 428-431.
- Kaminsky,R., Schmid,C., & Lun,Z.R. (1997) Susceptibility of dyskinetoplastic *Trypanosoma evansi* and *T. equiperdum* to isometamidium chloride. *Parasitol.Res.*, **83**, 816-818.
- Kaminsky,R. & Zweygarth,E. (1991) The effect of verapamil alone and in combination with trypanocides on multidrug-resistant *Trypanosoma brucei brucei*. *Acta Tropica*, **49**, 215-225.
- Kanmogne,G.D., Stevens,J.R., Asonganyi,T., & Gibson,W.C. (1996a) Characterization of *Trypanosoma brucei gambiense* isolates using restriction fragment length polymorphisms in 5 variant surface glycoprotein genes. *Acta Trop.*, **61**, 239-254.
- Kanmogne,G.D., Stevens,J.R., Asonganyi,T., & Gibson,W.C. (1996b) Genetic heterogeneity in the *Trypanosoma brucei gambiense* genome analysed by random amplification of polymorphic DNA. *Parasitol.Res.*, **82**, 535-541.
- Kinabo,L.D.B. (1993) Pharmacology of existing drugs for animal trypanosomiasis. *Acta Tropica*, **54**, 169-183.
- Koslowsky,D.J. (2009) Complex interactions in the regulation of trypanosome mitochondrial gene expression. *Trends in Parasitology*, **25**, 252-255.
- Lai,D.H., Hashimi,H., Lun,Z.R., Ayala,F.J., & Lukes,J. (2008) Adaptations of *Trypanosoma brucei* to gradual loss of kinetoplast DNA: *Trypanosoma*

- equiperdum and *Trypanosoma evansi* are petite mutants of *T. brucei*. *Proc.Natl.Acad.Sci.U.S.A*, **105**, 1999-2004.
- Landfear,S.M., Ullman,B., Carter,N.S., & Sanchez,M.A. (2004) Nucleoside and nucleobase transporters in parasitic protozoa. *Eukaryot.Cell*, **3**, 245-254.
- Laxman,S., Riechers,A., Sadilek,M., Schwede,F., & Beavo,J.A. (2006) Hydrolysis products of cAMP analogs cause transformation of *Trypanosoma brucei* from slender to stumpy-like forms. *Proceedings of the National Academy of Sciences*, **103**, 19194-19199.
- Leach,T.M. & Roberts,C.J. (1981) Present status of chemotherapy and chemoprophylaxis of animal trypanosomiasis in the eastern hemisphere. *pharmacology & therapeutics*, **13**, 91-147.
- Liu,B., Wang,J., Yaffe,N., Lindsay,M.E., Zhao,Z., Zick,A., Shlomai,J., & Englund,P.T. (2009) Trypanosomes have six mitochondrial DNA helicases with one controlling kinetoplast maxicircle replication. *Mol Cell*, **35**, 490-501.
- Liu,Z., Shen,J., Carbrey,J.M., Mukhopadhyay,R., Agre,P., & Rosen,B.P. (2002) Arsenite transport by mammalian aquaglyceroporins AQP7 and AQP9. *Proc.Natl.Acad.Sci U.S.A*, **99**, 6053-6058.
- Lun,Z.R., Fang,Y., Wang,C.J., & Brun,R. (1993) Trypanosomiasis of domestic animals in China. *Parasitol.Today*, **9**, 41-45.
- Luscher,A., de Koning,H.P., & Maser,P. (2007) Chemotherapeutic strategies against *Trypanosoma brucei*: drug targets vs. drug targeting. *Curr.Pharm.Des*, **13**, 555-567.
- Mackey,Z.B., O'Brien,T.C., Greenbaum,D.C., Blank,R.B., & McKerrow,J.H. (2004) A cathepsin B-like protease is required for host protein degradation in *Trypanosoma brucei*. *J Biol.Chem.*, **279**, 48426-48433.
- MacLeod,A., Tweedie,A., Welburn,S.C., Maudlin,I., Turner,C.M., & Tait,A. (2000) Minisatellite marker analysis of *Trypanosoma brucei*: reconciliation of clonal, panmictic, and epidemic population genetic structures. *Proc.Natl.Acad.Sci U.S.A*, **97**, 13442-13447.
- Majiwa,P.A., Thatthi,R., Mooloo,S.K., Nyeko,J.H., Otieno,L.H., & Maloo,S. (1994) Detection of trypanosome infections in the saliva of tsetse flies and buffy-coat samples from antigenaemic but aparasitaemic cattle. *Parasitology*, **108**, 313-322.
- Mandal,G., Sarkar,A., Saha,P., Singh,N., Sundar,S., & Chatterjee,M. (2009) Functionality of drug efflux pumps in antimonial resistant *Leishmania donovani* field isolates. *Indian J Biochem Biophys.*, **46**, 86-92.

- Maser,P. & Kaminsky,R. (1998) Identification of three ABC transporter genes in *Trypanosoma brucei* spp. *Parasitol.Res.*, **84**, 106-111.
- Maser,P., Luscher,A., & Kaminsky,R. (2003) Drug transport and drug resistance in African trypanosomes. *Drug Resist.Updat.*, **6**, 281-290.
- Maser,P., Sutterlin,C., Kralli,A., & Kaminsky,R. (1999) A nucleoside transporter from *Trypanosoma brucei* involved in drug resistance. *Science*, **285**, 242-244.
- Massussi,J.A., Djieto-Lordon,C., Njiokou,F., Laveissiere,C., & van der Ploeg,J.D. (2009) Influence of habitat and seasonal variation on wild mammal diversity and distribution with special reference to the *Trypanosoma brucei* gambiense host-reservoir in Bipindi (Cameroon). *Acta Trop.*, **112**, 308-315.
- Masterson,W.J., Doering,T.L., Hart,G.W., & Englund,P.T. (1989) A novel pathway for glycan assembly: Biosynthesis of the glycosyl-phosphatidylinositol anchor of the trypanosome variant surface glycoprotein. *Cell*, **56**, 793-800.
- Masterson,W.J., Raper,J., Doering,T.L., Hart,G.W., & Englund,P.T. (1990) Fatty acid remodeling: A novel reaction sequence in the biosynthesis of trypanosome glycosyl phosphatidylinositol membrane anchors. *Cell*, **62**, 73-80.
- Matovu,E., Iten,M., Enyaru,J.C., Schmid,C., Lubega,G.W., Brun,R., & Kaminsky,R. (1997) Susceptibility of Ugandan *Trypanosoma brucei* rhodesiense isolated from man and animal reservoirs to diminazene, isometamidium and melarsoprol. *Trop.Med.Int.Health*, **2**, 13-18.
- Matovu,E., Seebeck,T., Enyaru,J.C., & Kaminsky,R. (2001) Drug resistance in *Trypanosoma brucei* spp., the causative agents of sleeping sickness in man and nagana in cattle. *Microbes.Infect.*, **3**, 763-770.
- Matovu,E., Stewart,M.L., Geiser,F., Brun,R., Maser,P., Wallace,L.J., Burchmore,R.J., Enyaru,J.C., Barrett,M.P., Kaminsky,R., Seebeck,T., & de Koning,H.P. (2003) Mechanisms of arsenical and diamidine uptake and resistance in *Trypanosoma brucei*. *Eukaryot.Cell*, **2**, 1003-1008.
- Matthews,K.R. (2005) The developmental cell biology of *Trypanosoma brucei*. *J Cell Sci.*, **118**, 283-290.
- McDermott,J., Woitag,T., Sidibe,I., Bauer,B., Diarra,B., Ouedraogo,D., Kamuanga,M., Peregrine,A., Eisler,M., Zessin,K.H., Mehltz,D., & Clausen,P.H. (2003) Field studies of drug-resistant cattle trypanosomes in Kenedougou Province, Burkina Faso. *Acta Tropica*, **86**, 93-103.
- Michels,P.A.M., Hannaert,V., & Bringaud,F. (2000) Metabolic Aspects of Glycosomes in Trypanosomatidae-New Data and Views. *Parasitology Today*, **16**, 482-489.

- Munday, J.C., Rojas Lopez, K.E., Eze, A.A., Delespaux, V., Van Den Abbeele, J., Rowan, T., Barrett, M.P., Morrison, L.J., & de Koning, H.P. (2013) Functional expression of TcoAT1 reveals it to be a P1-type nucleoside transporter with no capacity for diminazene uptake. *International Journal for Parasitology: Drugs and Drug Resistance*, **3**, 69-76.
- Neupert, W. (1997) Protein import into mitochondria. *Annu. Rev Biochem*, **66**, 863-917.
- Nolan, D.P. & Voorheis, H.P. (1992) The mitochondrion in bloodstream forms of *Trypanosoma brucei* is energized by the electrogenic pumping of protons catalysed by the F1F0-ATPase. *European Journal of Biochemistry*, **209**, 207-216.
- Onyango, R.J., van Hove, K., & De Raadt, P. (1966) The epidemiology of *Trypanosoma rhodesiense* sleeping sickness in aleo location, Central Nyanza, Kenya I. Evidence that cattle may act as reservoir hosts of trypanosomes infective to man. *Transactions of the Royal Society of Tropical Medicine and Hygiene*, **60**, 175-182.
- Opperdoes, F.R. & Borst, P. (1977) Localization of nine glycolytic enzymes in a microbody-like organelle in *Trypanosoma brucei*: the glycosome. *FEBS Lett.*, **80**, 360-364.
- Opperdoes, F.R., Borst, P., & de Ruke, D. (1976) Oligomycin sensitivity of the mitochondrial ATPase as a marker for fly transmissibility and the presence of functional kinetoplast DNA in African trypanosomes. *Comparative Biochemistry and Physiology Part B: Comparative Biochemistry*, **55**, 25-30.
- Ortiz, D., Sanchez, M.A., Quecke, P., & Landfear, S.M. (2009) Two novel nucleobase/pentamidine transporters from *Trypanosoma brucei*. *Mol. Biochem Parasitol.*, **163**, 67-76.
- Osorio, A.L., Madruga, C.R., Desquesnes, M., Soares, C.O., Ribeiro, L.R., & Costa, S.C. (2008) *Trypanosoma* (*Duttonella*) *vivax*: its biology, epidemiology, pathogenesis, and introduction in the New World--a review. *Mem. Inst. Oswaldo Cruz*, **103**, 1-13.
- Overath, P. & Engstler, M. (2004) Endocytosis, membrane recycling and sorting of GPI-anchored proteins: *Trypanosoma brucei* as a model system. *Mol Microbiol.*, **53**, 735-744.
- Palenchar, J.B. & Bellofatto, V. (2006) Gene transcription in trypanosomes. *Molecular and Biochemical Parasitology*, **146**, 135-141.
- Parsons, M. (2004) Glycosomes: parasites and the divergence of peroxisomal purpose. *Molecular Microbiology*, **53**, 717-724.

- Pays,E. (1985) Selective telomere activation and the control of antigen gene expression in trypanosomes. *Annales de l'Institut Pasteur / Immunologie*, **136**, 25-39.
- Pays,E. (2006) The variant surface glycoprotein as a tool for adaptation in African trypanosomes. *Microbes.Infect.*, **8**, 930-937.
- Pays,E., Coquelet,H., Tebabi,P., Pays,A., Jefferies,D., Steinert,M., Koenig,E., Williams,R.O., & Roditi,I. (1990) Trypanosoma brucei: constitutive activity of the VSG and procyclin gene promoters. *EMBO J*, **9**, 3145-3151.
- Pays,E., Vanhollebeke,B., Vanhamme,L., Paturiaux-Hanocq,F., Nolan,D.P., & Perez-Morga,D. (2006) The trypanolytic factor of human serum. *Nat.Rev.Microbiol.*, **4**, 477-486.
- Penefsky,H.S. (1985) Mechanism of inhibition of mitochondrial adenosine triphosphatase by dicyclohexylcarbodiimide and oligomycin: relationship to ATP synthesis. *Proceedings of the National Academy of Sciences*, **82**, 1589-1593.
- Peregrine,A.S., Gray,M.A., & Moolo,S.K. (1997) Cross-resistance associated with development of resistance to isometamidium in a clone of Trypanosoma congolense. *Antimicrobial Agents and Chemotherapy*, **41**, 1604-1606.
- Preusser,C., Jae,N., & Bindereif,A. (2012) mRNA splicing in trypanosomes. *Int.J Med Microbiol.*, **302**, 221-224.
- Priest,J.W. & Hajduk,S.L. (1994) Developmental regulation of mitochondrial biogenesis in Trypanosoma brucei. *J Bioenerg.Biomembr.*, **26**, 179-191.
- Priotto,G., Kasparian,S., Mutombo,W., Ngouama,D., Ghorashian,S., Arnold,U., Ghabri,S., Baudin,E., Buard,V., Kazadi-Kyanza,S., Ilunga,M., Mutangala,W., Pohlig,G., Schmid,C., Karunakara,U., Torreele,E., & Kande,V. (2009) Nifurtimox-eflornithine combination therapy for second-stage African Trypanosoma brucei gambiense trypanosomiasis: a multicentre, randomised, phase III, non-inferiority trial. *The Lancet*, **374**, 56-64.
- Raz,B., Iten,M., Grether-Buhler,Y., Kaminsky,R., & Brun,R. (1997) The Alamar Blue assay to determine drug sensitivity of African trypanosomes (*T.b. rhodesiense* and *T.b. gambiense*) in vitro. *Acta Trop.*, **68**, 139-147.
- Reyes,P., Rathod,P.K., Sanchez,D.J., Mrema,J.E.K., Rieckmann,K.H., & Heidrich,H.G. (1982) Enzymes of Purine and Pyrimidine Metabolism from the Human Malaria, Plasmodium-Falciparum. *Molecular and Biochemical Parasitology*, **5**, 275-290.
- Riou,G.F., Belnat,P., & Benard,J. (1980) Complete loss of kinetoplast DNA sequences induced by ethidium bromide or by acriflavine in Trypanosoma equiperdum. *J Biol.Chem.*, **255**, 5141-5144.

- Ross, M.F., Kelso, G.F., Blaikie, F.H., James, A.M., Cocheme, H.M., Filipovska, A., Da, R.T., Hurd, T.R., Smith, R.A., & Murphy, M.P. (2005) Lipophilic triphenylphosphonium cations as tools in mitochondrial bioenergetics and free radical biology. *Biochemistry (Mosc.)*, **70**, 222-230.
- Roy Chowdhury, A., Bakshi, R., Wang, J., Yildirim, G., Liu, B., Pappas-Brown, V., Tolun, G., Griffith, J.D., Shapiro, T.A., Jensen, R.E., & Englund, P.T. (2010) The Killing of African Trypanosomes by Ethidium Bromide. *PLoS Pathog*, **6**, e1001226.
- Sambrook, J. & Russell, D.W. (2001) *Molecular Cloning: A laboratory Manual*, 3rd edn, p. 1.116-1.118. Cold Spring Harbor Laboratory Press, New York.
- Sanchez, M.A., Tryon, R., Green, J., Boor, I., & Landfear, S.M. (2002) Six related nucleoside/nucleobase transporters from *Trypanosoma brucei* exhibit distinct biochemical functions. *J Biol. Chem.*, **277**, 21499-21504.
- Sanders, O.I., Rensing, C., Kuroda, M., Mitra, B., & Rosen, B.P. (1997) Antimonite is accumulated by the glycerol facilitator GlpF in *Escherichia coli*. *J Bacteriol.*, **179**, 3365-3367.
- Schnauffer, A., Clark-Walker, G.D., Steinberg, A.G., & Stuart, K. (2005) The F1-ATP synthase complex in bloodstream stage trypanosomes has an unusual and essential function. *EMBO J*, **24**, 4029-4040.
- Schnauffer, A., Domingo, G.J., & Stuart, K. (2002) Natural and induced dyskinetoplastic trypanosomatids: how to live without mitochondrial DNA. *International Journal for Parasitology*, **32**, 1071-1084.
- Schonefeld, A., Rottcher, D., & Moloo, S.K. (1987) The sensitivity to trypanocidal drugs of *Trypanosoma vivax* isolated in Kenya and Somalia. *Trop. Med Parasitol.*, **38**, 177-180.
- Scoocca, J.R. & Shapiro, T.A. (2008) A mitochondrial topoisomerase IA essential for late theta structure resolution in African trypanosomes. *Mol Microbiol.*, **67**, 820-829.
- Seifi, H. (1995) Clinical trypanosomosis due to *Trypanosoma theileri* in a cow in Iran. *Tropical Animal Health and Production*, **27**, 93-94.
- Shahi, S.K., Krauth-Siegel, R.L., & Clayton, C.E. (2002) Overexpression of the putative thiol conjugate transporter TbMRPA causes melarsoprol resistance in *Trypanosoma brucei*. *Mol Microbiol.*, **43**, 1129-1138.
- Shapiro, T.A. (1993) Inhibition of topoisomerases in African trypanosomes. *Acta Trop.*, **54**, 251-260.

- Shapiro, T.A. & Englund, P.T. (1990) Selective cleavage of kinetoplast DNA minicircles promoted by antitrypanosomal drugs. *Proc. Natl. Acad. Sci. U.S.A.*, **87**, 950-954.
- Simarro, P.P., Jannin, J., & Cattand, P. (2008) Eliminating human African trypanosomiasis: where do we stand and what comes next? *PLoS. Med.*, **5**, e55.
- Simo, G., Cuny, G., Demonchy, R., & Herder, S. (2008) *Trypanosoma brucei* gambiense: Study of population genetic structure of Central African stocks using amplified fragment length polymorphism (AFLP). *Experimental Parasitology*, **118**, 172-180.
- Sinyangwe, L., Delespaux, V., Brandt, J., Geerts, S., Mubanga, J., Machila, N., Holmes, P.H., & Eisler, M.C. (2004) Trypanocidal drug resistance in eastern province of Zambia. *Veterinary Parasitology*, **119**, 125-135.
- Sow, A., Sidibe, I., Bengaly, Z., Marcotty, T., Sere, M., Diallo, A., Vitouley, H.S., Nebie, R.L., Ouedraogo, M., Akoda, G.K., Van den Bossche, P., van den Abbeele, J., De Deken, R., & Delespaux, V. (2012) Field detection of resistance to isometamidium chloride and diminazene aceturate in *Trypanosoma vivax* from the region of the Boucle du Mouhoun in Burkina Faso. *Veterinary Parasitology*, **187**, 105-111.
- Stephens, J.W.W. & Fantham, H.B. (1910) On the Peculiar Morphology of a Trypanosome from a Case of Sleeping Sickness and the Possibility of Its Being a New Species (*T. rhodesiense*). *Proceedings of the Royal Society of London. Series B, Containing Papers of a Biological Character*, **83**, 28-33.
- Steverding, D. (2007) The proteasome as a potential target for Chemotherapy of African trypanosomiasis. *Drug Development Research*, **68**, 205-212.
- Steverding, D. (2008) The history of African trypanosomiasis. *Parasit. Vectors.*, **1**, 3.
- Stewart, M.L., Burchmore, R.J., Clucas, C., Hertz-Fowler, C., Brooks, K., Tait, A., MacLeod, A., Turner, C.M., de Koning, H.P., Wong, P.E., & Barrett, M.P. (2010) Multiple genetic mechanisms lead to loss of functional TbAT1 expression in drug-resistant trypanosomes. *Eukaryot. Cell*, **9**, 336-343.
- Stewart, M.L., Bueno, G.J., Baliani, A., Klenke, B., Brun, R., Brock, J.M., Gilbert, I.H., & Barrett, M.P. (2004) Trypanocidal Activity of Melamine-Based Nitroheterocycles. *Antimicrobial Agents and Chemotherapy*, **48**, 1733-1738.
- Stuart, K.D., Schnauffer, A., Ernst, N.L., & Panigrahi, A.K. (2005) Complex management: RNA editing in trypanosomes. *Trends in Biochemical Sciences*, **30**, 97-105.

- Sutherland, I.A., Mounsey, A., & Holmes, P.H. (1992) Transport of isometamidium (Samorin) by drug-resistant and drug-sensitive *Trypanosoma congolense*. *Parasitology*, **104**, 461-467.
- Swallow, B.M. (1999) Impacts of trypanosomiasis on African agriculture. http://www.fao.org/waicent/Faoinfo/agricult/againfo/programmes/en/paa/t/documents/papers/Paper_1999.pdf.
- Swick, M.C., Morgan-Linnell, S.K., Carlson, K.M., & Zechiedrich, L. (2011) Expression of Multidrug Efflux Pump Genes *acrAB-tolC*, *mdfA*, and *norE* in *Escherichia coli* Clinical Isolates as a Function of Fluoroquinolone and Multidrug Resistance. *Antimicrobial Agents and Chemotherapy*, **55**, 921-924.
- Taladriz, A., Healy, A., Flores Perez, E.J., Herrero Garcia, V., Rios Martinez, C., Alkhalidi, A.A.M., Eze, A.A., Kaiser, M., de Koning, H.P., Chana, A., & Dardonville, C. (2012) Synthesis and Structure–Activity Analysis of New Phosphonium Salts with Potent Activity against African Trypanosomes. *Journal of Medicinal Chemistry*, **55**, 2606-2622.
- Taylor, M.C., Kaur, H., Blessington, B., Kelly, J.M., & Wilkinson, S.R. (2008) Validation of spermidine synthase as a drug target in African trypanosomes. *Biochemical Journal*, **409**, 563-569.
- Tegos, G.P., Masago, K., Aziz, F., Higginbotham, A., Stermitz, F.R., & Hamblin, M.R. (2008) Inhibitors of Bacterial Multidrug Efflux Pumps Potentiate Antimicrobial Photoinactivation. *Antimicrobial Agents and Chemotherapy*, **52**, 3202-3209.
- Teka, I.A. (2011) Diamidine Transporters of *Trypanosoma brucei*. *PhD thesis, University of Glasgow*, <http://theses.gla.ac.uk/2640/>.
- Teka, I.A., Kazibwe, A.J., El-Sabbagh, N., Al-Salabi, M.I., Ward, C.P., Eze, A.A., Munday, J.C., Maeser, P., Matovu, E., Barrett, M.P., & de Koning, H.P. (2011) The diamidine diminazene aceturate is a substrate for the High Affinity Pentamidine Transporter: implications for the development of high resistance levels in trypanosomes. *Mol Pharmacol*.
- ter Kuile, B.H. (1997) Adaptation of metabolic enzyme activities of *Trypanosoma brucei* promastigotes to growth rate and carbon regimen. *J Bacteriol.*, **179**, 4699-4705.
- Tetaud, E., Lecuix, I., Sheldrake, T., Baltz, T.o., & Fairlamb, A.H. (2002) A new expression vector for *Crithidia fasciculata* and *Leishmania*. *Molecular and Biochemical Parasitology*, **120**, 195-204.
- Tielens, A.G.M. & van Hellemond, J.J. (1998) Differences in Energy Metabolism Between Trypanosomatidae. *Parasitology Today*, **14**, 265-272.

- Tilley,A., Welburn,S.C., Fevre,E.M., Feil,E.J., & Hide,G. (2003) Trypanosoma brucei: trypanosome strain typing using PCR analysis of mobile genetic elements (MGE-PCR). *Exp.Parasitol.*, **104**, 26-32.
- Timms,M.W., van Deursen,F.J., Hendriks,E.F., & Matthews,K.R. (2002) Mitochondrial development during life cycle differentiation of African trypanosomes: evidence for a kinetoplast-dependent differentiation control point. *Mol Biol.Cell*, **13**, 3747-3759.
- Tsuhako,M.H., Alves,M.J., Colli,W., Filardi,L.S., Brener,Z., & Augusto,O. (1991) Comparative studies of nifurtimox uptake and metabolism by drug-resistant and susceptible strains of Trypanosoma cruzi. *Comp Biochem Physiol C.*, **99**, 317-321.
- Tsukaguchi,H., Shayakul,C., Berger,U.V., Mackenzie,B., Devidas,S., Guggino,W.B., van Hoek,A.N., & Hediger,M.A. (1998) Molecular Characterization of a Broad Selectivity Neutral Solute Channel. *Journal of Biological Chemistry*, **273**, 24737-24743.
- Upcroft,P. (1994) Multiple drug resistance in the pathogenic protozoa. *Acta Tropica*, **56**, 195-212.
- van Hellemond,J.J., Opperdoes,F.R., & Tielens,A.G. (2005) The extraordinary mitochondrion and unusual citric acid cycle in Trypanosoma brucei. *Biochem Soc.Trans.*, **33**, 967-971.
- Van,B. I & Haemers,A. (1989) Eflornithine. A new drug in the treatment of sleeping sickness. *Pharm.Weekbl.Sci.*, **11**, 69-75.
- Vanhamme,L. & Pays,E. (1995) Control of gene expression in trypanosomes. *Microbiological Reviews*, **59**, 223-240.
- Vanhamme,L. & Pays,E. (2004) The trypanosome lytic factor of human serum and the molecular basis of sleeping sickness. *Int.J Parasitol.*, **34**, 887-898.
- Vansterkenburg,E.L.M., Coppens,I., Wilting,J., Bos,O.J.M., Fischer,M.J.E., Janssen,L.H.M., & Opperdoes,F.R. (1993) The uptake of the trypanocidal drug suramin in combination with low-density lipoproteins by Trypanosoma brucei and its possible mode of action. *Acta Tropica*, **54**, 237-250.
- Vassella,E., Reuner,B., Yutzy,B., & Boshart,M. (1997) Differentiation of African trypanosomes is controlled by a density sensing mechanism which signals cell cycle arrest via the cAMP pathway. *Journal of Cell Science*, **110**, 2661-2671.
- Vaughan,S. & Gull,K. (2008) The structural mechanics of cell division in Trypanosoma brucei. *Biochem Soc.Trans.*, **36**, 421-424.

- Vaughan,S. & Gull,K. (2003) The trypanosome flagellum. *Journal of Cell Science*, **116**, 757-759.
- Verlinde,C.L., Callens,M., Van,C.S., Van,A.A., Herdewijn,P., Hannaert,V., Michels,P.A., Opperdoes,F.R., & Hol,W.G. (1994) Selective inhibition of trypanosomal glyceraldehyde-3-phosphate dehydrogenase by protein structure-based design: toward new drugs for the treatment of sleeping sickness. *J Med Chem.*, **37**, 3605-3613.
- Verlinde,C.L.M.J., Hannaert,V., Blonski,C., Willson,M., Pærië,J.J., Fothergill-Gilmore,L.A., Opperdoes,F.R., Gelb,M.H., Hol,W.G.J., & Michels,P.A.M. (2001) Glycolysis as a target for the design of new anti-trypanosome drugs. *Drug Resistance Updates*, **4**, 50-65.
- Vickerman,K. (1985) Developmental cycles and biology of pathogenic trypanosomes. *British Medical Bulletin*, **41**, 105-114.
- Vincent,I.M., Creek,D., Watson,D.G., Kamleh,M.A., Woods,D.J., Wong,P.E., Burchmore,R.J., & Barrett,M.P. (2010) A molecular mechanism for eflornithine resistance in African trypanosomes. *PLoS Pathog*, **6**, e1001204.
- Visser,N. & Opperdoes,F.R. (1980) Glycolysis in *Trypanosoma brucei*. *Eur.J Biochem*, **103**, 623-632.
- Vondruskova,E., van den Burg,J., Zikova,A., Ernst,N.L., Stuart,K., Benne,R., & Lukes,J. (2005) RNA Interference Analyses Suggest a Transcript-specific Regulatory Role for Mitochondrial RNA-binding Proteins MRP1 and MRP2 in RNA Editing and Other RNA Processing in *Trypanosoma brucei*. *Journal of Biological Chemistry*, **280**, 2429-2438.
- W.H.O. Control and Surveillance of African Trypanosomiasis, Report of WHO expert committee. 1998. Geneva, Switzerland, World Health Organisation. WHO Technical Report Series, no. 881.
- Ref Type: Report
- W.H.O. (2012) Trypanosomiasis, Human African (sleeping sickness). *W.H.O.Fact sheet*, **No. 259**.
<http://www.who.int/mediacentre/factsheets/fs259/en/index.html>.
- Wang,C.C. (1995) Molecular mechanisms and therapeutic approaches to the treatment of African trypanosomiasis. *Annu.Rev.Pharmacol.Toxicol.*, **35**, 93-127.
- Wang,Z. & Englund,P.T. (2001) RNA interference of a trypanosome topoisomerase II causes progressive loss of mitochondrial DNA. *EMBO J*, **20**, 4674-4683.
- Warburton,P.J., Ciric,L., Lerner,A., Seville,L.A., Roberts,A.P., Mullany,P., & Allan,E. (2013) TetAB(46), a predicted heterodimeric ABC transporter conferring

- tetracycline resistance in *Streptococcus australis* isolated from the oral cavity. *Journal of Antimicrobial Chemotherapy*, **68**, 17-22.
- Ward,C.P., Burgess,K.E.V., Burchmore,R.J.S., Barrett,M.P., & de Koning,H.P. (2010) A fluorescence-based assay for the uptake of CPD0801 (DB829) by African trypanosomes. *Molecular and Biochemical Parasitology*, **174**, 145-149.
- Ward,C.P., Wong,P.E., Burchmore,R.J., de Koning,H.P., & Barrett,M.P. (2011) Trypanocidal Furamide Analogues: Influence of Pyridine Nitrogens on Trypanocidal Activity, Transport Kinetics, and Resistance Patterns. *Antimicrobial Agents and Chemotherapy*, **55**, 2352-2361.
- Welburn,S.C., Fevre,E.M., Coleman,P.G., Odiit,M., & Maudlin,I. (2001) Sleeping sickness: a tale of two diseases. *Trends in Parasitology*, **17**, 19-24.
- Werbovets,K.A. (2000) Target-based drug discovery for malaria, leishmaniasis, and trypanosomiasis. *Curr.Med.Chem.*, **7**, 835-860.
- Wilkes,J.M., Mulugeta,W., Wells,C., & Peregrine,A.S. (1997) Modulation of mitochondrial electrical potential: a candidate mechanism for drug resistance in African trypanosomes. *Biochemical Journal*, **326**, 755-761.
- Wilkes,J.M., Peregrine,A.S., & Zilberstein,D. (1995) The accumulation and compartmentalization of isometamidium chloride in *Trypanosoma congolense*, monitored by its intrinsic fluorescence. *Biochemical Journal*, **312**, 319-327.
- Wilkinson,S.R., Bot,C., Kelly,J.M., & Hall,B.S. (2011) Trypanocidal activity of nitroaromatic prodrugs: current treatments and future perspectives. *Curr.Top.Med Chem.*, **11**, 2072-2084.
- Wilkinson,S.R. & Kelly,J.M. (2009) Trypanocidal drugs: mechanisms, resistance and new targets. *Expert.Rev.Mol.Med*, **11**, e31.
- Wilkinson,S.R., Taylor,M.C., Horn,D., Kelly,J.M., & Cheeseman,I. (2008) A mechanism for cross-resistance to nifurtimox and benznidazole in trypanosomes. *Proc.Natl.Acad.Sci.U.S.A*, **105**, 5022-5027.
- Willert,E.K. & Phillips,M.A. (2008) Regulated expression of an essential allosteric activator of polyamine biosynthesis in African trypanosomes. *PLoS.Pathog.*, **4**, e1000183.
- Williams,N. (1994) The mitochondrial ATP synthase of *Trypanosoma brucei*: Structure and regulation. *Journal of Bioenergetics and Biomembranes*, **26**, 173-178.
- Zikova,A., Schnauffer,A., Dalley,R.A., Panigrahi,A.K., & Stuart,K.D. (2009) The F(0)F(1)-ATP synthase complex contains novel subunits and is essential for procyclic *Trypanosoma brucei*. *PLoS Pathog*, **5**, e1000436.

